

Targeting of antigen presenting cells with mannosylated conjugates Hogervorst, T.P.

Citation

Hogervorst, T. P. (2020, March 17). *Targeting of antigen presenting cells with mannosylated conjugates*. Retrieved from https://hdl.handle.net/1887/136534

Version: Publisher's Version

License: License agreement concerning inclusion of doctoral thesis in the

Institutional Repository of the University of Leiden

Downloaded from: https://hdl.handle.net/1887/136534

Note: To cite this publication please use the final published version (if applicable).

Cover Page



Universiteit Leiden



The handle http://hdl.handle.net/1887/136534 holds various files of this Leiden University dissertation.

Author: Hogervorst, T.P.

Title: Targeting of antigen presenting cells with mannosylated conjugates

Issue Date: 2020-03-17

Targeting of antigen presenting cells with mannosylated conjugates

PROEFSCHRIFT

ter verkrijging van de graad van Doctor aan de Universiteit Leiden, op gezag van Rector Magnificus prof.mr. C.J.J.M. Stolker, volgens besluit van het College voor Promoties te verdedigen op 17 maart 2020 klokke 13:45

door

Tim Petrus Hogervorst

Geboren te Pijnacker in 1991

Promotiecommissie

Promotor : Dr. J.D.C. Codée

Copromotor: Prof.dr. G.A. van der Marel

Overige leden: Prof.dr. H.S. Overkleeft

Prof.dr. J. Brouwer

Prof. dr. Y. van Kooyk (Amsterdam UMC, Amsterdam)

Dr. D.V. Filippov

Dr. M. Verdoes (Radboud UMC, Nijmegen)

Print: Ridderprint | www.ridderprint.nl

ISBN: 978-94-6375-816-1

Table of Contents

List of Abbreviations	111
Chapter 1	1
Targeting of antigen presenting cells with mannosylated conjugates	
Chapter 2	21
Multivalent oligomannoside clusters to probe C-type lectin receptor binding	
Chapter 3	63
Large scale synthesis of a conjugation ready 2-butoxy-8-oxo-adenine analog TLR7-ligand	
	04
Chapter 4	81
Synthesis of trifunctional mannosylated peptide antigen conjugates targeting DC-SIGN and TLR7	

Chapter 5	111
Development of a C-mannoside functionalized lysine for the synthesis of acid-stable mannosylated peptides	
Chapter 6	145
Synthesis of glycosylated BTA-core monomers for the formation of dynamic self-assembling supramolecular fibers	
Chapter 7	177
Summary and future prospects	
Nederlandse Samenvatting	187
List of Publications	193
Curriculum Vitae	195

List of Abbreviations

Å	Ångstrom	DC dendritic cell		
Ac	acetyl	DCM	dichloromethane	
ACN	acetonitrile	DC-SIGN	SIGN DC-specific ICAM-3 grabbing	
AIBN	α,α'-azoisobutyronitrile		non-integrin	
APC	antigen-presenting cells	DIPEA	N,N-diisopropylethylamine	
APT	attached proton test	DMAP	4-(N,N-dimethylamino)pyridine	
aq.	aqueous	DMF	dimethylformamide	
arom	aromatic	DMSO	dimethylsulfoxide	
AuNP	gold nanoparticles	e.g.	exempli gratia	
Bn	benzyl	EBV	transfected B-cell line	
Boc-ON	2-(tert-butoxycarbonyloxyimino)-	ECD	extracellular domain	
	2-phenylacetonitrile	ECM	extracellular matrix	
Bu	butyl	eq	molar equivalents	
Bz	benzoyl	ESI	electrospray ionization	
CAR	chimeric antigen receptor	Et	ethyl	
CD	cluster of differentiation	et al.	et alia 'and others'	
СНО	Chinese hamster ovary	EtOAc	ethylacetate	
CLR	C-type lectin receptors	FACS	fluorescence-activated cell sorting	
COSY	correlation spectroscopy	FRET	Förster resonance energy transfer	
C_{q}	quarternary carbon	g	gram	
CRD	carbohydrate recognition domain	Gal	galactose	
CuAAC	copper(I)-catalyzed alkyne-azide	GalNAc	N-acetyl galactosamine	
	cycloaddition	Glu	glucose	
δ	chemical shift	h	hours	
d	coublet	HA	hyaluronic acid	
DAMP	danger/damage-associated molecular pattern	HFIP	1,1,1,3,3,3-hexafluoroisopropanol	

HPLC	high-performance liquid	PMB	para-Methoxybenzyl
	chromatography	PRR	pathogen recognizing receptor
HRMS	high resolution mass	q	quartet
	spectroscopy	qnt.	quantitative
HSQC	heteronuclear single quantum	RI	refractive index
	coherence	RIG-like	retinoic acid inducible gene-I-like
Hz	hertz	RLRs	retinoic acid-inducible gene-I-like
i.e.	id est		receptors
IL	interleukin	RP	reverse phase
IR	infrared	rt	room temperature
J	<i>J</i> -coupling	S	singlet
LC-MS	liquid chromatography mass-	sat.	saturated
	spectrometry	SLP	synthetic long peptide
LCP	lipid-core-peptide	SPPS	solid-phase peptide synthesis
m	multiplet	SPR	surface plasmon resonance
M	molar	STORM	stochastic optical reconstruction
Man	mannose		microscopy
MBL	mannose-binding lectin	TAAs	tumor-associated antigens
Me	methyl	t-Bu	<i>tert-</i> butyl
MGL	macrophage galactose-type lectin	TCR	T cell receptor
MHC	major histocompatibility complex	TFA	trifluoroacetic acid
min	minute	TFE	2,2,2-trifluoroethanol
Mmt	monomethoxy trityl	Th	T helper cell
moDC	monocyte derived dendritic cell	THPTA	tris(3-hydroxypropyl -
MR	mannose receptor		triazolylmethyl)amine
MS	molecular sieves	TIS	tri-isopropylsilane
MS	mass-spectrometry	TLR	Toll-Like Receptor
NBS	N-bromosuccinimide	TLR7	Toll-Like receptor-7
n.d.	not determined	TMS	trimethylsilyl
N.D.	not determined	TMSOTf	trimethylsilyl trifluoromethanesulfonate
NHS	N-hydroxysuccinimide		tilluoromethanesulionate
NIS	N-iodosuccinimide	Treg	regulatory T cells
NLR	NOD-like receptor	TTox	tetanus toxoid
NMR	nuclear magnetic resonance	UV	ultraviolet
NOD	nucleotide-binding oligomerization domain		
PAMP	pathogen-associated molecular pattern		
PE	petroleum ether		
PEG	polyethylene glycol		
Ph	phenyl		

Targeting of antigen presenting cells with mannosylated conjugates

Introduction

The immune system consists of a large variety of cells that continuously control and protect the body against foreign and aberrant cells. It can be divided into an innate and an adaptive part, that recognize these malignant cells through non-specific general traits (the innate part) or through highly specific interactions, as developed in the adaptive part of the immune system. Innate immune cells can instantly battle pathogens and aberrant cells after sensing danger or pathogen-associated molecular patterns (DAMPs and PAMPs). When the innate system does not suffice in eradication, adaptive immune cells are recruited to generate a selective response. The adaptive immune system serves two goals. It generates a strong tailored immune response with high specificity, and secondly, it generates lasting immunity by the formation of memory cells. Upon recognition of their specific target, the adaptive immune cells start to proliferate to form large numbers of specific cells. A small portion of these cells transforms into memory cells, which can be readily reactivated and allows the immune system to generate a fast and specific response when re-challenged by the same pathogen or aberrant cell.

The adaptive immune system has been exploited for centuries in the treatment of diseases. At the end of the eighteenth century, Edward Jenner successfully immunized the first human by challenging his immune system with cowpox, thereby effectively protecting him from smallpox.¹ Since Jenner, many other therapies that exploit the power and specificity of immune cells have been developed. In the last decades, immunotherapies have revolutionized cancer treatment with the development of chimeric antigen receptor (CAR) T cells and checkpoint inhibitors.^{2,3} The inhibition of checkpoints can result in the restoration of immune responses and has successfully treated various tumors were traditional cytotoxic therapies failed.^{4,5} Immunotherapies often rely on T cells, a specific set of adaptive immune cells and the amount of tumor-infiltrating T cells has been shown to be a prognostic marker for success in immunotherapy.^{6,7} However, the presence of T cells does not guarantee a sufficient response if the T cells are not tumor-reactive. For example, by sequencing the T cell receptor (TCR) of intratumoral T cells, Scheper et al.8, demonstrated that the majority of the T cells were not tumor-reactive. Furthermore, other immune cells, besides T cells, are required to generate a long-lasting response against malignant cells. A possible method to improve T cell based therapies is by active immunization against cancer cells by challenging the immune system with specific tumor-associated antigens (TAAs) to mount a specific T cell response to target aberrant cells or help improve and elongate the immune-response. 10,111

Innate immune cells can distinguish foreign and damaged cells from normal cells using pathogen recognizing receptors (PRRs). These receptors recognize distinct molecular motives that have been preserved in pathogens such as viral and bacterial DNA, RNA, carbohydrates, and lipids. Upon recognition, the innate immune cells are activated and generate signals to recruit other immune cells to the site of infection. Among the innate cells are dendritic cells (DCs) that play a pivotal role in the activation of the adaptive immune system. DCs are antigen-presenting cells (APCs) that can present (peptide) antigens on their cell surface in a protein called the major histocompatibility complex (MHC). Two types of (classic) MHC proteins exist of which class I (MHC-I) presents antigens from endogenous proteins from the cytosol and class II (MHC-II) antigens from endocytosed (pathogenic) proteins. MHC-I is present on all cells and presents epitopes containing 8-11 amino acids. It allows for the detection of aberrant cells through the interaction with cytotoxic T cells (CTL or CD8⁺), to induce programmed cell death. MHC-II is only expressed by professional APCs such as dendritic cells (DCs), B cells, and macrophages. MHC-II presents epitopes with a less stringent size restriction (generally in the 13-17 amino acids length range) to T helper cells (T_h cells or CD4⁺), that in turn stimulate effector cells and help prolong the immune response.¹² T cells recognize the combination of MHC occupied with an epitope via the T cell receptor (TCR). Although antigens presented in MHC-II are obtained via endocytosis of pathogens

and antigens presented in MHC-I are derived from the cytosol, professional APCs present a small amount of the endocytosed antigen in the MHC-I. This route is called antigen cross-presentation and allows for immunity against tumors and viruses.¹³ Importantly, the recognition of epitope-MHC is not sufficient to activate T cells and additional stimuli from the APC, in the form of costimulatory proteins such as CD40 and cytokines, are required. APCs upregulate the levels of these stimuli when their PRRs recognize PAMPs.

Mammalian immune cells express a multitude of PRRs which are divided into subfamilies based on their structure and the ligands they bind. The four well-defined families are the C-type lectin receptors (CLRs), toll-like receptors (TLRs), nucleotide-binding oligomerization domain-like receptors (NOD-like or NLRs) and the retinoic acid-inducible gene-I-like receptors (RIG-like, or RLRs). 14 Occasionally, new PRRs are identified that could potentially increase the number of PRR families. 15 The focus of this thesis is on the CLR and TLR families. TLRs recognize different type of PAMPs such as bacterial lipopeptides and bacterial and viral RNA and DNA and have been extensively explored to acquire adjuvants for vaccine development. 16,17 CLRs recognize viral, bacterial, and fungal derived glycans. Both soluble and transmembrane CLRs exist that bind carbohydrates in a calcium depending manner. The transmembrane CLRs are classified into two classes based on whether the position of their N-terminus is extra- (type I) or intra-cellular (type II). The CLR family recognizes various carbohydrates, for example, dectin-1 recognizes β-glucans, and the macrophage galactose-type lectin (MGL) recognizes N-acetyl galactosamine containing structures. Several CLRs can recognize mannose structures, which is the main subject of the research described in this Thesis. These include the mannose-binding lectin (MBL), the mannose receptor (MR, or CD206), dendritic cell-specific intercellular adhesion molecule-3-grabbing nonintegrin (DC-SIGN or CD209), and Langerin (CD207) and are discussed in the following sections.

MBL

The mannose-binding lectin (MBL) is a soluble CLR, which contains an N-terminal cysteine-rich region and a C-type lectin domain that can bind mannose, fucose, and GlcNAc type of carbohydrates. The cysteine-rich domain forms disulfide bonds with other MBL peptides, creating a trimeric structure with 45 Å spacing between the CRDs. ¹⁸ These subunits can multimerize further into a tetrameric complex, forming a bouquet-like structure with 12 CRDs per complex (See Figure 1). ¹⁹ The affinity of a single MBL protein is low, but when multimerized it can bind with high avidity to the neutral carbohydrates mentioned above. ²⁰ Pathogen recognition by MBL can initiate activation of the innate complement system via the lectin pathway. ²¹ Additionally, binding of MBL enhances phagocytosis, ²² thereby trafficking pathogens towards phagosomes, where it can lead to

the engagement of TLR2/TLR6, and MBL can thus act as a TLR co-receptor.²³ Due to the complexity of the complement system, antigen targeting using MBL is hardly explored. However, it can help to target antigens toward germinal centers which could start an appropriate adaptive immune response.²⁴

MR

The mannose receptor (MR, or CD206) is a C-type lectin receptor that is found on the surface of endothelial cells, macrophages, Langerhans cells (LCs) and (immature) DCs. The MR occurs both as a monomer and dimer, and both complexes can bind mannosides, 25,26 but dimerization is required for the binding of larger particles such as HIV-1.27 The receptor consists of a short Cterminal intracellular domain (type I CLR), a transmembrane domain linked to eight C-type carbohydrate recognition domains (CRDs), which can bind mannose, fucose, and N-acetyl glucosamine containing carbohydrates in a Ca²⁺ dependent manner.^{26,28} These are followed by a fibronectin type-II domain and a cysteine-rich domain on the N-terminus (see Figure 1). The cysteine-rich domain can bind sulfated carbohydrates in a Ca²⁺ independent manner, ^{29,30} and the fibronectin domain can bind and endocytose collagen.³¹ Human MR has eight CRDs with only a small amount of homology between them and varying affinities towards mannose structures.³² CRD-8 is the closest to the C-terminus and the transmembrane domain. Of all eight CRDs, only isolated CRD-4 is able to bind mannosides with a significant affinity, and it binds monosaccharides with similar specificity as the MBL.³³ However, CRDs 4-8 are required to achieve the binding affinities of the natural MR, indicating that these also have a role to play in the binding of mannosides.^{25,28} Targeting antigens towards the MR can serve two functions: enhancing cell maturation and antigen presentation. Although the MR lacks an intracellular signaling motive, engagement of the receptor can induce cytokine production, although the pathway through which this occurs remains unknown^{29,34} and it has been speculated that other mannose-binding receptors are responsible for these signals.³⁵ Colocalization of the MR and antigen suggest that they can be transported together toward early endosomes, which enables the cross-presentation of the antigen.36,37 Together, these findings make the MR an attractive target for cell-specific vaccine development, as described in previous reviews.^{38,39} However, it has proven to be challenging to study the binding affinity of this receptor in vivo because of the low expression levels of the MR on the cell surface. In addition, the poor stability of the receptor, when overexpressed, complicates the determination of ligand affinity in vitro. The stability of the MR can be improved through small alterations in the receptor's amino acid sequence, but this often modifies the properties of the receptor.40

DC-SIGN

Dendritic cell-specific intercellular adhesion molecule-3-grabbing non-integrin (DC-SIGN or CD209) is a C-type lectin present on dendritic cells and specific macrophage subsets. 41 DC-SIGN is a type II CLR and bears multiple internalization motives and a signaling motive on its intracellular domain. The extracellular part of DC-SIGN contains a flexible neck region and a CRD that can both bind mannose, fucose, and GlcNAc-like structures. DC-SIGN multimerizes into tetrameric structures on the cell surface, improving the binding avidity to pathogens (see Figure 1).⁴² In these tetrameric structures, the minimal distance between CRDs is 40 Å.⁴³ Upon binding of these CRDs, the receptor can induce signaling and it has been shown that mannosylated antigens can activate Ras-1 signaling resulting in an inflammatory response.⁴⁴ Binding the same CRD with fucosylated antigen, however, induces a different inflammatory response resulting in different T cell subsets. Thus, DC-SIGN can effectively skew the T cell response to stimulate T_H1 or T_H17 cell (through mannoside activation) or induce a T_H2 response (by binding of fucoses).⁴⁴ ⁴⁶ DC-SIGN is also a scavenging receptor that can rapidly internalize antigens upon binding. ^{47–49} These combined functions make DC-SIGN an attractive target for vaccine development. 50,51 DC-SIGN mediated endocytosis can traffic antigens towards different types of endosomes.⁵² For example, large structures such as HIV-1 are trafficked towards late endosomes/lysosomes resulting in MHC-II presentation,⁵³ while smaller fragments can be trafficked towards early endosomes, thereby improving cross-presentation.⁵⁴

Langerin

The skin is an attractive site for vaccinations since it contains large quantities of Langerhans cells (LCs), professional APCs which are a subset of DCs. ⁵⁵ LCs express the CLR Langerin (CD207), ⁵⁶ which is a type II transmembrane protein with a CRD that has a preference for mannose, fucose, and GlcNAc, similar to DC-SIGN. Affinity studies with an array of carbohydrates suggest that langerin can also bind sulfated oligosaccharides. ^{57,58} The receptor is expressed as a trimeric complex on the cell surface, binding multivalent carbohydrates (see Figure 1). Unlike DC-SIGN, scavenging by Langerin traffics antigens to Birbeck granules instead of endosomes. These Birbeck granules can degrade particles such as viruses, which allows LCs to act as a natural barrier against viral infections, for example, by HIV-1. ^{59,60} These findings have sparked a large interest in the development of ligands that are either specific for Langerin or DC-SIGN. ^{58,61} More information on vaccine strategies via Langerin is reviewed by Dam et al. ⁵¹ and Stoitzner et al. ⁶²

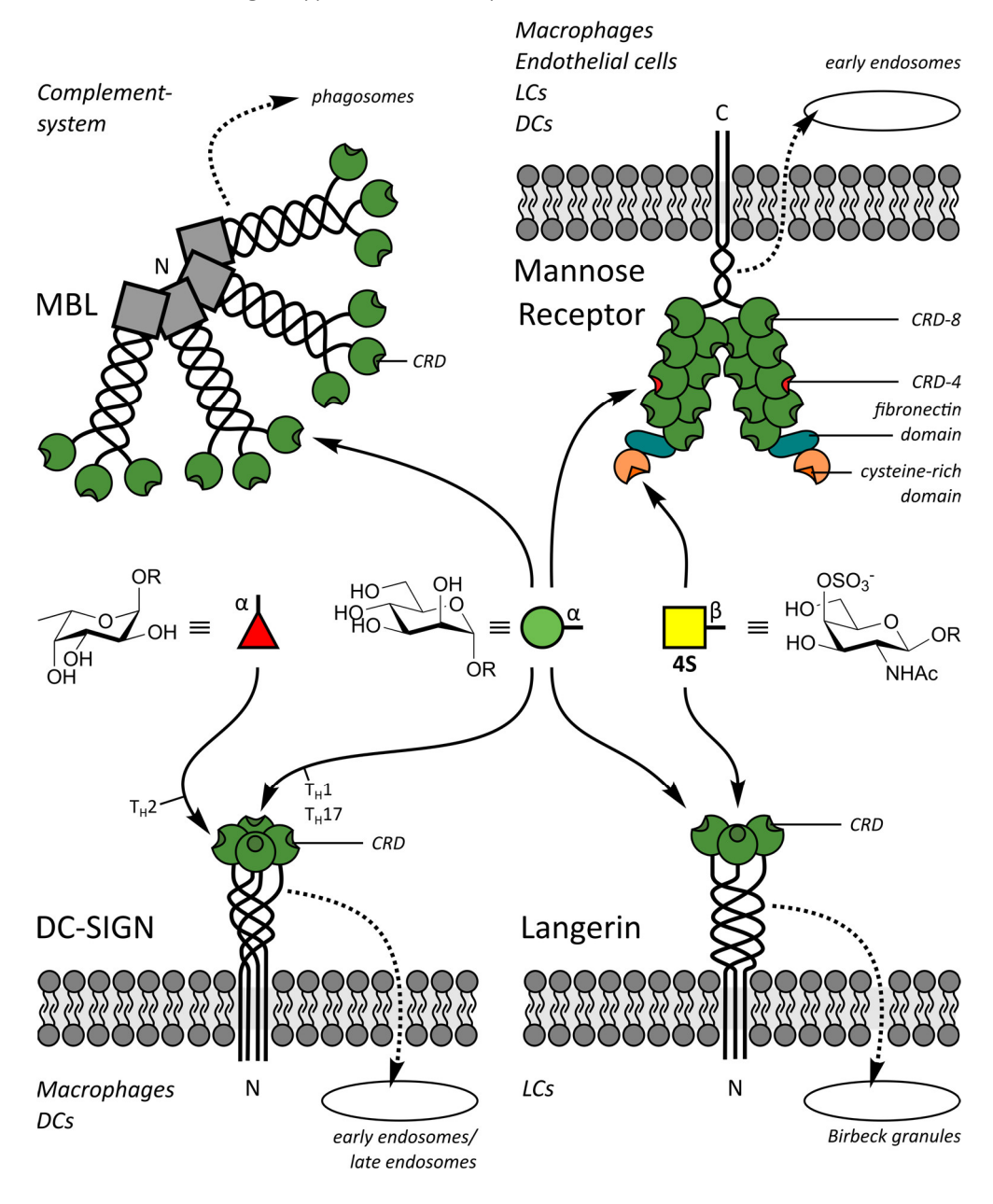


Figure 1: Mannose-binding C-type Lectin Receptors.

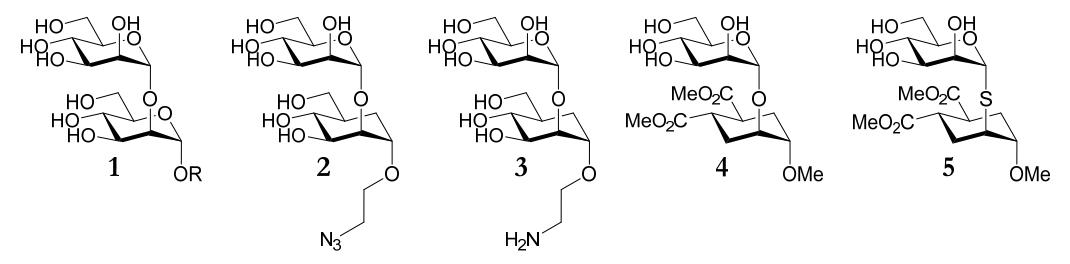
Schematic representation of mannose-binding C-type lectin receptors and the ligands that bind the different binding domains of the receptors.

Targeting of mannose-binding CLRs

Endocytosis by APCs via CLRs has gained much attention in the last decades, focusing on two distinct approaches. Ligands have been developed to block CLR-mediated endocytosis to prevent pathogens from hijacking the CLR internalization pathway for transfection. Alternatively, CLR-binders have been developed to target specific cargo into APCs *via* the CLRs. Although both strategies serve opposite functions, the design principles underlying the development of ligands

designed for either purpose is of relevance for the other application as well. The design of endocytosis blocking ligands has resulted in a large number of glycomimics that can bind with high affinity and selectivity for one CLR over another.^{63–69} Besides improved affinity and selectivity, replacing native ligands with glycomimics can improve their stability against enzymatic degradation.⁷⁰ For example, Bordoni et al.⁷¹ synthesized **2** and **3**, carba-analogues of the α1,2-dimannoside **1**, which lack the endocyclic oxygen, as enzymatic stable ligands for DC-SIGN (Figure 2). Tamburrini et al.⁷² improved the stability of the α1,2-glycosidic bond in carba pseudo mannoside **4** by the introduction of a thioglycosidic bond, forming pseudo disaccharide **5** (Figure 2). The affinity for CLRs can be further enhanced by the multivalent presentation of mannoside(-mimic)s by clustering the ligands on different types of carriers. Viral infection can be stopped effectively using ligands with nM affinities based on carriers systems such as dendrimers, ^{73,74} molecular rods, ⁷⁵ gold nanoparticles (AuNPs), ^{76,77} and polymers.⁴³

Figure 2: Stabilized pseudo mannosides.



Exploiting CLRs to target antigens towards antigen-presenting cells

The second approach to utilize CLR mediated endocytosis aims at the delivery of cargo towards APCs. One potential method to achieve this comprises the use of antibodies. Sehgal et al.⁷⁸ have recently reviewed different strategies for DC vaccination, including anti-CLR antibody conjugates. Cruz et al.⁷⁹ combined antigen-coated nanoparticles with anti-DC-SIGN antibodies and Breman et al.⁸⁰ combined anti-MR antibodies with a peptide antigen to deliver the antigens to APCs. Although both approaches improved the uptake efficacy, the level of T cell reactivity was similar to unconjugated antigens, suggesting that antigen presentation was not improved.

Carriers to deliver antigens.

Targeting CLRs with mannosylated constructs is a popular method to deliver cargo to APCs. This targeting is often achieved with multivalent carriers that contain mannosides and a cargo of interest, such as an antigen, and this approach has been reviewed extensively.^{78,81,82} Carriers exploited for selective targeting are often similar to those used for blocking of viral entry. For example, Zhu et al.⁸³ reported a mannosylated cationic lipid-hybrid polymersome, that combined

an ovalbumin antigen with two TLR agonists (Imiquimod and monophosphoryl lipid A) and induced strong activation and a synergistic antitumor immune response. Schulze and Wamhoff et al.61,84 selectively targeted antigens to LCs, using liposomes coated with Langerin specific glycomimic 6 or mannoses 7 (Figure 3). Liposomes with 6 could selectively deliver their content (e.g., fluorophore⁸⁴ or Doxorubicin⁶¹) to Langerin⁺ cells when compared with the mannosylated liposomes which were also endocytosed by other CLRs. As a proof of concept, Frison et al.⁸⁵ used an oligopeptide carrier with lysine repeats that were functionalized with carbohydrates to provide constructs such as **8** (See Figure 3). Incorporation of a fluorescein label allowed to track the uptake and routing of the conjugates via either the MR or DC-SIGN. Their results have shown that binding avidity increased with a higher number of mannosides (n=2 < n=3) and also that fucosylated constructs (Lewis A, Lewis B, or Lewis X) could be internalized by DC-SIGN, but not by the MR, demonstrating that these receptors can be discriminated using the appropriate glycans. Dong et al. 86 grafted mannosides on carbon nanotubes (9) which could adsorb a model OVA antigen. These nanotubes were efficiently engulfed by DCs indicating that such nanotubes could be potent nanovectors for antigen delivery, which could lead to selective drug delivery applications. Shinchi et al.⁸⁷ conjugated both mannosides and a TLR7 agonist to gold nanoparticles (10, Figure 3), which improved the activity of the TLR7 ligand. Co-administration of these nanoparticles with OVA as a model epitope resulted in a more efficient presentation due to improved activation of the APC. Wilson et al. 88 developed methacrylic acid co-polymers equipped with mannosides and a resiquimod analog as side groups, that were reversibly conjugated to an antigen (11, Figure 3). When both the mannoside and resiquimod were combined in a single polymer, the humoral response and the cellular immunity were improved. These results demonstrate that the introduction of ligands for both TLR7 and mannose-binding CLRs in one construct can improve the effectiveness of the immune response. Another mannosylated polymer carrier was synthesized by Jarvis et al.,⁵⁴ who utilized a ring-opening polymerization approach to generate multiple functionalized polymers (12, Figure 3). Both soluble polymers and polymer aggregates were obtained, and the fate of antigen routing proved to be dependent on the physical properties of the carrier. 89 These results showed that soluble antigen is routed toward early endosomes, ideal for antigen cross-presentation,⁵² while aggregates are directed to compartments that are more suitable for CD4⁺ presentation. ⁹⁰ This size-dependent routing is not only affected by the size of the carrier, but also by the type of CLR targeted. When Fehres et al.⁹¹ compared Lewis Y functionalized synthetic long peptides (SLPs) with liposomes, the routing fate and antigen presentation capacity proved to depend on the CLR responsible for the trafficking. The best antigen presentation via langerin was achieved with SLPs, and presentation via DC-SIGN using antigen-loaded liposomes.

Figure 3: Multivalent CLR targeting carriers.

Although multivalent systems, such as those described above, have been successfully applied for improvement of antigen (cross-)presentation, the heterogeneous character of the carriers can result in incoherent effects. Therefore, much effort has been directed at the development of well-defined

single molecules such as synthetic long peptides and defined dendrimers. For example, based on the results obtained with 8, Srinivas et al. 92 synthesized constructs such as 13 (Figure 4) in which four repeating lysines were functionalized with glycosyl residues and conjugated to a Melan-A/Mart-1 melanoma epitope (Melan-A₁₆₋₄₀). The antigen cross-presentation was enhanced by binding to MR or DC-SIGN. Similar immunological results were obtained by Rauen et al. 93 who generated mannosylated SLPs (14, Figure 4) comprising a lysine residue with two α -mannosides connected to either the MHC-I restricted OVA₂₅₇₋₂₆₄, the MHC-II restricted OVA₃₂₃₋₃₃₉, or the MHC-I restricted HPV E7₄₃₋₆₃ epitope. It was demonstrated that mannosylation^{94,95} of the synthetic long peptide enhanced cross-presentation but not MHC-II antigen presentation, indicating that the mannosides in this construct routes the antigen towards the early endosomes. Grandjeun et al.96 developed a synthetic approach to generate mannosylated dendrimers (15, Figure 4) to specifically target mannose-binding CLRs on DCs. Their dendrimers are based on branching lysines that were conjugated to an epitope via an N-terminal hydrazino-ligation. In an alternative approach, McIntosh et al. 97 conjugated one or two complex Man₉ structures to a synthetic peptide using an enzymatic glycosylation strategy to form native N glycan 16. The mannosylation improved binding to APCs, and the antigen was effectively presented as long as the epitope was not glycosylated. Glaffig et al. 98 combined a MUC-1 epitope with both a mannose targeting moiety and a tetanus toxoid (TTox) as an helper T cell epitope via squarate conjugation (17, Figure 4). Mouse immunized with this construct exhibited stronger IgG antibody titers in comparison with a control construct that lacked the mannosides.

The incorporation of additional adjuvants can further improve the effectiveness of mannosylated antigens.⁹⁹ For example, Moyle et al.¹⁰⁰ synthesized mannosylated conjugates **18** bearing an HPV E7₄₄₋₆₂ epitope and a lipid-core-peptide (LCP) adjuvant.¹⁰¹ The trifunctional conjugates were able to protect against TC-1 tumor cells. Sedaghat et al.¹⁰² synthesized similar constructs in which an OVA₃₂₃₋₃₃₉ MHC-II epitope was combined with self-adjuvating lipids, a reporter group, and targeting mannosides (**19**, Figure 5). Both the lipids and mannosides in the constructs played a significant role in the receptor-mediated uptake.

Figure 4: Mannosylated antigen.

Figure 5: Mannosylated trifunctional conjugates.

Outline of this Thesis

This Thesis presents studies on the targeting of mannosylated conjugates to C-type lectin receptors (CLRs) present on antigen presenting cells. Chapter 2 describes a systematic approach to determine the effect of both the number and type of mannosides on the affinity for the three mannoside binding transmembrane CLRs: the MR, DC-SIGN, and Langerin. The affinities of the clusters was determined using different in vitro techniques, including a new method that utilizes super-resolution microscopy. The established affinities directed the selection of the mannoside clusters to be used in follow-up studies in this Thesis. Chapter 3 describes improvements in the synthesis of a known Toll-like receptor (TLR) agonist which allows the use in solid-phase peptide synthesis. This agonist is combined with clusters selected from Chapter 2 to more effectively target the ligand to APCs. Combining the results of Chapters 2 and 3, Chapter 4 describes the synthesis of peptide conjugates in which the TLR agonist, the CLR targeting mannoside clusters, and a peptide antigen are incorporated. These peptides are evaluated for their ability to mature APCs and cross-present the antigen. Analogs of these conjugates in which amino acids, functionalized with an acid-stable C-mannoside is incorporated are the subject of **Chapter 5**. Both the synthesis of a C-mannosyl lysine building block and its use in the inline SPPS synthesis of peptides are described. The antigen-presenting capacities of these conjugates are assessed and compared to the O-mannose analogs. As an alternative to peptidic mannoside carriers, Chapter 6 describes the synthesis of glycosylated benzene tri-amides (BTAs) that can self-assemble into supramolecular fibers. Such systems could be considered in future work for a dynamic carrier for antigen and adjuvants. Finally, Chapter 7 summarizes all the findings in this Thesis and discusses future directions that could be taken to follow up on data generated in this Thesis.

References

- (1) Lakhani, S. Early Clinical Pathologists: Edward Jenner (1749-1823). *J. Clin. Pathol.* **1992**, *45*, 756–758. https://doi.org/10.1136/jcp.45.9.756.
- (2) Okazaki, T.; Honjo, T. PD-1 and PD-1 Ligands: From Discovery to Clinical Application. *Int. Immunol.* **2007**, 19, 813–824. https://doi.org/10.1093/intimm/dxm057.
- (3) June, C. H.; O'Connor, R. S.; Kawalekar, O. U.; Ghassemi, S.; Milone, M. C. CAR T Cell Immunotherapy for Human Cancer. *Science* (80-.). 2018, 359, 1361–1365. https://doi.org/10.1126/science.aar6711.
- (4) Ribas, A.; Wolchok, J. D. Cancer Immunotherapy Using Checkpoint Blockade. *Science (80-.).* **2018**, *359*, 1350–1355. https://doi.org/10.1126/science.aar4060.
- (5) Sharma, P.; Wagner, K.; Wolchok, J. D.; Allison, J. P. Novel Cancer Immunotherapy Agents with Survival Benefit: Recent Successes and next Steps. *Nat. Rev. Cancer* **2011**, *11*, 805–812. https://doi.org/10.1038/nrc3153.
- (6) Pagès, F.; Mlecnik, B.; Marliot, F.; Bindea, G.; Ou, F.-S.; Bifulco, C.; Lugli, A.; Zlobec, I.; Rau, T. T.; Berger, M. D.; Nagtegaal, I. D.; Vink-Börger, E.; Galon, J.; et al. International Validation of the Consensus Immunoscore for the Classification of Colon Cancer: A Prognostic and Accuracy Study. *Lancet (London, England)* 2018, 391, 2128–2139. https://doi.org/10.1016/S0140-6736(18)30789-X.
- (7) Denkert, C.; von Minckwitz, G.; Darb-Esfahani, S.; Lederer, B.; Heppner, B. I.; Weber, K. E.; Budczies, J.; Huober, J.; Klauschen, F.; Furlanetto, J.; Schmitt, W. D.; Blohmer, J.-U.; Karn, T.; Pfitzner, B. M.; Kümmel, S.; Engels, K.; Schneeweiss, A.; Hartmann, A.; Noske, A.; Fasching, P. A.; Jackisch, C.; van Mackelenbergh, M.; Sinn, P.; Schem, C.; Hanusch, C.; Untch, M.; Loibl, S. Tumour-Infiltrating Lymphocytes and Prognosis in Different Subtypes of Breast Cancer: A Pooled Analysis of 3771 Patients Treated with Neoadjuvant Therapy. *Lancet Oncol.* 2018, *19*, 40–50. https://doi.org/10.1016/S1470-2045(17)30904-X.
- (8) Scheper, W.; Kelderman, S.; Fanchi, L. F.; Linnemann, C.; Bendle, G.; de Rooij, M. A. J.; Hirt, C.; Mezzadra, R.; Slagter, M.; Dijkstra, K.; Kluin, R. J. C.; Snaebjornsson, P.; Milne, K.; Nelson, B. H.; Zijlmans, H.; Kenter, G.; Voest, E. E.; Haanen, J. B. A. G.; Schumacher, T. N.; Mezzadra, R.; Slagter, M.; Voest, E. E.; Zijlmans, H.; de Rooij, M. A. J.; Haanen, J. B. A. G.; Milne, K.; Kluin, R. J. C.; Nelson, B. H.; Snaebjornsson, P.; Hirt, C.; Bendle, G.; Kelderman, S.; Dijkstra, K.; Linnemann, C.; Schumacher, T. N.; Scheper, W.; Fanchi, L. F. Low and Variable Tumor Reactivity of the Intratumoral TCR Repertoire in Human Cancers. *Nat. Med.* 2019, 25, 89–94. https://doi.org/10.1038/s41591-018-0266-5.
- (9) Demaria, O.; Cornen, S.; Daëron, M.; Morel, Y.; Medzhitov, R.; Vivier, E. Harnessing Innate Immunity in Cancer Therapy. *Nature* **2019**, *574*, 45–56. https://doi.org/10.1038/s41586-019-1593-5.
- (10) Chandran, S. S.; Klebanoff, C. A. T Cell Receptor-based Cancer Immunotherapy: Emerging Efficacy and Pathways of Resistance. *Immunol. Rev.* **2019**, *290*, 127–147. https://doi.org/10.1111/imr.12772.
- (11) Disis, M. L.; Watt, W. C.; Cecil, D. L. Th1 Epitope Selection for Clinically Effective Cancer Vaccines. Oncoimmunology 2014, 3, e954971. https://doi.org/10.4161/21624011.2014.954971.
- (12) Neefjes, J.; Jongsma, M. L. M.; Paul, P.; Bakke, O. Towards a Systems Understanding of MHC Class I and MHC Class II Antigen Presentation. *Nat. Rev. Immunol.* **2011**, *11*, 823–836. https://doi.org/10.1038/nri3084.
- (13) Bevan, M. J. Cross-Priming. Nat. Immunol. 2006, 7, 363–365. https://doi.org/10.1038/ni0406-363.
- (14) Takeuchi, O.; Akira, S. Pattern Recognition Receptors and Inflammation. *Cell* **2010**, *140*, 805–820. https://doi.org/10.1016/j.cell.2010.01.022.
- (15) Broz, P.; Monack, D. M. Newly Described Pattern Recognition Receptors Team up against Intracellular Pathogens. *Nat. Rev. Immunol.* **2013**, *13*, 551–565. https://doi.org/10.1038/nri3479.
- (16) Coffman, R. L.; Sher, A.; Seder, R. A. Vaccine Adjuvants: Putting Innate Immunity to Work. *Immunity* **2010**, *33*, 492–503. https://doi.org/10.1016/j.immuni.2010.10.002.
- (17) Duthie, M. S.; Windish, H. P.; Fox, C. B.; Reed, S. G. Use of Defined TLR Ligands as Adjuvants within Human Vaccines. *Immunol. Rev.* **2011**, *239*, 178–196. https://doi.org/10.1111/j.1600-065X.2010.00978.x.
- (18) Sheriff, S.; Chang, C. Y.; Ezekowitz, R. A. Human Mannose-Binding Protein Carbohydrate Recognition Domain Trimerizes through a Triple Alpha-Helical Coiled-Coil. *Nat. Struct. Biol.* **1994**, *1*, 789–794.

- https://doi.org/10.1038/nsb1194-789.
- (19) Turner, M. W. Mannose-Binding Lectin: The Pluripotent Molecule of the Innate Immune System. *Immunol. Today* **1996**, *17*, 532–540. https://doi.org/10.1016/0167-5699(96)10062-1.
- (20) Teillet, F.; Dublet, B.; Andrieu, J.-P.; Gaboriaud, C.; Arlaud, G. J.; Thielens, N. M. The Two Major Oligomeric Forms of Human Mannan-Binding Lectin: Chemical Characterization, Carbohydrate-Binding Properties, and Interaction with MBL-Associated Serine Proteases. *J. Immunol.* **2005**, *174*, 2870–2877. https://doi.org/10.4049/jimmunol.174.5.2870.
- (21) Dahl, M. R.; Thiel, S.; Matsushita, M.; Fujita, T.; Willis, A. C.; Christensen, T.; Vorup-Jensen, T.; Jensenius, J. C. MASP-3 and Its Association with Distinct Complexes of the Mannan-Binding Lectin Complement Activation Pathway. *Immunity* **2001**, *15*, 127–135. https://doi.org/10.1016/S1074-7613(01)00161-3.
- (22) Jack, D. L.; Lee, M. E.; Turner, M. W.; Klein, N. J.; Read, R. C. Mannose-Binding Lectin Enhances Phagocytosis and Killing of Neisseria Meningitidis by Human Macrophages. *J. Leukoc. Biol.* **2005**, *77*, 328–336. https://doi.org/10.1189/jlb.0604342.
- (23) Eddie Ip, W. K.; Takahashi, K.; Alan Ezekowitz, R.; Stuart, L. M. Mannose-Binding Lectin and Innate Immunity. *Immunol. Rev.* **2009**, *230*, 9–21. https://doi.org/10.1111/j.1600-065X.2009.00789.x.
- (24) Tokatlian, T.; Read, B. J.; Jones, C. A.; Kulp, D. W.; Menis, S.; Chang, J. Y. H.; Steichen, J. M.; Kumari, S.; Allen, J. D.; Dane, E. L.; Liguori, A.; Sangesland, M.; Lingwood, D.; Crispin, M.; Schief, W. R.; Irvine, D. J. Innate Immune Recognition of Glycans Targets HIV Nanoparticle Immunogens to Germinal Centers. *Science* (80-.). 2019, 363, 649–654. https://doi.org/10.1126/science.aat9120.
- (25) Taylor, M. E.; Drickamer, K. Structural Requirements for High Affinity Binding of Complex Ligands by the Macrophage Mannose Receptor. *J. Biol. Chem.* **1993**, *268*, 399–404.
- (26) Napper, C. E.; Dyson, M. H.; Taylor, M. E. An Extended Conformation of the Macrophage Mannose Receptor. *J. Biol. Chem.* **2001**, *276*, 14759–14766. https://doi.org/10.1074/jbc.M100425200.
- (27) Lai, J.; Bernhard, O. K.; Turville, S. G.; Harman, A. N.; Wilkinson, J.; Cunningham, A. L. Oligomerization of the Macrophage Mannose Receptor Enhances Gp120-Mediated Binding of HIV-1. *J. Biol. Chem.* **2009**, *284*, 11027–11038. https://doi.org/10.1074/jbc.M809698200.
- (28) Mullin, N. P.; Hitchen, P. G.; Taylor, M. E. Mechanism of Ca 2+ and Monosaccharide Binding to a C-Type Carbohydrate-Recognition Domain of the Macrophage Mannose Receptor. *J. Biol. Chem.* **1997**, *272*, 5668–5681. https://doi.org/10.1074/jbc.272.9.5668.
- (29) Leteux, C.; Chai, W.; Loveless, R. W.; Yuen, C.-T.; Uhlin-Hansen, L.; Combarnous, Y.; Jankovic, M.; Maric, S. C.; Misulovin, Z.; Nussenzweig, M. C.; Ten Feizi. The Cysteine-Rich Domain of the Macrophage Mannose Receptor Is a Multispecific Lectin That Recognizes Chondroitin Sulfates a and B and Sulfated Oligosaccharides of Blood Group Lewis a and Lewis x Types in Addition to the Sulfated N -Glycans of Lutropin. *J. Exp. Med.* **2000**, *191*, 1117–1126. https://doi.org/10.1084/jem.191.7.1117.
- (30) Fiete, D. J.; Beranek, M. C.; Baenziger, J. U. A Cysteine-Rich Domain of the "Mannose" Receptor Mediates GalNAc-4-SO4 Binding. *Proc. Natl. Acad. Sci.* **1998**, *95*, 2089–2093. https://doi.org/10.1073/pnas.95.5.2089.
- (31) Paracuellos, P.; Briggs, D. C.; Carafoli, F.; Lončar, T.; Hohenester, E. Insights into Collagen Uptake by C-Type Mannose Receptors from the Crystal Structure of Endo180 Domains 1–4. *Structure* **2015**, *23*, 2133–2142. https://doi.org/10.1016/j.str.2015.09.004.
- (32) Taylor, M. E.; Bezouska, K.; Drickamer, K. Contribution to Ligand Binding by Multiple Carbohydrate-Recognition Domains in the Macrophage Mannose Receptor. *J. Biol. Chem.* **1992**, *267*, 1719–1726.
- (33) Mullin, N. P.; Hall, K. T.; Taylor, M. E. Characterization of Ligand Binding to a Carbohydrate-Recognition Domain of the Macrophage Mannose Receptor. *J. Biol. Chem.* **1994**, *269*, 28405–28413.
- (34) East, L.; Isacke, C. M. The Mannose Receptor Family. *Biochim. Biophys. Acta Gen. Subj.* **2002**, *1572*, 364–386. https://doi.org/10.1016/S0304-4165(02)00319-7.
- (35) Gazi, U.; Martinez-Pomares, L. Influence of the Mannose Receptor in Host Immune Responses. *Immunobiology* **2009**, *214*, 554–561. https://doi.org/10.1016/j.imbio.2008.11.004.
- (36) Burgdorf, S.; Kautz, A.; Bohnert, V.; Knolle, P. a; Kurts, C. Distinct Pathways of Antigen Uptake and Intracellular Routing in CD4 and CD8 T Cell Activation. *Science* (80-.). 2007, 316, 612–616.

- https://doi.org/10.1126/science.1137971.
- Burgdorf, S.; Schölz, C.; Kautz, A.; Tampé, R.; Kurts, C. Spatial and Mechanistic Separation of Cross-Presentation and Endogenous Antigen Presentation. *Nat. Immunol.* **2008**, *9*, 558–566. https://doi.org/10.1038/ni.1601.
- (38) Sedaghat, B.; Stephenson, R.; Toth, I. Targeting the Mannose Receptor with Mannosylated Subunit Vaccines. *Curr. Med. Chem.* **2014**, *21*, 3405–3418. https://doi.org/10.2174/0929867321666140826115552.
- (39) Tiwari, S. Mannosylated Constructs as a Platform for Cell-Specific Delivery of Bioactive Agents. *Crit. Rev. Ther. Drug Carrier Syst.* **2018**, *35*, 157–194. https://doi.org/10.1615/CritRevTherDrugCarrierSyst.2018020313.
- (40) Vigerust, D. J.; Vick, S. Stable Expression and Characterization of an Optimized Mannose Receptor. *J. Clin. Cell. Immunol.* **2015**, *06*. https://doi.org/10.4172/2155-9899.1000330.
- (41) Geijtenbeek, T. B.; Torensma, R.; van Vliet, S. J.; van Duijnhoven, G. C.; Adema, G. J.; van Kooyk, Y.; Figdor, C. G. Identification of DC-SIGN, a Novel Dendritic Cell-Specific ICAM-3 Receptor That Supports Primary Immune Responses. *Cell* **2000**, *100*, 575–585. https://doi.org/10.1016/s0092-8674(00)80693-5.
- (42) Feinberg, H.; Guo, Y.; Mitchell, D. A.; Drickamer, K.; Weis, W. I. Extended Neck Regions Stabilize Tetramers of the Receptors DC-SIGN and DC-SIGNR. *J. Biol. Chem.* **2005**, 280, 1327–1335. https://doi.org/10.1074/jbc.M409925200.
- (43) Garber, K. C. A.; Wangkanont, K.; Carlson, E. E.; Kiessling, L. L. A General Glycomimetic Strategy Yields Non-Carbohydrate Inhibitors of DC-SIGN. *Chem. Commun.* **2010**, *46*, 6747. https://doi.org/10.1039/c0cc00830c.
- (44) Gringhuis, S. I.; den Dunnen, J.; Litjens, M.; van der Vlist, M.; Geijtenbeek, T. B. H. Carbohydrate-Specific Signaling through the DC-SIGN Signalosome Tailors Immunity to Mycobacterium Tuberculosis, HIV-1 and Helicobacter Pylori. *Nat. Immunol.* **2009**, *10*, 1081–1088. https://doi.org/10.1038/ni.1778.
- Osorio, F.; Reis e Sousa, C. Myeloid C-Type Lectin Receptors in Pathogen Recognition and Host Defense. *Immunity* **2011**, *34*, 651–664. https://doi.org/10.1016/j.immuni.2011.05.001.
- (46) Geijtenbeek, T. B. H.; Gringhuis, S. I. C-Type Lectin Receptors in the Control of T Helper Cell Differentiation. *Nat. Rev. Immunol.* **2016**, *16*, 433–448. https://doi.org/10.1038/nri.2016.55.
- (47) Moris, A.; Pajot, A.; Blanchet, F.; Guivel-Benhassine, F.; Salcedo, M.; Schwartz, O. Dendritic Cells and HIV-Specific CD4+ T Cells: HIV Antigen Presentation, T-Cell Activation, and Viral Transfer. *Blood* **2006**, *108*, 1643–1651. https://doi.org/10.1182/blood-2006-02-006361.
- (48) Moris, A.; Nobile, C.; Buseyne, F.; Porrot, F.; Abastado, J. P.; Schwartz, O. DC-SIGN Promotes Exogenous MHC-I-Restricted HIV-1 Antigen Presentation. *Blood* **2004**, *103*, 2648–2654. https://doi.org/10.1182/blood-2003-07-2532.
- (49) GEIJTENBEEK, T. B. H. H.; Van Kooyk, Y. Pathogens Target DC-SIGN to Influence Their Fate DC-SIGN Functions as a Pathogen Receptor with Broad Specificity. *APMIS* **2003**, *111*, 698–714. https://doi.org/10.1034/j.1600-0463.2003.11107803.x.
- (50) Wolfert, M. A.; Boons, G. J. Adaptive Immune Activation: Glycosylation Does Matter. *Nat. Chem. Biol.* **2013**, 9, 776–784. https://doi.org/10.1038/nchembio.1403.
- (51) Dam, T. K.; Fred Brewer, C. Lectins as Pattern Recognition Molecules: The Effects of Epitope Density in Innate Immunity. *Glycobiology* **2009**, *20*, 270–279. https://doi.org/10.1093/glycob/cwp186.
- (52) Chatterjee, B.; Smed-Sörensen, A.; Cohn, L.; Chalouni, C.; Vandlen, R.; Lee, B.-C.; Widger, J.; Keler, T.; Delamarre, L.; Mellman, I. Internalization and Endosomal Degradation of Receptor-Bound Antigens Regulate the Efficiency of Cross Presentation by Human Dendritic Cells. *Blood* **2012**, *120*, 2011–2020. https://doi.org/10.1182/blood-2012-01-402370.
- (53) Engering, A.; Geijtenbeek, T. B. H.; van Vliet, S. J.; Wijers, M.; Liempt, E. van; Demaurex, N.; Lanzavecchia, A.; Fransen, J.; Figdor, C. G.; Piguet, V.; van Kooyk, Y. The Dendritic Cell-Specific Adhesion Receptor DC-SIGN Internalizes Antigen for Presentation to T Cells. *J. Immunol.* **2002**, *168*, 2118–2126. https://doi.org/10.4049/jimmunol.168.5.2118.
- (54) Jarvis, C. M.; Zwick, D. B.; Grim, J. C.; Alam, M. M.; Prost, L. R.; Gardiner, J. C.; Park, S.; Zimdars, L. L.; Sherer, N. M.; Kiessling, L. L. Antigen Structure Affects Cellular Routing through DC-SIGN. *Proc. Natl. Acad.*

- Sci. 2019, 116, 14862–14867. https://doi.org/10.1073/pnas.1820165116.
- (55) Prausnitz, M. R.; Langer, R. Transdermal Drug Delivery. Nat. Biotechnol. 2008, 26, 1261–1268. https://doi.org/10.1038/nbt.1504.
- Valladeau, J.; Ravel, O.; Dezutter-Dambuyant, C.; Moore, K.; Kleijmeer, M.; Liu, Y.; Duvert-Frances, V.; Vincent, C.; Schmitt, D.; Davoust, J.; Caux, C.; Lebecque, S.; Saeland, S. Langerin, a Novel C-Type Lectin Specific to Langerhans Cells, Is an Endocytic Receptor That Induces the Formation of Birbeck Granules. *Immunity* **2000**, *12*, 71–81. https://doi.org/10.1016/S1074-7613(00)80160-0.
- (57) Galustian, C.; Park, C. G.; Chai, W.; Kiso, M.; Bruening, S. A.; Kang, Y. S.; Steinman, R. M.; Feizi, T. High and Low Affinity Carbohydrate Ligands Revealed for Murine SIGN-R1 by Carbohydrate Array and Cell Binding Approaches, and Differing Specificities for SIGN-R3 and Langerin. *Int. Immunol.* 2004, *16*, 853–866. https://doi.org/10.1093/intimm/dxh089.
- (58) Ota, F.; Hirayama, T.; Kizuka, Y.; Yamaguchi, Y.; Fujinawa, R.; Nagata, M.; Ismanto, H. S.; Lepenies, B.; Aretz, J.; Rademacher, C.; Seeberger, P. H.; Angata, T.; Kitazume, S.; Yoshida, K.; Betsuyaku, T.; Kida, K.; Yamasaki, S.; Taniguchi, N. High Affinity Sugar Ligands of C-Type Lectin Receptor Langerin. *Biochim. Biophys. Acta Gen. Subj.* 2018, 1862, 1592–1601. https://doi.org/10.1016/j.bbagen.2018.04.004.
- (59) De Witte, L.; Nabatov, A.; Pion, M.; Fluitsma, D.; De Jong, M. A. W. P.; De Gruijl, T.; Piguet, V.; Van Kooyk, Y.; Geijtenbeek, T. B. H. Langerin Is a Natural Barrier to HIV-1 Transmission by Langerhans Cells. *Nat. Med.* **2007**, *13*, 367–371. https://doi.org/10.1038/nm1541.
- (60) Turville, S.; Wilkinson, J.; Cameron, P.; Dable, J.; Cunningham, A. L. The Role of Dendritic Cell C-Type Lectin Receptors in HIV Pathogenesis. *J. Leukov. Biol.* **2003**, *74*, 710–718. https://doi.org/10.1189/jlb.0503208.
- Wamhoff, E.-C.; Schulze, J.; Bellmann, L.; Rentzsch, M.; Bachem, G.; Fuchsberger, F. F.; Rademacher, J.; Hermann, M.; Del Frari, B.; van Dalen, R.; Hartmann, D.; van Sorge, N. M.; Seitz, O.; Stoitzner, P.; Rademacher, C. A Specific, Glycomimetic Langerin Ligand for Human Langerhans Cell Targeting. *ACS Cent. Sci.* 2019, acscentsci.9b00093. https://doi.org/10.1021/acscentsci.9b00093.
- (62) Stoitzner, P.; Sparber, F.; Tripp, C. H. Langerhans Cells as Targets for Immunotherapy against Skin Cancer. *Immunol. Cell Biol.* **2010**, *88*, 431–437. https://doi.org/10.1038/icb.2010.31.
- (63) Schuster, M. C.; Mann, D. A.; Buchholz, T. J.; Johnson, K. M.; Thomas, W. D.; Kiessling, L. L. Parallel Synthesis of Glycomimetic Libraries: Targeting a C-Type Lectin. *Org. Lett.* **2003**, *5*, 1407–1410. https://doi.org/10.1021/ol0340383.
- (64) Borrok, M. J.; Kiessling, L. L. Non-Carbohydrate Inhibitors of the Lectin DC-SIGN. *J. Am. Chem. Soc.* **2007**, *129*, 12780–12785. https://doi.org/10.1021/ja072944v.
- (65) Aretz, J.; Wamhoff, E. C.; Hanske, J.; Heymann, D.; Rademacher, C. Computational and Experimental Prediction of Human C-Type Lectin Receptor Druggability. Front. Immunol. 2014, 5, 1–12. https://doi.org/10.3389/fimmu.2014.00323.
- (66) Dehuyser, L.; Schaeffer, E.; Chaloin, O.; Mueller, C. G.; Baati, R.; Wagner, A. Synthesis of Novel Mannoside Glycolipid Conjugates for Inhibition of HIV-1 Trans -Infection. *Bioconjug. Chem.* **2012**, *23*, 1731–1739. https://doi.org/10.1021/bc200644d.
- (67) Varga, N.; Sutkeviciute, I.; Guzzi, C.; McGeagh, J.; Petit-Haertlein, I.; Gugliotta, S.; Weiser, J.; Angulo, J.; Fieschi, F.; Bernardi, A. Selective Targeting of Dendritic Cell-Specific Intercellular Adhesion Molecule-3-Grabbing Nonintegrin (Dc-Sign) with Mannose-Based Glycomimetics: Synthesis and Interaction Studies of Bis(Benzylamide) Derivatives of a Pseudomannobioside. *Chem. A Eur. J.* 2013, 19, 4786–4797. https://doi.org/10.1002/chem.201202764.
- (68) Thépaut, M.; Guzzi, C.; Sutkeviciute, I.; Sattin, S.; Ribeiro-Viana, R.; Varga, N.; Chabrol, E.; Rojo, J.; Bernardi, A.; Angulo, J.; Nieto, P. M.; Fieschi, F. Structure of a Glycomimetic Ligand in the Carbohydrate Recognition Domain of C-Type Lectin DC-SIGN. Structural Requirements for Selectivity and Ligand Design. *J. Am. Chem. Soc.* 2013, 135, 2518–2529. https://doi.org/10.1021/ja3053305.
- (69) Timpano, G.; Tabarani, G.; Anderluh, M.; Invernizzi, D.; Vasile, F.; Potenza, D.; Nieto, P. M.; Rojo, J.; Fieschi, F.; Bernardi, A. Synthesis of Novel DC-SIGN Ligands with an α-Fucosylamide Anchor. *ChemBioChem* **2008**, *9*, 1921–1930. https://doi.org/10.1002/cbic.200800139.

- (70) Tamburrini, A.; Colombo, C.; Bernardi, A. Design and Synthesis of Glycomimetics: Recent Advances. *Med. Res. Rev.* **2019**, No. April, 1–37. https://doi.org/10.1002/med.21625.
- (71) Bordoni, V.; Porkolab, V.; Sattin, S.; Thépaut, M.; Frau, I.; Favero, L.; Crotti, P.; Bernardi, A.; Fieschi, F.; Di Bussolo, V. Stereoselective Innovative Synthesis and Biological Evaluation of New Real Carba Analogues of Minimal Epitope Manα(1,2)Man as DC-SIGN Inhibitors. RSC Adv. 2016, 6, 89578–89584. https://doi.org/10.1039/c6ra20401e.
- (72) Tamburrini, A.; Achilli, S.; Vasile, F.; Sattin, S.; Vivès, C.; Colombo, C.; Fieschi, F.; Bernardi, A. Facile Access to Pseudo-Thio-1,2-Dimannoside, a New Glycomimetic DC-SIGN Antagonist. *Bioorg. Med. Chem.* **2017**, *25*, 5142–5147. https://doi.org/10.1016/j.bmc.2017.03.046.
- (73) Reina, J. J.; Rojo, J. Glycodendritic Structures: Tools to Interact with DC-SIGN. *Brazilian J. Pharm. Sci.* **2013**, 49, 109–124. https://doi.org/10.1590/S1984-82502013000700009.
- (74) Kantchev, E. A. B.; Chang, C. C.; Cheng, S. F.; Roche, A. C.; Chang, D. K. Direct Solid-Phase Synthesis and Fluorescence Labeling of Large, Monodisperse Mannosylated Dendrons in a Peptide Synthesizer. *Org. Biomol. Chem.* **2008**, *6*, 1377–1385. https://doi.org/10.1039/b719737c.
- (75) Ordanini, S.; Varga, N.; Porkolab, V.; Thépaut, M.; Belvisi, L.; Bertaglia, A.; Palmioli, A.; Berzi, A.; Trabattoni, D.; Clerici, M.; Fieschi, F.; Bernardi, A. Designing Nanomolar Antagonists of DC-SIGN-Mediated HIV Infection: Ligand Presentation Using Molecular Rods. *Chem. Commun.* **2015**, *51*, 3816–3819. https://doi.org/10.1039/C4CC09709B.
- (76) Martínez-Ávila, O.; Bedoya, L. M.; Marradi, M.; Clavel, C.; Alcamí, J.; Penadés, S. Multivalent Manno-Glyconanoparticles Inhibit DC-SIGN-Mediated HIV-1 Trans-Infection of Human T Cells. *ChemBioChem* **2009**, *10*, 1806–1809. https://doi.org/10.1002/cbic.200900294.
- (77) Martínez-Ávila, O.; Hijazi, K.; Marradi, M.; Clavel, C.; Campion, C.; Kelly, C.; Penadés, S. Gold Manno Glyconanoparticles: Multivalent Systems to Block HIV-1 Gp120 Binding to the Lectin DC-SIGN. *Chem. A Eur. J.* 2009, *15*, 9874–9888. https://doi.org/10.1002/chem.200900923.
- (78) Sehgal, K.; Dhodapkar, K. M.; Dhodapkar, M. V. Targeting Human Dendritic Cells in Situ to Improve Vaccines. *Immunol. Lett.* **2014**, *162*, 59–67. https://doi.org/10.1016/j.imlet.2014.07.004.
- (79) Cruz, L. J.; Tacken, P. J.; van der Schoot, J. M. S.; Rueda, F.; Torensma, R.; Figdor, C. G. ICAM3-Fc Outperforms Receptor-Specific Antibodies Targeted Nanoparticles to Dendritic Cells for Cross-Presentation. *Molecules* **2019**, *24*, 1825. https://doi.org/10.3390/molecules24091825.
- (80) Breman, E.; Ruben, J. M.; Franken, K. L.; Heemskerk, M. H. M.; Roelen, D. L.; Claas, F. H.; Van Kooten, C. Uptake of HLA Alloantigens via CD89 and CD206 Does Not Enhance Antigen Presentation by Indirect Allorecognition. *J. Immunol. Res.* **2016**, *2016*. https://doi.org/10.1155/2016/4215684.
- (81) Narasimhan, B.; Goodman, J. T.; Vela Ramirez, J. E. Rational Design of Targeted Next-Generation Carriers for Drug and Vaccine Delivery. *Annu. Rev. Biomed. Eng.* 2016, 18, 25–49. https://doi.org/10.1146/annurev-bioeng-082615-030519.
- [82] Joshi, M. D.; Unger, W. J.; Storm, G.; Van Kooyk, Y.; Mastrobattista, E. Targeting Tumor Antigens to Dendritic Cells Using Particulate Carriers. J. Control. Release 2012, 161, 25–37. https://doi.org/10.1016/j.jconrel.2012.05.010.
- (83) Zhu, D.; Hu, C.; Fan, F.; Qin, Y.; Huang, C.; Zhang, Z.; Lu, L.; Wang, H.; Sun, H.; Leng, X.; Wang, C.; Kong, D.; Zhang, L. Co-Delivery of Antigen and Dual Agonists by Programmed Mannose-Targeted Cationic Lipid-Hybrid Polymersomes for Enhanced Vaccination. *Biomaterials* **2019**, *206*, 25–40. https://doi.org/10.1016/j.biomaterials.2019.03.012.
- (84) Schulze, J.; Rentzsch, M.; Kim, D.; Bellmann, L.; Stoitzner, P.; Rademacher, C. A Liposomal Platform for Delivery of a Protein Antigen to Langerin-Expressing Cells. *Biochemistry* **2019**, *58*, 2576–2580. https://doi.org/10.1021/acs.biochem.9b00402.
- (85) Frison, N.; Taylor, M. E.; Soilleux, E.; Bousser, M.-T.; Mayer, R.; Monsigny, M.; Drickamer, K.; Roche, A.-C. Oligolysine-Based Oligosaccharide Clusters. *J. Biol. Chem.* **2003**, *278*, 23922–23929. https://doi.org/10.1074/jbc.M302483200.
- (86) Dong, Z.; Wang, Q.; Huo, M.; Zhang, N.; Li, B.; Li, H.; Xu, Y.; Chen, M.; Hong, H.; Wang, Y. Mannose-Modified Multi-Walled Carbon Nanotubes as a Delivery Nanovector Optimizing the Antigen Presentation of

- Dendritic Cells. Chemistry Open 2019, 8, 915–921. https://doi.org/10.1002/open.201900126.
- (87) Shinchi, H.; Yamaguchi, T.; Moroishi, T.; Yuki, M.; Wakao, M.; Cottam, H. B.; Hayashi, T.; Carson, D. A.; Suda, Y. Gold Nanoparticles Coimmobilized with Small Molecule Toll-Like Receptor 7 Ligand and α-Mannose as Adjuvants. *Bioconjug. Chem.* **2019**, acs.bioconjchem.9b00560. https://doi.org/10.1021/acs.bioconjchem.9b00560.
- (88) Wilson, D. S.; Hirosue, S.; Raczy, M. M.; Bonilla-Ramirez, L.; Jeanbart, L.; Wang, R.; Kwissa, M.; Franetich, J.-F. F.; Broggi, M. A. S. S.; Diaceri, G.; Quaglia-Thermes, X.; Mazier, D.; Swartz, M. A.; Hubbell, J. A. Antigens Reversibly Conjugated to a Polymeric Glyco-Adjuvant Induce Protective Humoral and Cellular Immunity. Nat. Mater. 2019, 18, 175–185. https://doi.org/10.1038/s41563-018-0256-5.
- (89) Park, J. H.; Oh, N. Endocytosis and Exocytosis of Nanoparticles in Mammalian Cells. *Int. J. Nanomedicine* **2014**, *9*, 51. https://doi.org/10.2147/IJN.S26592.
- (90) Platt, C. D.; Ma, J. K.; Chalouni, C.; Ebersold, M.; Bou-Reslan, H.; Carano, R. A. D.; Mellman, I.; Delamarre, L. Mature Dendritic Cells Use Endocytic Receptors to Capture and Present Antigens. *Proc. Natl. Acad. Sci.* 2010, 107, 4287–4292. https://doi.org/10.1073/pnas.0910609107.
- (91) Fehres, C. M.; Kalay, H.; Bruijns, S. C. M.; Musaafir, S. A. M.; Ambrosini, M.; Bloois, L. van; Van Vliet, S. J.; Storm, G.; Garcia-Vallejo, J. J.; Van Kooyk, Y.; Van Bloois, L.; Van Vliet, S. J.; Storm, G.; Garcia-Vallejo, J. J.; Van Kooyk, Y. Cross-Presentation through Langerin and DC-SIGN Targeting Requires Different Formulations of Glycan-Modified Antigens. *J. Control.* Release 2015, 203, 67–76. https://doi.org/10.1016/j.jconrel.2015.01.040.
- (92) Srinivas, O.; Larrieu, P.; Duverger, E.; Boccaccio, C.; Bousser, M. T.; Monsigny, M.; Fonteneau, J. F.; Jotereau, F.; Roche, A. C. Synthesis of Glycocluster Tumor Antigenic Peptide Conjugates for Dendritic Cell Targeting. *Bioconjug. Chem.* **2007**, *18*, 1547–1554. https://doi.org/10.1021/bc070026g.
- (93) Rauen, J.; Kreer, C.; Paillard, A.; van Duikeren, S.; Benckhuijsen, W. E.; Camps, M. G.; Valentijn, A. R. P. M.; Ossendorp, F.; Drijfhout, J. W.; Arens, R.; Burgdorf, S. Enhanced Cross-Presentation and Improved CD8+ T Cell Responses after Mannosylation of Synthetic Long Peptides in Mice. *PLoS One* **2014**, *9*, e103755. https://doi.org/10.1371/journal.pone.0103755.
- (94) Bergen, J.; Ossendorp, F.; Jordens, R.; Mommaas, A. M.; Drijfhout, J.-W.; Koning, F. Get into the Groovel Targeting Antigens to MHC Class II. *Immunol. Rev.* **1999**, *172*, 87–96. https://doi.org/10.1111/j.1600-065X.1999.tb01358.x.
- (95) Tan, M. C. A. A.; Mommaas, A. M.; Drijfhout, J. W.; Jordens, R.; Onderwater, J. J. M. M.; Verwoerd, D.; Mulder, A. A.; van der Heiden, A. N.; Scheidegger, D.; Oomen, L. C. J. M. J. M.; Ottenhoff, T. H. M. M.; Tulp, A.; Neefjes, J. J.; Koning, F. Mannose Receptor-Mediated Uptake of Antigens Strongly Enhances HLA Class II-Restricted Antigen Presentation by Cultured Dendritic Cells. *Eur. J. Immunol.* 1997, 27, 2426–2435. https://doi.org/10.1002/eji.1830270942.
- (96) Grandjean, C.; Gras-Masse, H.; Melnyk, O. Synthesis of Clustered Glycoside-Antigen Conjugates by Two One-Pot, Orthogonal, Chemoselective Ligation Reactions: Scope and Limitations. *Chemistry (Easton).* **2001**, 7, 230–239. https://doi.org/10.1002/1521-3765(20010105)7:1<230::AID-CHEM230>3.0.CO;2-L.
- (97) McIntosh, J. D.; Brimble, M. A.; Brooks, A. E. S.; Dunbar, P. R.; Kowalczyk, R.; Tomabechi, Y.; Fairbanks, A. J. Convergent Chemo-Enzymatic Synthesis of Mannosylated Glycopeptides; Targeting of Putative Vaccine Candidates to Antigen Presenting Cells. *Chem. Sci.* **2015**, *6*, 4636–4642. https://doi.org/10.1039/c5sc00952a.
- (98) Glaffig, M.; Stergiou, N.; Hartmann, S.; Schmitt, E.; Kunz, H. A Synthetic MUC1 Anticancer Vaccine Containing Mannose Ligands for Targeting Macrophages and Dendritic Cells. *ChemMedChem* **2018**, *13*, 25–29. https://doi.org/10.1002/cmdc.201700646.
- (99) Moyle, P. M.; Toth, I. Modern Subunit Vaccines: Development, Components, and Research Opportunities. *ChemMedChem* **2013**, *8*, 360–376. https://doi.org/10.1002/cmdc.201200487.
- (100) Moyle, P. M.; Olive, C.; Ho, M.-F.; Pandey, M.; Dyer, J.; Suhrbier, A.; Fujita, Y.; Toth, I. Toward the Development of Prophylactic and Therapeutic Human Papillomavirus Type-16 Lipopeptide Vaccines. *J. Med. Chem.* **2007**, *50*, 4721–4727. https://doi.org/10.1021/jm070287b.
- (101) Skwarczynski, M.; Toth, I. Lipid-Core-Peptide System for Self-Adjuvanting Synthetic Vaccine Delivery; 2011; pp 297–308. https://doi.org/10.1007/978-1-61779-151-2_18.

(102) Sedaghat, B.; Stephenson, R. J.; Giddam, A. K.; Eskandari, S.; Apte, S. H.; Pattinson, D. J.; Doolan, D. L.; Toth, I. Synthesis of Mannosylated Lipopeptides with Receptor Targeting Properties. *Bioconjug. Chem.* **2016**, 27, 533–548. https://doi.org/10.1021/acs.bioconjchem.5b00547.

Multivalent oligomannoside clusters to probe C-type lectin receptor binding

Introduction

Mannose-binding C-type lectin receptors (CLRs) have been studied extensively because of the role they play on immune cells in signaling and internalization of antigens. ⁴⁻⁷ The mannose receptor (MR or CD206), DC-specific ICAM-3 grabbing non-integrin (DC-SIGN or CD209), and Langerin (CD207) have been successfully exploited for the (prevention of) uptake of antigens, via multiple strategies including the use of antibodies and ligands that can bind the receptor's carbohydrate-recognition domains (CRDs, see Chapter 1). Although all three receptors contain mannose-binding CRDs, the structures of the receptors are quite distinct (see Chapter 1). Where DC-SIGN and Langerin both have only one CRD, the human MR has eight CRDs that can bind mannosides with differing affinities. The receptors are able to multimerize: DC-SIGN can form a tetramer, while Langerin forms a trimeric structure. The MR occurs as either a monomer or as a dimer to the presence of Ca²⁺. As a result of the multimerization of the receptor and the multiple CRDs,

Part of this work is published in Hogervorst & Li et al. 2019¹

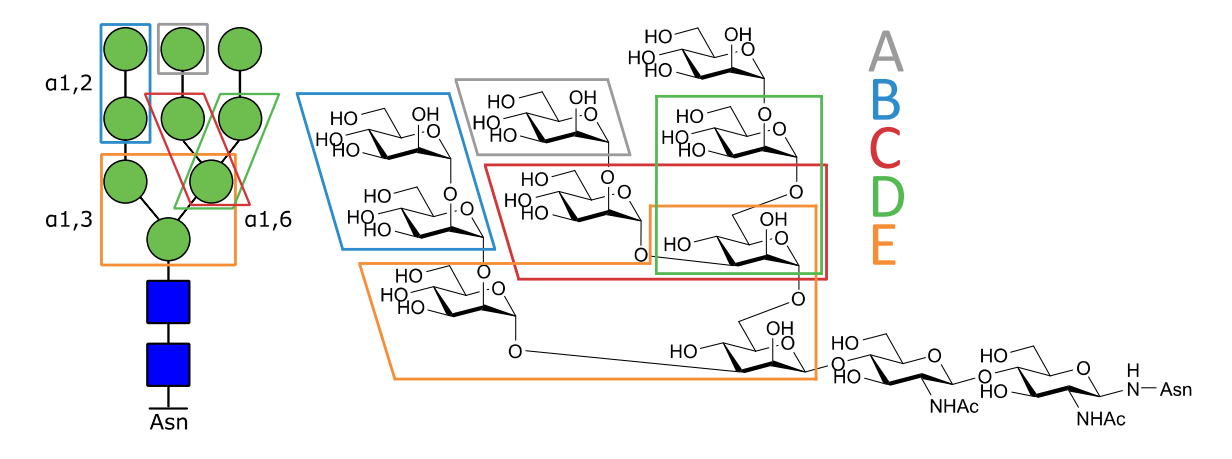
Part of this work has been submitted by Hogervorst & Li et al. 2020²

Part of this work is part of Riera Brillas et al. 20203, manuscript in preparation

the affinity for mannosides increases when mannosides are presented in a clustered manner with multiple mannosides in close proximity of each other. This so-called multivalent effect, in which the affinity increases more than the sum of affinities of the presented mannosides, is often exploited when targeting ligands to these CLRs. By incorporating readily available monomannosides in dendrimers, nanoparticles, liposomes or viral particles, these mannosides are presented in a multivalent manner resulting in high-avidity binding. ¹³⁻¹⁷ The binding affinity of a mono-mannoside however, is generally smaller than the affinity of more complex oligomannosides. ¹⁸ Targeting the CLRs with more complex larger oligomannosides with distinct stereoand regio-isomers and intrinsic multivalency results in increased affinity. ^{19,20} An often-utilized mannoside is the Man₉ scaffold (Figure 1) that is known to bind DC-SIGN with high affinity. Both strategies have previously been used to deliver cargo to DCs to enhance uptake of constructs. ²¹⁻²⁵ Utilizing more complex mannosides allows for a smaller scaffold and fewer number of mannoside copies. However, the synthesys of high mannose structures is time and labor-intensive and obtaining these structures in large quantities is challenging. ²⁶⁻²⁹

Due to the differences in the receptors, different preferences for mannosides in terms of their configuration and multivalent presentation is expected. However, studies that simultaneously study the effect of mannoside configuration and varying multivalent presentation in a defined manner are scarce, and often only determine binding affinity for one of the receptors. The goal of the present chapter is to study the effect of different mannoside configurations and the number of presented oligomannosides on binding affinity, in a defined and systematic approach. By dissecting the Man₉-structure in smaller oligomannosides, five fragments were selected that each represents a part of the main structure. The selected fragments are the mono-, α 1,2-di-, α 1,3-di-, α 1,6-di- and α 1,3- α 1,6-tri-mannoside, coded as **A-E** (See Figure 1). By the use of a scaffold that allowed the incorporation of 1, 2, 3, or 6 copies of these mannoside fragments, an array of constructs was obtained that can be used to systematically study the effect of multivalency and configuration on the affinity for each of the three CLRs.

Figure 1. Man₉ "high mannose" N-glycan structure.



Mono-, di- and tri-mannosides used in this chapter are based on the substructures in the "high mannose" N-glycan above.

Results and Discussion

The assembly of the mannoside array hinges on the Cu(I) catalyzed azide-alkyne cycloaddition (CuAAC) of propargyl mannosides with azide functionalized peptide scaffolds. The synthesis of the scaffolds was achieved via solid-phase peptide synthesis (SPPS) and resulted in five different backbones with 1, 2, 3, or 6 azides, forming scaffolds **20-24** (Scheme 1).

Scheme 1: Synthesis of backbone.

Reagents and conditions: HCTU, DIPEA, DMF (20: 81%; 21: 50%; 22: 44%; 23: 44%; 24: 30%).

The design of the scaffolds **20-24** is based on the following considerations. To match the length of the largest, hexavalent scaffold **23** with the trivalent backbone **22**, glycine residues were incorporated in the latter scaffold to separate the azidolysines. Similarly, the azidolysines in the divalent scaffold **21** were also separated by glycine residues. In divalent scaffold **24**, the same spacing in terms of the number of atoms between the outermost azides, as in hexavalent scaffold **23**, was introduced. This spacing was achieved with a glycine and a tri-ethylene glycol moiety, to ensure water solubility while maintaining similar spacing. All scaffolds contained a lysine at the C-terminus for further functionalization. SPPS of the scaffolds started with the coupling of Fmoc-Lys(Boc)-OH as the first amino acid on Tentagel® S-RAM amide resin followed by elongation using standard Fmoc protocol with HCTU as condensating agent. After completion of the oligopeptides, the scaffolds were deprotected and cleaved from resin under acidic conditions followed by purification via RP-HPLC resulting in peptides: **20** (in 81% yield, 93% per step); **21**: (in 50% yield, 87% per step); **22**: (in 44% yield, 89% per step); **23**: (in 44% yield, 90% per step) and **24**: (in 30% yield, 82% per step).

With the azidopeptide scaffolds **20-24** in hand, propargyl mannosides **25-29**, galactose **30** and sulfo GalNAc **31** were prepared using reported procedures (Scheme 2).^{1,3,33-35} These propargyl glycosides were selected based on their ability to bind the CLRs of interest. They can either bind all three CLRs (mannosides **25-29**), none of the three receptors (galactose **30**, to be used as a negative control) or only the MR via its cysteine-rich domain (sulfo GalNAc **31**). Series **A-E** are derived from the N-glycan high mannose structure Man₉ (see Figure 1). The **A** series combines the azido peptides with propargyl α-D-mannose (**25**);³³ the **B** series uses propargyl α1,2-di-α-D-mannosides (**26**);¹ representing the mono- and di-saccharides found at the end of the Man₉-antennas; the **C** series uses propargyl α1,3-di-α-D-mannosides (**27**);¹ the **D** series uses propargyl α1,6-di-α-D-mannosides (**28**);¹ the **E** series employs propargyl α1,3-α1,6-tri-α-D-mannosides (**29**),³⁴ representing the di- and tri-saccharides found in the core motive. The **G** series uses propargyl β-D-galactoside (**30**);³⁵ and the **S** series uses a propargyl 4-sulfo-β-D-N-acetyl-galactosamine (**31**).³

The assembly of the array was achieved by conjugation of the propargyl glycosides **25-29** and azido peptides **20-24** by CuAAC (Scheme 2). Many aqueous CuAAC conjugations have been described in literature,³⁶ but many of these require the use of significant amounts of copper.^{37–39} Although the use of a large amount of copper catalyst did provide fast and high yielding conjugation reactions, the purification and especially the removal of copper, proved to be troublesome. An

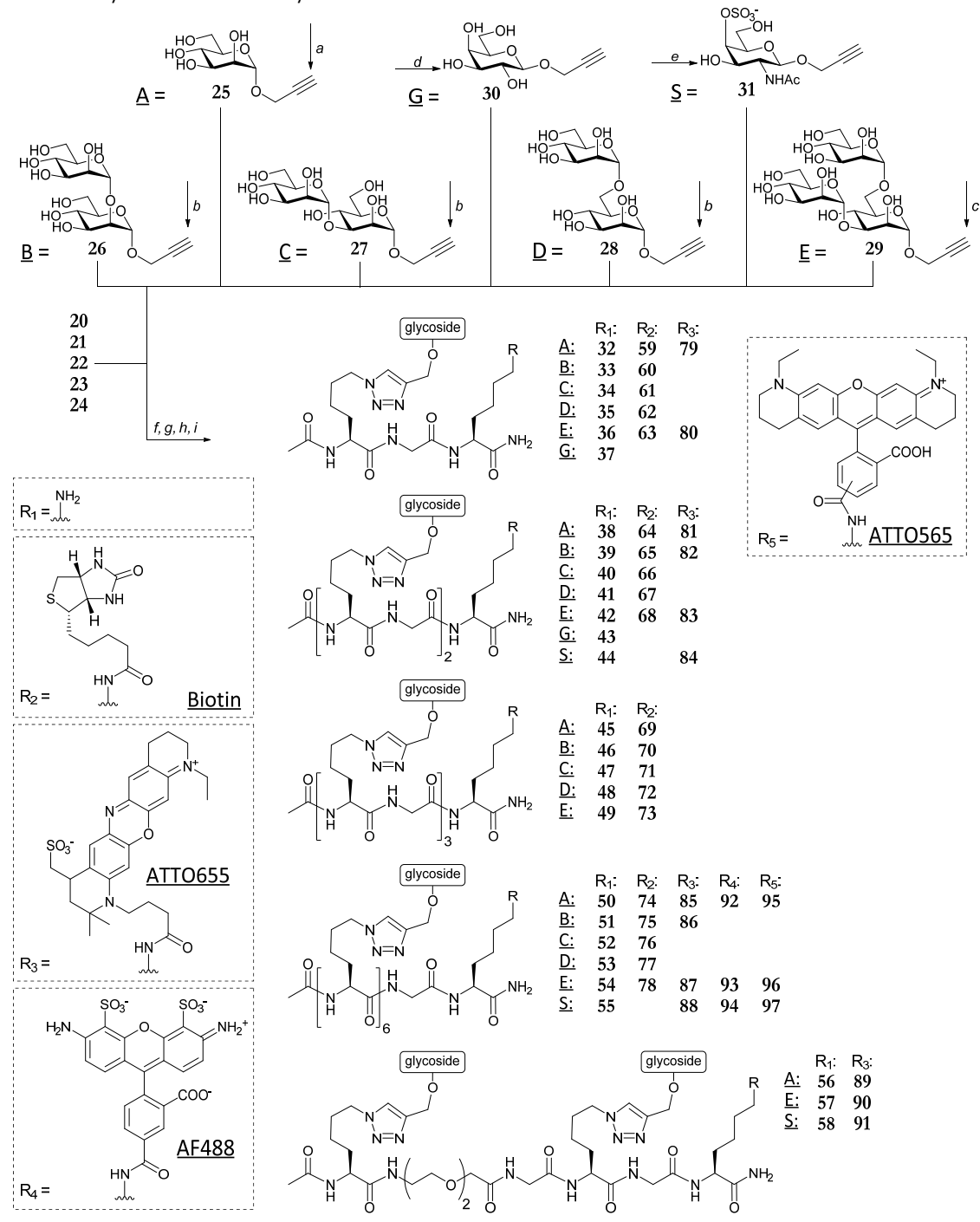
24

^a Whether the low conversion for **24** is caused by the lower temperature during the coupling or whether the product is lost during workup and/or purification was not determined.

earlier described method to remove copper with CuprisorbTM,⁴⁰ gave variable results. Attempts to circumvent these issues by reducing the amount of copper resulted in varying yields. Major improvements in the conjugation were achieved by i) lowering the amount of copper in combination with the addition of tris(3-hydroxypropyltriazolylmethyl)amine (THPTA) to stabilize the Cu(I) species;³⁶ ii) reducing the concentration of dissolved oxygen in the reaction mixture by purging solvents with argon; iii) increasing the temperature of the reaction; iv) addition of *N*,*N*-diisopropylethylamine (DIPEA); and v) reduction of Cu(II) with a smaller amount of sodium ascorbate to prevent over-reduction of Cu cations to metallic copper. The remaining copper was scavenged using Quadrasil[®] AP resin, and the 27 prepared clusters **32-58** were purified by either HPLC or gel filtration.

All the conjugation reactions leading to the clusters 32-58 required separation of unreacted glycosides from the desired products, for which size exclusion gel filtration and RP-HPLC were explored. Due to the hydrophilic character of both the products and unreacted propargyl glycosides only minimal differences in retention times were observed using either C18 or C30 RP-HPLC columns. To prevent co-elution, only small injection volumes were tolerated, making purification by RP-HPLC very solvent and time-demanding. In addition, the constructs showed little UV absorption and tended to fragment during electron spray ionization (ESI), leading to relatively high loss of product during HPLC purification when relying on these monitoring techniques. On the other hand, the use of an HW40S size exclusion column provided a large difference in retention time between the clusters and the monomers, allowing for single run purifications. Unlike the HPLC, the gel filtration setup allowed for fraction monitoring by refractive index (RI) and the synthesized clusters displayed a strong RI signal. This high sensitivity allowed for high recovery during fraction collection. Altogether, the larger difference in elution time, the single run purifications, and the smaller losses because of the more sensitive monitoring, made gel filtration the method of choice for purification of these clusters. In total 27 clusters (32-58) were obtained that varied in the type of glycosides and varied in number of presented glycosides (Scheme 2). All 27 clusters contain an unfunctionalized C-terminal lysine for further conjugation purposes.

Scheme 2: Synthesis of library.



Reagents and conditions: a) starting from D-mannose ³³; b) starting from **25** ¹; c) starting from **25** ³⁴; d) starting from D-galactose ³⁵; e) starting from D-galactose ³; f) CuI, THPTA, DIPEA, DMSO, H₂O (32: 39%; 33: 68%; 34: 99%; 35: 85%; 36: 99%; 37: 57%; 38: 61%; 39: 41%; 40: 14%; 41: 28%; 42: 43%; 43: 53%; 44: 30%; 45: 69%; 46: 80%; 47: 82%; 48: 85%; 49: 80%; 50: 82%; 51: 98%; 52: 99%; 53: 57%; 54: 85%; 55: 88%; 56: 83%; 57: 99%; 58: 17%); g) BiotinO-NHS, DIPEA, DMSO (59: 99%; 60: 16%; 61: 17%; 62: 50%; 63: 14%; 64: 19%; 65: 49%; 66: 99%; 67: 76%; 68: 49%; 69: 63%; 70: 33%; 71: 96%; 72: 90%; 73: 51%; 74: 59%; 75: 62%; 76: 62%; 77: 56%; 78: 85%); g) ATTO655-NHS, DIPEA, DMSO (79: 88%; 80: 84%; 81: 45%; 82: 95%; 83: 100%; 84: 6%; 85: 62%; 86: 34%; 87: 81%; 88: 89%; 89: 43%; 90: 26%; 91: 11%); h) AlexaFluor488-NHS, DIPEA, DMSO (92: 46%; 93: 34%; 94: 6%); i) ATTO565-NHS, DIPEA, DMSO (95: 43%; 96: 43%; 97: 17%).

Table 1: SPR results.

	DC-SIGN		Langerin	
Cluster	K_d app (μM)	$IC_{50} (\mu M)$	K_d app (μM)	$IC_{50} (\mu M)$
1A = 32		N.D.		N.D
2A = 38		2605±95		2424±30
3A = 45		736.7 ± 3.4	43	
6A = 50	7.8±0.4		3.4±1.4	
1B = 33		2343±109		4138±773
2B = 39		189.3±3.4		181±4
3B = 46	19.5±0.5		48	
6B = 51	0.95±0.04		3.2±1.7	
1C = 34		N.D		N.D.
2C = 40		567.5±1.2		1415±13
3C = 47		172.0 ± 1.5		281±14
6C = 52	1.17±0.25		3.9±1.5	
1D = 35		6961.5±3038.5		N.D.
2D = 41		410.9±0.3	16	
3D = 48	48.7±2.6		9.8	
6D = 53	6.6±1.2		12.3±0.7	
1E = 36		1518.5±250.5		N.D.
2E = 42		305.6 ± 4.8	278	
3E = 49	2.44±0.04		4.2	
6E = 54	2.78±0.02		6.5±2.7	
1G = 37		N.D.		N.D.
2G = 43		N.D.		N.D.

Surface plasmon resonance (SPR) analysis of clusters for ECD DC-SIGN and ECD Langerin. Direct interaction experiments resulted in an apparent K_{ab} and competition experiments resulted in an IC_{50} . N.D. = Not Determined because binding affinity was too low to assess a reliable IC_{50} .

The majority of the constructs were tested for their affinity for DC-SIGN and Langerin via Surface plasmon resonance (SPR) assays (Table 1).⁴¹ The apparent K_d was calculated in direct interaction mode using a surface functionalized with the DC-SIGN extracellular domains (ECDs) in an oriented manner. In this assay, the tetrameric DC-SIGN ECD was attached to the surface of the sensor chip via the N-terminus of its neck oligomerization domain, thus presenting its four carbohydrate recognition domains towards the solvent, realistically mimicking the presentation of the receptor on the cell surface.⁴² For some of the low-affinity ligands, binding in the mM range, it was not possible to determine their affinity with this assay, and therefore a competition experiment was performed providing IC_{50} values.⁴³ When the galactose clusters **37** and **43** were tested, their affinity was too low to be determined, thereby excluding a-specific binding interactions

of the scaffold. When comparing equivalent clusters, the α 1,2-di-mannoside (**B** series) bound with the highest affinity. The hexavalent presentation (n=6) of the oligomannosides led to micromolar affinity of these clusters for DC-SIGN. **51** showed the highest affinity in the library with an apparent K_d of 0.95 μ M, followed by the α 1,3-dimannoside cluster **52** (1.17 μ M), the trimannoside clusters **49** (2.44 μ M) and **54** (2.78 μ M). Interestingly, the affinity of the trisaccharide series (**E** series) did not improve from the tri- to the hexavalent representation (**49** versus **54**). A potential explanation for this effect could be that the spacing of clusters is more important for the larger trimannosides. For the monovalent mannosides **32** and **34**, a reliable IC₅₀ could not be determined in this setup, indicating that their binding affinity for DC-SIGN is too weak to establish a reliable measurement. For Langerin the results were very similar to DC-SIGN with avidity improving with an increasing amount of mannoside copies, although the effect of the mannoside configuration appeared to be less prominent (Table 1).

To enable visualization of the clusters in cellular experiments, a biotin handle was introduced that could be identified using fluorescent streptavidin antibodies. Treatment of mannoside clusters 32-54 with biotin-N-hydroxysuccinimide (NHS) ester gave biotinylated mannoside clusters 59-78 (R = R₂, Scheme 2). Because of the large differences in polarity between the products and starting compounds, and the small scale of the biotinylation, RP-HPLC proved to be the most efficient purification method for the biotinylated clusters. The twenty biotinylated mannoside clusters (59-78) were next tested for their affinity for and uptake by CLRs on monocyte derived DCs (moDCs).

When the biotinylated clusters were assessed for their binding to cellular DC-SIGN, similar trends as revealed by the SPR experiments were observed. In the used assay, clusters **59-78** were allowed to bind to moDCs for 30 minutes at 4° C. After washing of the cells at 4° C, the number of attached clusters were quantified by staining with a fluorescent streptavidin and quantification by flow cytometry (Figure 2, top). The α 1,2-mannosides (**B** series) showed enhanced binding in comparison to the mono-mannoside and the α 1,6- or α 1,3-dimannosides, in line with the SPR data and earlier results. When increasing the number of mannosides from 3 to 6 for the tri-mannoside (**73** to **78**) and the α 1,6-dimannoside (**72** to **77**), the affinity did not increase, again illustrating the potential influence of the spacing in the used scaffold. Similar experiments were performed with a transfected B-cell line expressing Langerin (EBV Langerin⁺). Again, the results were in line with the affinities obtained *via* SPR, showing a strong effect of the number of mannoside copies. The type of mannoside appeared to have relatively little influence on binding in this assay, although the highest affinities were observed for the α 1,6-di and tri-mannoside clusters. (Figure 2, bottom)

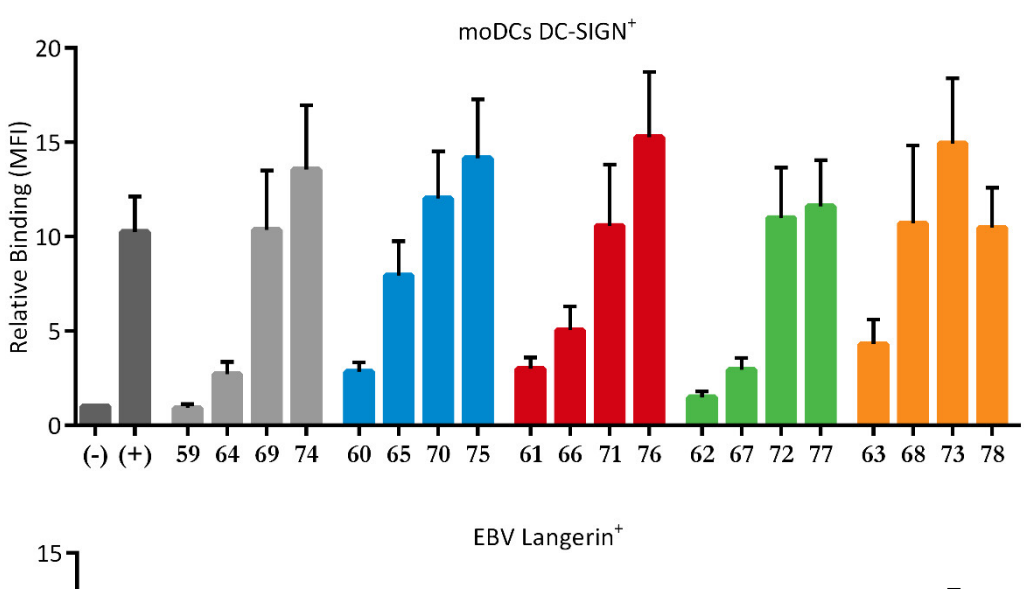
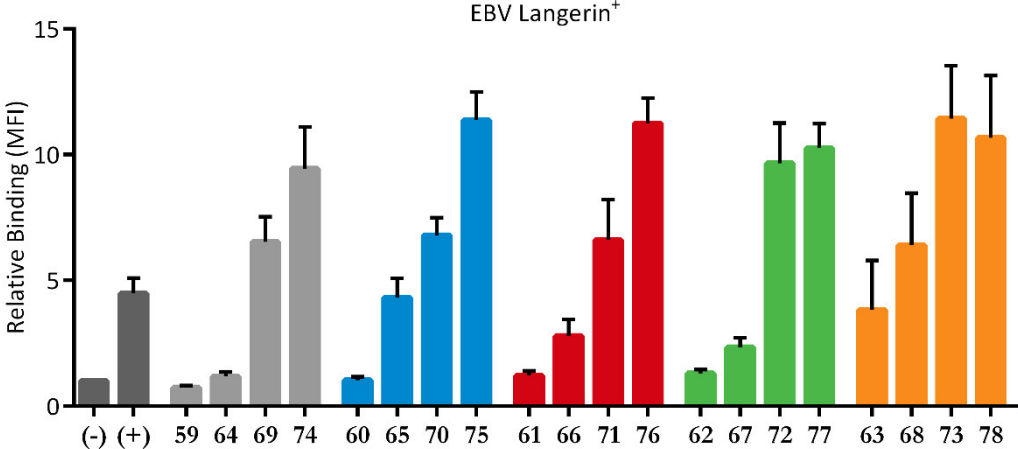


Figure 2: Affinity towards DC-SIGN (top) or Langerin (bottom) via FACS.



Binding of the biotinylated mannoside library to DC-SIGN on moDCs (top) or to Langerin on EBV cells (bottom) was measured by flow cytometry. Normalized to the negative control. MoDCs were incubated with biotinylated constructs (30 min, 4 °C, 10 μ M). (-) = negative control (PBS); (+) = positive control (1 μ g/mL of Lewis Y conjugated polyacrylamide); Serie A in gray; B in blue; C in red; D in green; and E in orange.

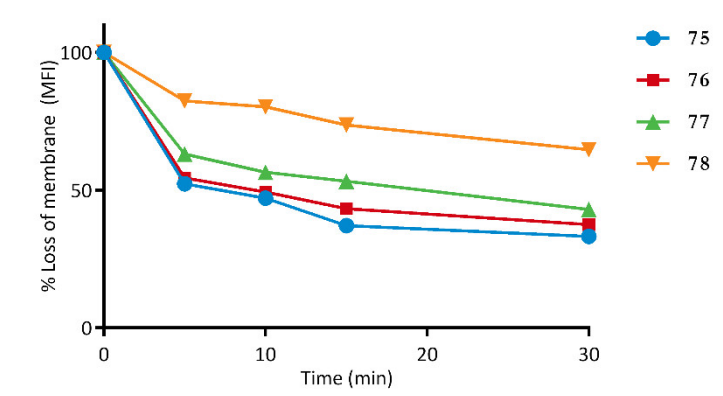


Figure 3: Internalization of cluster by moDCs (DC-SIGN) via FACS.

The internalization of the mannoside clusters by moDCs was measured by flow cytometry. One donor is depicted here as representation of four. Cells were incubated with clusters (20 μ M on ice for one hour and after incubated at 37 °C for different time spans). Quantification with an external fluorophore allowed quantification of the remaining clusters on the cell surface as an indirect measure of uptake. clusters 75, 76 $\stackrel{.}{c}$ 77 are rapidly internalized, while 78 remains longer at the surface.

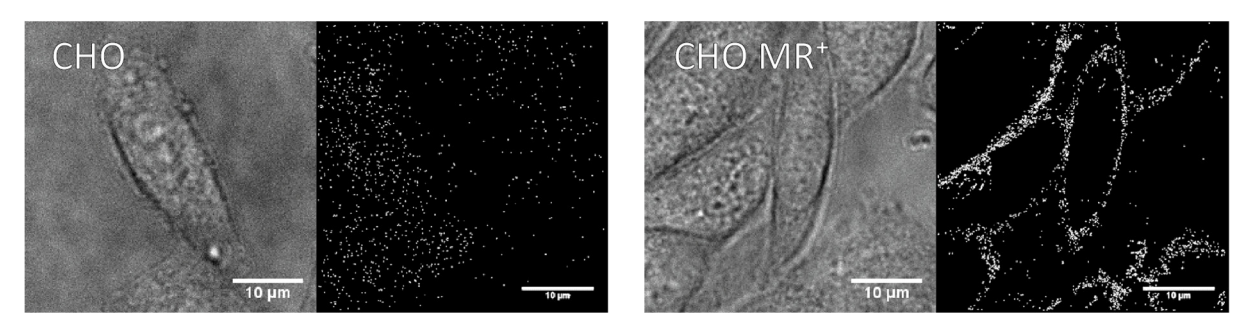
Active internalization can take place when the cells are allowed to warm up, leading to the diminished presence of the ligand on the surface of the cells. Quantifying the amount of biotinylated clusters on the cell surface as a function of time can then provide an indication for the rate of uptake over time (Figure 3). Using this assay, the rate of uptake for clusters 75-78 was determined to show a difference with respect to the affinity for DC-SIGN. The di-mannosides 75-77 were internalized relatively fast, while the tri-mannoside 78 remained longer on the cell surface. Although the DC-SIGN mediated uptake mechanism is known, 45 the initiation trigger for endocytosis upon DC-SIGN-ligand binding remains unclear. Recognition of the di-mannoside clusters could lead to different signaling and a difference in the rate of uptake. Experiments to determine the affinity on cellular langerin are still ongoing.

Although affinity for, and uptake *via* the MR of mannose ligands has been the subject of many studies, stable expression of functional MR remains challenging. The receptor can be stabilized through small alterations in its amino acid sequence, but this often modifies the properties of the receptor. ⁴⁶ In an attempt to study the kinetics of the MR in a more natural setting, the kinetics of the natural cellular receptor was studied with stochastic optical reconstruction microscopy (STORM). A selection of conjugates was functionalized with a laser dye using their activated *N*-hydroxysuccinimide (NHS) esters to generate the clusters within minutes with high conversion (Scheme 2). Besides the default ATTO655 dye ($R = R_3$), AlexaFluor488 ($R = R_4$) and ATTO565 ($R = R_5$) were appended on the clusters, to allow for co-localization and Förster resonance energy transfer (FRET) experiments. For optimal results, the clusters containing the sulfate-carrying glycans 44, 55, 58 were converted from the ammonium salts, obtained after their purification using aqueous NH₄HCO₃, into the corresponding sodium salts using a Na⁺-exchange resin. The clusters decorated with the ATTO655 or ATTO565 laser dyes allow for tracking of single molecules binding to the mannose receptor (also see Chapter 5).

In this STORM experiment, only clusters that remain at the same location for a certain time will be observed. Since unbound clusters move to fast due to diffusion, only clusters that are fixed will be observed. This can be either in cellular compartments or bound to receptors. When Chinese hamster ovary (CHO) cells transfected with the MR were subjected to cluster 81, the clusters localized on the cell surface (see Figure 4, right panel). When the same experiments were performed with CHO cells that lack the MR, the clusters did not localize, indicating that this localization is MR dependent (Figure 4, left panel). When these MR⁺ CHO cells were subjected to a selection of ATTO655 clusters, cellular localization of fluorophores showed a trend with more signal for the hexavalent clusters, indicating that larger clusters are trafficked more readily into the CHO cells (see Figure 5). Additionally, by following individual fluorescent events, an average

binding time can be determined, which correlates with the affinity of the cluster for the receptor (Figure 6). This binding time was determined for a selection of clusters and demonstrated that affinity increases from mono- to di- to tri-mannoside. When comparing clusters bearing the monomannoside (79, 81, 89, and 85), affinity is similar for the clusters bearing one or two mannoside copies, and only increases for the hexavalent clusters 85. One potential explanation for the increase in affinity could be that the distance between the two outermost mannosides in the hexavalent cluster is long enough to bind two CRDs simultaneously. However, since bi-valent cluster 89 was designed to match the spacer length with that of hexavalent cluster 85, and these do not match in affinity, this hypothesis seems unlikely. For the trisaccharide series (80, 83, 90, and 87) similar trends were observed. The α12-dimannoside cluster 82 shows an affinity between the mono- and tri-mannoside analogs. Finally, clusters bearing the sulfo GalNAc were tested (84, 91, and 88). These clusters are designed to bind the cysteine-rich domain, of which unlike CRDs, only one is present per receptor. Strikingly, no change in affinity was observed when the number of sulfo GalNAc copies were increased. This observation, in combination with the fact that increasing the spacing between two mannoside copies did not increase the affinity, could indicate that the multivalent effect observed for the mannoside clusters is due to the presence of multiple CRDs in one receptor and not due to binding multiple receptors simultaneously.

Figure 4: comparison between CHO and MR transfected CHO cells using 81.



CHO-K1 (left) and CHO-MR (right) cells were incubated with 81 (5 nM, at 4 °C), in this experiment the focus area is photo-bleach, followed by a short restoration time in which new ATTO-655 clusters can bind the receptors present on the cell surface. Area imaged with a 640 nm laser (40 mW).

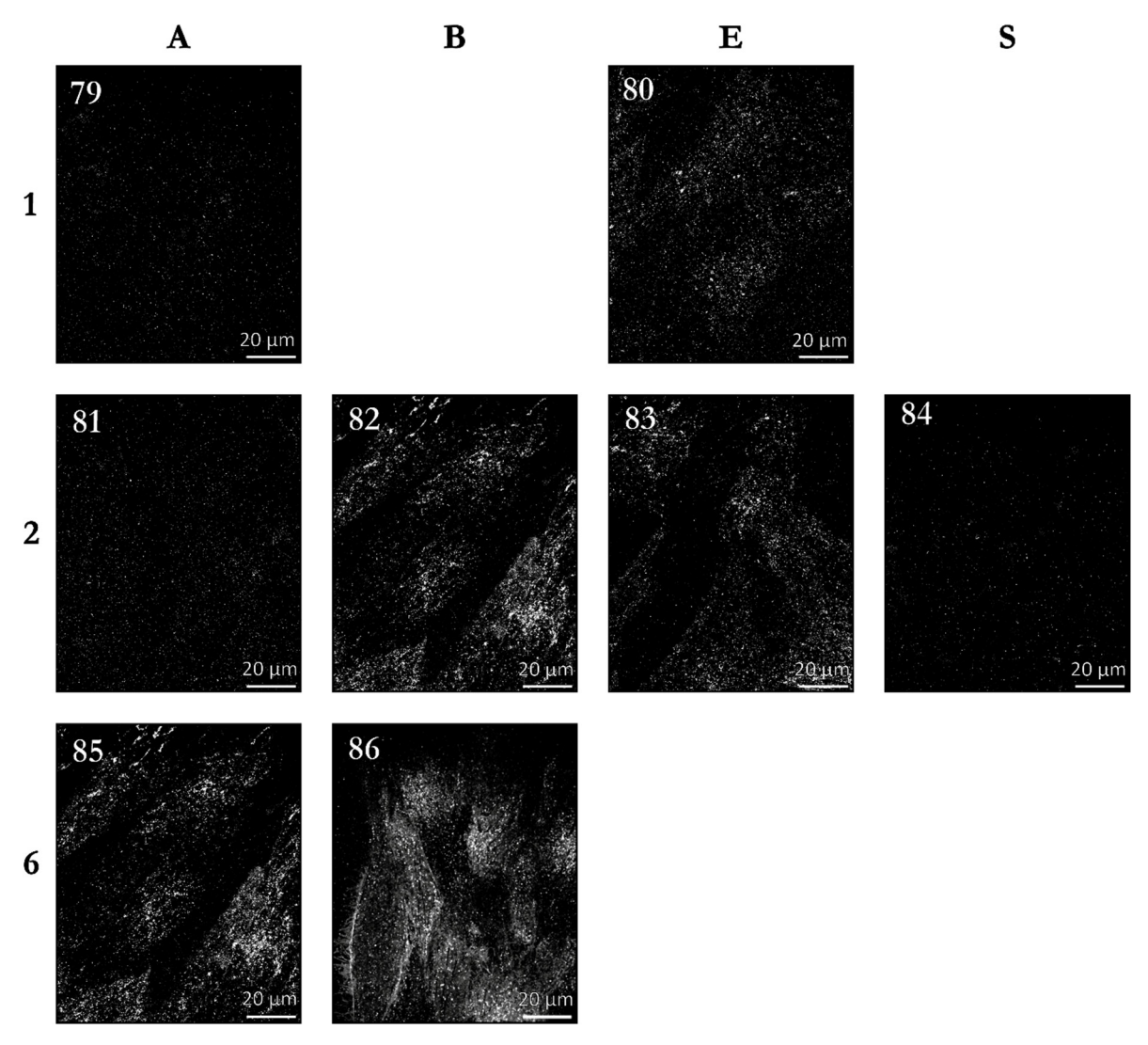


Figure 5: Density map using STORM microscopy.

CHO-MR cells were incubated with ATTO655 functionalized mannoside clusters (5 nM) and imaged with a 640 nm laser (40 mW) Clusters with high affinity are endocytosed faster compared with lower affinity clusters, resulting in higher density of clusters within the cells.

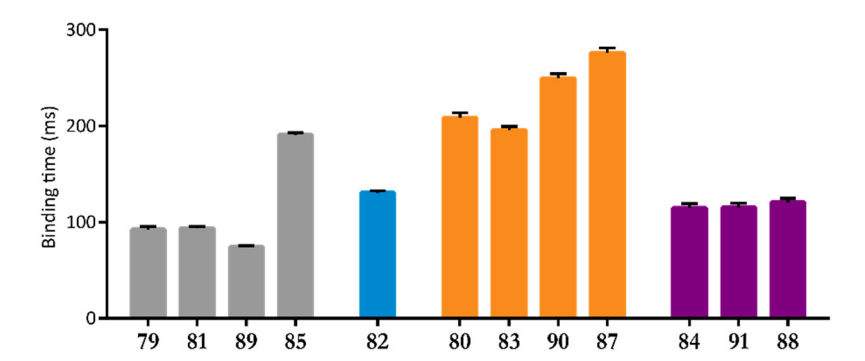


Figure 6: binding time (τ) from combined trajectories (\pm SE) determined by STORM.

Incubation of CHO-MR cells with ATTO655 functionalized mannoside clusters at 37°C allowed for single particle tracking. Trajectory lengths from at least 5 images per probes were combined, plotted in a histogram and fitted with a single exponential decay function wherefrom τ was determined. Serie A in gray; B in blue; E in orange; and S in purple.

Conclusion

This chapter has described the synthesis of a systematic library of clusters, consisting of defined mannosides (mono-, di- and tri-mannosides) that are presented in an increasing number (n=1, 2, 3, or 6) on a well-defined oligopeptide scaffold, which allowed the simultaneous studying of the effect of mannoside configuration and multivalency on the binding affinity for DC-SIGN, langerin, and the MR. The reaction conditions to conjugate the azidopeptides with the propargyl mannosides and the purification procedures were optimized to allow for the effective assembly of the sizable library of clusters. Further decoration of the constructs via the C-terminal lysine with either a biotin affinity tag or fluorescent dyes was successful and enabled the use of the conjugates in FACS and STORM experiments. The highest affinity for DC-SIGN can be obtained by the highest number of copies and the α1,2-dimannoside (B series). The type of mannoside appeared to have relatively little influence on the affinity for Langerin, and the highest affinity is mainly obtained by the highest number of copies. The introduction of laser dyes allowed for the MR to be studied in a more natural setting. These results indicate that the binding affinity for either one or two mannoside copies does not differ significantly, however affinity increases when six copies are presented. This increase is most likely not caused by the simultaneous binding of the outermost mannosides since bivalent clusters with similar spacing do not display this increment in affinity. Clusters that target the cysteine-rich domain show no multivalent effect, which would indicate that the multivalent effect observed for the mannoside clusters is not due to the simultaneous binding of two receptors.

Experimental

General procedures:

Reactions: All reactions were carried out in oven-dried glassware (85 °C). Prior to reactions traces of water and solvents were removed by co-evaporation with toluene where appropriate. Reactions sensitive to oxygen or moisture were carried out under an atmosphere of nitrogen. Solvents for reactions were of reagent grade and when anhydrous conditions were required, were stored over 4Å molecular sieves (3Å for CH₂Cl₂, MeOH & HFIP) Et₃N was dried over KOH pellets; and pyridine and DMF were used without molecular sieves. Solvents used for workup and column chromatography were of technical grade and used as received. Unless stated otherwise, solvents were removed by rotary evaporation under reduced pressure at 40 °C. All other chemicals (Sigma-Aldrich, TCI, Carbosynth, Iris-Biotech, Merck, Boom, Honeywell & Biosolve) were used as received. The solid-phase peptide synthesis was performed on a TRIBUTE® Peptide Synthesizer (Gyros Protein Technologies AB, Arizona, USA) applying Fmoc based protocol.

Purification: Silica gel column chromatography was performed on Screening Devices silica gel 60 (0.004 - 0.063 mm). Gel filtrations were performed with an ÄKTATMexplorer (GE Healthcare, Illinois, USA) using either a 1.6 x 60 cm, or 2.6 x 60 cm column with Toyopearl HW-40S resin eluting with a solution of NH₄HCO₃ (150 mM) or NH₄OAc (150 mM) in MilliQ with 0 – 20% ACN. Fraction monitoring was performed using refractive index and with UV absorption at 260 nm unless stated otherwise. Preparative high-pressure liquid chromatography was conducted on either a Gilson GX281 with an automatic fraction collector, Waters auto purifier prep LCMS coupled to a Waters SQ detector, or an Agilent1200 semi-prep system coupled to an Agilent 6120 quadruple detector. Columns used are either: Gemini-NX 5µm C18, 110 Å, 250 x 10.0 mm, 5 mL/min or Develosil RPAQUEOUS 10.0 x 250 mm, 5 mL/min in combination with eluents A: 0.1% TFA in MilliQ in B: ACN.

Analysis: Reaction progress was monitored using LC-MS analysis or TLC-analysis. TLC-analysis was performed on Merck 25 DC plastikfolien 60 F254. Visualization was carried out by irradiation with UV light (λ: 254 nm, 360 nm), followed by spraying with either 20% H₂SO₄ in EtOH (w/v); (NH₄)₆Mo₇O₂₄·4H₂O (25 g/L) and (NH₄)₄Ce(SO₄)₄·2H₂O (10 g/L) in 10% H₂SO₄ (aq.); ninhydrin (3 g/L) in EtOH/AcOH (20/1, v/v); or by dipping in anisaldehyde/H₂SO₄/EtOH (1/1/18, v/v/v); followed by charring >150 °C. LC-MS analysis was performed on one of the following LC-MS systems: A Thermo Finnigan LCQ Advantage MAX ion-trap mass spectrometer with an electrospray ion source coupled to Surveyor HPLC system (Thermo Finnegan), A Thermo Finnigan LCQ Fleet MAX ion-trap mass spectrometer with an electrospray ion source coupled to

Vanquish UHPLC system (Thermo Finnegan) or an Agilent Technologies 1260 Infinity LC system (detection simultaneously at 214 and 254 nm) coupled to a Agilent Technologies 6120 Quadrupole MS. Using an analytical Gemini C18 column (Phenomex, 50 x 4.60 mm, 3 microns) in combination with eluents A: H₂O; B: ACN and C: 1% TFA (aq.) as the solvent system, in which the gradient was modified by changing the ratio of A in B in combination with 10% C. ¹H and ¹³C NMR spectra were recorded on a 300/75, 400/100, or a 500/125 MHz spectrometer. Chemical shifts (δ) are given in ppm relative to tetramethylsilane as an internal standard. Coupling constants are given in Hz. All individual signals were assigned using 2D-NMR spectroscopy, HH-COSY, and HSQC. Optical rotations were measured on an Anton Paar Modular Circular Polarimeter MCP 100/150. IR spectra are reported in cm⁻¹, and recorded on a Shimadzu FTIR-8300 or a PerkinElmer universal attenuated total reflectance (UATR; Single Reflection Diamond) Spectrum Two instrument. High resolution mass spectra were recorded either by direct injection (2 µL of a 2 µM solution in water/acetonitrile 50/50 (v/v) and 0.1% formic acid) on a Thermo Finnigan LTQ Orbitrap equipped with an electrospray ion source in positive mode (source voltage 3.5 kV, sheath gas flow 10, capillary temperature 250°C) with resolution R = 60,000 at m/z 400 (mass range m/z = 150-2,000) and dioctylphthalate (m/z = 391.2843) as a "lock mass". Or were measured by direct injection (2 µL of a 1 µM solution in water/acetonitrile 50/50 (v/v) and 0.1% formic acid) using an ultimate 3000 UHPLC on a Thermo Finnigan Q executive HF Orbitrap equipped with an electrospray ion source in positive mode (source voltage 3.5 kV, sheath gas flow 10, capillary temperature 250°C) with resolution R = 240,000 at m/z 400 (mass range m/z = 150-3,000) with external lock and calibration. The high-resolution mass spectrometers were calibrated prior to measurements when $\delta \ge 1$ ppm with a calibration mixture (Thermo Finnigan).

General procedure for automated solid-phase synthesis:

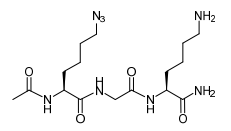
The solid-phase peptide synthesis was performed on a TRIBUTE® Peptide Synthesiser (Gyros Protein Technologies AB, Arizona, USA) applying Fmoc based protocol starting with Tentagel® S-RAM resin (~0.22 mmol/g) on a 100 µmol scale using established synthetic protocols.⁴⁷ The consecutive steps performed in each cycle were:

1) DMF wash (1x) followed by nitrogen purge; 2) Deprotection of the Fmoc-group with 20% piperidine in DMF (4 mL)(3 x 5 min); 3) DMF wash (3x) followed by nitrogen purge; 4) Coupling of the appropriate

amino acida in five-fold excess (unless stated otherwise); 5) DMF wash (3x) followed by nitrogen purge; 6) capping with an Ac₂O/DMF/DIPEA solution (4mL, 20/88/2, v/v/v) for 2 min; 7) DMF wash (2x).

After the complete sequence capping was achieved by utilization of steps 1,2, 3, and 6 followed by washing with DMF (3x), DCM (3x), Et₂O (2x), and nitrogen purge.

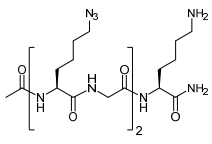
Ac-Lys(N₃)-Gly-Lys-NH₂ (20).



Ac-Lys(N₃)-Gly-Lys(Boc)-Tentagel® S-RAM was transferred to a flask and treated for 90 minutes with a cleavage cocktail (10 mL, TFA/TIS/H₂O, 190/5/5, v/v/v). the resin was filtered off and washed with neat TFA (3 x 1 mL). The filtrate was concentrated, co-evaporated with toluene (2x). Purification via RP-HPLC (linear-gradient 5-30% B, 10 min)

yielded title compound **20** as an clear oil after lyophilization (32.2 mg, 80.9 μ mol, 81%). <u>LC-MS</u>: R_t = 2.79 min (0 - 90% ACN; 13 min); ¹H NMR (500 MHz, DMSO) δ 8.27 (t, I = 5.8 Hz, 1H, NH (G)), 8.14 (d, I = 7.2 Hz, 1H, NH (K)), 7.77 (d, J = 8.2 Hz, 1H, NH (K)), 7.68 (s, 2H, CH₂NH₂), 7.29 (s, 1H, (CO)NHH), 7.08 (s, 1H, (CO)NHH), 4.18 - 4.10 (m, 2H, CH), 3.75 (dd, J = 16.6, 6.0 Hz, 1H, CHH (G)), 3.66 (dd, J = 16.6) 16.6, 5.6 Hz, 1H, CHH (G)), 3.31 (td, J = 6.8, 1.2 Hz, 2H, CH₂-N₃), 2.74 (p, J = 6.5 Hz, 2H, CH₂-NH₂), 1.85 (s, 3H, Ac), 1.75 - 1.61 (m, 2H, CH₂), 1.51 (td, J = 12.1, 10.9, 4.7 Hz, 6H, CH₂), 1.42 - 1.21 (m, 4H, CH₂); ¹³C NMR (126 MHz, DMSO) δ 173.5, 172.4, 169.8, 168.7 (C=O), 52.9, 52.1 (CH), 50.5 (CH₂-N₃), 42.2 (CH₂ (G)), 38.7 (CH₂-NH₂), 31.3, 31.0, 27.9, 26.6, 22.6 (CH₂), 22.5 (Ac), 22.2 (CH₂); HRMS $[C_{16}H_{30}N_8O_4 + H]^+$: 399.2475 found, 399.2463 calculated.

$Ac-Lys(N_3)-Gly-Lys(N_3)-Gly-Lys-NH_2$ (21).



Ac-Lys(N3)-Gly-Lys(N3)-Gly-Lys(Boc)-Tentagel® S-RAM was transferred to a flask and treated for 90 minutes with a cleavage cocktail (10 mL, TFA/TIS/H₂O, 190/5/5, The mixture was concentrated to approximately one mL after which the resin

was filtered off into a cold mixture of diethylether/pentane (45 mL, 5/4, v/v) and the resin was washed off with neat TFA (3 x 1 mL) into the ether solution. This solution was centrifuged (10 minutes, 5000 rpm) after which the supernatant was removed and the precipitate was dried under nitrogen flow. Purification via RP-HPLC (linear-gradient 10-40% B, 10 min) yielded title compound 21 as a white powder after lyophilization (30.47 mg, 49.9 μ mol, 49.9%). LC-MS: $R_t = 4.21 \text{ min } (0 - 90\% \text{ ACN}; 13 \text{ min}); 1H NMR (500)$ MHz, DMSO) δ 8.25 (dt, J = 17.2, 5.5 Hz, 2H, NH (G)), 8.13 (d, J = 7.1 Hz, 1H, NH (K)), 7.90 (d, J = 7.6Hz, 1H, NH (K)), 7.82 - 7.69 (m, 3H, NH (K), CH₂NH₂), 7.32 (s, 1H, (CO)NHH), 7.05 (s, 1H, (CO)NHH), 4.28 - 4.06 (m, 3H, CH), 3.79 - 3.64 (m, 4H, CH₂ (G)), 3.29 (q, J = 6.8 Hz, 4H, CH₂-N₃), 2.75 (q, J = 6.3Hz, 2H, CH₂NH₂), 1.85 (s, 3H, Ac), 1.75 - 1.44 (m, 12H, CH₂), 1.42 - 1.20 (m, 6H, CH₂); 13C NMR (126

^a The Fmoc amino acids applied in this synthesis were: Fmoc-Lys(Boc)-OH, Fmoc-Gly-OH, Fmoc-AEEA-OH (Carbosynth) and Fmoc-Lys(N₃)-OH (4eq per coupling, IRIS biotech).

^b Generally, the Fmoc amino acid was dissolved in a HCTU solution in DMF (2.50 mL ,0.20 M, 0.5 mmol, 5 eq) This solution was transferred to the reaction vessel followed by a DIPEA solution in DMF (2.00 mL, 0.50 M, 1.0 mmol, 10 eq) to initiate the coupling. Next, the reaction vessel was shaken for 60 min at room temperature.

MHz, DMSO) δ 173.5, 172.3, 172.0, 169.8, 169.1, 168.6 (C=O), 52.9, 52.6, 52.1 (CH), 50.5 (CH₂-N₃), 42.2, 42.1 (CH₂ (G)), 38.7 (CH₂-NH₂), 31.3, 31.2, 31.2, 31.1, 27.9, 27.9, 26.6, 22.6, 22.5 (CH₂), 22.5 (Ac), 22.3 (CH₂); <u>HRMS</u> [C₂₄H₄₃N₁₃O₆ + H]⁺: 610.3539 found, 610.3532 calculated.

$Ac-Lys(N_3)-Gly-Lys(N_3)-Gly-Lys(N_3)-Gly-Lys-NH_2$ (22).

Ac-Lys(N₃)-Gly-Lys(N₃)-Gly-Lys(N₃)-Gly-Lys(Boc)-Tentagel® S-RAM was transferred to a flask and treated for 90 minutes with a cleavage cocktail (10 mL, TFA/TIS/H₂O, 190/5/5, v/v/v). The resin was filtered off into a cold mixture of diethylether/pentane (45 mL, 5/4, v/v) and the resin was washed off with neat TFA (3 x 1 mL) into the ether solution. This solution was centrifuged (10 minutes, 5000 rpm) after which the supernatant was removed and the precipitate was dried under nitrogen flow. Purification via RP-HPLC (linear-gradient 16-38% B, 10 min) yielded title compound **22** as a white powder after lyophilization (36.01 mg, 43.9 μmol, 43.9% (89% per step)). LC-MS: R_t = 4.80 min (0 - 90% ACN; 13 min); H NMR (400 MHz, DMSO) δ 8.33 - 8.20 (m, 3H, NH (G)), 8.14 (d, J = 7.3 Hz, 1H, NH (K)), 7.97 (d, J = 7.7 Hz, 1H, NH (K)), 7.90 (d, J = 7.8 Hz, 1H, NH (K)), 7.85 (d, J = 8.2 Hz, 1H, NH (K)), 7.70 (s, 2H, CH₂NH₂), 7.36 (s, 1H, (CO)N*H*H), 7.09 (s, 1H, (CO)NHH), 4.33 - 4.09 (m, 4H, CH), 3.87 - 3.63 (m, 6H, CH₂ (G)), 3.31 (tt, J = 6.9, 2.8 Hz, 6H, CH₂N₃), 2.76 (t, J = 7.2 Hz, 2H, CH₂NH₂), 1.86 (s, 3H, Ac), 1.76 - 1.20 (m, 24H, CH₂); $\frac{13}{12}$ C NMR (101 MHz, DMSO) δ 173.9, 172.7, 172.4, 172.3, 170.2, 169.4, 169.3, 169.0 (C=O), 53.2, 52.9, 52.5 (CH), 51.0 (CH₂N₃), 42.5 (CH₂ (G)), 39.2 (CH₂NH₂), 31.7, 28.4, 28.3, 27.1, 23.1 (CH₂), 22.9 (Ac), 22.9, 22.7 (CH₂); HRMS [C₃2H₅6N₁₈O₈ + H]+: 821.4608 found, 821.4601 calculated.

$Ac-Lys(N_3)-Lys(N_3)-Lys(N_3)-Lys(N_3)-Lys(N_3)-Gly-Lys-NH_2$ (23).

Ac-Lys(N₃)-Lys(N₃)-Lys(N₃)-Lys(N₃)-Lys(N₃)-Lys(N₃)-Lys(N₃)-Gly-Lys(Boc)-Tentagel® S-RAM was transferred to a flask and treated for 90 minutes with a cleavage cocktail (10 mL, TFA/TIS/H₂O, 190/5/5, v/v/v). The mixture was concentrated to approximately one mL after which the resin was filtered off into a cold mixture of diethylether/pentane (45 mL, 5/4, v/v) and the resin was washed off with neat TFA (3 x 1 mL) into the ether solution. This solution was centrifuged (10 minutes, 5000 rpm) after which the supernatant was removed and the precipitate was dried under nitrogen flow and dissolved (1mL, t-BuOH/ACN/H₂O, 1/1/1, v/v/v). Purification via RP-HPLC (linear-gradient 30-60% B, 10 min) yielded title compound **23** as a white powder after lyophilization (51.57 mg, 44.1 µmol, 44.1% (90% per step)). LC-MS: R_t = 6.70 min (0 - 90% ACN; 13 min); $\frac{1}{1}$ H NMR (400 MHz, DMSO) δ 8.14 (t, J = 5.6 Hz, 1H, NH (G)), 8.09 - 8.01 (m, 2H, NH (K)), 7.92 (dt, J = 18.6, 6.4 Hz, 5H, NH (K)), 7.70 (s, 2H, CH₂NH₂), 7.36 (s, 1H, (CO)NHH), 7.09 (s, 1H, (CO)NHH), 4.32 - 4.10 (m, 7H, CH), 3.78 - 3.72 (m, 2H, CH₂(G)), 3.34 - 3.26 (m, 12H, CH₂N₃), 2.76 (s, 2H, CH₂NH₂), 1.86 (s, 3H, Ac), 1.77 - 1.18 (m, 42H, CH₂); $\frac{13}{1}$ C NMR (101 MHz, DMSO) δ 173.4, 171.9, 171.8, 171.5, 171.4, 169.5, 168.5 (C=O), 52.3, 52.0 (CH), 50.5 (CH₂N₃), 42.5 (CH₂ (G)), 38.7 (CH₂NH₂), 31.4, 27.9, 26.7, 22.6 (CH₂), 22.5 (Ac), 22.4 (CH₂); $\frac{1}{1}$ HRMS [C₄6H₈0N₂8O₉ + H]+: 1169.6738 found, 1169.6736 calculated.

Ac-Lys(N₃)-AEEA-Gly-Lys(N₃)-Gly-Lys-NH2 (24).

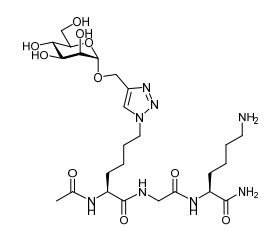
Ac-Lys(N₃)-AEEA-Gly-Lys(N₃)-Gly-Lys(Boc)-Tentagel® S-RAM was synthesized using the general protocol, with 1 hour couplings at rt after it was washed and transferred to a flask and treated for 90 minutes with a cleavage cocktail (10 mL, TFA/TIS/H₂O, 190/5/5, v/v/v). The mixture was concentrated to approximately one mL after which the resin was filtered off into a cold mixture of diethylether/pentane (45 mL, 5/4, v/v) and the resin was washed off with neat TFA (3 x 1 mL) into the ether solution. This solution was centrifuged (10 minutes, 5000 rpm) after which the supernatant was removed and the precipitate was dried under nitrogen flow and dissolved (1mL, t-BuOH/ACN/H₂O, 1/1/1, v/v/v). Purification via RP-HPLC (linear-gradient 30-60% B, 10 min) yielded title compound 24 as a white powder after lyophilization (22.57 mg, 29.6 µmol, 29.6% (82% per step)). LC-MS: R_t = 5.08 min (0 - 90% ACN; 13 min); $1H NMR (400 MHz, DMSO) \delta 8.28 (t, J = 5.7 Hz, 1H, NH), 8.17 (d, J = 7.6 Hz, 1H, NH), 8.04 –$ 7.96 (m, 2H, NH), 7.88 – 7.81 (m, 2H, NH), 7.72 (s, 2H, NH₂), 7.34 (s, 1H, CONHH), 7.08 (s, 1H, CONHH), 4.29 - 4.09 (m, 3H, CH (K)), 3.92 (s, 2H, O-CH₂-CO), 3.81 (t, J = 4.9 Hz, 2H, CH₂ (PEG)), 3.72 (t, J = 5.8 Hz, 2H, CH_2 (PEG)), 3.63 - 3.52 (m, 4H, CH_2 (G, 2x)), 3.41 (t, J = 5.9 Hz, 2H, CH_2 (PEG)), 3.30 (td, J = 6.8, 2.8 Hz, 4H, CH₂-N₃), 3.25 – 3.16 (m, 2H, CH₂ (PEG)), 2.75 (q, J = 6.5 Hz, 2H, CH₂-NH₂), 1.83 (s, 3H, Ac), 1.76 – 1.16 (m, 18H, CH₂ (K)); $\frac{13}{12}$ C NMR (101 MHz, DMSO) δ 173.9, 172.4, 172.3, 170.0, 169.7, 169.3, 169.0 (C=O), 70.7, 70.3, 69.8, 69.4 (CH₂ (PEG, 2x), CH₂ (G, 2x)), 53.0, 52.7, 52.5 (CH (K)), 51.0 (CH₂-N₃), 42.6, 41.9, 39.2 (CH₂ (PEG, 3x)), 38.9 (CH₂-NH₂), 32.1, 31.8, 31.7, 28.4, 27.1, 23.0, 23.0 (CH₂ (K)), 22.9 (Ac), 22.7(CH₂ (K)); HRMS [C₃₀H₅₄N₁₄O₉ + 2H]²⁺: 378.21718 found, 378.21719

General procedure for propargyl azide conjugation:

All solvents used in these reactions were degassed by sonicating while bubbling argon through the solutions. The "general click protocol" used was the following procedure: A solution of azidopeptides in DMSO (0.5 M, 1eq) was mixed with a solution of propargyl glycoside in water (0.5 M, 1.2eq per azide) followed by addition of an aliquot of a stock solution of CuI (0.1 eq), THPTA (0.3 eq) and DIPEA (0.2 eq) in water ([Cu⁺] = 0.5 M). The reaction was stirred at 40°C, and the process was followed via LC-MS. When reactions do not progress and turn blue, a sodium ascorbate solution (0.2 - 1 eq, 1 M, aq.) was added. Generally, reactions were stirred overnight at 40°C. When not complete after 16 hours, an extra aliquot of the copper stock was added. After completion a small amount of Quadrasil® AP (washed with water) was added, stirred for 1 h, filtered and applied on gel filtration (Toyopearl HW40S, 150 mM NH4HCO₃ (aq., in some cases a percentage of ACN was added to the elution buffer), 1.6x60 cm, 1 mL/min) followed by lyophilization.

calculated.

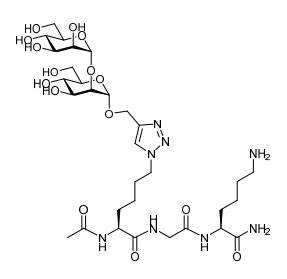
Ac-Lys(Man₁)-Gly-Lys-NH₂ (32).



Azide 20 (5.37 mg, 13.48 μ mol) was conjugated to propargyl mannoside 25 using the general click protocol. Compound 32 was obtained after purification by gel filtration (eluting buffer contains 10% ACN, eluted at 49.5 - 57 mL) followed by RP-HPLC (linear-gradient 8 - 16% B, 12 min) as a white powder (3.30 mg, 5.34 μ mol, 39%). LC-MS: $R_t = 4.01$ min (0 - 50% ACN; 13 min); $\frac{1}{1}$ NMR (400 MHz,

D₂O) δ 8.03 (s, 1H, trzl), 4.94 (d, J=1.6, 1H, H-1), 4.68 (d, J=12.5, 1H Hz, CHH), 4.42 (t, J=6.6 Hz, 2H), 4.27 (dd, J=9.4, 4.9 Hz, 1H), 4.18 (dd, J=8.7 Hz, 5.9, 1H), 3.97 - 3.52 (m, 8H), 2.94 (t, J=7.6 Hz, 2H), 1.98 (s, 3H, Ac), 1.96 - 1.56 (m, 8H), 1.51 - 1.18 (m, 4H); <u>HRMS</u> [C₂₅H₄₄N₈O₁₀ + H]⁺: 617.3254 found, 617.3253 calculated.

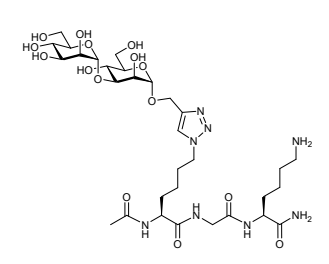
Ac-Lys(1,2-Man₂)-Gly-Lys-NH₂ (33).



Azide **20** (11.03 mg, 27.67 µmol) was conjugated to propargyl mannosides **26** using the general click protocol. Compound **33** was obtained after purification by gel filtration (eluted at 50-62 mL) followed by RP-HPLC (linear-gradient 8 - 16% B, 12 min) as a white powder (14.71 mg, 18.88 µmol, 68%). <u>LC-MS</u>: $R_t = 3.87$ min (0 - 50% ACN; 13 min); <u>1H NMR</u> (500 MHz, D₂O) δ 8.07 (s, 1H, trzl), 5.19 (d, J = 1.6 Hz, 1H, H-1), 5.01 (d, J = 1.8 Hz, 1H, H-1), 4.84 (d, J = 12.6 Hz, 1H, O-

CHH-trzl), 4.73 (d, J = 12.6 Hz, 1H, O-CHH-trzl), 4.47 (t, J = 6.9 Hz, 2H, CH₂-trzl), 4.32 (dd, J = 9.5, 5.0 Hz, 1H, CH), 4.23 (dd, J = 8.8, 5.7 Hz, 1H, CH), 4.08 (dd, J = 3.3, 1.8 Hz, 1H, H-2), 3.99 - 3.58 (m, 14H, CH, H-2', H-3, H-3', H-4, H-4', H-5, H-5', H-6, H-6', CH₂ (G)), 3.01 (td, J = 8.0, 2.1 Hz, 2H, CH₂-NH₂), 2.03 (s, 3H, Ac), 2.00 - 1.64 (m, 8H, CH₂), 1.54 - 1.24 (m, 4H, CH₂); HRMS [C₃₁H₅₄N₈O₁₅ + H]+: 779.3784 found, 779.3781 calculated.

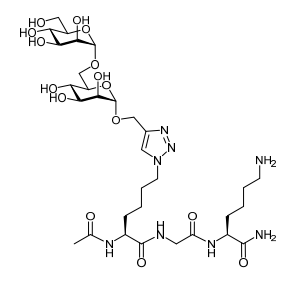
Ac-Lys(1,3-Man₂)-Gly-Lys-NH₂ (34).



Azide **20** (5.28 mg, 13.24 μ mol) was conjugated to propargyl mannosides **27** using the general click protocol. Compound **34** was obtained after purification by gel filtration (eluted at 42-55 mL) followed by RP-HPLC (linear-gradient 8 - 16% B, 12 min) as a white powder (10.16 mg, 13.05 μ mol, 99%). <u>LC-MS</u>: R_t = 3.89 min (0 - 50% ACN; 13 min); <u>1H NMR</u> (500 MHz, D₂O) δ 8.07 (s, 1H,

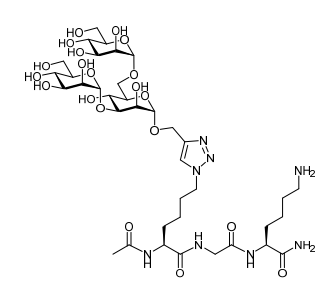
trzl), 5.12 (d, J = 1.6 Hz, 1H, H-1), 4.97 (d, J = 1.7 Hz, 1H, H-1'), 4.85 (d, J = 12.4 Hz, 1H, O-CHH-trzl), 4.76 - 4.72 (m, 1H, O-CHH-trzl), 4.47 (t, J = 7.1 Hz, 2H, CH₂-trzl), 4.32 (dd, J = 9.4, 5.0 Hz, 1H, CH), 4.23 (dd, J = 8.8, 5.8 Hz, 1H, CH), 4.09 (ddd, J = 12.9, 3.3, 1.8 Hz, 2H), 4.00 - 3.62 (m, 12H, CH₂ (G), H-2, H-2', H-3, H-3', H-4, H-4', H-5, H-5', H-6, H-6'), 3.06 - 2.95 (m, 2H, CH₂NH₂), 2.03 (s, 3H, Ac), 2.00 - 1.63 (m, 8H, CH₂), 1.54 - 1.27 (m, 4H, CH₂); H₂MS [C₃₁H₅₄N₈O₁₅ + H]⁺: 779.3785 found, 779.3781 calculated.

$Ac-Lys(1,6-Man_2)-Gly-Lys-NH_2$ (35).



Azide 20 (4.81 mg, 12.06 μmol) was conjugated to propargyl mannosides 28 using the general click protocol. Compound 35 was obtained after purification by gel filtration (eluted at 51 - 60 mL) followed by RP-HPLC (linear-gradient 8 - 16% B, 12 min) as a white powder (7.99 mg, 10.26 μ mol, 85%). <u>LC-MS</u>: $R_t = 3.95 \text{ min } (0.26 \text{ ms})$ - 50% ACN; 13 min); <u>HRMS</u> [C₃₁H₅₄N₈O₁₅ + H]⁺: 779.3785 found, 779.3781

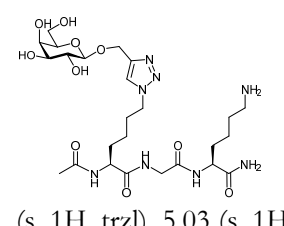
$Ac-Lys(Man_3)-Gly-Lys-NH_2$ (36).



Azide 20 (5.52 mg, 13.84 µmol) was conjugated to propargyl mannosides 29 using the general click protocol. Compound (36) was obtained after purification by gel filtration (eluted at 46 - 55 mL) followed by RP-HPLC (linear-gradient 8 - 16% B, 12 min) as a white powder (12.99 mg, 13.80 µmol, 99%). LC-MS: $R_t = 4.15 \text{ min } (0 - 50\% \text{ ACN}; 13 \text{ min}); \frac{1 \text{H NMR}}{2} (500 \text{ MHz}, 13 \text{ min}); \frac{1}{2} (500 \text{ min}); \frac$ D₂O) δ 8.06 (s, 1H, trzl), 5.09 (s, 1H), 4.94 (s, 1H), 4.90 (s, 1H, H-1, H-1', H-

1"), 4.82 (d, J = 12.4 Hz, 1H, O-CHH-trzl), 4.74 (d, J = 12.6 Hz, 1H, O-CHH-trzl), 4.46 (t, J = 6.8 Hz, 2H, CH2-trzl), 4.30 (dd, J = 9.4, 4.9 Hz, 1H, CH), 4.22 (dd, J = 8.6, 5.8 Hz, 1H, CH), 4.14 - 3.58 (m, 20H, $CH_2(G)$, H-2, H-2', H-3', H-3', H-3', H-4', H-4', H-5, H-5', H-5', H-6, H-6', H-6'), 3.00 (t, $J = \frac{1}{2}$ 7.4 Hz, 2H, CH₂NH₂), 2.02 (s, 3H, Ac), 1.92 - 1.23 (m, 18H, CH₂); HRMS [C₃₇H₆₄N₈O₂₀ + H]⁺: 941.4316 found, 941.4310 calculated.

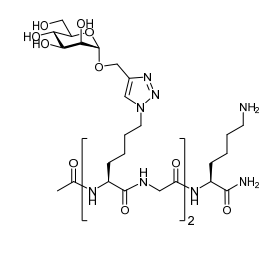
Ac-Lys(Gal)-Gly-Lys-NH2 (37).



Azide 20 (5.54 mg, 13.90 μmol) was conjugated to propargyl galactoside 30 using the general click protocol. Compound 37 was obtained after purification by gel filtration (eluted at 46.5 - 51 mL) as a white powder (4.93 mg, 7.99 µmol, 57%). <u>LC-MS</u>: $R_t = 4.02 \text{ min } (0 - 50\% \text{ ACN}; 13 \text{ min}); \frac{1 \text{H NMR}}{1} (500 \text{ MHz}, D_2O) \delta 7.97$ (s, 1H, trzl), 5.03 (s, 1H, H-1), 4.75 (d, J = 13.4 Hz, 1H, O-CHH-trzl), 4.73 - 4.67 (m, 1H, O-CHH-trzl), $4.39 \text{ (t, } J = 6.8 \text{ Hz, } 2\text{H, } \text{CH}_2\text{-trzl}), 4.23 \text{ (dd, } J = 9.5, 5.0 \text{ Hz, } 1\text{H, } \text{CH}), 4.14 \text{ (dd, } J = 8.7, 5.7 \text{ Hz, } 1\text{H, } \text{CH}),$

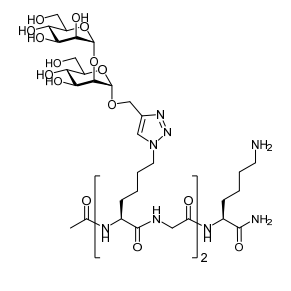
 $4.00 \text{ (dd, } I = 3.6, 1.7 \text{ Hz, } 2H, \text{CH}_2), 3.92 - 3.71 \text{ (m, } 4H, \text{H-2, H-3, H-4, H-5)}, 3.64 - 3.50 \text{ (m, } 2H, \text{H-6)}, 2.93$ (td, $J = 8.0, 2.1 \text{ Hz}, 2H, CH_2NH_2), 1.94$ (s, 3H, Ac), 1.92 - 1.14 (m, 12H, CH₂); HRMS $[C_{25}H_{44}N_8O_{10} +$ H]+: 617.32531 found, 617.3253 calculated.

Ac-Lys(Man₁)-Gly-Lys(Man₁)-Gly-Lys-NH₂ (38).



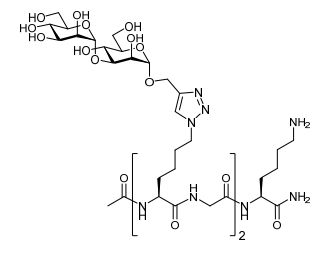
Azide 21 (17.00 mg, 27.89 umol) was conjugated to propargyl mannoside 25 using the general click protocol. Compound 38 was obtained after purification by gel filtration (eluted at 42-52 mL) as a white powder (17.66 mg, 16.88 µmol, 61%). LC- $\underline{MS}\!\!:R_t$ = 4.37 min (0 - 50% ACN; 13 min); $\underline{^1H\ NMR}$ (500 MHz, $D_2O)$ δ 8.07 (s, 2H, trzl), 4.98 (s, 2H, H-1), 4.84 (dd, J = 12.5, 2.1 Hz, 2H, O-CHH-trzl), 4.73 (d, J = 12.4 Hz, 2H, O-CHH-trzl), 4.51 - 4.42 (m, 4H, CH₂-trzl), 4.36 (d, J = 2.6 Hz, 1H), 4.34 - 4.19 (m, 3H, CH), 4.14 - 4.10 (m, 1H), 4.05 (d, J = 2.6 Hz, 2H), 4.03 - 3.57 (m, 16H, H-2, H-3, H-4, H-5, H-6, CH₂ (G)), 3.01 (t, J = 6.6 Hz, 2H, CH₂-NH₂), 2.01 (s, 3H, Ac), 1.98 - 1.23 (m, 18H, CH₂); HRMS [C₄₂H₇₁N₁₃O₁₈ + H]⁺: 1046.5118 found, 1046.5113 calculated.

Ac-Lys(1,2-Man₂)-Gly-Lys(1,2-Man₂)-Gly-Lys-NH₂ (39).



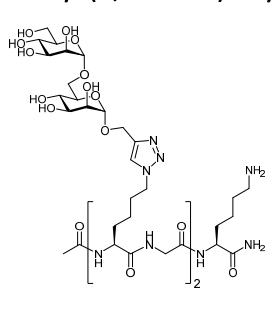
Azide **21** (4.58 mg, 7.51 µmol) was conjugated to propargyl mannosides **26** using the general click protocol. Compound **39** was obtained after purification by gel filtration (instead of HW40S resin a superdex30, 1.6x60 cm, column was used with 150 mM NH₄HCO₃ aq. 1 mL/min as elution buffer; eluted at 65 - 76 mL) as a white powder (4.27 mg, 3.12 µmol, 41%). <u>LC-MS</u>: $R_t = 4.31$ min (0 - 50% ACN; 13 min); <u>HRMS</u> [C₅₄H₉₁N₁₃O₂₈ + H]⁺: 1370.6175 found 1370.6169 calculated.

Ac-Lys(1,3-Man₂)-Gly-Lys(1,3-Man₂)-Gly-Lys-NH₂ (40).



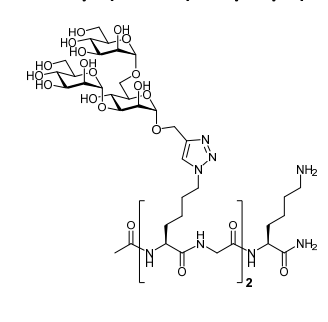
Azide **21** (8.14 mg, 13.36 µmol) was conjugated to propargyl mannosides **27** using the general click protocol. Compound **40** was obtained after purification by gel filtration (eluted at 38.5 - 46 mL) as a white powder (2.48 mg, 1.81 µmol, 14%). <u>LC-MS</u>: $R_t = 4.46$ min (0 - 50% ACN; 13 min); <u>HRMS</u> [$C_{54}H_{91}N_{13}O_{28} + H$]+: 1370.6176 found, 1370.6169 calculated.

Ac-Lys(1,6-Man₂)-Gly-Lys(1,6-Man₂)-Gly-Lys-NH₂ (41).



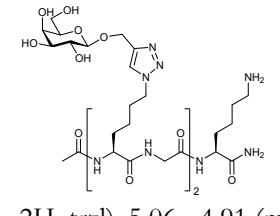
Azide **21** (4.22 mg, 6.92 µmol) was conjugated to propargyl mannosides **28** using the general click protocol. Compound **41** was obtained after purification by gel filtration (eluted at 39.5 - 47 mL) as a white powder (2.69 mg, 1.96 µmol, 28%). <u>LC-MS</u>: $R_t = 4.31 \text{ min}$ (0 - 50% ACN; 13 min); <u>HRMS</u> [$C_{54}H_{91}N_{13}O_{28} + H$]+: 1370.6177 found, 1370.6169 calculated.

Ac-Lys(Man₃)-Gly-Lys(Man₃)-Gly-Lys-NH₂ (42).



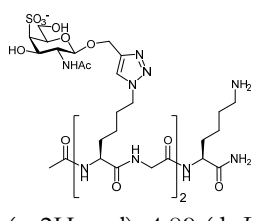
Azide **21** (7.91 mg, 12.98 µmol) was conjugated to propargyl mannosides **29** using the general click protocol. Compound **42** was obtained after purification by gel filtration (eluted at 34 - 44.5 mL) as a white powder (9.44 mg, 5.57 µmol, 43%). <u>LC-MS</u>: $R_t = 4.18 \text{ min}$ (0 - 50% ACN; 13 min); <u>HRMS</u> [$C_{66}H_{111}N_{13}O_{38} + H$]+: 1694.7229 found, 1694.7226 calculated.

Ac-Lys(Gal)-Gly-Lys(Gal)-Gly-Lys-NH₂ (43).



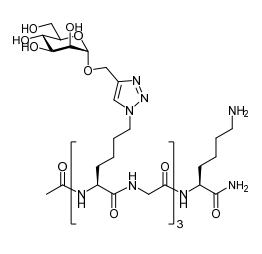
Azide 21 (6.07 mg, 9.95 μmol) was conjugated to propargyl galactoside 30 using the general click protocol. Compound 43 was obtained after purification by gel filtration (eluted at 44 - 52 mL) as a white powder (5.54 mg, 5.29 µmol, 53%). LC-MS: $R_t = 4.38 \text{ min } (0 - 50\% \text{ ACN}; 13 \text{ min}); \frac{1 \text{H NMR}}{2} (500 \text{ MHz}, D_2 O) \delta 7.97 \text{ (s,})$ 2H, trzl), 5.06 - 4.91 (m, 2H, H-1), 4.72 - 4.68 (m, 4H, O-CH₂-trzl), 4.38 (t, J = 6.7 Hz, 4H, CH₂-trzl), 4.27- 4.17 (m, 2H, CH), 4.14 (dd, I = 8.8, 5.7 Hz, 1H, CH), 4.04 - 3.98 (m, 4H, CH₂ (G)), 3.92 - 3.71 (m, 8H, H-2, H-3, H-4, H-5), 3.64 - 3.50 (m, 4H, H-6), 2.92 (td, J = 8.0, 2.2 Hz, 2H, CH_2NH_2), 1.93 (s, 3H, Ac), 1.91 - 1.07 (m, 18H, CH_2 (K)); HRMS [$C_{42}H_{71}N_{13}O_{18} + H$]+: 1046.51147 found, 1046.5113 calculated.

Ac-Lys(4-SO₃-GalNAc)-Gly-Lys(4-SO₃-GalNAc)-Gly-Lys-NH₂ (44).



Azide 21 (5.0 μL, 0.2 M, 1.0 μmol) was conjugated to propargyl mannosides 31 using the general click protocol. Compound 44 was obtained after purification by gel filtration (eluted at 34 - 44.5 mL) as a white powder (0.395 mg, 299 nmol, 30%). <u>LC-MS</u>: $R_t = 3.69 \text{ min } (0 - 50\% \text{ ACN}; 13 \text{ min}); {}^{1}H \text{ NMR} (400 \text{ MHz}, D_2O) \delta 7.98$ (s, 2H, trzl), 4.89 (d, J = 12.9 Hz, 2H, O-CHH-trzl), 4.76 (d, J = 1.8 Hz, 2H, O-CHH-trzl), 4.65 (d, J = 2.9Hz, 2H, H-1), 4.57 (d, J = 7.8 Hz, 2H, H-2), 4.41 (t, J = 6.8 Hz, 4H, CH₂-trzl), 4.24 (ddd, J = 11.8, 9.1, 5.3Hz, 2H, CH (K)), 4.17 (dd, J = 8.7, 5.8 Hz, 1H, CH (K)), 3.94 - 3.74 (m, 14H, H-3, H-4, H-5, H-6, CH₂ (G, 2x), 2.95 (t, J = 7.0 Hz, 2H, CH_2 -NH₂), 1.96 (s, 3H, Ac), 1.92 – 1.59 (m, 18H, NH $A\varepsilon$ (2x), CH₂ (K)), 1.46 - 1.20 (m, 6H, CH₂ (K)); <u>HRMS</u> [C₄₆H₇₇N₁₅O₂₄S₂ + 2H]²⁺: 644.74259 found, 644.74264 calculated.

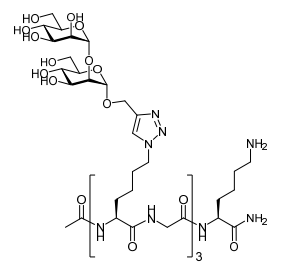
Ac-Lys(Man₁)-Gly-Lys(Man₁)-Gly-Lys(Man₁)-Gly-Lys-NH₂ (45).



Azide 22 (2.92 mg, 3.56 µmol) was conjugated to propargyl mannosides 25 using the general click protocol. Compound 45 was obtained after purification by gel filtration (eluted at 38-46 mL) followed by RP-HPLC as a white powder (3.61 mg, 2.44 μ mol, 69%). <u>LC-MS</u>: R_t = 4.60 min (0 - 50% ACN; 13 min); <u>1H NMR</u> (400 MHz, D₂O) δ 7.96 - 7.89 (m, 3H, trzl), 4.84 (s, 3H, H-1), 4.71 - 4.67 (m, 3H, O-

CHH-trzl), 4.58 (d, I = 12.5 Hz, 3H, O-CHH-trzl), 4.32 (t, I = 6.8 Hz, 6H, CH₂-trzl), 4.22 - 4.04 (m, 4H, CH), 3.90 - 3.43 (m, 24H, CH_2 (G), H-2, H-3, H-4, H-5, H-6), 2.87 (t, J=7.5 Hz, 2H, CH_2NH_2), 1.87 (s, 3H, Ac), 1.84 - 1.07 (m, 24H, CH₂); 13C NMR (101 MHz, D₂O) 8 143.4, 99.4 (C-1), 72.9, 70.4, 69.9, 66.6 (C-2, C-3, C-4, C-5), 60.8 (C-6), 28.7; <u>HRMS</u> $[C_{59}H_{98}N_{18}O_{26} + 2H]^{2+}$: 738.3528 found, 738.3523 calculated.

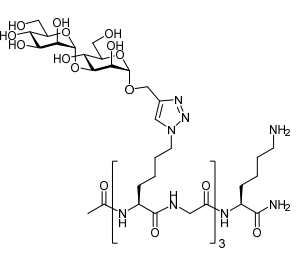
$Ac-Lys(1,2-Man_2)-Gly-Lys(1,2-Man_2)-Gly-Lys(1,2-Man_2)-Gly-Lys-NH_2$ (46).



Azide **22** (4.20 mg, 5.12 µmol) was conjugated to propargyl mannosides **26** using the general click protocol. Compound **46** was obtained after purification by gel filtration (eluted at 34 - 44.5 mL) as a white powder (8.01mg, 4.08 µmol, 80%). LC-MS: $R_t = 4.45 \text{ min } (0 - 50\% \text{ ACN}; 13 \text{ min}); \frac{1 \text{H NMR}}{1} (500 \text{ MHz}, D_2O) \delta 8.07 (d, <math>J = 2.3 \text{ Hz}, 3\text{H}, \text{trzl}), 5.18 (s, 3\text{H}, \text{H-1}), 5.01 (s, 3\text{H}, \text{H-1}'), 4.83 (d, <math>J = 12.4 \text{ Hz}, 3\text{H}, O\text{-CHH-trzl}), 4.72 (d, <math>J = 12.7 \text{ Hz}, 3\text{H}, O\text{-CHH-trzl}), 4.45 (t, <math>J = 6.9 \text{ Hz}, 6\text{H}, 6\text{Hz})$

CH₂-trzl), 4.30 (tt, J = 9.4, 5.1 Hz, 3H, CH), 4.23 (dd, J = 8.5, 6.0 Hz, 1H, CH), 4.08 (dd, J = 3.3, 1.8 Hz, 3H, H-2), 4.00 - 3.59 (m, 42H, CH₂ (G), H-2', H-3, H-3', H-4, H-4', H-5, H-5', H-6, H-6'), 3.01 (t, J = 7.0 Hz, 2H, CH₂NH₂), 2.01 (s, 3H, Ac), 1.98 - 1.60 (m, 16H, CH₂), 1.55 - 1.28 (m, 8H, CH₂); <u>HRMS</u> [C₇₇H₁₂₈N₁₈O₄₁ + H]⁺: 1961.8643 found, 1961.8557 calculated.

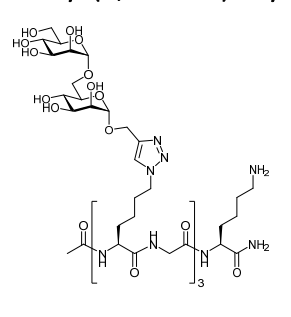
Ac-Lys(1,3-Man₂)-Gly-Lys(1,3-Man₂)-Gly-Lys(1,3-Man₂)-Gly-Lys-NH₂ (47).



Azide 22 (2.92 mg, 3.56 µmol) was conjugated to propargyl mannosides 27 using the general click protocol. Compound 47 was obtained after purification by gel filtration (buffer contains 10% ACN, eluted at 33.5 - 42.5 mL) as a white powder (5.71 mg, 2.91 µmol, 82%). <u>LC-MS</u>: R_t = 4.37 min (0 - 50% ACN; 13 min); <u>1H NMR</u> (400 MHz, D₂O) δ 7.99 - 7.84 (m, 3H, trzl), 4.98 (s, 3H, H-1),

4.83 (d, J = 1.5 Hz, 3H, H-1'), 4.76 - 4.66 (m, 3H, O-CHH-trzl), 4.60 (d, J = 12.4 Hz, 3H, O-CHH-trzl), 4.32 (t, J = 6.8 Hz, 6H, CH₂-trzl), 4.22 - 4.12 (m, 3H, CH), 4.09 (dd, J = 8.7, 5.6 Hz, 1H, CH), 4.00 - 3.42 (m, 42H, CH₂ (G), H-2, H-2', H-3, H-3', H-4, H-4', H-5, H-5', H-6, H-6'), 2.85 (t, J = 7.5 Hz, 2H, CH₂NH₂), 1.87 (s, 3H, Ac), 1.85 - 1.09 (m, 24H, CH₂); <u>HRMS</u> [C₇₇H₁₂₈N₁₈O₄₁ + H]+: 1961.8589 found 1961.8557 calculated.

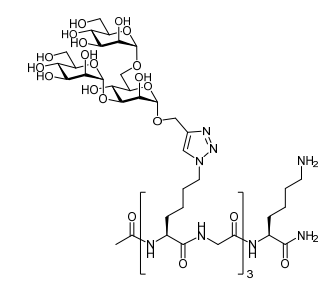
Ac-Lys(1,6-Man₂)-Gly-Lys(1,6-Man₂)-Gly-Lys(1,6-Man₂)-Gly-Lys-NH₂ (48).



Azide **22** (3.92 mg, 3.56 µmol) was conjugated to propargyl mannosides **28** using the general click protocol. Compound **48** was obtained after purification by gel filtration (eluted at 34 - 41.5 mL) as a white powder (5.96 mg, 3.04 µmol, 85%). LC-MS: $R_t = 4.37 \text{ min}$ (0 - 50% ACN; 13 min); ¹H NMR (500 MHz, D_2O) δ 8.03 - 7.91 (m, 3H, trzl), 4.88 (s, 3H, H-1), 4.83 (s, 3H, H-1'), 4.74 (d, J = 12.6 Hz, 3H, O-CHH-trzl), 4.64 (d, J = 12.5 Hz, 3H, O-CHH-trzl), 4.37 (t, J = 6.9 Hz, 6H,

CH₂-trzl), 4.21 (tt, J = 9.2, 5.3 Hz, 3H, CH), 4.14 (dd, J = 8.8, 5.7 Hz, 1H, CH), 3.95 - 3.56 (m, 42H, CH₂ (G), H-2, H-2', H-3, H-3', H-4, H-4', H-5, H-5', H-6, H-6'), 2.88 (t, J = 7.1 Hz, 2H, CH₂NH₂), 1.92 (s, 3H, Ac), 1.90 - 1.51 (m, 16H, CH₂), 1.44 - 1.14 (m, 8H, CH₂); <u>HRMS</u> [C₇₇H₁₂₈N₁₈O₄₁ + H]⁺: 1961.8616 found, 1961.8557 calculated.

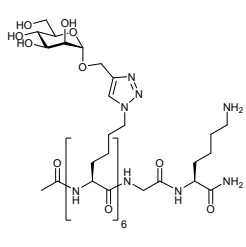
Ac-Lys(Man₃)-Gly-Lys(Man₃)-Gly-Lys(Man₃)-Gly-Lys-NH₂ (49).



Azide **22** (2.92 mg, 3.56 μmol) was conjugated to propargyl mannosides **29** using the general click protocol. Compound **49** was obtained after purification by gel filtration (eluted at 31- 39.5 mL) as a white powder (6.97 mg, 2.85 μmol, 80%). <u>LC-MS</u>: $R_t = 4.54$ min (0 - 50% ACN; 13 min); <u>1H NMR</u> (500 MHz, D₂O) δ 8.06 (d, J = 1.8 Hz, 3H, trzl), 5.10 (s, 3H), 4.95 (d, J = 1.5 Hz, 3H), 4.91 (d, J = 1.2 Hz, 3H, H-1, H-1' & H-1"), 4.83 (d, J = 12.7 Hz, 3H, O-CHH-

trzl), 4.74 (d, J = 12.6 Hz, 3H, O-CHH-trzl), 4.46 (t, J = 6.9 Hz, 6H, CH₂-trzl), 4.35 - 4.27 (m, 3H, CH), 4.23 (dd, J = 8.8, 5.7 Hz, 1H, CH), 4.13 - 3.60 (m, 60H, CH₂(G), H-2, H-2', H-2', H-3, H-3', H-3'', H-4, H-4'', H-5, H-5', H-5'', H-6, H-6', H-6''), 2.95 (t, J = 7.3 Hz, 2H, CH₂NH₂), 2.01 (s, 3H, Ac), 1.99 - 1.23 (m, 24H, CH₂); <u>HRMS</u> [C₉₅H₁₅₈N₁₈O₅₆ + 2H]²⁺: 1225.0138 found, 1225.01225 calculated.

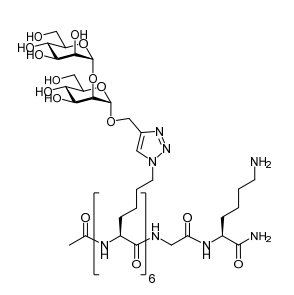
$Ac-Lys(Man_1)-Lys(Ma$



Azide **23** (2.51 mg, 2.15 μ mol) was conjugated to propargyl mannosides **25** using the general click protocol. Compound **50** was obtained after purification by gel filtration (buffer contained 20% ACN, eluted at 39-47 mL) as a white powder (4.31 mg, 1.76 μ mol, 82%). LC-MS: R_t = 4.73 min (0 - 50% ACN; 13 min); 1H NMR (500 MHz, D₂O) δ 8.03 (d, J = 5.1 Hz, 6H, trzl), 4.96 (d, J = 1.8 Hz, 6H, H-1), 4.89 - 4.71 (m,

146H, HDO, O-C*H*H-trzl), 4.67 (dd, J = 12.5, 2.9 Hz, 6H, O-CH*H*-trzl), 4.40 (t, J = 6.4 Hz, 12H, CH₂-trzl), 4.34 - 4.09 (m, 7H, CH (K)), 3.99 - 3.57 (m, 38H, H-2, H-3, H-4, H-5, H-6, CH₂ (G)), 3.05 - 2.98 (m, 2H, CH₂-NH₂), 2.01 (s, 3H, Ac), 1.97 - 1.20 (m, 42H, CH₂); $\frac{13}{12}$ C NMR (126 MHz, D₂O) δ 160.3, 143.5, 125.0 (CH-trzl), 99.5 (C-1), 73.0, 70.6, 70.0, 66.7 (C-2, C-3, C-4, C-5), 60.9 (C-6), 59.8 (O-*C*H₂-trzl), 50.1 (*C*H₂-trzl), 39.3 (CH₂-NH₂), 28.9, 22.1 (CH₂); HRMS [C₁₀₀H₁₆₄N₂₈O₄₅ + 2H]²⁺: 1240.0857 found, 1240.0790 calculated.

Ac-Lys(1,2-Man₂)-Lys(1,2-Man

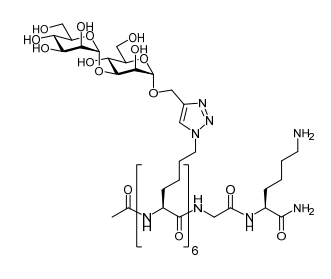


Azide 23 (3.84 mg, 3.28 μ mol) was conjugated to propargyl mannosides 26 using the general click protocol. Compound 51 was obtained after purification by gel filtration (buffer contained 20% ACN, eluted at 28 - 38 mL) as a white powder (11.10 mg, 3.21 μ mol, 98%). <u>LC-MS</u>: R_t = 4.51 min (0 - 50% ACN; 13 min); 1 H NMR (500 MHz, D₂O) δ 8.09 - 7.91 (m, 6H, trzl), 5.13 (s, 6H, H-1), 4.95 (s, 6H, H-1'), 4.74 (d, J=12.6, 6H, O-CHH-trzl), 4.63 (d, J=12.5, 6H, O-CHH-trzl), 4.36

(s, 12H, CH₂-trzl), 4.30 - 4.05 (m, 7H, CH), 4.02 (dd, J = 3.2, 1.7 Hz, 6H, H-2), 4.01 - 3.50 (m, 68H, CH₂ (G), H-2', H-3, H-3', H-4', H-5, H-5', H-6, H-6'), 2.98 - 2.92 (m, 2H, CH₂NH₂), 1.95 (s, 3H, Ac), 1.91 - 1.12 (m, 42H, CH₂); $\frac{13}{2}$ NMR (126 MHz, D₂O) δ 143.4, 125.0 (CH-trzl), 105.0 (CH₂), 102.3, 97.7 (C-1,

C-1'), 78.6, 73.2, 72.9, 70.3, 70.1, 69.9, 69.5, 66.8, 66.7, 60.9, 60.8, 59.8, 50.0, 22.0; <u>HRMS</u> [C₁₃₆H₂₂₄N₂₈O₇₅ + 2H]²⁺: 1726.2408 found, 1726.2375 calculated.

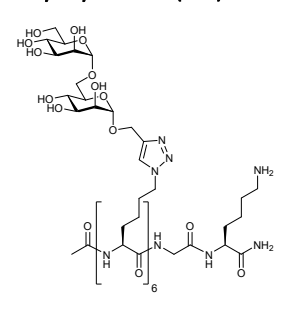
Ac-Lys(1,3-Man₂)-Lys(1,3-Man



Azide **23** (3.78 mg, 3.23 µmol) was conjugated to propargyl mannosides **27** using the general click protocol. Compound **52** was obtained after purification by gel filtration (eluted at 30.5 - 39 mL) as a white powder (11.04 mg, 3.19 µmol, 99%). <u>LC-MS</u>: $R_t = 4.63$ min (0 - 50% ACN; 13 min); <u>1H NMR</u> (500 MHz, D₂O) δ 7.92 (d, J = 4.1 Hz, 6H, trzl), 4.97 (s, 6H, H-1), 4.81 (s, 6H, H-1), 4.69 - 4.66 (m, 6H, O-CHH-trzl), 4.56 (d, J = 12.6 Hz, 6H, O-CHH-trzl),

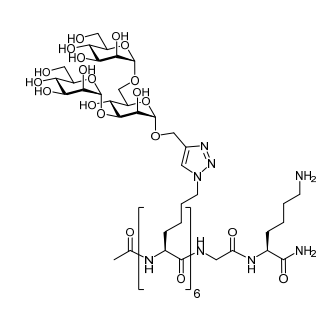
4.28 (s, 12H, CH₂-trzl), 4.19 - 3.97 (m, 7H, CH), 3.97 - 3.48 (m, 74H, CH₂ (G), H-2, H-2', H-3, H-3', H-4, H-4', H-5, H-5', H-6, H-6'), 2.79 - 2.72 (m, 2H, CH₂NH₂), 1.87 (s, 3H, Ac), 1.84 - 1.44 (m, 28H, CH₂), 1.40 - 1.05 (m, 14H, CH₂); 13 C NMR (126 MHz, D₂O) δ 143.5, 125.0, 102.4, 99.5 (C-1, C-1'), 78.3, 73.4, 73.1, 70.4, 70.1, 69.6, 66.8, 66.0, 61.0, 60.8, 59.9, 50.1, 28.9; 13 HRMS [C₁₃₆H₂₂₄N₂₈O₇₅ + 2H]²⁺: 1726.2405 found, 1726.2375 calculated.

Ac-Lys(1,6-Man₂)-Lys(1,6-Ma



Azide 23 (2.63 mg, 2.25 μ mol) was conjugated to propargyl mannosides 28 using the general click protocol. Compound 53 was obtained after purification by gel filtration (eluted at 36 - 50 mL) as a white powder (4.45 mg, 1.29 μ mol, 57%). <u>LC-MS</u>: R_t = 4.63 min (0 - 50% ACN; 13 min); <u>HRMS</u> [C₁₃₆H₂₂₄N₂₈O₇₅ + 2H]²⁺: 1726.2408 found, 1726.2375 calculated.

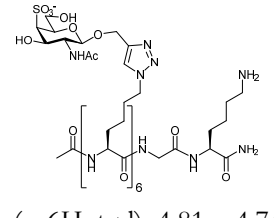
Ac-Lys(Man₃)-Lys(Man₃)-Lys(Man₃)-Lys(Man₃)-Lys(Man₃)-Lys(Man₃)-Gly-Lys-NH₂ (54).



Azide **23** (6.90 mg, 5.90 µmol) was conjugated to propargyl mannosides **29** using the general click protocol. Compound **54** was obtained after purification by gel filtration (eluted at 28 - 39 mL) as a white powder (22.22 mg, 5.02 µmol, 85%). <u>LC-MS</u>: $R_t = 4.34 \text{ min } (0 - 50\% \text{ ACN}; 13 \text{ min}); 1H NMR (500 MHz, D₂O) <math>\delta$ 8.01 (s, 6H, trzl), 5.04 (s, 6H), 4.89 (s, 6H), 4.86 (s, 6H, H-1, H-1', H-1''), 4.77 - 4.73 (m, 6H, O-CHH-trzl), 4.69 - 4.62 (m, 6H, O-CHH-trzl), 4.37

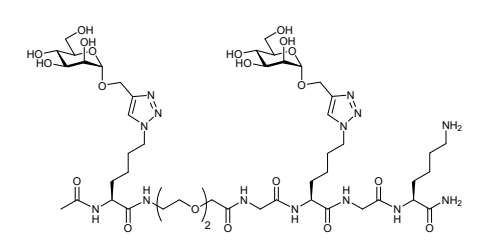
(s, 12H, CH₂-trzl), 4.28 - 4.14 (m, 7H, CH), 4.13 - 3.50 (m, 110H, CH₂(G), H-2, H-2', H-2", H-3, H-3', H-3", H-4, H-4', H-4", H-5, H-5', H-5", H-6, H-6', H-6"), 2.93 (t, J = 6.7 Hz, 2H, CH₂NH₂), 1.96 (s, 3H, Ac), 1.91 - 1.14 (m, 42H, CH₂); $\frac{13C}{13}$ NMR (126 MHz, D₂O) δ 143.4, 124.9, 102.4, 99.6, 99.4 (C-1,C-1'& C-1"), 78.6, 73.3, 72.6, 71.2, 70.6, 70.3, 70.0, 69.9, 69.5, 69.5, 66.7, 65.4, 64.9, 60.9, 60.0, 50.0, 39.2, 28.9, 22.0; $\frac{18}{12}$ HRMS [C₁₇₂H₂₈₄N₂₈O₁₀₅ + 2H]²⁺: 2212.9033 found, 2212.8975 calculated.

Ac-Lys(4-SO₃-GalNAc)-Lys GalNAc)-Lys(4-SO₃-GalNAc)-Gly-Lys-NH₂ (55).



Azide 23 (5.0 μL, 0.2 M, 1.0 μmol) was conjugated to propargyl mannosides 31 using the general click protocol. Compound 55 was obtained after purification by gel filtration (eluted at 28 - 39 mL) as a white powder (1.17 mg, 884 nmol, 88%). <u>LC-MS</u>: $R_t = 3.75 \text{ min } (0 - 50\% \text{ ACN}; 13 \text{ min}); \frac{1 \text{H NMR}}{1 \text{H NMR}} (400 \text{ MHz}, D_2O) \delta 7.87$ (s, 6H, trzl), 4.81 - 4.74 (m, 6H, O-CHH-trzl), 4.68 - 4.64 (m, 6H, O-CHH-trzl), 4.57 (d, J = 2.2 Hz, 6H, H-1), 4.47 (d, J = 7.4 Hz, 6H, H-2), 4.27 (d, J = 6.3 Hz, 12H, CH_2 -trzl), 4.19 - 3.93 (m, 7H, CH (K)), 3.84-3.64 (m, 32H, H-3, H-4, H-5, H-6, CH₂ (G)), 2.87 (t, J = 7.6 Hz, 2H, CH₂NH₂), 1.87 (s, 3H, Ac), 1.81 – 1.48 (m, 46H, NHAc (6x), CH₂ (K)), 1.20 (d, J = 7.0 Hz, 14H, CH₂ (K)); HRMS [C₁₁₂H₁₈₂N₃₄O₆₃S₆ + 3H]³⁺: 1069.02205 found, 1069.02176 calculated.

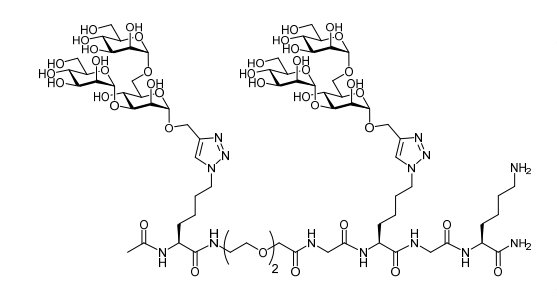
Ac-Lys(Man₁)-AEEA-Gly-Lys(Man₁)-Gly-Lys-NH2 (56).



Azide 24 (5.28 mg, 7.00 µmol) was conjugated to propargyl mannosides 25 using the general click protocol. Compound 56 was obtained after purification by gel filtration (buffer contained 20% ACN, eluted at 39.5 - 47.5 mL)_as a white powder (6.95 mg, 5.84 μ mol, 83%). <u>LC-MS</u>: $R_t = 4.11 \min (0 - 50\% ACN; 13 \min);$

<u>1H NMR</u> (400 MHz, D₂O) δ 8.01 (d, J = 1.4 Hz, 2H, trzl), 4.92 (d, J = 1.5 Hz, 2H, H-1), 4.79 – 4.75 (m, 2H, O-CHH-trzl), 4.67 (d, I = 2.3 Hz, 2H, O-CHH-trzl), 4.47 – 4.35 (m, 4H, CH₂-trzl), 4.25 (td, I = 9.2, 4, H-5, H-6, CH₂ (PEG, 3x), CH₂ (G, 2x)), 3.41 - 3.26 (m, 2H, CH₂ (PEG)), 2.95 (t, J = 7.5 Hz, 2H, CH₂-NH₂), 1.95 (s, 3H, Ac), 1.93 – 1.56 (m, 12H, CH₂ (K)), 1.48 – 1.14 (m, 6H, CH₂ (K)); HRMS [C₄₈H₈₂N₁₄O₂₁ + H] +: 1191.58528 found, 1191.58517 calculated.

Ac-Lys(Man₃)-AEEA-Gly-Lys(Man₃)-Gly-Lys-NH2 (57).

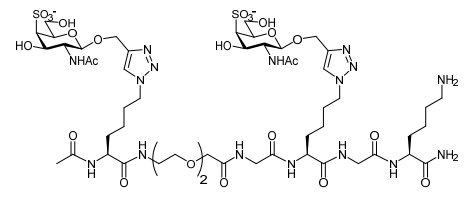


Azide 24 (5.28 mg, 7.00 µmol) was conjugated to propargyl mannosides 29 using the general click protocol. Compound 57 was obtained after purification by gel filtration (buffer contained 20% ACN, eluted at 38 - 46 mL) as a white powder (12.8 mg, 7.00 μ mol, 99%). <u>LC-MS</u>: $R_t = 3.89 \min (0 - 50\%)$ ACN; 13 min); 1 H NMR (400 MHz, D₂O) δ 8.01 (d, J = 1.7

Hz, 2H, trzl), 5.03 (d, I = 1.5 Hz, 2H), 4.89 (s, 2H), 4.85 (d, I = 1.4 Hz, 2H, H-1, H-1', H-1''), 4.77 – 4.75 (m, 2H, O-CHH-trzl), 4.68 (dd, J = 12.6, 1.5 Hz, 2H, O-CHH-trzl), 4.40 (q, J = 4.7 Hz, 4H, CH₂-trzl), 4.24(td, J = 8.6, 7.9, 5.5 Hz, 2H, CH (K)), 4.13 (dd, J = 8.6, 5.9 Hz, 1H, CH (K)), 4.09 (s, 2H, CH₂ (PEG)), 4.07- 3.53 (m, 46H, H-2, H-2', H-2', H-3, H-3', H-3', H-4, H-4', H-4', H-5, H-5', H-5', H-6, H-6', H-6', CH₂ $(PEG, 3x), CH_2(G, 2x)), 3.34 (q, J = 5.3 Hz, 2H, CH_2(PEG)), 2.95 (t, J = 7.5 Hz, 2H, CH_2-NH_2), 1.95 (s, J = 7.5 Hz,$

3H, Ac), 1.93 - 1.56 (m, 12H, CH_2 (K)), 1.46 - 1.15 (m, 6H, CH_2 (K)); <u>HRMS</u> [$C_{72}H_{122}N_{14}O_{41} + 2H$] ²⁺: 920.40110 found, 920.40187 calculated.

Ac-Lys(4-SO₃-GalNAc)-AEEA-Gly-Lys(4-SO₃-GalNAc)-Gly-Lys-NH2 (58).



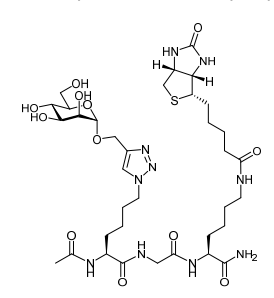
Azide 24 (5.0 μ L, 0.2 M, 1.0 μ mol) was conjugated to propargyl mannosides 31 using the general click protocol. Compound 58 was obtained after purification by gel filtration (buffer contained 20% ACN, eluted at 38 - 46 mL) as a white powder (0.25 mg, 167

nmol, 17%). <u>LC-MS</u>: $R_t = 3.91 \text{ min } (0 - 50\% \text{ ACN}; 13 \text{ min}); \frac{1 \text{H NMR}}{1} (400 \text{ MHz}, \text{D}_2\text{O}) \delta 7.99 (d, \textit{J} = 2.3 \text{ Hz}, 2\text{H, trzl}), 4.90 (d, \textit{J} = 12.9 \text{ Hz}, 2\text{H, O-CHH-trzl}), 4.81 - 4.72 (m, 2\text{H, O-CHH-trzl}), 4.66 (d, \textit{J} = 2.8 \text{ Hz}, 2\text{H, H-1}), 4.58 (d, \textit{J} = 7.8 \text{ Hz}, 2\text{H, H-2}), 4.41 (q, \textit{J} = 3.5 \text{ Hz}, 4\text{H, CH}_2\text{-trzl}), 4.29 - 4.21 (m, 2\text{H, CH}_2\text{Hz}), 4.18 - 4.11 (m, 1\text{H, CH (K)}), 4.10 (s, 2\text{H, CH}_2\text{ (PEG)}), 4.04 - 3.63 (m, 18\text{H, H-3}, \text{H-4}, \text{H-5}, \text{H-6}, \text{CH}_2\text{ (PEG}, 2x), \text{CH}_2\text{ (G, 2x)}), 3.57 (t, \textit{J} = 5.5 \text{ Hz}, 2\text{H, CH}_2\text{ (PEG)}), 3.41 - 3.30 (m, 2\text{H, CH}_2\text{ (PEG)}), 2.96 (t, \textit{J} = 7.3 \text{ Hz}, 2\text{H, CH}_2\text{NH}_2), 1.96 (s, 3\text{H, Ac}), 1.93 - 1.57 (m, 18\text{H, NH}_4c (2x), \text{CH}_2\text{ (K)}), 1.48 - 1.18 (m, 6\text{H, CH}_2\text{ (K)}); <u>HRMS</u> [C₅₂H₈₈N₁₆O₂₇S₂ + 2\text{H}]²⁺: 717.27926 found, 717.27959 calculated.$

General procedure for biotinylation:

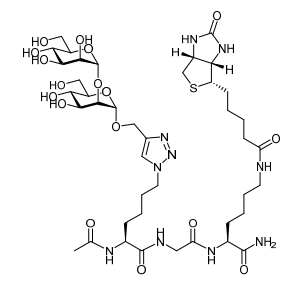
The "general procedure" to introduce the biotin handle: Glycoclusters described above with a free amine were dissolved in DMSO (0.02 M). To this, a stock solution of Biotin-NHS (0.15 M, 3-4 eq) and DIPEA (0.015 M, 0.3-0.4 eq) in DMSO was added and shaken overnight after which compounds were purified via RP-HPLC (linear gradient 10 - 16 % B in A, 12 min, 5 mL/min, Develosil RPAQUEOUS 10.0 x 250 mm) followed by lyophilization.

Ac-Lys(Man₁)-Gly-Lys(biotin)-NH₂(59).



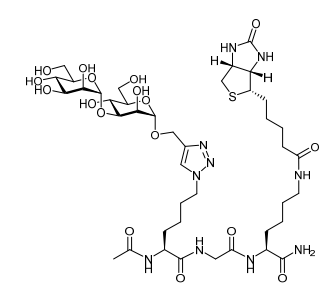
Compound **32** (1.01 mg, 1.64 μ mol) was coupled with biotin-NHS using the general procedure. Compound **59** was obtained after purification by RP-HPLC as a white powder (1.37 mg, 1.62 μ mol, 99%). <u>LC-MS:</u> R_t = 5.28 min (0 - 50% ACN; 13 min); <u>HRMS</u> [C₃₅H₅₈N₁₀O₁₂S + H]+: 843.4031 found, 843.4029 calculated.

Ac-Lys(1,2-Man₂)-Gly-Lys(biotin)-NH₂(60).



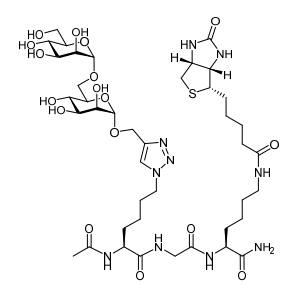
Compound **33** (8.97 mg, 11.51 µmol) was coupled with biotin-NHS using the general procedure. Compound **60** was obtained after purification by RP-HPLC as a white powder (1.90 mg, 1.89 µmol, 16%). <u>LC-MS:</u> $R_t = 5.18 \text{ min}$ (0 - 50% ACN; 13 min); <u>HRMS</u> $[C_{41}H_{68}N_{10}O_{17}S + 2H]^{2+}$: 503.2315 found, 503.2315 calculated.

Ac-Lys(1,3-Man₂)-Gly-Lys(biotin)-NH₂ (61).



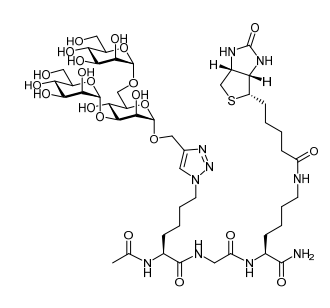
Compound **34** (6.46 mg, 8.30 µmol) was coupled with biotin-NHS using the general procedure. Compound **61** was obtained after purification by RP-HPLC as a white powder (1.44 mg, 1.44 µmol, 17%). <u>LC-MS:</u> $R_t = 5.23 \text{ min}$ (0 - 50% ACN; 13 min); <u>HRMS</u> [C₄₁H₆₈N₁₀O₁₇S +2H]²⁺: 503.2316 found, 503.2315 calculated.

Ac-Lys(1,6-Man₂)-Gly-Lys(biotin)-NH₂ (62).



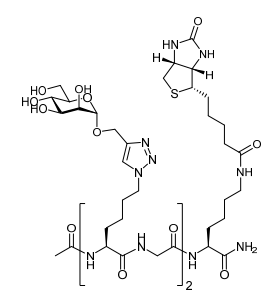
Compound **35** (1.50 mg, 1.93 µmol) was coupled with biotin-NHS using the general procedure. Compound **62** was obtained after purification by RP-HPLC as a white powder (0.97 mg, 0.97 µmol, 50 %). <u>LC-MS:</u> $R_t = 5.23 \text{ min}$ (0 - 50% ACN; 13 min); <u>HRMS</u> $[C_{41}H_{68}N_{10}O_{17}S + 2H]^{2+}$: 503.2314 found, 503.2315 calculated.

Ac-Lys(Man₃)-Gly-Lys(biotin)-NH₂ (63).



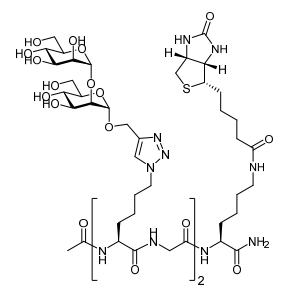
Compound **36** (8.25 mg, 8.77 µmol) was coupled with biotin-NHS using the general procedure. Compound **63** was obtained after purification by RP-HPLC as a white powder (1.48 mg, 1.26 µmol, 14%). <u>LC-MS</u>: $R_t = 5.15$ min (0 - 50% ACN; 13 min); <u>HRMS</u> [C₄₇H₇₈N₁₀O₂₂S + 2H]²⁺: 584.2582 found, 584.2579 calculated.

Ac-Lys(Man₁)-Gly-Lys(Man₁)-Gly-Lys(biotin)-NH₂(64).



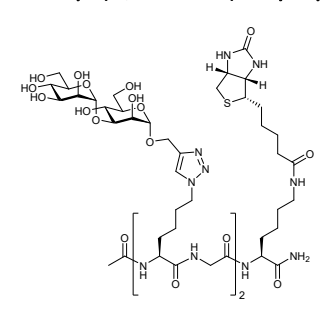
Compound **38** (11.06 mg, 10.57 µmol) was coupled with biotin-NHS using the general procedure. Compound **64** was obtained after purification by RP-HPLC as a white powder (2.62 mg, 2.06 µmol, 19%). <u>LC-MS:</u> $R_t = 5.30 \text{ min } (0 - 50\% \text{ ACN}; 13 \text{ min}); \frac{HRMS}{LC-MS} [C_{52}H_{85}N_{15}O_{20}S + 2H]^{2+}: 636.7984 found, 636.7981 calculated.$

$Ac-Lys(1,2-Man_2)-Gly-Lys(1,2-Man_2)-Gly-Lys(biotin)-NH_2 (65).$



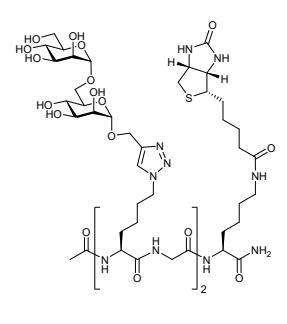
Compound **39** (2.67 mg, 1.95 μ mol) was coupled with biotin-NHS using the general procedure. Compound **65** was obtained after purification by RP-HPLC as a white powder (1.52 mg, 0.95 μ mol, 49%). <u>LC-MS</u>: $R_t = 5.14 \min (0 - 50\% ACN; 13 \min); <u>HRMS</u> [C₆₄H₁₀₅N₁₅O₃₀S+2H]²⁺: 798.8514 found, 798.8509 calculated.$

Ac-Lys(1,3-Man₂)-Gly-Lys(1,3-Man₂)-Gly-Lys(biotin)-NH₂ (66).



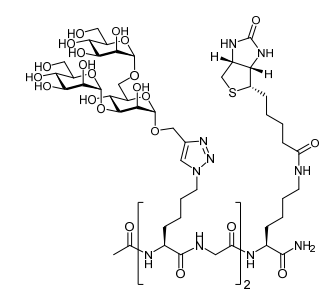
Compound **40** (1.50 mg, 1.10 µmol) was coupled with biotin-NHS using the general procedure. Compound **66** was obtained after purification by RP-HPLC as a white powder (1.74 mg, 1.09 µmol, 99%). <u>LC-MS</u>: $R_t = 5.18$ min (0 - 50% ACN; 13 min); <u>HRMS</u> $[C_{64}H_{105}N_{15}O_{30}S+2H]^{2+}$: 798.8516 found, 798.8509 calculated.

Ac-Lys(1,6-Man₂)-Gly-Lys(1,6-Man₂)-Gly-Lys(biotin)-NH₂ (67).



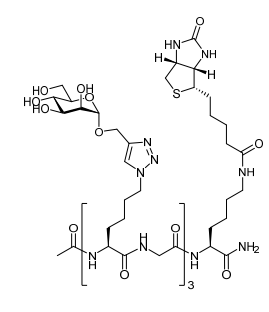
Compound **41** (1.68 mg, 1.22 µmol) was coupled with biotin-NHS using the general procedure. Compound **67** was obtained after purification by RP-HPLC as a white powder (1.48 mg, 0.93 µmol, 76%). <u>LC-MS</u>: $R_t = 5.11$ min (0 - 50% ACN; 13 min); <u>HRMS</u> [$C_{64}H_{105}N_{15}O_{30}S + 2H$]²⁺: 798.8512 found, 798.8509 calculated.

Ac-Lys(Man₃)-Gly-Lys(Man₃)-Gly-Lys(biotin)-NH₂ (68).



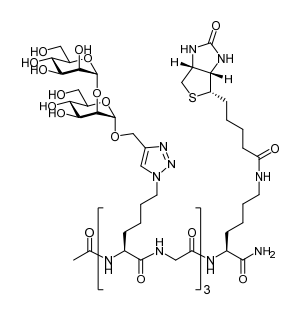
Compound **42** (6.02 mg, 3.55 μ mol) was coupled with biotin-NHS using the general procedure. Compound **68** was obtained after purification by RP-HPLC as a white powder (3.34 mg, 1.74 μ mol, 49%). <u>LC-MS:</u> $R_t = 5.02$ min (0 - 50% ACN; 13 min); <u>HRMS</u> [C₇₆H₁₂₅N₁₅O₄₀S+ 2H]²⁺: 960.9051 found, 960.9037 calculated.

$Ac-Lys(Man_1)-Gly-Lys(Man_1)-Gly-Lys(biotin)-NH_2(69)$.



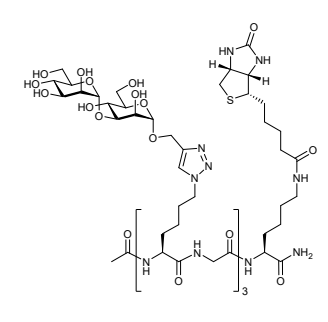
Compound **45** (2.63 mg, 1.78 µmol) was coupled with biotin-NHS using the general procedure. Compound **69** was obtained after purification by RP-HPLC as a white powder (1.92 mg, 1.13 µmol, 63%). <u>LC-MS:</u> $R_t = 5.26 \text{ min } (0 - 50\% \text{ ACN}; 13 \text{ min});$ <u>HRMS</u> $[C_{69}H_{112}N_{20}O_{28}S + 2H]^{2+}$: 851.3912 found, 851.3911 calculated.

Ac-Lys(1,2-Man₂)-Gly-Lys(1,2-Man₂)-Gly-Lys(1,2-Man₂)-Gly-Lys(biotin)-NH₂ (70).



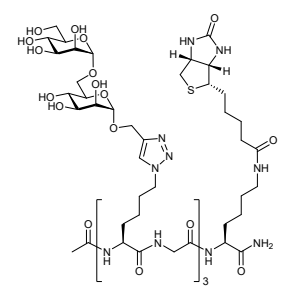
Compound **46** (4.91 mg, 2.50 μ mol) was coupled with biotin-NHS using the general procedure. Compound **70** was obtained after purification by RP-HPLC as a white powder (1.82 mg, 0.83 μ mol, 33%). <u>LC-MS:</u> R_t = 5.07 min (0 - 50% ACN; 13 min); <u>HRMS</u> [C₈₇H₁₄₂N₂₀O₄₃S + 2H]²⁺: 1094.9727 found, 1094.9718 calculated.

$Ac-Lys(1,3-Man_2)-Gly-Lys(1,3-Man_2)-Gly-Lys(biotin)-NH_2$ (71).



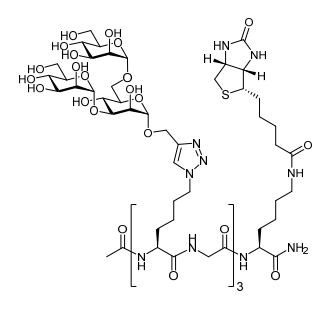
Compound 47 (3.53 mg, 1.80 μ mol) was coupled with biotin-NHS using the general procedure. Compound 71 was obtained after purification by RP-HPLC as a white powder (3.78 mg, 1.72 μ mol, 96%). <u>LC-MS</u>: R_t = 5.13 min (0 - 50% ACN; 13 min); <u>HRMS</u> [C₈₇H₁₄₂N₂₀O₄₃S + 2H]²⁺: 1094.9719 found, 1094.9718 calculated.

$Ac-Lys(1,6-Man_2)-Gly-Lys(1,6-Man_2)-Gly-Lys(biotin)-NH_2$ (72).



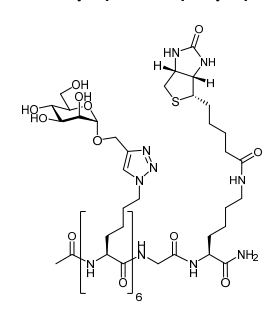
Compound **48** (3.53 mg, 1.80 μ mol) was coupled with biotin-NHS using the general procedure. Compound **72** was obtained after purification by RP-HPLC as a white powder (3.55 mg, 1.62 μ mol, 90%). <u>LC-MS</u>: R_t = 5.09 min (0 - 50% ACN; 13 min); <u>HRMS</u> [C₈₇H₁₄₂N₂₀O₄₃S + 2H]²⁺: 1094.9721 found, 1094.9718 calculated.

Ac-Lys(Man₃)-Gly-Lys(Man₃)-Gly-Lys(biotin)-NH₂ (73).



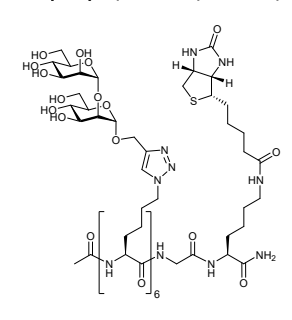
Compound **49** (4.41 mg, 1.80 μ mol) was coupled with biotin-NHS using the general procedure. Compound **73** was obtained after purification by RP-HPLC as a white powder (2.44 mg, 0.91 μ mol, 51%). <u>LC-MS</u>: $R_t = 4.94$ min (0 - 50% ACN; 13 min); <u>HRMS</u> [$C_{105}H_{172}N_{20}O_{58}S + 2H]^{2+}$: 1338.0503 found, 1338.0510 calculated.

$Ac-Lys(Man_1)-Lys(Ma$



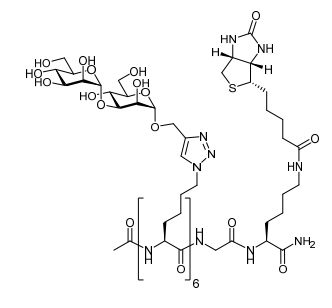
Compound **50** (1.75 mg, 0.72 µmol) was coupled with biotin-NHS using the general procedure. Compound **74** was obtained after purification by RP-HPLC as a white powder (1.14 mg, 0.42 µmol, 59%). <u>LC-MS:</u> $R_t = 5.26 \, \text{min} \, (0 - 50\% \, \text{ACN}; 13 \, \text{min});$ <u>HRMS</u> [C₁₁₀H₁₇₈N₃₀O₄₇S + 2H]²⁺: 1353.1169 found, 1353.1178 calculated.

Ac-Lys(1,2-Man₂)-Lys(1,2-Ma



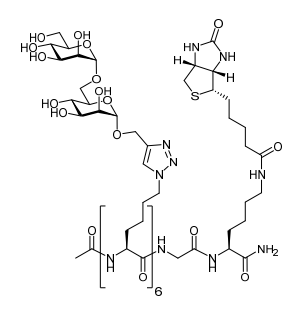
Compound **51** (5.24 mg, 1.60 µmol) was coupled with biotin-NHS using the general procedure. Compound **75** was obtained after purification by RP-HPLC as a white powder (3.65 mg, 0.99 µmol, 62%). <u>LC-MS:</u> $R_t = 4.94 \text{ min } (0 - 50\% \text{ ACN}; 13 \text{ min}); <u>HRMS</u> [<math>C_{146}H_{238}N_{30}O_{77}S + 3H]^{3+}$: 1226.5201 found, 1226.5200 calculated.

Ac-Lys(1,3-Man₂)-Lys(1,3-Ma



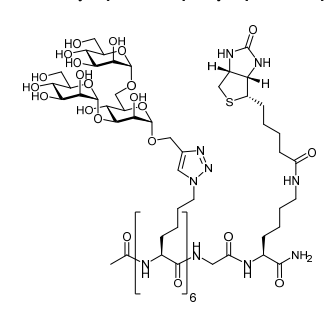
Compound **52** (5.24 mg, 1.60 µmol) was coupled with biotin-NHS using the general procedure. Compound **76** was obtained after purification by RP-HPLC as a white powder (3.65 mg, 0.99µmol, 62%). <u>LC-MS</u>: $R_t = 5.00$ min (0 - 50% ACN; 13 min); <u>HRMS</u> [$C_{146}H_{238}N_{30}O_{77}S + 3H$]³⁺: 1226.5195 found, 1226.5200 calculated.

Ac-Lys(1,6-Man₂)-Lys(1,6-Ma



Compound **53** (1.82 mg, 0.53 µmol) was coupled with biotin-NHS using the general procedure. Compound **77** was obtained after purification by RP-HPLC as a white powder (1.08 mg, 0.29 µmol, 56%). <u>LC-MS</u>: $R_t = 4.94 \text{ min } (0 - 50\% \text{ ACN}; 13 \text{ min}); <u>HRMS</u> [C₁₄₆H₂₃₈N₃₀O₇₇S + 3H]³⁺: 1226.5203 found, 1226.5200 calculated.$

Ac-Lys(Man₃)-Lys(Man₃)-Lys(Man₃)-Lys(Man₃)-Lys(Man₃)-Lys(Man₃)-Gly-Lys(biotin)-NH₂ (78).

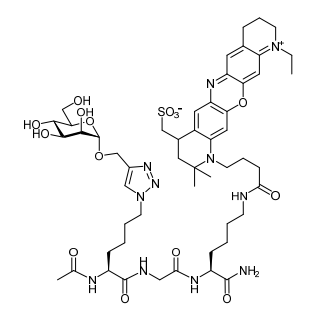


Compound **54** (8.40 mg, 1.90 μ mol) was coupled with biotin-NHS using the general procedure. Compound **78** was obtained after purification by RP-HPLC as a white powder (7.50 mg, 1.61 μ mol, 85%). <u>LC-MS</u>: $R_t = 4.68$ min (0 - 50% ACN; 13 min); <u>HRMS</u> [$C_{182}H_{298}N_{30}O_{107}S + 3H$]³⁺: 1550.9603 found, 1550.9599 calculated.

General procedure to introduce ATTO655:

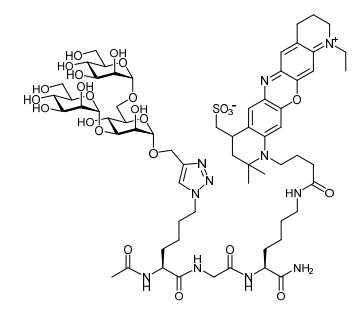
Glycoclusters with a free amine were dissolved in DMSO (2.0 mM). To this, a stock solution of ATTO655-NHS (5.0 mM, 2 eq) and DIPEA (0.01 M, 2 eq) in DMSO was added and shaken protected from light for one hour. After which the product was isolated either via RP-HPLC (linear gradient B in A, Gemini-NX 5μm C18, 110 Å, 250 x 10.0 mm, 5 mL/min, collection on λ: 610 nm), or gel filtration (Toyopearl HW-40S, 150 mM NH₄HCO₃ aq. with 20% ACN, 1.6x60 cm, UV monitoring λ: 610 nm) followed by lyophilization.

Ac-Lys(Man₁)-Gly-Lys(ATTO655)-NH₂ (79).



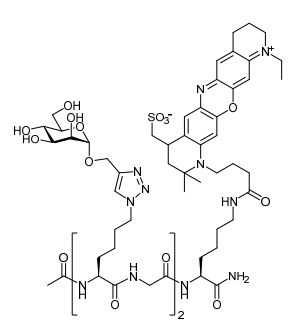
Compound **32** (267 nmol) was coupled with ATTO655-NHS using the general procedure. Compound **79** was obtained after purification by gel filtration (eluted at 130 - 165 mL) as a blue powder after lyophilization (0.265 mg, 235 nmol, 88%). LC-MS: $R_t = 6.01 \text{ min } (0 - 50\% \text{ ACN}; 13 \text{ min}); \frac{HRMS}{C_{52}H_{75}N_{11}O_{15}S} + 2H]^{2+}: 563.76566$ found, 563.76552 calculated.

Ac-Lys(Man₃)-Gly-Lys(ATTO655)-NH₂ (80).



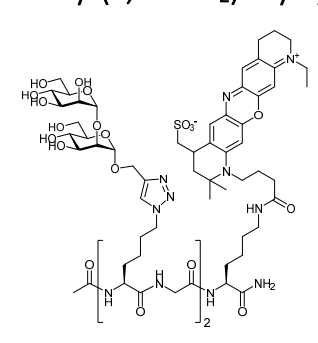
Compound **36** (200 nmol) was coupled with ATTO655-NHS using the general procedure. Compound **80** was obtained after purification by gel filtration (eluted at 95 - 110 mL) as a blue powder after lyophilization (0.245 mg, 169 nmol, 84%). <u>LC-MS:</u> $R_t = 6.83 \text{ min } (0 - 50\% \text{ ACN; } 13 \text{ min}); \underline{HRMS}$ $[C_{64}H_{95}N_{11}O_{25}S + 2H]^{2+}$: 725.81835 found, 725.81834 calculated.

$Ac-Lys(Man_1)-Gly-Lys(Man_1)-Gly-Lys(ATTO655)-NH_2 (81).$



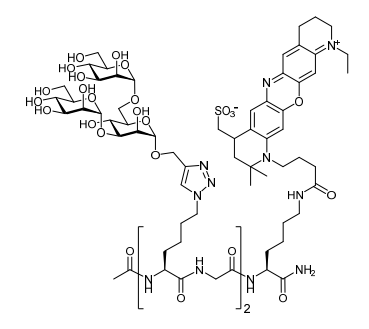
Compound **38** (200 nmol) was coupled with ATTO655-NHS using the general procedure. Compound **81** was obtained after purification by RP-HPLC (5 - 50 % B in A, 10 min) as a blue powder after lyophilization (0.140 mg, 89 nmol, 45%). <u>LC-MS</u>: $R_t = 6.05 \text{ min}$ (0 - 50% ACN; 13 min); <u>HRMS</u> [$C_{69}H_{102}N_{16}O_{23}S + 2H$]²⁺: 778.35840 found, 778.35850 calculated.

$Ac-Lys(1,2-Man_2)-Gly-Lys(1,2-Man_2)-Gly-Lys(ATTO655)-NH_2(82)$.



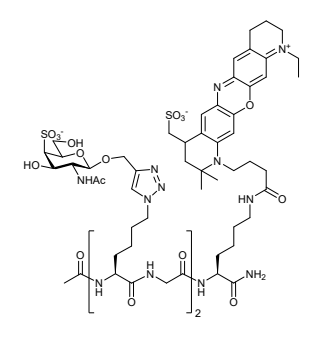
Compound **39** (100 nmol) was coupled with ATTO655-NHS using the general procedure. Compound **82** was obtained after purification by RP-HPLC (5 - 50 % B in A, 10 min) as a blue powder after lyophilization (0.18 mg, 95 nmol, 95%). <u>LC-MS:</u> $R_t = 5.95 \text{ min}$ (0 - 50% ACN; 13 min); <u>HRMS</u> $[C_{81}H_{122}N_{16}O_{33}S + 2H]^{2+}$: 940.41153 found, 940.41132 calculated.

Ac-Lys(Man₃)-Gly-Lys(Man₃)-Gly-Lys(ATTO655)-NH₂ (83).



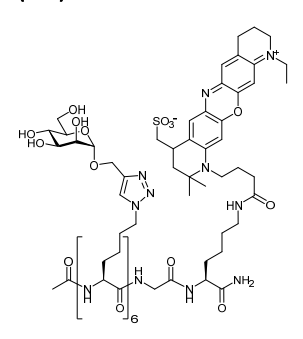
Compound 42 (200 nmol) was coupled with ATTO655-NHS using the general procedure. Compound 83 was obtained after purification by RP-HPLC (5 - 50 % B in A, 10 min) as a blue powder after lyophilization (0.45 mg, 204 nmol, qnt). <u>LC-MS</u>: $R_t = 5.86$ min (0 - 50% ACN; 13 min); <u>HRMS</u> $[C_{93}H_{142}N_{16}O_{43}S + 2H]^{2+}$: 1102.96588 found, 1102.96567 calculated.

Ac-Lys(4-SO₃-GalNAc)-Gly-Lys(4-SO₃-GalNAc)-Gly-Lys(ATTO655)-NH₂ (84).



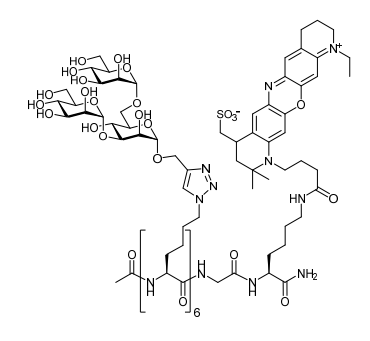
Compound **44** (100 nmol) was coupled with ATTO655-NHS using the general procedure. Compound **84** was obtained after purification by RP-HPLC (linear-gradient 7 - 46 % B in A, 10 min) as a blue powder after lyophilization (5.82 nmol, 6%, ABS = 0.364 (2 mL, λ = 663 nm)). <u>LC-MS</u>: R_t = 5.29 min (0 - 50% ACN; 13 min); <u>HRMS</u> [C₇₃H₁₀₈N₁₈O₂₉S₃ + 2H]²⁺: 899.34175 found, 899.34186 calculated.

Ac-Lys(Man₁)-Lys(Man₁)-Lys(Man₁)-Lys(Man₁)-Lys(Man₁)-Gly-Lys(ATTO655)-NH₂ (85).



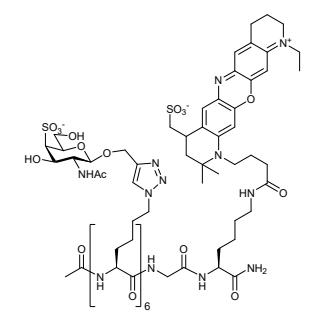
Compound **50** (293 nmol) was coupled with ATTO655-NHS using the general procedure. Compound **85** was obtained after purification by gel filtration (eluted at 46 - 58 mL) as a blue powder after lyophilization (0.54 mg, 180 nmol, 62%). LC-MS: $R_t = 5.46 \, \text{min} \, (0 - 50\% \, \text{ACN}; 13 \, \text{min}); \frac{HRMS}{LC-MS-1000} \, [C_{127}H_{195}N_{31}O_{50}S + 3H]^{3+}: 996.78798 \, \text{found}, 996.78791 \, \text{calculated}.$

Ac-Lys(1,2-Man₂)-Lys(1,2-Ma



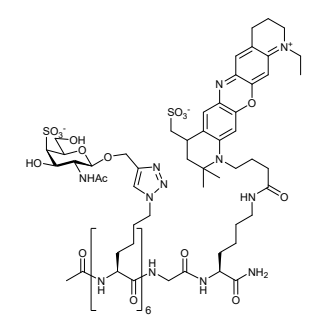
Compound **51** (100 nmol) was coupled with ATTO655-NHS using the general procedure. Compound **86** was obtained after purification by gel filtration (eluted at 36 - 48 mL) as a blue powder after lyophilization (34 nmol, 34%, ABS = 1.063 (4 mL, λ = 663 nm)). <u>LC-MS</u>: R_t = 5.32 min (0 - 50% ACN; 13 min); <u>HRMS</u> [C₁₆₃H₂₅₅N₃₁O₈₀S + 3H]³⁺: 1320.89485 found, 1320.89359 calculated.

Ac-Lys(Man₃)-Lys(Man₃)-Lys(Man₃)-Lys(Man₃)-Lys(Man₃)-Gly-Lys(ATTO655)-NH₂ (87).



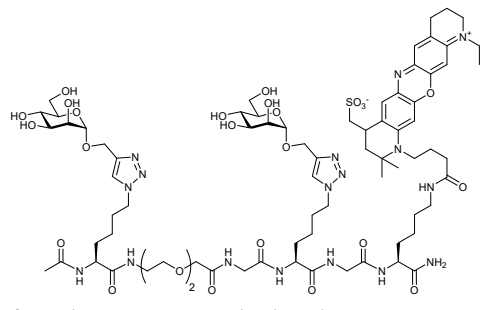
Compound **54** (234 nmol) was coupled with ATTO655-NHS using the general procedure. Compound **87** was obtained after purification by gel filtration (eluted at 33 - 45 mL) as a blue powder after lyophilization (0.935 mg, 190 nmol, 81%). LC-MS: $R_t = 5.78$ min (0 - 50% ACN; 13 min); HRMS [$C_{199}H_{315}N_{31}O_{110}S + 3H$]³⁺: 1645.33311 found, 1645.33352 calculated.

Ac-Lys(4-SO₃-GalNAc)-Ly



Compound **55** (100 nmol) was coupled with ATTO655-NHS using the general procedure. Compound **90** was obtained after purification by RP-HPLC (linear-gradient 7 - 47 % B in A, 10 min) as a blue powder after lyophilization (89 nmol, 89%, ABS = 1.597 (7 mL, λ = 663 nm)). <u>LC-MS:</u> R_t = 4.57 min (0 - 50% ACN; 13 min); <u>HRMS</u> [C₁₃₉H₂₁₃N₃₇O₆₈S₇ + 2H + Na]³⁺: 1246.41578 found, 1246.41561 calculated.

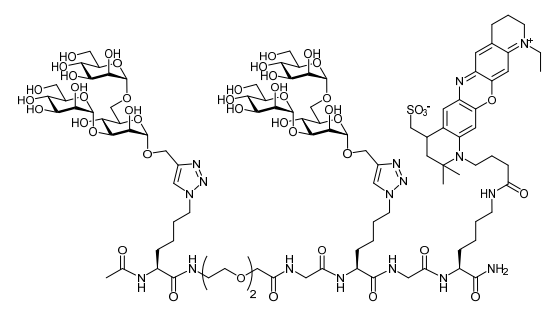
$Ac-Lys(Man_1)-AEEA-Gly-Lys(Man_1)-Gly-Lys(ATTO655)-NH_2$ (89).



found, 850.89544 calculated.

Compound **56** (100 nmol) was coupled with ATTO655-NHS using the general procedure. Compound **89** was obtained after purification by RP-HPLC (linear-gradient 7 - 46 % B in A, 10 min) as a blue powder after lyophilization (43 nmol, 43%, ABS = 1.344 (4 mL, λ = 663 nm)). <u>LC-MS</u>: R_t = 5.44 min (0 - 50% ACN; 13 min); <u>HRMS</u> [C₇₅H₁₁₃N₁₇O₂₆S + 2H]²⁺: 850.89550

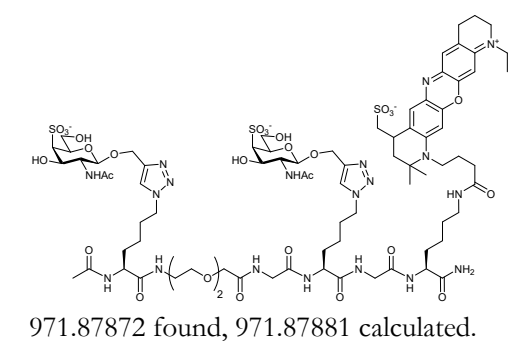
Ac-Lys(Man₃)-AEEA-Gly-Lys(Man₃)-Gly-Lys(ATTO655)-NH₂ (90).



Compound **57** (100 nmol) was coupled with ATTO655-NHS using the general procedure. Compound **90** was obtained after purification by RP-HPLC (linear-gradient 7 - 47 % B in A, 10 min) as a blue powder after lyophilization (26.1 nmol, 26%, ABS = 0.818 (4 mL, λ = 663 nm)). <u>LC-MS</u>: $R_t = 5.23 \text{ min}$ (0 - 50% ACN; 13 min);

<u>HRMS</u> $[C_{99}H_{153}N_{17}O_{46}S + 2H]^{2+}$: 1175.50270 found, 1175.50253 calculated.

Ac-Lys(4-SO₃-GalNAc)-AEEA-Gly-Lys(4-SO₃-GalNAc)-Gly-Lys(ATTO655)-NH₂ (91).

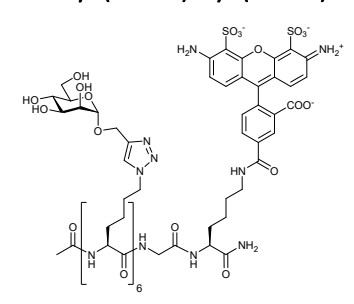


Compound **58** (100 nmol) was coupled with ATTO655-NHS using the general procedure. Compound **91** was obtained after purification by RP-HPLC (linear-gradient 7 - 47 % B in A, 10 min) as a blue powder after lyophilization (10.6 nmol, 11%, ABS = 0.666 (2 mL, λ = 663 nm)). <u>LC-MS</u>: R_t = 5.30 min (0 - 50% ACN; 13 min); <u>HRMS</u> [$C_{79}H_{119}N_{19}O_{32}S_3 + 2H$]²⁺:

General procedure for the introduction of AlexaFluor488:

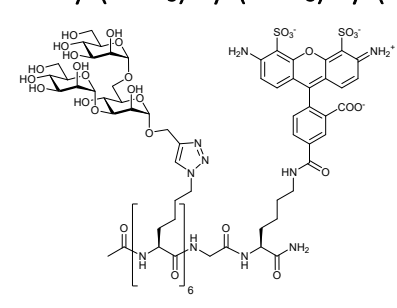
Glycoclusters with a free amine were dissolved in DMSO (2.0 mM). To this, a stock solution of AF488-NHS (5.0 mM, 2 eq) and DIPEA (0.01 M, 2 eq) in DMSO was added and shaken protected from light for one hour. After which the product was isolated via gel filtration (Toyopearl HW-40S, 1.6x60 cm, 150 mM NH₄HCO₃, 20% ACN, UV monitoring λ: 494 nm) followed by lyophilization.

Ac-Lys(Man₁)-Lys(Man₁)-Lys(Man₁)-Lys(Man₁)-Lys(Man₁)-Lys(Man₁)-Gly-Lys(AF488)-NH₂ (92).



Compound **50** (200 nmol) was coupled with AF488-NHS using the general procedure. Compound **92** was obtained after purification by gel filtration (eluted at 28 – 35.5 mL) as a green solution or orange powder after lyophilization (94 nmol, 47%, ABS = 0.869 (8 mL, λ = 494 nm)). <u>LC-MS:</u> $R_t = 5.59 \text{ min } (0 - 50\% \text{ ACN}; 13 \text{ min}); <u>HRMS</u> [C₁₂₁H₁₇₆N₃₀O₅₅S₂ + 3H]³⁺: 999.05260 found, 999.05286 calculated.$

Ac-Lys(Man₃)-Lys(Man₃)-Lys(Man₃)-Lys(Man₃)-Lys(Man₃)-Lys(Man₃)-Gly-Lys(AF488)-NH₂ (93).



Compound **54** (200 nmol) was coupled with AF488-NHS using the general procedure. Compound **87** was obtained after purification by gel filtration (eluted at 26.5 - 34 mL) as a green solution or orange powder after lyophilization (68 nmol, 34%, ABS = 1.243 (4 mL, λ = 494 nm)). LC-MS: $R_t = 4.88$ min (0 - 50% ACN; 13 min); HRMS $[C_{193}H_{296}N_{30}O_{115}S_2 + 3H]^{3+}$: 1647.59818 found, 1647.59842 calculated.

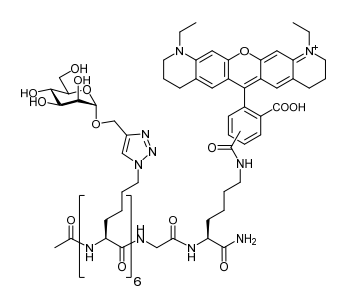
Ac-Lys(4-SO₃-GalNAc)-Ly

Compound **55** (100 nmol) was coupled with AF488-NHS using the general procedure. Compound **90** was obtained after purification by gel filtration (eluted at 28 – 37 mL) as a green solution or orange powder after lyophilization (5.9 nmol, 6%, ABS = 0.216 (2 mL, λ = 494 nm)). <u>LC-MS:</u> $R_t = 5.60$ min (0 - 50% ACN; 13 min); <u>HRMS</u> [C₁₃₃H₁₉₄N₃₆O₇₃S₈ + Na+3NH₃]⁴⁺: 948.72085 found, 948.77796 calculated.

General procedure for the introduction of ATTO565:

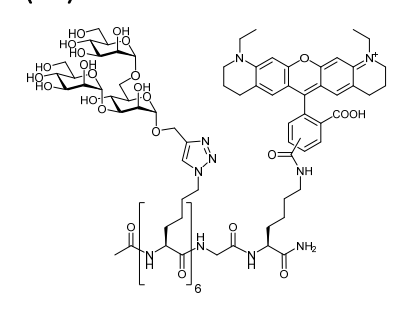
Glycoclusters with a free amine were dissolved in DMSO (2.0 mM). To this, a stock solution of ATTO565-NHS (10 mM, 2 eq) and DIPEA (0.01 M, 2 eq) in DMSO was added and shaken protected from light for one hour. After which the product was isolated via gel filtration (Toyopearl HW-40S, 1.6x60 cm, 150 mM NH₄HCO₃, 20% ACN, UV monitoring λ : 564 nm) followed by lyophilization.

Ac-Lys(Man₁)-Lys(Man₁)-Lys(Man₁)-Lys(Man₁)-Lys(Man₁)-Gly-Lys(ATTO565)-NH₂ (95).



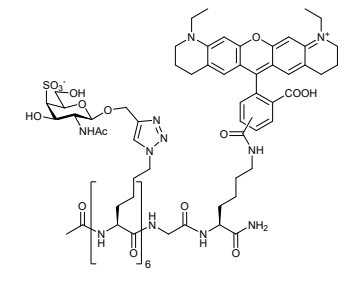
Compound **50** (300 nmol) was coupled with ATTO565-NHS using the general procedure. Compound **95** was obtained after purification by gel filtration (eluted at 29.5 – 37 mL) as a pink powder after lyophilization (127.8 nmol, 43%, ABS = 1.704 (9 mL, λ = 564 nm)). <u>LC-MS</u>: R_t = 6.42 min (0 - 50% ACN; 13 min); <u>HRMS</u> [C₁₃₁H₁₉₂N₃₀O₄₉ + 3H]³⁺: 991.12431 found, 991.12341 calculated.

Ac-Lys(Man₃)-Lys(Man₃)-Lys(Man₃)-Lys(Man₃)-Lys(Man₃)-Lys(Man₃)-Gly-Lys(ATTO565)-NH₂ (96).



Compound **54** (300 nmol) was coupled with ATTO565-NHS using the general procedure. Compound **96** was obtained after purification by gel filtration (eluted at 26.5 – 34 mL) as a pink powder after lyophilization (128.6 nmol, 43%, ABS = 1.715 (9 mL, λ = 564 nm)). <u>LC-MS</u>: R_t = 5.75 min (0 - 50% ACN; 13 min); <u>HRMS</u> [$C_{203}H_{312}N_{30}O_{109}$ + 4H]⁴⁺: 1230.00614 found, 1230.00363 calculated.

$Ac-Lys(4-SO_3-GaINAc)-Lys(4-SO$



Compound **55** (100 nmol) was coupled with ATTO565-NHS using the general procedure. Compound **97** was obtained after purification by gel filtration (eluted at 30 – 42 mL) as a pink powder after lyophilization (17 nmol, 17%, ABS = 1.031 (2 mL, λ = 564 nm)). <u>LC-MS</u>: R_t = 5.82 min (0 - 50% ACN; 13 min); <u>HRMS</u> [C₁₄₃H₂₁₀N₃₆O₆₇S₆ + 3H]³⁺: 1233.42735 found, 1233.42389 calculated.

References

- (1) Li, R.-J. E.; Hogervorst, T. P.; Achilli, S.; Bruijns, S. C.; Arnoldus, T.; Vivès, C.; Wong, C. C.; Thépaut, M.; Meeuwenoord, N. J.; van den Elst, H.; Overkleeft, H. S.; van der Marel, G. A.; Filippov, D. V.; van Vliet, S. J.; Fieschi, F.; Codée, J. D. C. C.; van Kooyk, Y. Systematic Dual Targeting of Dendritic Cell C-Type Lectin Receptor DC-SIGN and TLR7 Using a Trifunctional Mannosylated Antigen. *Front. Chem.* **2019**, 7. https://doi.org/10.3389/fchem.2019.00650.
- (2) Hogervorst, T. P.; Li, E. R. J.; Achilli, S.; Bruijns, S. C. M.; Vivès, C.; van Vliet, S. J.; Fieschi, F.; Codée, J. D. C.; Van Kooyk, Y. Targeting of the Langerhans Cell C-Type Lectin Receptor Langerin Using Bifunctional Mannosylated Antigens. [Submitted] 2020.
- (3) Brillas, R. R.; Hogervorst, T. P.; Doelman, W.; van Kasteren, S. I.; Codée, J. D. C.; Albertazzi, L. [Working Title]. [Manuscript Prep. 2020.
- (4) Sedaghat, B.; Stephenson, R.; Toth, I. Targeting the Mannose Receptor with Mannosylated Subunit Vaccines. *Curr. Med. Chem.* **2014**, *21*, 3405–3418. https://doi.org/10.2174/0929867321666140826115552.
- (5) Wolfert, M. A.; Boons, G. J. Adaptive Immune Activation: Glycosylation Does Matter. *Nat. Chem. Biol.* **2013**, *9*, 776–784. https://doi.org/10.1038/nchembio.1403.
- (6) Dam, T. K.; Fred Brewer, C. Lectins as Pattern Recognition Molecules: The Effects of Epitope Density in Innate Immunity. *Glycobiology* **2009**, *20*, 270–279. https://doi.org/10.1093/glycob/cwp186.
- (7) Li, R. E.; van Vliet, S. J.; van Kooyk, Y. Using the Glycan Toolbox for Pathogenic Interventions and Glycan Immunotherapy. *Curr. Opin. Biotechnol.* **2018**, *51*, 24–31. https://doi.org/10.1016/j.copbio.2017.11.003.
- (8) Taylor, M. E.; Bezouska, K.; Drickamer, K. Contribution to Ligand Binding by Multiple Carbohydrate-Recognition Domains in the Macrophage Mannose Receptor. *J. Biol. Chem.* **1992**, *267*, 1719–1726.
- (9) Mitchell, D. A.; Fadden, A. J.; Drickamer, K. A Novel Mechanism of Carbohydrate Recognition by the C-Type Lectins DC-SIGN and DC-SIGNR. *J. Biol. Chem.* **2001**, 276, 28939–28945. https://doi.org/10.1074/jbc.M104565200.
- (10) Feinberg, H.; Powlesland, A. S.; Taylor, M. E.; Weis, W. I. Trimeric Structure of Langerin. *J. Biol. Chem.* **2010**, *285*, 13285–13293. https://doi.org/10.1074/jbc.M109.086058.
- (11) Taylor, M. E.; Drickamer, K. Structural Requirements for High Affinity Binding of Complex Ligands by the Macrophage Mannose Receptor. *J. Biol. Chem.* **1993**, *268*, 399–404.
- (12) Napper, C. E.; Dyson, M. H.; Taylor, M. E. An Extended Conformation of the Macrophage Mannose Receptor. *J. Biol. Chem.* **2001**, *276*, 14759–14766. https://doi.org/10.1074/jbc.M100425200.
- (13) Berzi, A.; Ordanini, S.; Joosten, B.; Trabattoni, D.; Cambi, A.; Bernardi, A.; Clerici, M. Pseudo-Mannosylated DC-SIGN Ligands as Immunomodulants. *Sci. Rep.* **2016**, *6*, 35373. https://doi.org/10.1038/srep35373.
- (14) Le Moignic, A.; Malard, V.; Benvegnu, T.; Lemiègre, L.; Berchel, M.; Jaffrès, P.-A.; Baillou, C.; Delost, M.; Macedo, R.; Rochefort, J.; Lescaille, G.; Pichon, C.; Lemoine, F. M.; Midoux, P.; Mateo, V. Preclinical Evaluation of MRNA Trimannosylated Lipopolyplexes as Therapeutic Cancer Vaccines Targeting Dendritic Cells. *J. Control. Release* 2018, 278, 110–121. https://doi.org/10.1016/j.jconrel.2018.03.035.
- (15) Fehres, C. M.; Kalay, H.; Bruijns, S. C. M.; Musaafir, S. A. M.; Ambrosini, M.; Bloois, L. van; van Vliet, S. J.; Storm, G.; Garcia-Vallejo, J. J.; Van Kooyk, Y. Cross-Presentation through Langerin and DC-SIGN Targeting Requires Different Formulations of Glycan-Modified Antigens. *J. Control. Release* **2015**, *203*, 67–76. https://doi.org/10.1016/j.jconrel.2015.01.040.
- (16)Silva, J. M.; Zupancic, E.; Vandermeulen, G.; Oliveira, V. G.; Salgado, A.; Videira, M.; Gaspar, M.; Graca, L.; Préat, V.; Florindo, H. F. In Vivo Delivery of Peptides and Toll-like Receptor Ligands by Mannose-Functionalized Polymeric Nanoparticles Induces Prophylactic and Therapeutic Anti-Tumor Immune Responses in a Melanoma Model. Control. Release 198, 91-103. J. 2015, https://doi.org/10.1016/j.jconrel.2014.11.033.
- (17) Ordanini, S.; Varga, N.; Porkolab, V.; Thépaut, M.; Belvisi, L.; Bertaglia, A.; Palmioli, A.; Berzi, A.; Trabattoni, D.; Clerici, M.; Fieschi, F.; Bernardi, A. Designing Nanomolar Antagonists of DC-SIGN-Mediated HIV Infection: Ligand Presentation Using Molecular Rods. *Chem. Commun.* **2015**, *51*, 3816–3819. https://doi.org/10.1039/C4CC09709B.

- van Liempt, E.; Bank, C. M. C.; Mehta, P.; Garcı´a-Vallejo, J. J.; Kawar, Z. S.; Geyer, R.; Alvarez, R. A.; Cummings, R. D.; Van Kooyk, Y.; van Die, I. Specificity of DC-SIGN for Mannose- and Fucose-Containing Glycans. FEBS Lett. 2006, 580, 6123–6131. https://doi.org/10.1016/j.febslet.2006.10.009.
- (19) McIntosh, J. D.; Brimble, M. A.; Brooks, A. E. S.; Dunbar, P. R.; Kowalczyk, R.; Tomabechi, Y.; Fairbanks, A. J. Convergent Chemo-Enzymatic Synthesis of Mannosylated Glycopeptides; Targeting of Putative Vaccine Candidates to Antigen Presenting Cells. *Chem. Sci.* **2015**, *6*, 4636–4642. https://doi.org/10.1039/c5sc00952a.
- (20) Ni, J.; Song, H.; Wang, Y.; Stamatos, N. M.; Wang, L.-X. X. Toward a Carbohydrate-Based HIV-1 Vaccine: Synthesis and Immunological Studies of Oligomannose-Containing Glycoconjugates. *Bioconjug. Chem.* **2006**, 17, 493–500. https://doi.org/10.1021/bc0502816.
- Glaffig, M.; Stergiou, N.; Hartmann, S.; Schmitt, E.; Kunz, H. A Synthetic MUC1 Anticancer Vaccine Containing Mannose Ligands for Targeting Macrophages and Dendritic Cells. *ChemMedChem* **2018**, *13*, 25–29. https://doi.org/10.1002/cmdc.201700646.
- (22) Moyle, P. M.; Olive, C.; Ho, M.-F.; Pandey, M.; Dyer, J.; Suhrbier, A.; Fujita, Y.; Toth, I. Toward the Development of Prophylactic and Therapeutic Human Papillomavirus Type-16 Lipopeptide Vaccines. *J. Med. Chem.* **2007**, *50*, 4721–4727. https://doi.org/10.1021/jm070287b.
- (23) Buskas, T.; Ingale, S.; Boons, G.-J. Towards a Fully Synthetic Carbohydrate-Based Anticancer Vaccine: Synthesis and Immunological Evaluation of a Lipidated Glycopeptide Containing the Tumor-Associated Tn Antigen. *Angew. Chemie Int. Ed.* **2005**, *44*, 5985–5988. https://doi.org/10.1002/anie.200501818.
- (24) McIntosh, J. D.; Brimble, M. A.; Brooks, A. E. S.; Dunbar, P. R.; Kowalczyk, R.; Tomabechi, Y.; Fairbanks, A. J. Convergent Chemo-Enzymatic Synthesis of Mannosylated Glycopeptides; Targeting of Putative Vaccine Candidates to Antigen Presenting Cells. *Chem. Sci.* **2015**, *6*, 4636–4642. https://doi.org/10.1039/C5SC00952A.
- (25) Srinivas, O.; Larrieu, P.; Duverger, E.; Boccaccio, C.; Bousser, M. T.; Monsigny, M.; Fonteneau, J. F.; Jotereau, F.; Roche, A. C. Synthesis of Glycocluster Tumor Antigenic Peptide Conjugates for Dendritic Cell Targeting. *Bioconjug. Chem.* **2007**, *18*, 1547–1554. https://doi.org/10.1021/bc070026g.
- (26) Umekawa, M.; Huang, W.; Li, B.; Fujita, K.; Ashida, H.; Wang, L. X.; Yamamoto, K. Mutants of Mucor Hiemalis Endo-β-N-Acetylglucosaminidase Show Enhanced Transglycosylation and Glycosynthase-like Activities. *J. Biol. Chem.* **2008**, *283*, 4469–4479. https://doi.org/10.1074/jbc.M707137200.
- (27) Evers, D. L.; Hung, R. L.; Thomas, V. H.; Rice, K. G. Preparative Purification of a High-Mannose Type N-Glycan from Soy Bean Agglutinin by Hydrazinolysis and Tyrosinamide Derivatization. *Anal. Biochem.* **1998**, 265, 313–316. https://doi.org/10.1006/abio.1998.2895.
- (28) Amin, M. N.; Huang, W.; Mizanur, R. M.; Wang, L.-X. Convergent Synthesis of Homogeneous Glc 1 Man 9 GlcNAc 2 -Protein and Derivatives as Ligands of Molecular Chaperones in Protein Quality Control. *J. Am. Chem. Soc.* **2011**, *133*, 14404–14417. https://doi.org/10.1021/ja204831z.
- (29) Temme, J. S.; Drzyzga, M. G.; MacPherson, I. S.; Krauss, I. J. Directed Evolution of 2G12-Targeted Nonamannose Glycoclusters by SELMA. *Chem. A Eur. J.* **2013**, *19*, 17291–17295. https://doi.org/10.1002/chem.201303848.
- (30) Geijtenbeek, T. B.; Torensma, R.; van Vliet, S. J.; van Duijnhoven, G. C.; Adema, G. J.; van Kooyk, Y.; Figdor, C. G. Identification of DC-SIGN, a Novel Dendritic Cell-Specific ICAM-3 Receptor That Supports Primary Immune Responses. *Cell* **2000**, *100*, 575–585. https://doi.org/10.1016/s0092-8674(00)80693-5.
- (31) Feinberg, H.; Mitchell, D. A.; Drickamer, K.; Weis, W. I. Structural Basis for Selective Recognition of Oligosaccharides by DC-SIGN and DC-SIGNR. *Science* (80-.). **2001**, 294, 2163–2166. https://doi.org/10.1126/science.1066371.
- (32) Frison, N.; Taylor, M. E.; Soilleux, E.; Bousser, M.-T.; Mayer, R.; Monsigny, M.; Drickamer, K.; Roche, A.-C. Oligolysine-Based Oligosaccharide Clusters. *J. Biol. Chem.* **2003**, *278*, 23922–23929. https://doi.org/10.1074/jbc.M302483200.
- Oaly, R.; Vaz, G.; Davies, A. M.; Senge, M. O.; Scanlan, E. M. Synthesis and Biological Evaluation of a Library of Glycoporphyrin Compounds. *Chem. A Eur. J.* **2012**, *18*, 14671–14679. https://doi.org/10.1002/chem.201202064.
- (34) Wong, C. S.; Hoogendoorn, S.; van der Marel, G. A.; Overkleeft, H. S.; Codée, J. D. C. C. Targeted Delivery

- of Fluorescent High-Mannose-Type Oligosaccharide Cathepsin Inhibitor Conjugates. *Chempluschem* **2015**, *80*, 928–937. https://doi.org/10.1002/cplu.201500004.
- (35) Mereyala, H. B.; Gurrala, S. R. Design, Development and Utility of Glycosyl Donors Bearing an Acetoxymethoxy Leaving Group. *Chem. Lett.* **1998**, *27*, 863–864. https://doi.org/10.1246/cl.1998.863.
- (36) Meldal, M.; Tornøe, C. W. Cu-Catalyzed Azide-Alkyne Cycloaddition. *Chem. Rev.* **2008**, *108*, 2952–3015. https://doi.org/10.1021/cr0783479.
- (37) Zhao, X. Z.; Semenova, E. A.; Liao, C.; Nicklaus, M.; Pommier, Y.; Burke, T. R. Biotinylated Biphenyl Ketone-Containing 2,4-Dioxobutanoic Acids Designed as HIV-1 Integrase Photoaffinity Ligands. *Bioorg. Med. Chem.* **2006**, *14*, 7816–7825. https://doi.org/10.1016/j.bmc.2006.07.064.
- Wilkinson, B. L.; Bornaghi, L. F.; Poulsen, S.-A.; Houston, T. A. Synthetic Utility of Glycosyl Triazoles in Carbohydrate Chemistry. *Tetrahedron* **2006**, *62*, 8115–8125. https://doi.org/10.1016/j.tet.2006.06.001.
- (39) Aucagne, V.; Leigh, D. A. Chemoselective Formation of Successive Triazole Linkages in One Pot: "Click—Click" Chemistry. Org. Lett. 2006, 8, 4505–4507. https://doi.org/10.1021/ol061657d.
- (40) Wong, C. S. The Synthesis of Mannose-Derived Bioconjugates and Enzyme Inhibitors (Dissertation), Leiden University, 2015.
- (41) Tabarani, G.; Thépaut, M.; Stroebel, D.; Ebel, C.; Vivès, C.; Vachette, P.; Durand, D.; Fieschi, F. DC-SIGN Neck Domain Is a PH-Sensor Controlling Oligomerization. *J. Biol. Chem.* **2009**, *284*, 21229–21240. https://doi.org/10.1074/jbc.M109.021204.
- (42) Porkolab, V.; Pifferi, C.; Sutkeviciute, I.; Ordanini, S.; Taouai, M.; Thepaut, M.; Vivès, C.; Benazza, M.; Bernardi, A.; Renaudet, O.; Fieschi, F. Development of C-Type Lectin Oriented Surfaces for High Avidity Glycoconjugates: Towards Mimicking Multivalent Interactions on the Cell Surface. *bioRxiv* [Preprint] 2019. https://doi.org/10.1101/780452.
- (43) Timpano, G.; Tabarani, G.; Anderluh, M.; Invernizzi, D.; Vasile, F.; Potenza, D.; Nieto, P. M.; Rojo, J.; Fieschi, F.; Bernardi, A. Synthesis of Novel DC-SIGN Ligands with an α-Fucosylamide Anchor. *ChemBioChem* 2008, 9, 1921–1930. https://doi.org/10.1002/cbic.200800139.
- (44) Feinberg, H.; Castelli, R.; Drickamer, K.; Seeberger, P. H.; Weis, W. I. Multiple Modes of Binding Enhance the Affinity of DC-SIGN for High Mannose N-Linked Glycans Found on Viral Glycoproteins. *J. Biol. Chem.* **2007**, *282*, 4202–4209. https://doi.org/10.1074/jbc.M609689200.
- (45) Cambi, A.; Beeren, I.; Joosten, B.; Fransen, J. A.; Figdor, C. G. The C-Type Lectin DC-SIGN Internalizes Soluble Antigens and HIV-1 Virions via a Clathrin-Dependent Mechanism. *Eur. J. Immunol.* **2009**, *39*, 1923–1928. https://doi.org/10.1002/eji.200939351.
- (46) Vigerust, D. J.; Vick, S. Stable Expression and Characterization of an Optimized Mannose Receptor. *J. Clin. Cell. Immunol.* **2015**, *06*. https://doi.org/10.4172/2155-9899.1000330.
- (47) Chan, W. C.; White, P. D. Fmoc Solid Phase Peptide Synthesis: A Practical Approach; Oxford University Press, 2000.

Large scale synthesis of a conjugation-ready 2-butoxy-8-oxo-adenine analog TLR7-ligand

Introduction

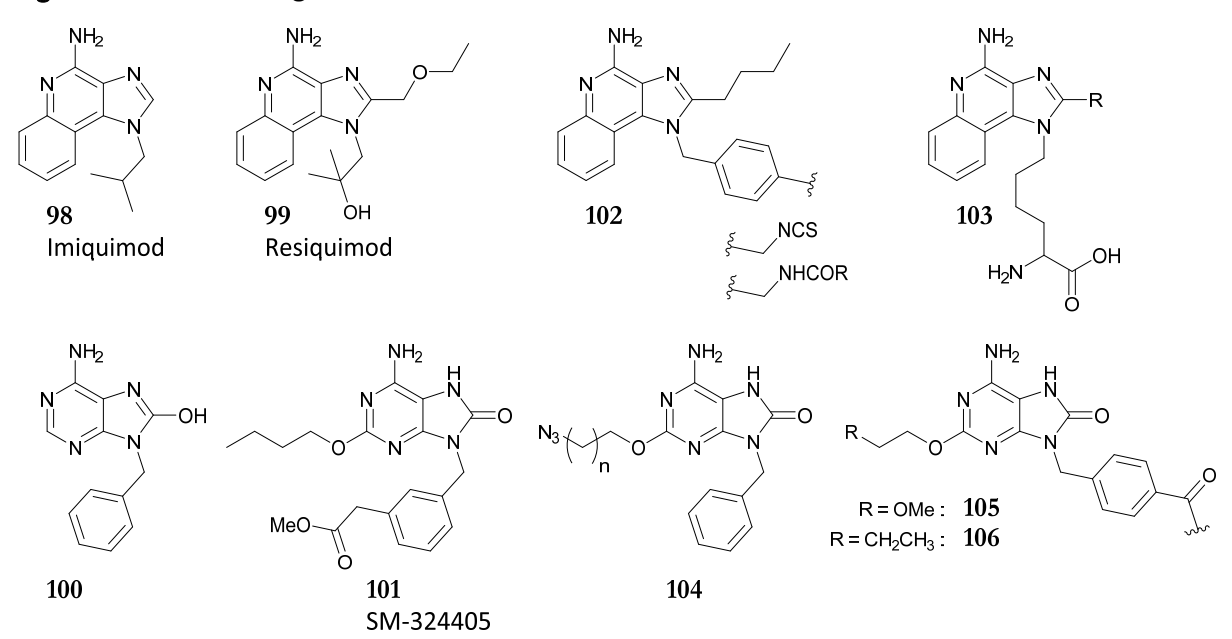
Effective vaccines require at least two functionalities, a recognizable disease-related antigen and an adjuvant. Adjuvants can be derived from pathogen-associated molecular patterns (PAMPs) that induce signaling through binding of pattern recognition receptors (PRRs) stimulating antigen-presenting cells (APCs) to mature. Maturation results in the secretion of inflammatory cytokines and upregulation of antigen processing and presentation, which are a necessity for an adequate adaptive response. The Toll-like receptor (TLR) family is intensively explored for the development of new vaccine adjuvants.² Ten different TLRs which recognize different types of PAMPs can be found on human immune cells. They are either expressed on the cell surface (TLR1, TLR2, TLR4, TLR5, TLR6, and TLR10) or endosomal (TLR3, TLR7, TLR8, and TLR9).^{3,4} Endosomal TLRs

Part of this work is published in Hogervorst & Gential et al. 2019¹

recognize nucleic acid-based PAMPs such as viral double-stranded RNA (TLR3),⁵ single-stranded bacterial and viral RNA (TLR7 and TLR8)⁶⁻⁸ and bacterial and viral DNA (TLR9).⁹

Small molecule agonists have been discovered as ligands for TLR7 and TLR8. Prime examples are imidazoquinolines based structures such as imiquimod (98) and resiquimod (99, Figure 1),¹⁰ of which the latter is used in the clinic for the treatment of an uncommon epidermal cancer¹¹ and is tested as vaccine adjuvant.¹² Derivatives of 8-oxo-adenine and 8-hydroxy-adenine are another class of TLR7/TLR8 agonists. Based on lead compound 100 (Figure 1), developed by Hirota et al.¹³ a multitude of structure-activity relationship studies have been described resulting in agonists such as SM-324405 (101).¹⁴⁻¹⁷

Figure 1: TLR7/TLR8 agonists.



Both classes of agonists have been functionalized to give conjugation-ready compounds such as **102**, which can be conjugated *via* either an isothiocyanate or a maleimide handle.¹⁸ Fujita et al. described the norleucine amino acid derivative **103** that can be incorporated in a peptide via solid-phase peptide synthesis.¹⁹ Several derivatives of 8-oxo-adenine have been used for conjugation to antigens. For example, Weterings et al.²⁰ generated **104**, having an 2-azidoalkoxy spacer for attachment to a peptide antigen. The resulting conjugate showed enhanced antigen presentation but lost the ability to induce maturation.²⁰ Conjugation of **105** via its 9-benzyl function as first described by Chan et al.,²¹ resulted in conjugates that maintained the maturation ability and **105** has since been successfully used in peptide-adjuvant conjugates.²² Similar results were obtained with the 2-butoxy analog **106**.¹⁷

Although structures such as **106** and **105** have been successfully used in adjuvant-antigen conjugates, their synthesis and subsequent conjugation are far from ideal. Two synthetic routes towards **106** have been described. Akinbobuyi et al.²³ obtained **106** in four steps with an 61% overall yield starting from 6-amino-2-chloropurine (**107**, Scheme 1, route A). In this route, the benzoic acid was introduced with cyanobenzylbromide (**108**) to afford (**109**), which was converted to free acid **110**, after the butoxy group was installed. Subsequent bromination, followed by sodium hydroxide treatment gave ligand **106**. The authors described that the main advantage of this route is that all intermediates could be purified via precipitation in reactions with high conversion.

In the second route to **106**, developed by G.P.P. Gential,²⁴ the benzoic acid is masked as a butylester that was deprotected in the final stage of the synthesis (route B, Scheme 1). Starting from purine (**107**), adenine **106** was obtained in four steps in a 23% overall yield. In this route, the butylester protection circumvented solubility issues caused by the free benzoic acid as experienced in route A. It was described that the electrophilic aromatic bromination to obtain **115** proceeded sluggishly and could only be achieved in high yield with the aid of a large excess of bromine. Nucleophilic aromatic substitution, demethylation and ester hydrolysis resulted in **106**. The main advantage of route B is the solubility of all intermediates, allowing the purification by for example flash column chromatography. A major disadvantage is the large excess of reagents that are needed to introduce and substitute the bromine and the low overall yield of the route.

A drawback of small molecule agonists for TLR7 and TLR8 is their toxicity. Therefore, imiquimod can only be administered topically.²⁵ Chan et al.²¹ achieved a significant reduction of toxicity by conjugation of TLR ligand **105** to phospholipids and polyethylene glycols. Unfortunately, conjugation of ligands **106** and **105** via their carboxylic acid function resulted in poor yields, due to the poor solubility of the ligand.²¹ The solubility of **106** could be improved by the introduction of a *tert*-butoxycarbonyl (Boc) protecting group, but the yield of a small scale (0.15 mmol) synthesis of **116** did not exceed 10% (Scheme 1).²⁴

Scheme 1: Previously described routes towards **106**.

This Chapter presents an improved route of synthesis of **116**. Because Route A could not be reproduced providing enough material in sufficient purity, Route B was optimized to enable the production of **116** on a large scale. Having sufficient amounts of **116** available, conjugates can be developed that can be targeted to the endosomes of immune cells, thereby potentially increasing their effectiveness. Conjugation of **116** to the oligomannoside clusters, described in Chapter 2, would not only increase the water solubility of the TLR7 ligand, but also allow for the active transport toward endosomes. To test this hypothesis, this Chapter also describes the synthesis of three bifunctional conjugates that target both TLR7 and trafficking receptors.

Results and Discussion

An improved synthetic route towards Boc protected TLR7 agonist **116** is described in Scheme 2. To allow for the synthesis of **116** with higher yields and on a larger scale, the synthetic procedures applied in route B (Scheme 1)²⁴ were modified, learning lessons from route A.²³ The main drawback in route B was the conversion of **114** to **116**, requiring a large excess of reagents for the introduction and the substitution of the bromine, hindering efficient scale-up. Furthermore, 90% of **106** was lost in the final step introducing the Boc protection group.

The electrophilic aromatic bromination of 114, according to route B, required nineteen equivalents of bromine. Subsequent quenching of the excess of bromine with a sodium thiosulphate solution generated HBr that lowered the pH of the solution, leading to the formation of solid elementary sulfur.²⁶ On a small scale, these solids made the work-up time consuming, because they clogged the glassware and filters. On a larger scale, this problem was so prominent that it made work-up impossible. The addition of sodium acetate (as in route A)²³ improved both the efficiency of reaction and the work-up procedure. Using only five equivalents of bromine, 115 was obtained within an hour in 94% yield on a 40 mmol scale (Scheme 2). Not only did the smaller excess of bromine reduce the amount of required thiosulphate, but the presence of sodium acetate also increased the pH resulting in the formation of less solid sulfur.

Attempts to hydrolyze bromine 115 directly with NaOH were unsuccessful in route B. This was circumvented by using a more nucleophilic methoxide, followed by acidic cleavage of the resulting methyl ether and finally saponification of the remaining benzoic ester under basic condition. The large amount of acidic and basic solutions required for scale-up of the reaction made this three-step method cumbersome. The two extra steps could be circumvented by refluxing 115 for three days in a solution of NaOH in a mixture of methanol and water. In this procedure, *in situ* formed methanolate can displace the bromine while the ether and ester are also cleaved. After acidification of the resulting solution, 106 could be precipitated and filtered off to provide the free acid in 89% yield on a multigram scale.

106 proved to be insoluble in most organic solvents, which makes this building block unsuitable for conjugation. Gential described the enhancement of the solubility of the building block by the introduction of a Boc group. To introduce the *tert*-butyl carbamate, 106 was suspended in a water/dioxane mixture after which it was stirred with triethylamine and ten equivalents of 2-(*tert*-butoxycarbonyloxyimino)-2-phenylacetonitrile (Boc-ON) for five days. The reaction proceeded sluggishly with only 10% conversion after five days. This result was explained by the poor solubility of both 106 and Boc-ON and the moderate nucleophilicity of the aromatic amine. ²⁴ Optimization

of this reaction (Table 1) by either changing the solvent system (entries 2 and 3), changing to the more soluble di-*tert*-butyl dicarbonate (Boc₂O, entries 4-11) or changing Et₃N to DMAP (entries 2-5) improved the reaction slightly but still more than 80% of product was lost. Notably, in all entries, **106** was not completely dissolved, not even when diluted in DMSO (entries 2,4,8). In an attempt to obtain a homogenous solution, **106** was dissolved in a NaOH (1.0 M, aq.) generating its sodium salt, after which a solution of Boc₂O in dioxane was added dropwise (entry 9). Upon neutralization with HCl (1.0 M, aq.) both **106** and **116** crashed out, and subsequent centrifugation of the suspension allowed for removal of excess reagents after which extraction of the solids with chloroform gave **116** in 30-40% yield while starting compound **106** could be recovered from the residue (entries 9-11).

Scheme 2: Synthesis of building block 116

Reagents and conditions a) **112**, K₂CO₃, DMSO, 63%; b) i. NaH, n-BuOH, 120 °C; ii. H₂SO₄, 80 °C, 71%; c) Br₂, NaOAc, DCM, 94%; d) NaOH, H₂O, MeOH, reflux, 89%; e) NaOH, Boc₂O, H₂O, Dioxane, 35% (95% recovery of **106**).

When the reaction was performed on a 30 mmol scale (entry 11), the final extraction proved to be more difficult due to large amounts of solids. However, using a Soxhlet extraction apparatus, 116 could be isolated in high yield, delivering 10.5 mmol of product (35%). By extraction of the remaining residue in the sock using a NaOH solution (1 M, aq.) and subsequent acidification of the filtrate, the precipitated 106 could be recovered in high yield (18.5 mmol, 95% recovery) and it could be re-subjected to the bocylation reaction. Together these optimizations improved the

conversion of **114** into **116** from 4% to 29%. The synthesis of **116** on a multi-mmol scale makes it a feasible conjugation-ready building block to be used in SPPS (as described in Chapter 4 and 5) or solution-based synthesis (below).

Before conjugation of 116 to the projected glycoside clusters, a spacer was introduced (Scheme 3). Condensation of 116 with known triethylene glycol 117, 27,28 obtained via previously described procedures resulted in tert-butyl ester protected 118. Simultaneous acid-mediated removal of the Boc group and butyl ester²⁹ resulted in a compound that caused gelation in water and DMSO, thereby hindering its purification. In the end, the compound could be dissolved using NH₄OAc (0.033 M) in a mixture of H₂O/ACN/t-BuOH/AcOH (4/1/1/3, v/v/v) allowing the purification of 119 via RP-HPLC. Conversion of carboxylic acid 119 into the pentafluorophenol (Pfp) ester 120 improved the solubility in water and DMSO which enabled the synthesis of three bi-functional conjugates (Scheme 3). The mannoside clusters 50 and 54 (mono- or tri-mannoside clusters on a hexavalent scaffold), described in Chapter 2, were conjugated to Pfp ester 120 resulting in clusters 121 and 122. Both clusters should be able to target DC-SIGN (see Chapter 2) and could route the bi-functional conjugates toward endosomes. A similar hexavalent scaffold 123 containing six mannose-6-phosphates, described by R.N.M. Reintjes, 30 was conjugated to Pfp ester 120 forming cluster 124. This conjugate was designed to target the mannose-6-phospate receptor which could result in endo-/lysosomal routing. Unlike the previously described 9-benzyl-8-oxo adenine analog, all these bi-functional conjugates are highly water-soluble. All three conjugates are being tested for their ability to mature APCs and this evaluation is ongoing.

Table 1: Optimization of Boc introduction

Entry	Boc source	Solvent	Base	[106]	Yield
124	Boc-ON (13 eq)	H ₂ O/dioxane (1/1)	Et ₃ N (3 eq)	0.5 M	10%a
2	Boc-ON (2 eq)	DMSO	DMAP (0.1 eq)	0.5 M	$8^{0}/_{0}^{a}$
3	Boc-ON (2 eq)	THF	DMAP (0.1 eq)	0.5 M	$7^{0}/_{0^{a}}$
4	Boc ₂ O (4 eq)	DMSO	DMAP (0.1 eq)	0.5 M	14%
5	Boc ₂ O (4 eq)	THF	DMAP (0.1 eq)	0.5 M	13%
6	Boc ₂ O (4 eq)	MeOH/H ₂ O/Et ₃ N (10/10/7)	$\mathrm{Et}_{3}N$	0.5 M	0%
7	Boc ₂ O (8 eq)	H ₂ O/dioxane (1/1)	$\mathrm{Et_3}N$ (3 eq)	0.5 M	13%
8	Boc ₂ O (8 eq)	DMSO	$\mathrm{Et}_{3}N$	0.15 M	15%
9	Boc ₂ O (1.5 eq)	H ₂ O/dioxane (1/1)	NaOH (2 eq)	0.5 M	24%
10	Boc_2O (1.2 eq)	H ₂ O/dioxane (3/1)	NaOH (3 eq)	0.25 M	41%
11	Boc ₂ O (1.2 eq)	H ₂ O/dioxane (3/1)	NaOH (3 eq)	0.25 M	35%
	l				

^a Formation of butyl ester was observed on LC-MS

Scheme 3: Synthesis of mannosylated - TLR7 agonist - conjugates

Reagents and conditions: a) HCTU, DIPEA, DCM/DMF, 84%; b) H_3PO_4 , $H_2O/toluene$, 43%; c) pentafluorophenol, DIC, DMAP, DMSO; d) 50, 120, DIPEA, DMSO/ H_2O , 73%; e) 54, 120, DIPEA, DMSO/ H_2O , 46%; f) 120, DIPEA, DMSO/ H_2O , 2.8%.

Conclusion

A major improvement in the synthesis of 2-butoxy-8-oxo-adenine analog 116 was achieved. In particular, the overall total yield for the conversion of 114 into 116, comprising electrophilic aromatic bromination, bromine hydrolysis, and introduction of a Boc group, was increased from 4% to 29%. Furthermore, it was possible to regenerate unprotected adenine 106 during the introduction of the Boc group, by which the Boc-protection could be repeated, increasing the total overall yield further. The new synthetic procedures improved the workability of the synthetic route, in terms of work-up and purification, allowing for a significant increment of reaction scale. Which resulted in the isolation of 116 on a 10.5 mmol scale, making this building block readily available for further conjugations. Together with the improvement in solubility due to the introduction of the Boc-group, makes 116 a suitable building block for application in both solution and solid-phase peptide syntheses. The applicability of 116 was successfully demonstrated by the solution phase conjugation to three mannoside clusters forming three highly water-soluble bifunctional conjugates of which their effectiveness to induce DC-maturation is under current evaluation.

Experimental

General procedures:

All reactions, purifications, and analyses were performed as described in the general procedures of Chapter 2.

Butyl 4-methylbenzoate (125).

p-Toluic acid (53.3 g, 390 mmol) was dissolved in dry n-BuOH (500 mL, 0.8 M). H₂SO₄ (1.9 mL 35 mmol, 0.09 eq) was added and the mixture was refluxed for 5 hours, after which the reaction mixture was diluted with DCM (1 L) and washed with NaHCO₃ (sat. aq.) twice. The organic layer was collected, dried over MgSO₄, filtered and concentrated *in vacuo*. The mixture was co-evaporated with toluene (2x) yielding ester **125** as a clear oil (56.13 g, 370 mmol, 95%). <u>TLC R_f</u> 0.63 (Et₂O/PE, 5/95, v/v); <u>IR</u> (neat, cm⁻¹): 2957, 1713; ¹H NMR (400 MHz, CDCl₃, HH-COSY, HSQC): δ 7.93 (d, J = 8.3 Hz, 2H, H-3/H-4), 7.20 (d, J = 8.0 Hz, 2H, H-3/H-4), 4.30 (t, J = 6.6 Hz, 2H, H-7), 2.37 (s, 3H, H-1), 1.80 - 1.66 (m, 2H, H-8), 1.53 - 1.39 (m, 2H, H-9), 0.97 (t, J = 7.4 Hz, 3H, H-10); ¹³C NMR (100 MHz, CDCl₃, HSQC): δ 166.7 (C-6), 143.4 (C-5), 129.6, 129.0 (C-3, C-4), 127.8 (C-2), 64.6 (C-7), 30.8 (C-8), 21.6 (C-1), 19.3 (C-9), 13.8 (C-10); HRMS [C₁₂H₁₆O₂ +H]⁺: 193.12226 found, 193.12231 calculated.

Butyl 4-(bromomethyl) benzoate (112).

Compound **125** (54.45 g, 283 mmol) was dissolved in CCl₄ (283 mL, 1.0 M) in a three liter flask equipped with a bump-trap and a large cooler loosely stoppered with a septum under nitrogen. NBS (86.5 g, 311 mmol, 1.1 eq) and α , α '-Azoisobutyronitrile (AIBN, 2.4 g, 14.6 mmol, 0.05 eq) were added and the mixture was carefully heated to 90 °C for six hours. After TLC analysis showed full conversion of the starting material the reaction mixture was concentrated *in vacuo*, diluted in EtOAc and washed with H₂O. The organic layer was collected, dried over MgSO₄, filtered and concentrated. Compound **112** was obtained after purification by silica gel chromatography (absorbed on Celite \rightarrow 1/199 \rightarrow 2/98, Et₂O/PE, v/v) as a yellow oil (49.62 g, 183 mmol, 65%). TLC R_f 0.55 (Et₂O/PE, 5/95, v/v); IR (neat, cm⁻¹): 3197, 2957, 1713; ¹H NMR (400 MHz, CDCl₃): δ 8.04 (d, J = 8.3 Hz, 2H, H-3/H-4), 7.48 (d, J = 8.3 Hz, 2H, H-3/H-4), 4.52 (s, 2H, H-1), 4.35 (t, J = 6.6 Hz, 2H, H-7), 1.83 - 1.72 (m, 2H, H-8), 1.56 - 1.44 (m, 2H, H-9), 1.01 (t, J = 7.4 Hz, 3H, H-10); ¹³C NMR (100 MHz, CDCl₃): δ 166.2 (C-6), 142.6 (C-2), 130.6 (C-5), 130.1, 129.1 (C-3, C-4), 65.1 (C-7), 32.4 (C-1), 30.9 (C-8), 19.4 (C-9), 13.9 (C-10); HRMS [C₁₂H₁₅BrO₂ + H]⁺: 271.11816 found, 271.03282 calculated.

Butyl 4-((6-amino-2-chloro-9H-purin-9-yl)methyl)benzoate (113).

To a suspension of 6-amino-2-chloropurine (107) (22.11 g, 130 mmol) in DMSO (300 mL, final 0.3 M) at 0 °C, K₂CO₃ (54 g, 390 mmol, 3 eq) and a solution of compound 112 (42.3 g, 156 mmol, 1.2 eq) in DMSO (133 mL) were added successively and the mixture was stirred for a day. After complete consumption of 107 the mixture was poured in H₂O (3 L) and stored at 4 °C overnight. The suspension was filtered off, washed with H₂O (3x) and the powder was dried *in vacuo*. Purification by

silica gel column chromatography (absorbed on Celite \rightarrow 1/99 \rightarrow 6/94, MeOH/DCM, v/v) yielded title compound **113** as an off-white solid (29.88 g, 83.0 mmol, 63%). TLC R_J 0.34 (MeOH/DCM, 5/95, v/v); IR (neat, cm⁻¹): 3297, 3122, 2957, 1736, 1597; ¹H NMR (400 MHz, CDCl₃): δ 8.03 (d, J = 8.3 Hz, 2H, H-12/H-13), 7.72 (s, 1H, H-8), 7.33 (d, J = 8.3 Hz, 2H, H-12/H-13), 6.06 (s, 2H, NH₂), 5.39 (s, 2H, H-10), 4.32 (t, J = 6.7 Hz, 2H, H-16), 1.80 - 1.71 (m, 2H, H-17), 1.51 - 1.42 (m, 2H, H-18), 0.97 (t, J = 7.4 Hz, 3H, H-19); ¹³C NMR (101 MHz, CDCl₃): δ 166.1, 156.3 (C-2, C-4, C-5, C-6, C-11, C-14), 140.7 (C-8), 140.0 (C-2, C-4, C-5, C-6, C-11, C-14), 130.5, 127.8 (C-12, C-13), 65.2 (C-16), 47.1 (C-10), 30.9 (C-17), 19.4 (C-18), 13.9 (C-19); HRMS [C₁₇H₁₈ClN₅O₂ + H]⁺: 360.12143 found, 360.12218 calculated.

Butyl 4-((6-amino-2-butoxy-9H-purin-9-yl)methyl)benzoate (114).

Compound 113 (29.88 g, 83.0 mmol) was dissolved in anhydrous n-BuOH (500 mL, 0.17 M) and cooled to 0 °C. To this solution NaH (33.2 g, 830 mmol, 10 eq) was added in small portions over three hours. The mixture was stirred at 120°C overnight, after which LC-MS analysis showed full conversion of the starting material into the product and a small portion hydrolyzed product. The mixture was cooled to 0°C and H₂SO₄ (53 mL, 1 mol, 1.2 eq, 98%) was added dropwise over three hours under vigorous stirring. After addition the reaction mixture was stirred at 80 °C for two hours. The mixture was diluted in DCM (1.5 L), washed with NaHCO₃ (sat. aq., 3x) after which the organic layer was collected, dried over MgSO₄, filtered and concentrated in vacuo. Remaining n-BuOH was removed by coevaporating with toluene (3x). Purification by silica gel column chromatography (applied in CHCl₃ \rightarrow 1/99 → 1/1, MeOH/DCM, v/v) followed by crystallization (CHCl₃/toluene, 1/1, v/v) yielding title compound 114 as an off-white solid (23.46 g, 59.0 mmol, 71%). TLC R_f 0.26 (MeOH/DCM, 5/95, v/v); IR (neat, cm⁻ 1): 3282, 3110, 2955, 1736, 1597; 1H NMR (400 MHz, CDCl₃): δ 8.01 (d, J = 8.3 Hz, 2H, H-12/H-13), 7.61 (s, 1H, H-8), 7.34 (d, J = 8.3 Hz, 2H, H-12/H-13), 5.69 (s, 2H, NH2), 5.33 (s, 2H, H-10), 4.35 - 4.25 (m, 4H, H-16, H-20), 1.83 - 1.69 (m, 4H, H-17, H-21), 1.56 - 1.40 (m, 4H, H-22, H-18), 0.97 (td, *J* = 7.4, 2.0 Hz, 6H, H-19, H-23); 13 C NMR (100 MHz, CDCl₃): δ 166.2, 162.6, 156.6, 152.1, 140.8, 138.8, 130.6 (C-2, C-4, C-5, C-6, C-11, C-14), 130.3, 127.8 (C-12, C-13), 67.2, 65.1 (C-16, C-20), 46.7 (C-10), 31.2, 30.8 (C-17, C-21), 19.4, 19.4, 14.0, 13.9; HRMS [C₂₁H₂₇N₅O₃ + H]⁺: 398.21702 found, 398.21867 calculated.

Butyl 4-((6-amino-8-bromo-2-butoxy-9H-purin-9-yl)methyl)benzoate (115).

Compound **114** (16.93 g, 42.5 mmol) was dissolved in DCM (430 mL, 0.1 M), cooled to 0 °C and NaOAc (13.95 g, 85 mmol, 2 eq) and Br₂ (10.9 mL, 212.5 mmol, 5 eq) were added successively. After one hour the reaction was quenched with Na₂S₂O₃ (sat. aq.). The mixture was transferred to a separation funnel and the organic layer was washed with Na₂S₂O₃ (sat. aq. 3x) and H₂O (1x), dried over MgSO₄, filtered and concentrated *in vacuo*. Purification by silica gel column chromatography (1/99, MeOH/DCM, v/v) yielded title compound **115** as an orange solid (19.0 g, 39.9 mmol, 94%). <u>TLC R</u> $_2$ 0.52 (MeOH/DCM, 5/95, v/v); <u>IR</u> (neat, cm⁻¹): 3320, 3196, 2957, 1722, 1652, 1589; ¹H NMR (400 MHz, CDCl3): δ 8.00 (d, J = 8.3 Hz, 2H, H-12/13), 7.37 (d, J = 8.4 Hz, 2H, H-12/13), 5.89 (s, 2H, NH₂), 5.35 (s, 2H, H-10), 4.31 (td, J = 6.1, 0.9 Hz, 4H, H-16, H-20), 1.81 - 1.68 (m, 4H, H-17, H-21), 1.55 - 1.40 (m, 4H,

H-18, H-22), 0.96 (td, J = 7.4, 1.1 Hz, 6H, H-19, H-23); 13 C NMR (100 MHz, CDCl3): δ 166.2, 162.4, 155.4, 153.1,140.2, 130.5 (C-2, C-4, C-5, C-6, C-11, C-14, C-15), 130.2, 127.8, (C-12, C-13), 124.5 (C-8), 116.2 (C-2, C-4, C-5, C-6, C-11, C-14, C-15), 67.4, 65.1 (C-16, C-20), 47.1 (C-10), 31.1, 30.9 (C-17, C-21), 19.4, 19.2 (C-18, C-22), 14.0, 13.9 (C-19, C-23); HRMS [C₂₁H₂₆BrN₅O₃ + H]⁺: 478.12507 measured, 478.12740 calculated.

4-((6-Amino-2-butoxy-8-oxo-7,8-dihydro-9H-purin-9-yl)methyl)benzoic acid (106).

Compound **115** (13.03 g, 27.3 mmol) was dissolved in MeOH (182 mL, 0.15 M) and NaOH (240 mL, 10 M, aq., 2.4 mol, 88 eq) was added dropwise after which the cream white suspension was refluxed for three days. After LC-MS analysis showed full conversion of the starting material the clear brown solution was cooled to 0 °C and quenched with HCl (420 mL, 6 M, aq., 2.52 mol, 92 eq). The solution changed to a white suspension and the reaction volume was reduced by halve under reduced pressure. The solids were filtered off and washed with water and dried *in vacuo* yielding compound **106** as an orange solid (8.71 g, 24.4 mmol, 89%). <u>LC-MS</u>: Rt = 5.09 min (0 - 50% ACN; 13 min); <u>IR</u> (neat, cm⁻¹): 3418, 3168, 1689; 1 <u>H NMR</u> (400 MHz, DMSO-d6): δ 12.94 (s, 1H, CO₂H), 10.93 (s, 1H, NH-7), 7.88 (d, J = 8.1 Hz, 2H, H-12/H-13), 7.36 (d, J = 8.1 Hz, 2H, H-12/H-13), 6.98 (s, 2H, NH₂), 4.92 (s, 2H, H-10), 4.11 (t, J = 6.6 Hz, 2H, H-16), 1.67 - 1.51 (m, 2H, H-17), 1.42 - 1.27 (m, 2H, H-18), 0.87 (t, J = 7.3 Hz, 3H, H-19); 13 <u>C NMR</u> (101 MHz, DMSO-d6): δ 167.0, 160.0, 152.0, 148.9, 148.0, 142.2, 129.8 (C-2, C-4, C-5, C-6, C-11, C-14, C-15), 129.6, 127.3 (C-13, C-12), 98.4 (C-2, C-4, C-5, C-6, C-11, C-14, C-15), 65.9 (C-16), 42.1 (C-10), 30.6 (C-17), 18.7 (C-18), 13.7 (C-19); <u>HRMS</u> [C₁₇H₁₉N₅O₄ + H]+: 358.15009 found, 358.15098 calculated.

4-((6-amino-2-butoxy-7-(tert-butoxycarbonyl)-8-oxo-7,8-dihydro-9H-purin-9-yl) methyl) benzoic acid (116).

Compound **106** (10.7 g, 30.0 mmol) was dissolved in a NaOH solution (1.0 M, 100 mL, 100 mmol, 3.3 eq). To this clear dark-brown solution a solution of Boc₂O in dioxane (1.2 M, 33 mL, 39.6 mmol, 1.3 eq) was added dropwise over 10 minutes under vigorous stirring. After 2.5 hours the reaction mixture was diluted with CHCl₃ (200 mL) and acidified with HCl (1.0 M, 100 mL, 100 mmol, 3.3 eq) dropwise over 20 minutes in which a clouded suspension formed. Separation of layers was achieved by spinning the mixture down at 4000 rpm for 5 min. The aqueous layer was removed and the solid and organic layer were combined and transferred to a soxhlet extractor. This solid was extracted with CHCl₃ in the soxhlet apparatus until no clear color emerged from the sock (7 times). The organic layer was dried over MgSO₄, filtered and concentrated. Purification by silica gel column chromatography (1/99 → 4/96, MeOH/DCM, v/v) yielded title compound **116** as an off-white solid. (4.83 g, 10.5 mmol, 35%) Starting material was recovered by rinsing the soxhlet with NaOH (1 M, aq.) followed by acidification of the aqueous layer (HCl, 1 M, aq.), results in starting material **106** as a solid that could be obtained by filtration (6.60 g, 18.5 mmol, 95% recovery). TLC R_f 0.27 (MeOH/DCM, 1/9, v/v); IR (neat, cm⁻¹): 3431, 3163, 2958, 1753, 1720, 1637; ¹H NMR (400 MHz, DMSO-d6): δ 12.96 (s, 1H, CO₂H), 7.90 (d, *f* = 8.0 Hz, 2H,

H-12/H-13), 7.41 (d, J = 8.0 Hz, 2H, H-12/H-13), 7.06 (s, 2H, NH₂), 4.94 (s, 2H, H-10), 4.16 (t, J = 6.5 Hz, 2H, H-16), 1.66 - 1.57 (m, 2H, H-17), 1.54 (s, 9H, t-Bu), 1.35 (dq, J = 14.7, 7.4 Hz, 2H, H-18), 0.89 (t, J = 7.3 Hz, 3H, H-19); ¹³C NMR (101 MHz, DMSO-d6): δ 167.0, 161.2, 150.5, 150.2, 149.6, 149.1, 141.1, 130.0 (C-2, C-4, C-5, C-6, C-11, C-14, C-15), 129.6, 127.6 (C-13, C-12), 96.4 (C-2, C-4, C-5, C-6, C-11, C-14, C-15), 85.2 (C_q t-Bu), 66.2 (C-16), 42.7 (C-10), 30.5 (C-17), 27.6 (t-Bu), 18.7 (C-18), 13.7 (C-19); HRMS [C₂₂H₂₇N₅O₆ + H]⁺: 458.2046 found, 458.2034 calculated.

tert-butyl 6-amino-2-butoxy-9-(4-((13,13-dimethyl-11-oxo-3,6,9,12-tetraoxatetradecyl) carbamoyl) benzyl)-8-oxo-8,9-dihydro-7H-purine-7-carboxylate (118).



Amine 117 (313.9 mg, 1.19 mmol 1.03 eq), Boc protected adenine 116 (528.3 mg, 1.15 mmol, 1 eq) and HCTU (475 mg, 1.15 mmol, 1 eq) were combined and dissolved in DCM/DMF (4 mL, 0.28 M, 3/1, v/v) to which DIPEA (400 μ L, 2.30 mmol, 2eq) was added dropwise. After two hours the mixture was diluted with CHCl₃ washed with HCl (1 M, aq., 1x) dried

over MgSO₄ (s), filtered, concentrated *in vacuo* and purified by silica gel column chromatography (1/19 \rightarrow 3/22, acetone/DCM, v/v) to yield title compound **118** as a yellow oil (678 mg, 0.96 mmol, 84%). <u>TLC R</u>₂ 0.65 (MeOH/DCM, 1/49, v/v); <u>1H NMR</u> (500 MHz, CDCl₃) δ 8.01 (s, 1H), 7.75 (d, J = 8.3 Hz, 2H, H-12/H-13), 7.47 (d, J = 8.2 Hz, 2H, H-12/H-13), 7.00 (s, 2H, NH₂), 5.01 (s, 2H, H-10), 4.27 (t, J = 6.7 Hz, 2H, H-16), 3.99 (s, 2H, O-CH₂-CO), 3.69 - 3.62 (m, 12H, CH₂ PEG), 1.77 - 1.68 (m, 2H, H-17), 1.62 (s, 9H, t-Bu), 1.47 - 1.39 (m, 11H, t-Bu, H-18), 0.95 (t, J = 7.4 Hz, 3H, H-19); <u>13C NMR</u> (126 MHz, CDCl₃) δ 170.2, 167.9, 161.9 (C=O), 150.9, 150.3, 150.1, 149.6, 139.2, 134.0, 128.9 (C_q), 128.7, 127.6 (C-12/C-13), 125.9, 120.3, 109.7, 97.2 (C_q), 86.4 (C_q t-Bu), 82.5, 70.8, 70.2, 70.1, 70.0, 69.9 (CH₂ PEG), 68.7 (O-CH₂-CO), 67.5 (C-16), 55.6 (C_q), 43.4 (C-10), 31.0 (C-17), 28.1, 28.1 (t-Bu), 18.6 (C-18), 13.9 (C-19); <u>HRMS</u> [C₃₄H₅₀N₆O₁₀ + H]⁺: 703.36517 found, 703.36612 calculated.

1-(4-((6-amino-2-butoxy-8-oxo-7,8-dihydro-9H-purin-9-yl)methyl)phenyl)-1-oxo-5,8,11-trioxa-2-azatridecan-13-oic acid (119).



Butyl ester 118 (170.7 mg, 0.243 mmol, 1 eq) was dissolved in toluene (0.4 mL, 0.5 M) and H₃PO₄ (0.1 mL, 85-90% wt) was added. After LCMS analysis indicated complete conversion the mixture was concentrated *in vacuo*, dissolved in a solution of NH₄OAc (0.033 M) in a mixture of AcOH/ACN/*t*-BuOH/H₂O (3/1/1/4, v/v/v/v, 6 mL) and purified via RP-

HPLC (linear gradient 25 - 40% B in A, 10 min, Gemini-NX 5μm C18, 110 Å, 250 x 10.0 mm, 5 mL/min) to yield title compound **119** as a white powder after lyophilization (57.54 mg, 105 μmol, 43%). <u>LC-MS:</u> R_t = 4.80 min (10 - 90% ACN; 13 min); <u>1H NMR</u> (400 MHz, DMSO) δ 10.17 (s, 1H, COOH), 8.50 (t, J = 5.6 Hz, 1H, NH), 7.79 (d, J = 8.3 Hz, 2H, H-12/H-13), 7.34 (d, J = 8.3 Hz, 2H, H-12/H-13), 6.56 (s, 2H, NH₂), 4.90 (s, 2H, H-10), 4.12 (t, J = 6.6 Hz, 2H, H-16), 4.00 (s, 2H, O-CH₂-CO), 3.57 - 3.48 (m, 11H, CO)NH, CH₂ PEG), 3.39 (q, J = 5.8 Hz, 2H, CH₂-NH), 1.65 - 1.56 (m, 2H, H-17), 1.35 (dq, J = 14.7, 7.4

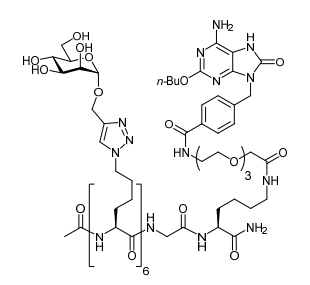
Hz, 2H, H-18), 0.89 (t, J = 7.4 Hz, 3H, H-19); ^{13}C NMR (101 MHz, DMSO) δ 171.7, 166.0, 160.1 (C=O), 152.3, 149.1, 147.8, 140.2, 133.5 (C_q), 127.4, 127.2 (C-12/C-13), 98.3 (C_q), 69.8, 69.7, 69.7, 69.6, 68.9 (CH₂ PEG), 67.6 (O-CH₂-CO), 65.9 (C-16), 42.1 (C-10), 39.2 (CH₂-NH), 30.6 (C-17), 18.8 (C-18), 13.7 (C-19); $\frac{1}{2}$ HRMS [C₂₅H₃₄N₆O₈ + H]⁺: 547.25105 found, 547.25109 calculated.

perfluorophenyl 1-(4-((6-amino-2-butoxy-8-oxo-7,8-dihydro-9H-purin-9-yl)methyl)phenyl)-1-oxo-5,8,11-trioxa-2-azatridecan-13-oate (120).



Carboxylic acid **119** (11.04 mg, 20.1 μ mol, 1 eq) was dissolved in a solution of pentafluorophenol (120 μ L, 0.34 M, 40.8 μ mol, 2 eq) and N,N'-Diisopropylcarbodiimide (3.42 μ L, 22.1 μ mol, 1.1 eq) was added. After two hours, this solution was used without further workup.

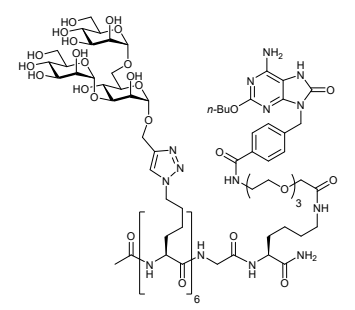
Ac-Lys(Man₁)-Lys(Man₁)-Lys(Man₁)-Lys(Man₁)-Lys(Man₁)-Lys(Man₁)-Gly-Lys[1-(4-((6-amino-2-butoxy-8-oxo-7,8-dihydro-9H-purin-9-yl)methyl)phenyl)-1-oxo-5,8,11-trioxa-2-azatridecan-13-oic amide]-NH₂ (121).



To a solution of **50** in water (250uL, 4.0 mM, 1.0 μ mol, 1 eq) a stock solution of Pfp ester **120** (30 μ L, 0.17 M, 5.0 μ mol, 5 eq) and DIPEA (0.5 μ L, 3 μ mol, 3 eq) were added. The mixture was further diluted with DMSO (250 μ L) until the mixture was a homogenous solution, and shaken overnight. After purification via RP-HPLC (linear gradient 7 - 55% B in A, 10 min, Gemini-NX 5 μ m C18, 110 Å, 250 x 10.0 mm, 5 mL/min) compound **121** was isolated as a white powder after

lyophilization (2.19 mg, 727 nmol, 73%). <u>LC-MS</u>: $R_t = 3.68$ min (10 - 90% ACN; 13 min); <u>1H NMR</u> (500 MHz, D₂O) δ 8.01 - 7.91 (m, 6H, trzl), 7.71 (d, J = 8.3 Hz, 2H, H-12*/H-13*), 7.40 (d, J = 8.2 Hz, 2H, H-12*/H-13*), 5.01 (s, 2H, H-10*), 4.92 (s, 6H, H-1), 4.77 - 4.70 (m, 6H, O-CHH-trzl), 4.65 - 4.56 (m, 6H, O-CHH-trzl), 4.37 - 4.25 (m, 12H, CH₂-trzl), 4.24 - 4.15 (m, 8H, H-16*, CH (K)), 4.13 - 4.08 (m, 1H, CH (K)), 3.93 - 3.50 (m, 52H, H-2, H-3, H-4, H-5, H-6, CH₂ (G), CH₂ (PEG, 7x)), 3.04 - 2.99 (m, 2H, CH₂-NH(CO) (K)), 1.97 (s, 3H, Ac), 1.87 - 1.62 (m, 24H, CH₂ (K)), 1.61 - 1.53 (m, 2H, H-17*), 1.37 - 1.18 (m, 20H, H-18*, CH₂ (K)), 0.82 (t, J = 7.4 Hz, 3H, H-19*); <u>HRMS</u> [C₁₂₅H₁₉₆N₃₄O₅₂ + 3H]³⁺: 1003.13252 found, 1003.13283 calculated.

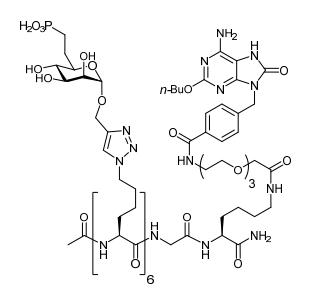
Ac-Lys(Man₃)-Lys(Man₃)-Lys(Man₃)-Lys(Man₃)-Lys(Man₃)-Lys(Man₃)-Gly-Lys(1-(4-((6-amino-2-butoxy-8-oxo-7,8-dihydro-9H-purin-9-yl)methyl)phenyl)-1-oxo-5,8,11-trioxa-2-azatridecan-13-oic amide)-NH₂ (122).



To a solution of **54** in water (250uL, 3.74 mM, 0.935 μ mol, 1 eq) a stock solution of Pfp ester **120** (30 μ L, 0.17 M, 5.0 μ mol, 5.3 eq) and DIPEA (0.5 μ L, 3 μ mol, 3.2 eq) were added. The mixture was further diluted with DMSO (250 μ L) until the mixture was a homogenous solution, and shaken overnight. After purification via RP-HPLC (linear gradient 7 - 55% B in A, 10 min, Gemini-NX 5 μ m C18, 110 Å, 250 x 10.0 mm, 5 mL/min)

compound **122** was isolated as a white powder after lyophilization (2.15 mg, 429 nmol, 46%). <u>LC-MS</u>: $R_t = 3.33 \text{ min} (10 - 90\% \text{ ACN}; 13 \text{ min}); \frac{1 \text{H NMR}}{1} (500 \text{ MHz}, D_2\text{O}) \delta 8.02 - 7.92 (m, 6H, trzl), 7.72 (d, <math>J = 8.1 \text{ Hz}, 2\text{H}, \text{H-}12*/\text{H-}13*), 7.40 (d, <math>J = 8.2 \text{ Hz}, 2\text{H}, \text{H-}12*/\text{H-}13*), 5.06 (s, 6\text{H}, \text{H-}1/\text{H-}1'/\text{H-}1''), 5.02 (s, 2\text{H}, \text{H-}10*), 4.90 (s, 6\text{H}), 4.88 (s, 6\text{H}, \text{H-}1/\text{H-}1'/\text{H-}1''), 4.69 - 4.59 (m, 6\text{H}, \text{O-CH}H-\text{trzl}), 4.42 - 4.27 (m, 12\text{H}, \text{CH}_2-\text{trzl}), 4.27 - 4.16 (m, 8\text{H}, \text{H-}16*, \text{CH (K)}), 4.14 (dd, <math>J = 5.5, 1.8 \text{ Hz}, 1\text{H}, \text{CH (K)}), 4.10 - 3.50 (m, 124\text{H}, \text{H-}2, \text{H-}2', \text{H-}3', \text{H-}3', \text{H-}4, \text{H-}4', \text{H-}4'', \text{H-}5, \text{H-}5', \text{H-}5'', \text{H-}6, \text{H-}6', \text{H-}6'', \text{CH}_2 (G), \text{CH}_2 (\text{PEG}, 7\text{x})), 3.02 (d, <math>J = 6.8 \text{ Hz}, 2\text{H}, \text{C}H_2-\text{NH}(\text{CO}) (\text{K})), 1.98 (s, 3\text{H}, \text{Ac}), 1.91 - 1.62 (m, 24\text{H CH}_2 (\text{K})), 1.62 - 1.52 (m, 2\text{H}, \text{H-}17*), 1.42 - 1.16 (m, 20\text{H}, \text{H-}18*, \text{CH}_2 (\text{K})), 0.83 (t, <math>J = 7.4 \text{ Hz}, 3\text{H}, \text{H-}19*); \frac{\text{HRMS}}{1} (\text{C}_{197}\text{H}_{316}\text{N}_{34}\text{O}_{112} + 4\text{H}_1^{14+}: 1239.01239 \text{ found}, 1239.01069 \text{ calculated}.$

Ac-Lys(M6P)-Lys(M6P)-Lys(M6P)-Lys(M6P)-Lys(M6P)-Gly-Lys(1-(4-((6-amino-2-butoxy-8-oxo-7,8-dihydro-9H-purin-9-yl)methyl)phenyl)-1-oxo-5,8,11-trioxa-2-azatridecan-13-oic amide)-NH₂ (124).



Mannose-6-phospate clusters **123**³⁰ (2.45 mg, 8.3 μmol, 1 eq) was dissolved in a stock solution of Pfp ester **120** (90 μL, 0.17 M, 15.0 μmol, 1.9 eq) and DIPEA (2 μL, 12 μmol, 1.5 eq) was added. After overnight shaking the mixture was purified via gel filtration (Toyopearl HW-40S, 1.6x60 cm, 150 mM NH₄OAc, 20% ACN, 1mL/min) (25 - 37 mL) followed by RP-HPLC (linear gradient 5 - 55% B in A, 10 min, Gemini-NX 5μm C18, 110 Å, 250 x 10.0 mm, 5 mL/min)

to isolate compound **124** as a white powder after lyophilization (0.80 mg, 231 nmol, 2.8%). <u>LC-MS:</u> $R_t = 5.68 \text{ min}$ (0 - 50% ACN; 13 min); <u>HRMS</u> [$C_{131}H_{208}N_{34}O_{64}P_6^{6-} + 4NH_4^+ + 2 Na^+ + 3H^+$]³⁺: 1197.05295 found, 1197.13554 calculated.

References

- (1) Gential, G. P. P.; Hogervorst, T. P.; Tondini, E.; van de Graaff, M. J.; Overkleeft, H. S.; Codée, J. D. C.; van der Marel, G. A.; Ossendorp, F.; Filippov, D. V. Peptides Conjugated to 2-Alkoxy-8-Oxo-Adenine as Potential Synthetic Vaccines Triggering TLR7. *Bioorg. Med. Chem. Lett.* **2019**, *29*, 1340–1344. https://doi.org/10.1016/j.bmcl.2019.03.048.
- (2) Apostólico, J. D. S.; Lunardelli, V. A. S.; Coirada, F. C.; Boscardin, S. B.; Rosa, D. S. Adjuvants: Classification, Modus Operandi, and Licensing. *J. Immunol. Res.* **2016**, *2016*, 1–16. https://doi.org/10.1155/2016/1459394.
- (3) Zom, G. G. P.; Khan, S.; Filippov, D. V.; Ossendorp, F. TLR Ligand-Peptide Conjugate Vaccines. Toward Clinical Application., 1st ed.; Elsevier Inc., 2012; Vol. 114. https://doi.org/10.1016/B978-0-12-396548-6.00007-X.
- (4) Muñoz-Wolf, N.; Lavelle, E. C. Innate Immune Receptors. In Nod Like Receptors, Pelegrin, P., Virgilio, F. Di, Eds.; Springer, 2016; pp 1–43. https://doi.org/10.1007/978-1-4939-3566-6_9.
- (5) Gay, N. J.; Gangloff, M. Structure and Function of Toll Receptors and Their Ligands. *Annu. Rev. Biochem.* **2007**, *76*, 141–165. https://doi.org/10.1146/annurev.biochem.76.060305.151318.
- (6) Jung, S.; von Thülen, T.; Laukemper, V.; Pigisch, S.; Hangel, D.; Wagner, H.; Kaufmann, A.; Bauer, S. A Single Naturally Occurring 2'-O-Methylation Converts a TLR7- and TLR8-Activating RNA into a TLR8-Specific Ligand. PLoS One 2015, 10, e0120498. https://doi.org/10.1371/journal.pone.0120498.
- (7) Leslie, A. J.; Pichulik, T.; Khatamzas, E.; Mayer, A.; McMichael, A.; Simmons, A. Early Phosphorylation Events Induced in Dendritic Cells by the HIV Derived TLR8 Ligand SsRNA40. **2011**.
- (8) Gantier, M. P.; Tong, S.; Behlke, M. A.; Xu, D.; Phipps, S.; Foster, P. S.; Williams, B. R. G. TLR7 Is Involved in Sequence-Specific Sensing of Single-Stranded RNAs in Human Macrophages. *J. Immunol.* **2008**, 180, 2117–2124. https://doi.org/10.4049/jimmunol.180.4.2117.
- (9) Krieg, A. M.; Yi, A.-K.; Matson, S.; Waldschmidt, T. J.; Bishop, G. A.; Teasdale, R.; Koretzky, G. A.; Klinman, D. M. CpG Motifs in Bacterial DNA Trigger Direct B-Cell Activation. *Nature* **1995**, *374*, 546–549. https://doi.org/10.1038/374546a0.
- (10) Gibson, S. J.; Lindh, J. M.; Riter, T. R.; Gleason, R. M.; Rogers, L. M.; Fuller, A. E.; Oesterich, J. L.; Gorden, K. B.; Qiu, X.; McKane, S. W.; Noelle, R. J.; Miller, R. L.; Kedl, R. M.; Fitzgerald-Bocarsly, P.; Tomai, M. A.; Vasilakos, J. P. Plasmacytoid Dendritic Cells Produce Cytokines and Mature in Response to the TLR7 Agonists, Imiquimod and Resiquimod. *Cell. Immunol.* 2002, 218, 74–86. https://doi.org/10.1016/S0008-8749(02)00517-8.
- (11) Mirer, E.; El Sayed, F.; Ammoury, A.; Lamant, L.; Messer, L.; Bazex, J. Treatment of Mammary and Extramammary Paget's Skin Disease with Topical Imiquimod. *J. Dermatolog. Treat.* **2006**, *17*, 167–171. https://doi.org/10.1080/09546630600788877.
- (12) Bernhardt, S. L.; Buanes, T. A.; Møller, M.; Eriksen, J. A.; Geudernack, G. Imiquimod a New Adjuvant for Telomerase Peptide Vaccine: A Phase I Trial in Patients with Inoperable Pancreatic Cancer. J. Clin. Oncol. 2005, 23, 9623–9623. https://doi.org/10.1200/jco.2005.23.16_suppl.9623.
- (13) Hirota, K.; Kazaoka, K.; Niimoto, I.; Kumihara, H.; Sajiki, H.; Isobe, Y.; Takaku, H.; Tobe, M.; Ogita, H.; Ogino, T.; Ichii, S.; Kurimoto, A.; Kawakami, H. Discovery of 8-Hydroxyadenines as a Novel Type of Interferon Inducer. *J. Med. Chem.* **2002**, *45*, 5419–5422. https://doi.org/10.1021/jm0203581.
- (14) Moyle, P. M.; Toth, I. Modern Subunit Vaccines: Development, Components, and Research Opportunities. *ChemMedChem* **2013**, *8*, 360–376. https://doi.org/10.1002/cmdc.201200487.
- (15) Jin, G.; Wu, C. C. N.; Tawatao, R. I.; Chan, M.; Carson, D. A.; Cottam, H. B. Synthesis and Immunostimulatory Activity of 8-Substituted Amino 9-Benzyladenines as Potent Toll-like Receptor 7 Agonists. *Bioorg. Med. Chem. Lett.* 2006, 16, 4559–4563. https://doi.org/10.1016/j.bmcl.2006.06.017.
- (16) Yoo, E.; Crall, B. M.; Balakrishna, R.; Malladi, S. S.; Fox, L. M.; Hermanson, A. R.; David, S. A. Structure-Activity Relationships in Toll-like Receptor 7 Agonistic 1H-Imidazo[4,5-c]Pyridines. *Org. Biomol. Chem.* 2013, 11, 6526–6545. https://doi.org/10.1039/c3ob40816g.
- (17) Kurimoto, A.; Hashimoto, K.; Nakamura, T.; Norimura, K.; Ogita, H.; Takaku, H.; Bonnert, R.; McInally,

- T.; Wada, H.; Isobe, Y. Synthesis and Biological Evaluation of 8-Oxoadenine Derivatives as Toll-like Receptor 7 Agonists Introducing the Antedrug Concept. *J. Med. Chem.* **2010**, *53*, 2964–2972. https://doi.org/10.1021/jm100070n.
- (18) Shukla, N. M.; Lewis, T. C.; Day, T. P.; Mutz, C. A.; Ukani, R.; Hamilton, C. D.; Balakrishna, R.; David, S. A. Toward Self-Adjuvanting Subunit Vaccines: Model Peptide and Protein Antigens Incorporating Covalently Bound Toll-like Receptor-7 Agonistic Imidazoquinolines. *Bioorg. Med. Chem. Lett.* **2011**, *21*, 3232–3236. https://doi.org/10.1016/j.bmcl.2011.04.050.
- (19) Fujita, Y.; Hirai, K.; Nishida, K.; Taguchi, H. 6-(4-Amino-2-Butyl-Imidazoquinolyl)-Norleucine: Toll-like Receptor 7 and 8 Agonist Amino Acid for Self-Adjuvanting Peptide Vaccine. *Amino Acids* **2016**, *48*, 1319–1329. https://doi.org/10.1007/s00726-016-2190-7.
- (20) Weterings, J. J.; Khan, S.; van der Heden van Noort, G. J.; Melief, C. J. M.; Overkleeft, H. S.; van der Burg, S. H.; Ossendorp, F.; van der Marel, G. A.; Filippov, D. V. 2-Azidoalkoxy-7-Hydro-8-Oxoadenine Derivatives as TLR7 Agonists Inducing Dendritic Cell Maturation. *Bioorganic Med. Chem. Lett.* **2009**, *19*, 2249–2251. https://doi.org/10.1016/j.bmcl.2009.02.095.
- (21) Chan, M.; Hayashi, T.; Kuy, C. S.; Gray, C. S.; Wu, C. C. N.; Corr, M.; Wrasidlo, W.; Cottam, H. B.; Carson, D. A. Synthesis and Immunological Characterization of Toll-Like Receptor 7 Agonistic Conjugates. *Bioconjug. Chem.* **2009**, *20*, 1194–1200. https://doi.org/10.1021/bc900054q.
- (22) Wang, X.-D.; Gao, N.-N.; Diao, Y.-W.; Liu, Y.; Gao, D.; Li, W.; Wan, Y.-Y.; Zhong, J.-J.; Jin, G.-Y. Conjugation of Toll-like Receptor-7 Agonist to Gastric Cancer Antigen MG7-Ag Exerts Antitumor Effects. *World J. Gastroenterol.* **2015**, *21*, 8052. https://doi.org/10.3748/wjg.v21.i26.8052.
- (23) Akinbobuyi, B.; Byrd, M. R.; Chang, C. A.; Nguyen, M.; Seifert, Z. J.; Flamar, A.-L.; Zurawski, G.; Upchurch, K. C.; Oh, S.; Dempsey, S. H.; Enke, T. J.; Le, J.; Winstead, H. J.; Boquín, J. R.; Kane, R. R. Facile Syntheses of Functionalized Toll-like Receptor 7 Agonists. *Tetrahedron Lett.* **2015**, *56*, 458–460. https://doi.org/10.1016/j.tetlet.2014.11.126.
- (24) Gential, G. P. P. Self Adjuvanting Immunopeptides: Design and Synthesis (Dissertation), Leiden University, 2018.
- (25) Savage, P.; Horton, V.; Moore, J.; Owens, M.; Witt, P.; Gore, M. A Phase I Clinical Trial of Imiquimod, an Oral Interferon Inducer, Administered Daily. *Br. J. Cancer* **1996**, *74*, 1482–1486. https://doi.org/10.1038/bjc.1996.569.
- (26) Xiang, Y.; Caron, P.-Y.; Lillie, B. M.; Vaidyanathan, R. Sulfur Contamination Due to Quenching of Halogenation Reactions with Sodium Thiosulfate: Resolution of Process Problems via Improved Quench Protocols. *Org. Process Res. Dev.* **2008**, *12*, 116–119. https://doi.org/10.1021/op700227p.
- (27) Heller, K.; Ochtrop, P.; Albers, M. F.; Zauner, F. B.; Itzen, A.; Hedberg, C. Covalent Protein Labeling by Enzymatic Phosphocholination. *Angew. Chemie Int. Ed.* **2015**, *54*, 10327–10330. https://doi.org/10.1002/anie.201502618.
- (28) Peterse, E. [To Be Determined] (Dissertation), Leiden University, 2020.
- (29) Li, B.; Berliner, M.; Buzon, R.; Chiu, C. K. F.; Colgan, S. T.; Kaneko, T.; Keene, N.; Kissel, W.; Le, T.; Leeman, K. R.; Marquez, B.; Morris, R.; Newell, L.; Wunderwald, S.; Witt, M.; Weaver, J.; Zhang, Z. Aqueous Phosphoric Acid as a Mild Reagent for Deprotection of Tert -Butyl Carbamates, Esters, and Ethers. *J. Org. Chem.* **2006**, *71*, 9045–9050. https://doi.org/10.1021/jo061377b.
- (30) Reintjens, N. R. M. Synthetic Carbohydrate Ligands for Immune Receptors (Dissertation), Leiden University, 2020.

Synthesis of trifunctional mannosylated peptide antigen conjugates targeting DC-SIGN and TLR7

Introduction

The last decades, immunotherapies have proven to be powerful in the treatment of cancers. For instance, inhibition of immune regulatory checkpoints can result in the restoration of immune responses, which has led to the successful treatment of various tumors where traditional cytotoxic therapies failed.^{3,4} To be effective, immunotherapies have to elicit or sustain a strong and tumor-specific T cell response.^{5,6} A possible method to achieve this is by the use of vaccine strategies, In which tumor-associated antigens (TAAs) are combined with an adjuvant to generate a specific immune response against these antigens. Adjuvants can be derived from pathogen-associated molecular patterns (PAMPs) that induce immune activation *via* binding to pattern recognition receptors (PRRs), thereby stimulating antigen presenting cells (APCs) to mature and initiate an immune response. Maturation results in the secretion of inflammatory cytokines and upregulation

Part of this work is published in Hogervorst & Li et al. 2019¹

Part of this work has been submitted by Hogervorst & Li et al. 2020²

of antigen processing and presentation, which are a necessity for an adequate adaptive immune response. ⁷ Target antigens can be common TAAs, neoantigens, neo open reading frame peptides⁸ or a combination of these, allowing to combat each cancer with a personalized treatment.9 One possible strategy to obtain such vaccines is to generate them via a synthetic approach. An advantage of a synthetic approach is the fact that they can be obtained as well-defined molecular structures, reducing the potential risk of raising autoimmune responses against self-antigens, a possible side effect when antigens are isolated from cancer cells. In addition, this strategy allows for the covalent attachment of adjuvants and antigens, an approach which has previously been successfully demonstrated with ligands for the Toll-Like Receptor (TLR) family, 10-14 the NOD-like receptor (NLR) family 15 or combinations thereof. 16-19 It has become clear that the covalent attachment of a TLR agonist to an antigen can enhance antigen presentation while DC maturation via the TLRligands is maintained. 20,21 Another class of PRRs that is often targeted are the C-type lectin receptors (CLRs) as described in Chapter 1 and 2. For example, DC-SIGN has previously been successfully exploited to deliver cancer antigens to DCs by enhancing uptake and antigen presentation, generating more effective anti-cancer immunotherapies. 16,17,22-24 Furthermore, it has been shown that the simultaneous targeting of CLRs and TLRs can lead to a synergistic more powerful immune response. For example, simultaneous triggering of DC-SIGN and TLR4 strengthened and prolonged TLR-signaling leading to enhanced pro-inflammatory cytokine production in DCs. 25,26 Based on these results, it is hypothesized that a peptide-antigen conjugate, equipped with both a mannose-based DC-SIGN targeting glycan and a TLR-ligand, could lead to synergy in antigen presentation and improve specific T cell activation.

This Chapter describes the design and synthesis of trifunctional conjugates composed of CLR-targeting clusters, a synthetic long peptide, and a TLR7-agonist (Figure 1). Targeting of DC-SIGN will be achieved with the mannoside clusters, as described in Chapter 2. As a model antigen, the effector T cell epitope gp100₂₈₀₋₂₈₈ and helper T cell epitope gp100₄₄₋₅₉ are combined to form a synthetic long peptide (SLP). The addition of a helper T cell epitope can result in a more durable immune response when compared with a stand-alone effector T cell epitope and is included for future assays.²⁷ As agonist of endosomal TLR7 the 8-oxo-adenosine analog, described in Chapter 3, is selected.^{28–30} The hypothesis is, that upon binding and internalization *via* DC-SIGN, these conjugates are trafficked towards the endosomes where they can activate TLR7. The benefit of using an endosomal receptor, instead of a PRRs residing on the cell surface, would be the prevention of competition between the binding of DC-SIGN and other surface PRRs.

1 3 Mannoside clusters gp100₂₈₀₋₂₈₈ gp10044-59 HN αAbuWRGK -NH₂ YLEPGPVTA-NRQLYPEWTEAQRLD Targeting of DC-SIGN for CD8⁺ and CD4⁺ Improve maturation by addition improved uptake of antigens model antigens of additional adjuvant (Mannoside clusters, Chapter 2) (gp100)(TLR7 agonist, Chapter 3)

Figure 1: The global structure of trifunctional mannosylated conjugates.

Results and Discussion

To determine the effect of the mannoside clusters on the activity of the antigen conjugates, control peptides were synthesized lacking these clusters (Scheme 1). These peptides were obtained using a Fmoc-SPPS strategy starting from Tentagel® S-RAM amide resin. A monomethoxy trityl (Mmt) protected lysine was used as the first amino acid to introduce an orthogonal side-chain protecting group that could later be selectively removed for further functionalization. The immobilized lysine was elongated using standard Fmoc protected amino acids generating the gp100₂₈₀₋₂₈₈ sequence (YLEPGPVTA) for antigen cross-presentation to CD8⁺ T cells connected to the N-terminus of the gp100₄₄₋₅₉ sequence for antigen presentation to CD4⁺ T cells (NRQLYPEWTEAQRLD). The presence of both CD8⁺ and CD4⁺ epitopes in the same antigen-conjugate platform will allow the study of both cross-presentation and presentation, which in combination with different adjuvants can help to determine the optimal adjuvant combinations on the same conjugate platform. The epitope was extended both at the C- and the N-terminus with four extra amino acids, acting as spacers (Figure 1). To prevent potential oxidation, Cys_{60} was replaced by its isosteric analog α aminobutyric acid, a modification that should have minimal impact on biological processing.³¹ Acetylation of the N-terminus yielded immobilized peptide 126. For further functionalization of this peptide, the Mmt group on the C-terminal lysine was removed selectively, after which the lysine was elongated with spacer moiety 127 and TLR7 ligand 116 (see Chapter 3) to give immobilized TLR7 conjugate 128. Both 126 and 128 were released from resin by treatment with a cleavage cocktail (TFA/TIS/H₂O, 190/5/5, v/v/v) to generate gp100 peptide 129 and bifunctional conjugate 130, containing the gp100 peptide and the TLR7 agonist.²⁹ To validate that the replacement of cysteine by α -aminobutyric acid does not hamper the antigen presentation capacity, bifunctional conjugate **133** was synthesized via similar chemistry as its isosteric isomer **130** (Scheme 1). Both TLR-antigen conjugates **130** and **133** were tested for their antigen cross-presentation ability. In short, five-day-old monocyte-derived dendritic cells (moDCs) were incubated with these conjugates, after which the moDCs were washed and co-cultured with a CD8⁺ cell clone that is specific for the gp100₂₈₀₋₂₈₈ MHC-I epitope. Interferon γ cytokine secretion was measured by sandwich ELISA as a measure for T cell activation. Quantification of antigen presentation was achieved by normalization of the interferon γ cytokine production to secretion levels induced by short gp100 peptide (gp100₂₈₀₋₂₈₈ set to 100%). Both **130** and **133** resulted in similar levels of antigen presentation, indicating that the replacement of cysteine in the epitope indeed did not hamper the presentation capacity (See Figure 2).

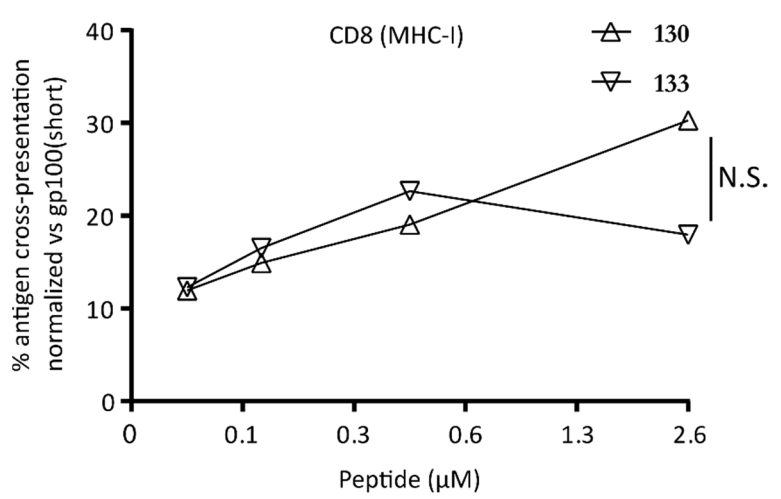


Figure 2: Comparison of the antigen cross-presenting ability of 130 and 133.

The gp100(Cys) (133) was compared to the gp100 methyl analog (130). No significant difference was seen between the two peptides in presence of TLR7 ligand. One representative donor out of six is shown.

соон

Scheme 1: Synthesis of control gp100 peptide and control gp100-TLR7 conjugates.

[[AA₁]*]:-Trp(Boc)-Arg(Pbf)-Gly-

[AA₁] : -Trp-Arg-Gly-

FmocHN 127 BuO 116

[AA₂]*]:-Val-Thr(tBu)-His(Trt)-Thr(tBu)-Tyr(tBu)-Leu-Glu(OtBu)-Pro-Gly-Pro-Val-Thr(tBu)-Ala-Asn(Trt)-Arg(Pbf)-Gln(Trt)-Leu-Tyr(tBu)-Pro-Glu(OtBu)-Red (Trt)-Leu-Tyr(tBu)-Pro-Glu(OtBu)-Red (Trt)-Red (Trt)-Trp(Boc)-Thr(tBu)-Glu(OtBu)-Ala-Gln(Trt)-Arg(Pbf)-Leu-Asp(OtBu)-

[AA2]: -Val-Thr-His-Thr-Tyr-Leu-Glu-Pro-Gly-Pro-Val-Thr-Ala-Asn-Arg-Gln-Leu-Tyr-Pro-Glu-Trp-Thr-Glu-Ala-Gln-Arg-Leu-Asp-

Reagents and conditions: a) i. Fmoc-SPPS (HCTU, DIPEA, DMF); ii. Ac₂O, DIPEA, DMF; b) i. TFA, DCM; ii. Fmoc-SPPS (127 or 116, HCTU, DIPEA, DMF); c) TFA, TIS, H₂O,(phenol) (129: 9.1% over 33 couplings (93% per step); 130: 1.78% over 35 couplings (89% per step); 133: 0.23% over 35 couplings (84% per step)).

Two different strategies for the incorporation of the mannose clusters in mannosylated-gp100-TLR7 conjugates were considered (Scheme 2). Route A comprises the synthesis of a gp100-TLR7 conjugate provided with six azides (n = 6) followed by copper(I)-catalyzed alkyne-azide cycloadditions (CuAACs) with propargylated mannosides. The modular approach of route B applies the pre-assembled mannoside clusters described in Chapter 2 for a single CuAAC with a gp100-TLR7 conjugate provided with a single azide (Route B, Scheme 2). Both routes allow for the introduction of different ligands in the final stage of assembly, enabling screening of different PAMP combinations on the same gp100 platform. Route A would be most straightforward as six simultaneous cycloadditions and one purification are required. However, incomplete CuAACs may result in a complicated product mixture necessitating a challenging purification. Although route B is more lengthy, the availability of the well-defined mannoside clusters (see Chapter 2) and the introduction of different PAMPs via a single CuAAC could make this approach overall more effective. Based on these considerations, both strategies were evaluated.

The azido-gp100-peptides were obtained using a similar Fmoc-SPPS strategy as for the control peptides described above. Both routes started with immobilized peptide 134, that was further elongated on the N-terminal valine with either one (135) or six azidolysines (136, Scheme 3). Treatment of resin 136, bearing six azides, with the cleavage cocktail (described above) generated a crude mixture of poor quality and attempts to isolate the desired peptide in sufficient amount failed. When resin 135, bearing only one azide, was treated with the same cocktail, the quality of the crude peptide was somewhat better but still too poor for large scale isolation of 137. Optimization of the synthesis of peptide 137 was achieved by the use of double couplings at an elevated temperature. The quality was further improved by the addition of phenol to the cleavage cocktail as an additional scavenger. Together, this allowed for the isolation of 137 in sufficient quantities after purification. En route to trifunctional mannosylated conjugates, the monomethoxy trityl (Mmt) on the C-terminal lysine of immobilized peptide 135 was selectively removed, followed by elongation of this position with a spacer moiety (127) and the TLR7 ligand 116 (as described in Scheme 1) to provide resin 138 bearing the TLR7 agonist on the C-terminus. Release of the peptide-TLR7 conjugate from the resin and concomitant global deprotection of the side chains with the optimized scavenger cocktail resulted in the azido-gp100-TLR7 conjugate 139. Because of the successful assembly of the TLR7-functionalized antigens with the conjugation ready azide handle, this route was further explored and the first route, with six azidolysines incorporated in the antigenic peptide, was abandoned.

The modular approach of route B requires the introduction of an alkyne handle on the mannoside clusters, the synthesis of which is described in Chapter 2. Treatment of mono- and hexa-valent

mannoside clusters 32, 33, 35, 36, and 50-54 with pent-4-ynoic acid-N-hydroxysuccinimide (NHS) ester (140) and purification *via* gel filtration yielded alkyne clusters 141-149, suitable for ensuing CuAAC (Scheme 4). CuAAC of the monovalent monomannoside cluster 141 with either azidogp100 137 or azido-gp100-TLR7 conjugate 139 yielded the bi-functional (containing both CLR ligand and gp100 antigen) conjugate 150 and the tri-functional (containing both CLR ligand, gp100 antigen, and TLR ligand) conjugate 151 (Scheme 4). Applying the same procedure to hexavalent monomannosides cluster 145 gave comparable results, resulting in bifunctional and trifunctional conjugates 152 and 153, respectively. The four conjugates obtained in this manner could be purified and were isolated in sufficient yield, proving the feasibility of route B. This result, in combination with the difficulties to obtain a gp100 peptide bearing six azides (i.e. 136), the availability of the mannoside clusters described in Chapter 2, the ease of alkyne introduction on these clusters, and the possibility to introduce other ligands in a single ligation, made the modular route B preferred over direct route A (Scheme 2). The compound library was finalized by the assembly of the remaining seven mannoside clusters (142-144 and 146-149) with 137 and 139 to yield bi- and trifunctional conjugates 154-167 (Scheme 4).

Scheme 2: Retrosynthesis of route A and B towards (hexavalent) mannosylated gp100 conjugates.

Scheme 3: Synthesis of azido-gp100 and azido-gp100-TLR7 conjugates.

[AA]* : -Val-Thr(tBu)-His(Trt)-Thr(tBu)-Tyr(tBu)-Leu-Glu(OtBu)-Pro-Gly-Pro-Val-Thr(tBu)-Ala-Asn(Trt)-Arg(Pbf)-Gln(Trt)-Leu-Tyr(tBu)-Pro-Glu(OtBu)-Trp(Boc)-Thr(tBu)-Glu(OtBu)-Ala-Gln(Trt)-Arg(Pbf)-Leu-Asp(OtBu)-αAbu-Trp(Boc)-Arg(Pbf)-Gly-

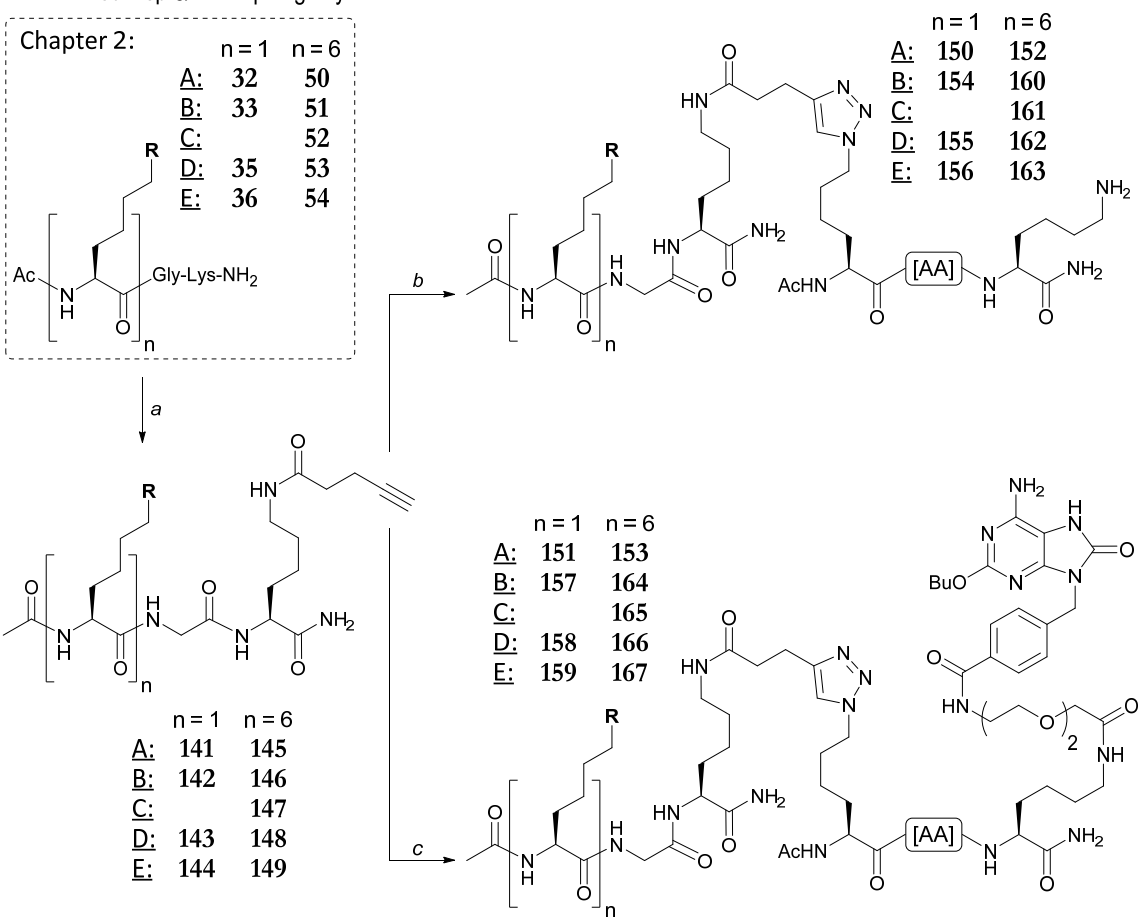
[AA] : -Val-Thr-His-Thr-Tyr-Leu-Glu-Pro-Gly-Pro-Val-Thr-Ala-Asn-Arg-Gln-Leu-Tyr-Pro-Glu-Trp-Thr-Glu-Ala-Gln-Arg-Leu-Asp-αAbu-Trp-Arg-Gly-

Reagents and conditions: a) Fmoc-SPPS (HCTU, DIPEA, DMF); b) Ac₂O, DIPEA, DMF; c) i. TFA, DCM; ii. Fmoc-SPPS (127 or 116, HCTU, DIPEA, DMF); d) TFA, TIS, H₂O, (phenol) (137: 8.33% over 34 couplings (93% per step); 139: 5.09% over 36 couplings (92% per step)).

Finally these conjugates with either the monovalent clusters bearing the monomannoside (150 & 151), α 1,2-di-mannoside (154 & 157), α 1,6-di-mannoside (155 & 158), or α 1,3- α 1,6-tri-mannoside (156 & 159), or the hexavalent clusters with the monomannosides (152 & 153), α 1,2-di-mannosides (160 & 164), α 1,3-di-mannosides (161 & 165), α 1,6-di-mannosides (162 & 166), or α 1,3- α 1,6-tri-mannosides (163 & 167) were evaluated for their capacity to induce DC-maturation and present the model gp100 antigen. Since the number of available moDCs was limited, only the hexavalent series (160-167) have been tested. The mono mannoside clusters 150-153 have been evaluated in comparison to their *C*-mannoside analogs as described in Chapter 5.

Scheme 4: Assembly of mannosylated – (TLR7) – bi- and tri-functional gp100 conjugates.

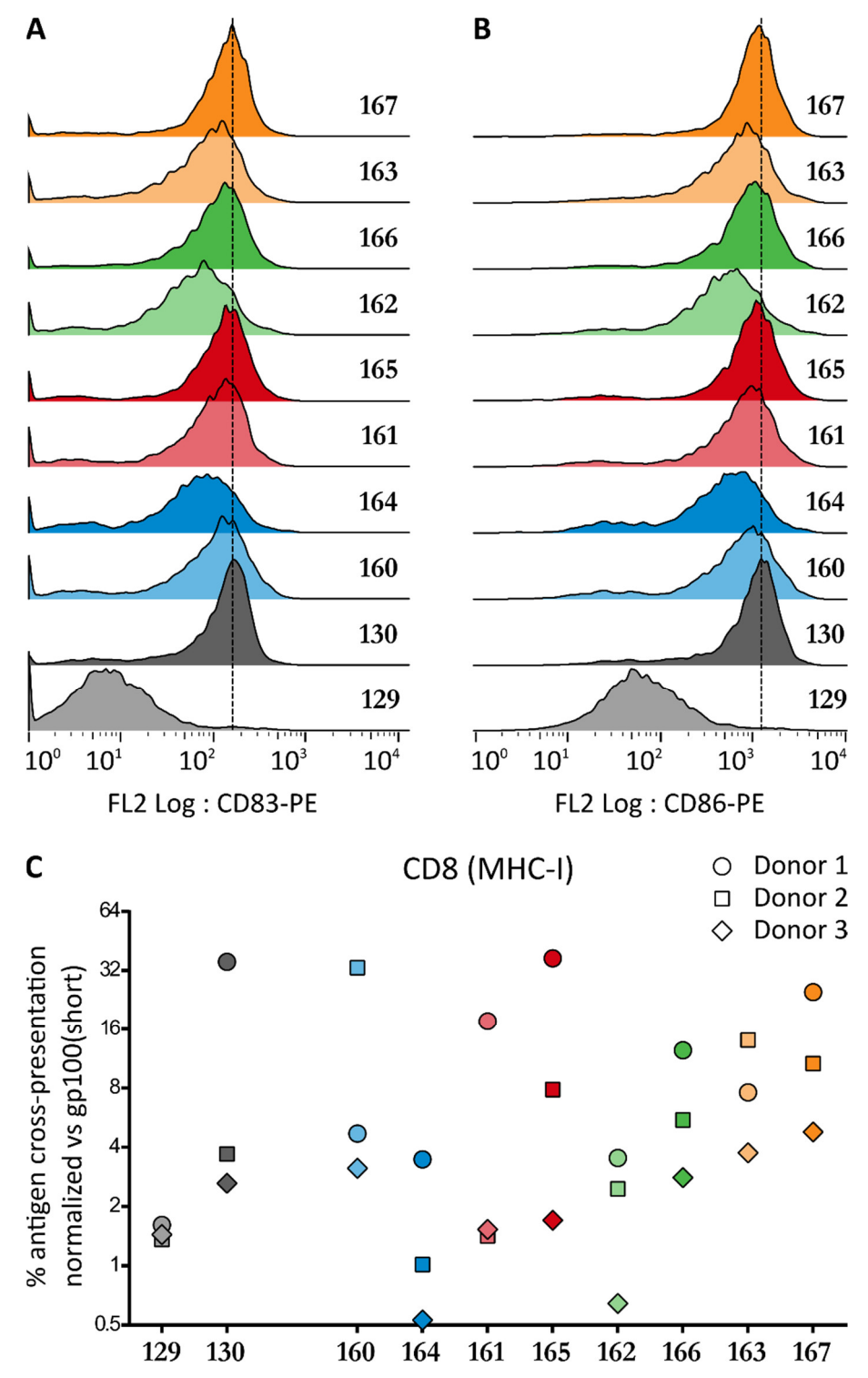
[AA]: -Val-Thr-His-Thr-Tyr-Leu-Glu-Pro-Gly-Pro-Val-Thr-Ala-Asn-Arg-Gln-Leu-Tyr-Pro-Glu-Trp-Thr-Glu-Ala-Gln-Arg-Leu-Asp-αAbu-Trp-Arg-Gly-



Reagents and conditions: a) 140, DIPEA, DMSO (141: 62%; 142: 71%; 143: 71%; 144: 18%; 145: 66%; 146: 96%; 147: 95%; 148: 95%; 149: 94%); b) 137, CuI, THPTA, DIPEA, H₂O, DMSO (150: 52%; 152: 34%; 154: 91%; 155: 90%; 156: 88%; 160: 39%; 161: 62%; 162: 68%; 163: 45%;); c) 139, CuI, THPTA, DIPEA, H₂O, DMSO (151: 34%; 153: 29%; 157: 21%; 158: 19%; 159: 32%; 164: 24%; 165: 41%; 166: 18%; 167: 27%).

The ability to mature moDCs was quantified by measuring the expression of CD83 and CD86 after overnight stimulation with a selection of conjugates (Figure 3A and 3B). As expected, 129, the gp100 peptide without any adjuvant, did not induce maturation. All bi- and tri-functional conjugates induce the expression of both maturation markers. Generally, the conjugates bearing the TLR7 agonist led to enhanced maturation. These results show that the presence of either the TLR7 ligand or the mannoside clusters in conjugates does not hamper the maturation abilities of the ligands. Inclusion of the TLR agonist improves the maturation capacity of the conjugates most significantly. Besides maturation, a selection of the prepared conjugates was tested for their antigen cross-presentation ability using gp100 specific T cell clones as described above for 130 and 133 (see Figure 3C). Although significant donor variability was observed, almost all conjugates showed improvements when mannoside clusters were attached (Figure 3C). Unexpectedly, conjugate 164, bearing both the TLR7 agonist and an α 1,2-di-mannoside cluster, did not enhance antigen presentation. Whether this outcome is due to differences in processing, signaling, uptake, or conjugate stability is unclear and needs additional experiments. Overall, conjugate 167 demonstrated the most consistent and strongest response of the tested conjugates. This conjugate, bearing both TLR7 ligand and the tri-mannoside cluster, also effectively induced maturation, which would make it a good candidate for further development. Except for 164, all conjugates that contained both the mannoside clusters and TLR agonist, induced more maturation and higher levels of antigen cross-presentation when compared with their counterpart only bearing the mannoside cluster. This result indicates that the combination of two different adjuvants in a single adjuvant-antigen conjugate can further improve the effectiveness of antigen conjugates and could serve as a starting point for further development of antigen conjugates bearing multiple functionalities.

Figure 3: Conjugates **160-167** were compared with conjugates **129** and **130** for their ability to induce maturation (A and B) and their capacity to cross-present antigen (C).



A, B) Expression of the DC maturation marker CD83 and CD86 upon overnight stimulation with the trifunctional conjugates is measured by flow cytometry. LPS stimulation (10 ng/mL) is used as positive control; **C)** Antigen presentation by the moDCs was determined by IFNy release of the activated T cells, after stimulation with conjugates (20 μ M, 30 min).

Conclusion

The synthesis of conjugates that combine a model epitope with both TLR7 and DC-SIGN ligands has been reported. All conjugates are assembled on the same gp100 platform, which includes both a CD4⁺ and CD8⁺ epitope. The gp100 peptides were assembled using automated SPPS. C-terminal functionalization of the gp100 epitope with the TLR7 agonist, described in Chapter 3, could be achieved on resin via selective removal of the Mmt group on lysine. The assembly of azido functionalized gp100 peptides of sufficient quality and quantity required double couplings at elevated temperature and the presence of phenol in the cleavage cocktail. For the introduction of mannoside clusters, the simultaneous CuAACs of multiple propargylmannosides with the azides in the gp100 platform and a single CuAAC of alkyne functionalized pre-assembled clusters with one azide in the gp100 were planned. However, isolation of gp100 peptides bearing six azides in sufficient quantities proved difficult. Because the alkyne functionalized mannoside clusters were readily obtained and the CuAAC of these alkyne functionalized clusters to the gp100 platform was successful, the former route was abandoned and the latter was used to assemble a set of trifunctional conjugates. A selection of these conjugates was tested for their ability to induce DC maturation and their capacity to induce antigen cross-presentation. Although significant variation between DC-donors was observed, the results have shown that the combination of a TLR7 and DC-SIGN ligand improves the effectiveness of the antigen conjugates. Additional experiments with the monovalent clusters will show whether the hexavalent presentation of the mannosides is a requirement for the activity of the conjugates. Overall, the conjugate that combines the TLR7 agonist with the hexavalent tri-mannoside cluster has demonstrated the most potential, inducing strong maturation and consistent levels of antigen-presentation, and could serve as a starting point for further conjugate development.

With the here described gp100 platform and optimized synthetic protocols, further conjugates can be designed bearing different combinations of adjuvants that could target different PRRs such as other members of the TLR-, NLR- or CLR-families. Adjuvants with carboxylic acid handles could be introduced on either the C-terminal lysine or N-terminus on resin. The azide handle could be used for either addition of other alkyne functionalized adjuvants or be used in conjunction with "clickable" reporter groups to study the fate of these conjugates during the processing from uptake to presentation. The presence of the CD4⁺ epitope in the peptide would allow determining the level of antigen presentation of helper T cell epitopes. The trifunctional conjugates described in this Chapter and novel conjugates based on the methods described in combination with the current cross-presentation assay could be used to determine the best combination of adjuvants to obtain the most durable anti-cancer response with a single vaccine modality.

Experimental

General procedures:

All reactions, purifications, and analyses were performed as described in the general procedures of Chapter 2.

General procedure for automated solid-phase synthesis of gp100 peptides:

The solid-phase peptide synthesis was performed on a TRIBUTE® Peptide Synthesizer (Gyros Protein Technologies AB, Arizona, USA) applying Fmoc based protocol starting with Tentagel® S-RAM resin (~0.22 mmol/g) on a 100-250 µmol scale using established synthetic protocols.³² The consecutive steps for synthesis on 250 µmol scale^a performed in each cycle were:

1) DMF wash (1x) followed by nitrogen purge; 2) Deprotection of the Fmoc-group with 20% piperidine in DMF (8 mL)(3 x 3 min at 50 °C); 3) DMF wash (3x) followed by nitrogen purge; 4.1) Coupling of the appropriate amino acid^b in four-fold excess (unless stated otherwise);^{c,d} 4.2) Step 4.1 was repeated 5) DMF wash (3x) followed by nitrogen purge; 6) capping with a solution of Ac₂O/DMF/DIPEA (8 mL, 10/88/2, v/v/v) for 2 min; 7) DMF wash (2x).

After the complete sequence the resin was washed with DMF (3x), DCM (3x), Et₂O (3x), followed by nitrogen purge before treatment with the cleavage cocktail.

 $Val-Thr(tBu)-His(Trt)-Thr(tBu)-Tyr(tBu)-Leu-Glu(OtBu)-Pro-Gly-Pro-Val-Thr(tBu)-Ala-Asn(Trt)-Arg(Pbf)-Gln(Trt)-Leu-Tyr(tBu)-Pro-Glu(OtBu)-Trp(Boc)-Thr(tBu)-Glu(OtBu)-Ala-Gln(Trt)-Arg(Pbf)-Leu-Asp(OtBu)-<math>\alpha$ Abu-Trp(Boc)-Arg(Pbf)-Gly-Lys(Mmt)-Tentagel S-Rink amide (134).

Peptide synthesis was performed on a 250 µmol scale using the general procedure. Resulting in functionalized resin 134, which was used in further reactions.

^a All amounts are scaled-down in equimolar proportions for smaller scale.

^b The amino acids applied in this synthesis were: Fmoc-Lys(Mmt)-OH, Fmoc-Gly-OH, Fmoc-Arg(Pbf)-OH, Fmoc-Trp(Boc)-OH, Fmoc-Leu-OH^d, Fmoc-Glu(OfBu)-OH, Fmoc-Ala-OH, Fmoc-Glu(OfBu)-OH, Fmoc-Thr(fBu)-OH, Fmoc-Pro-OH, Fmoc-Tyr(fBu)-OH, Fmoc-Asn(Trt)-OH, Fmoc-Val-OH, Fmoc-His(Trt)-OH, Fmoc-Cys(Trt)-OH and Fmoc-Lys(N₃)-OH (IRIS biotech). Fmoc-AEEA-OH (Fmoc-8-amino-3,6-dioxaoctanoic acid)(Carbosynth) and 116.

^c Generally, the Fmoc amino acid is dissolved in a HCTU solution in DMF (5.00 mL ,0.20 M, 1.0 mmol, 4 eq) The resulting solution was transferred to the reaction vessel followed by a DIPEA solution in DMF (4.00 mL, 0.50 M, 2.0 mmol, 8 eq) to initiate the coupling. The reaction vessel was shaken for 30 min at 50 °C (unless stated otherwise).

 $^{^{\}rm d}$ Aspartic acid and the adjacent Leucine and Arginine were introduced at with one hour reaction time at room temperature. Fmoc removal was achieved with piperide/DMF in 3 x 5 min at room temperature. 35

Ac-Val-Thr-His-Thr-Tyr-Leu-Glu-Pro-Gly-Pro-Val-Thr-Ala-Asn-Arg-Gln-Leu-Tyr-Pro-Glu-Trp-Thr-Glu-Ala-Gln-Arg-Leu-Asp- α Abu-Trp-Arg-Gly-Lys-NH₂ (129).

Resin 134 (theoretical loading of 25 μ mol), was capped with Ac₂O/DMF/DIPEA (4 mL, 10/88/2, purge to yield Ac-Val-Thr(tBu)-His(Trt)-Thr(tBu)-Tyr(tBu)-Leu-Glu(OtBu)-Pro-Gly-Pro-Val-Thr(tBu)-Ala-Asn(Trt)-Arg(Pbf)-Gln(Trt)-Leu-Tyr(tBu)-Pro-Glu(OtBu)-Trp(Boc)-Thr(tBu)-Glu(OtBu)-Ala-Gln(Trt)-Arg(Pbf)-Leu-Asp(OtBu)- $_{\alpha}$ Abu-Trp(Boc)-Arg(Pbf)-Gly-Lys(Mmt)-Tentagel S-RAM. The resin was transferred to a flask and treated for 120 minutes with a cleavage cocktail (10 mL, TFA/TIS/H₂O, 190/5/5, v/v/v). The resin was filtered off and washed with neat TFA (3 x 1 mL). The filtrate was concentrated and transferred dropwise into a cold mixture of Et₂O/pentane (45 mL, 5/4, v/v). This solution was centrifuged (10 minutes, 5000 rpm) after which the supernatant was removed and the precipitate was dried under nitrogen flow and dissolved (4 mL, DMF/H₂O, 1/3, v/v). Purification via RP-HPLC (linear-gradient 19.5 - 29.5 % B in A, 10 min, 5 mL/min, Gemini-NX 5 μ m C18, 110 Å, 250 x 10.0 mm) yielded title compound 129 as a white powder after lyophilization (8.97 mg, 2.28 μ mol, 9.1% over 33 couplings, 93% per step). LC-MS: R_t = 6.01 min (10 - 50% ACN; 13 min); R_t = 4.25 min (10 - 90% ACN; 13 min); HRMS [C₁₇₈H₂₆₉N₅₁O₅₁ + 5H]⁵⁺: 788.8100 found, 788.80888 calculated.

Ac-Lys(N_3)-Val-Thr-His-Thr-Tyr-Leu-Glu-Pro-Gly-Pro-Val-Thr-Ala-Asn-Arg-Gln-Leu-Tyr-Pro-Glu-Trp-Thr-Glu-Ala-Gln-Arg-Leu-Asp- α Abu-Trp-Arg-Gly-Lys-NH $_2$ (137).

Resin 134 (theoretical loading of 250 μmol) was elongated using the general protocol after which the N-terminus was capped with Ac₂O/DMF/DIPEA (4mL, 10/88/2, v/v/v, 3 x 5 min) and the resin was washed with DMF (3x), DCM (3x), Et₂O (3x) and dried by nitrogen purge to yield Ac-Lys(N₃)-Val-Thr(*I*Bu)-His(Trt)-Thr(*I*Bu)-Tyr(*I*Bu)-Leu-Glu(O*I*Bu)-Pro-Gly-Pro-Val-Thr(*I*Bu)-Ala-Asn(Trt)-Arg(Pbf)-Gln(Trt)-Leu-Tyr(*I*Bu)-Pro-Glu(O*I*Bu)-Trp(Boc)-Thr(*I*Bu)-Glu(O*I*Bu)-Ala-Gln(Trt)-Arg(Pbf)-Leu-Asp(O*I*Bu)-αAbu-Trp(Boc)-Arg(Pbf)-Gly-Lys(Mmt)-Tentagel® S-RAM. The resin was transferred to a flask and treated for 120 minutes with a cleavage cocktail (25 mL, TFA/TIS/H₂O/phenol, 188/5/5/2, v/v/v/w). The mixture was concentrated to approximately one mL and the resin was filtered off into a cold mixture of Et2O/pentane (45 mL, 5/4, v/v). The resin was washed off extra with neat TFA (3x 1 mL) into the ether solution. This solution was centrifuged (10 minutes, 5000 rpm) after which the supernatant was removed and the precipitate was dried under nitrogen flow. Purification via RP-HPLC (linear-gradient 23 - 34% B in A, 11 min, 5 mL/min, Gemini-NX 5 μm C18, 110 Å, 250 x 10.0 mm) yielded title compound 137 as a white powder after lyophilization (85.2 mg, 20.8μmol, 8.33% over 34 couplings, 93% per step). LC-MS: R_t = 4.32 min (10 - 90% ACN; 13 min); HRMS [C₁₈₄H₂₇₉N₅₅O₅₂ + 5H]⁵⁺: 819.6255 found, 819.62596 calculated.

Ac-Val-Thr-His-Thr-Tyr-Leu-Glu-Pro-Gly-Pro-Val-Thr-Ala-Asn-Arg-Gln-Leu-Tyr-Pro-Glu-Trp-Thr-Glu-Ala-Gln-Arg-Leu-Asp- α Abu-Trp-Arg-Gly-Lys(Peg-TLR7L)-NH₂ (130).

Resin 134 (100 µmol scale, single couplings at room temperature) was loaded in a syringe with frit and treated with a TFA solution (1% in DCM) shaken for five minutes followed by filtration. This was repeated until the filtrate lost the orange/yellow color (~ 12x). After which the resin was washed with DCM (5x), DMF (5x) Piperidine (20% in DMF, 1x) and DMF (5x). The lysine was elongated with Fmoc-AEEA-OH using the general protocol followed by introduction of 116 (91.5 mg, 200 µmol, 2 eq) by shaking for two hour with HCTU (82.7 mg, 200 μmol, 2 eq) and DIPEA (69.7 μL, 400 μmol, 4 eq) in DMF (1.8 mL, 0.11 M of 116). The resin was washed with DMF (3x), DCM (3x) and Et₂O (2x) followed by nitrogen purge, transferred to a flask and treated for 120 minutes with a cleavage cocktail (10 mL, TFA/TIS/H₂O, 190/5/5, v/v/v). The mixture was concentrated to approximately one mL and the resin was filtered off into a cold mixture of Et₂O/pentane (45 mL, 5/4, v/v). The resin was washed off extra with neat TFA (3x 1 mL) into the ether solution. This solution was centrifuged (10 minutes, 5000 rpm) after which the supernatant was removed and the precipitate was dried under nitrogen flow. Purification via RP-HPLC (linear-gradient 24 -36 % B in A, 12 min, 5 mL/min, Gemini-NX 5 µm C18, 110 Å, 250 x 10.0 mm) yielded title compound 130 as a white powder after lyophilization (7.85 mg, 1.78 μmol, 1.78% over 35 couplings, 89% per step). <u>LC-MS</u>: $R_t = 4.94 \text{ min } (10 - 90\% \text{ ACN}; 13 \text{ min}); <u>HRMS</u> [C₂₀₁H₂₉₇N₅₇O₅₇ + 5H]⁵⁺: 885.6479 found,$ 885.65029 calculated.

Ac-Lys(N_3)-Val-Thr-His-Thr-Tyr-Leu-Glu-Pro-Gly-Pro-Val-Thr-Ala-Asn-Arg-Gln-Leu-Tyr-Pro-Glu-Trp-Thr-Glu-Ala-Gln-Arg-Leu-Asp- $_{\alpha}$ Abu-Trp-Arg-Gly-Lys(Peg-TLR7L)-NH $_2$ (139).

Resin 134 (theoretical loading of 100 μmol) was elongated using the general protocol resulting in Ac- $Lys(N_3)-Val-Thr(tBu)-His(Trt)-Thr(tBu)-Tyr(tBu)-Leu-Glu(OtBu)-Pro-Gly-Pro-Val-Thr(tBu)-Ala-Interval (Bu)-Interval (Bu)-Interv$ Asn(Trt)-Arg(Pbf)-Gln(Trt)-Leu-Tyr(tBu)-Pro-Glu(OtBu)-Trp(Boc)-Thr(tBu)-Glu(OtBu)-Ala-Gln(Trt)-Arg(Pbf)-Glu(OtBu)-Ala-Gln(Trt)-Arg(Pbf)-Glu(OtBu)-Ala-Gln(Trt)-Arg(Pbf)-Glu(OtBu)-Ala-Gln(Trt)-Arg(Pbf)-Glu(OtBu)-Ala-Gln(Trt)-Arg(Pbf)-Glu(OtBu)-Ala-Gln(Trt)-Arg(Pbf)-Glu(OtBu)-Ala-Gln(Trt)-Arg(Pbf)-Glu(OtBu)-Ala-Gln(Trt)-Arg(Pbf)-Glu(OtBu)-Ala-Gln(Trt)-Arg(Pbf)-Glu(OtBu)-Ala-Gln(Trt)-Arg(Pbf)-Glu(OtBu)-Ala-Gln(Trt)-Arg(Pbf)-Glu(OtBu)-Ala-Gln(Trt)-Arg(Pbf)-Glu(OtBu)-Ala-Gln(Trt)-Arg(Pbf)-Glu(OtBu)-Ala-Gln(Trt)-Arg(Pbf)-Arg(Pbf)-Ala-Gln(Trt)-Arg(Pbf)-Ala-Gln(Trt)-Arg(Pbf)-Ala-Gln(Trt)-Arg(Pbf)-Ala-Gln(Trt)-Arg(Pbf)-Ala-Gln(Trt)-Arg(Pbf)-Ala-Gln(Trt)-Arg(Pbf)-Ala-Gln(Trt)-Arg(Pbf)-Ala-Gln(Trt)-Arg(Pbf)-ArgArg(Pbf)-Leu-Asp(OtBu)-αAbu-Trp(Boc)-Arg(Pbf)-Gly-Lys(Mmt)-Tentagel® S-RAM. This was loaded in a syringe with frit and treated with a TFA solution (1% in DCM) shaken for five minutes, followed by filtration. This was repeated until the filtrate lost the orange/yellow color (~ 12x). After which the resin was washed with DCM (5x), DMF (5x) Piperidine (20% in DMF, 1x) and DMF (5x). The lysine was elongated with Fmoc-AEEA-OH using the general protocol followed by introduction of 116 (183 mg, 400 µmol, 4 eq) by shaking for one hour with HCTU (165.4 mg, 400 µmol, 4 eq) and DIPEA (140 µL, 800 µmol, 8 eq) in DMF (3.6 mL, 0.11 M of 116). The resin was washed with DMF (3x), DCM (3x) and Et₂O (2x) followed by nitrogen purge, transferred to a flask and treated for 120 minutes with a cleavage cocktail (25 mL, TFA/TIS/H₂O/phenol, 188/5/5/2, v/v/v/w). The mixture was concentrated to approximately one mL and the resin was filtered off into a cold mixture of Et₂O/pentane (45 mL, 5/4, v/v). The resin was washed off extra with neat TFA (3x 1 mL) into the ether solution. This solution was centrifuged (10 minutes, 5000 rpm) after which the supernatant was removed and the precipitate was dried under nitrogen flow. Purification via RP-HPLC (linear-gradient 23 - 36 % B in A, 12 min, 5 mL/min, Gemini-NX 5 µm C18,

110 Å, 250 x 10.0 mm) yielded title compound **139** as a white powder after lyophilization (23.30 mg, 5.09 μ mol, 5.09% over 36 couplings, 92% per step). <u>LC-MS:</u> $R_t = 7.05 \text{ min}$ (10 - 50% ACN; 13 min); $R_t = 4.71 \text{ min}$ (10 - 90% ACN; 13 min); <u>HRMS</u> [$C_{207}H_{307}N_{61}O_{58} + 5H]^{5+}$: 916.4700 found, 916.46737 calculated.

Ac-Val-Thr-His-Thr-Tyr-Leu-Glu-Pro-Gly-Pro-Val-Thr-Ala-Asn-Arg-Gln-Leu-Tyr-Pro-Glu-Trp-Thr-Glu-Ala-Gln-Arg-Leu-Asp-Cys-Trp-Arg-Gly-Lys(Peg-TLR7L)-NH₂ (133).

Ac-Val-Thr(tBu)-His(Trt)-Thr(tBu)-Tyr(tBu)-Leu-Glu(OtBu)-Pro-Gly-Pro-Val-Thr(tBu)-Ala-Asn(Trt)-Arg(Pbf)-Gln(Trt)-Leu-Tyr(tBu)-Pro-Glu(OtBu)-Trp(Boc)-Thr(tBu)-Glu(OtBu)-Ala-Gln(Trt)-Arg(Pbf)-Leu-Asp(OtBu)-Cys(Trt)-Trp(Boc)-Arg(Pbf)-Gly-Lys(Mmt)-Tentagel® S-RAM (100 µmol scale, single couplings at room temperature) was loaded in a syringe with frit and treated with a TFA (1% in DCM) shaken for five minutes followed by filtration. This was repeated until the filtrate lost the orange/yellow color (12x). After which the resin was washed with DCM (5x), DMF (5x) Piperidine (20% in DMF, 1x) and DMF (5x). The lysine was elongated with Fmoc-AEEA-OH using the general protocol followed by introduction of 116 (91.5 mg, 200 μmol, 2 eq) by shaking for two hour with HCTU (82.7 mg, 200 μmol, 2 eq) and DIPEA (69.7 µL, 400 µmol, 4 eq) in DMF (1.8 mL, 0.11 M of 116). The resin was washed with DMF (3x), DCM (3x) and Et₂O (2x) followed by nitrogen purge, transferred to a flask and treated for 120 minutes with a cleavage cocktail (10 mL, TFA/TIS/H₂O, 190/5/5, v/v/v). The mixture was concentrated to approximately one mL and the resin was filtered off into a cold mixture of Et₂O/pentane (45 mL, 5/4, v/v). The resin was washed off extra with neat TFA (3x 1 mL) into the ether solution. This solution was centrifuged (10 minutes, 5000 rpm) after which the supernatant was removed and the precipitate was dried under nitrogen flow. Purification via RP-HPLC (linear-gradient 24 - 36 % B in A, 12 min, 5 mL/min, Gemini-NX 5 µm C18, 110 Å, 250 x 10.0 mm) yielded title compound 133 as a white powder after lyophilization (1.03 mg, 0.232 μ mol, 0.23% over 35 couplings, 84% per step). <u>LC-MS</u>: $R_t = 5.01 \text{ min}$ (10 -90% ACN; 13 min); <u>HRMS</u> $[C_{201}H_{296}N_{56}O_{57}S + 5H]^{5+}$: 889.0417 found, 889.04249 calculated.

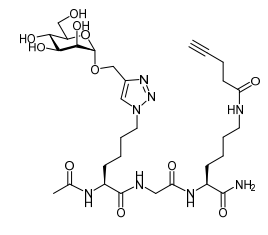
Pent-4-ynoic acid succinimidyl ester (140).

Synthesis and spectral data were as described in previous literature.³³

General alkyne introduction procedure:

The "general procedure" to introduce the alkyne handle: A solution of glycoclusters with a free amine (0.2 M, aq., 1 eq) was mixed with a stock solution of **140** (0.15 M, 3 eq) and DIPEA (0.05 M, 1 eq) in DMSO and shaken for one hour. Reaction progress was followed via LC-MS and when completed, the 4-pentynoic amides were purified via gel filtration (Toyopearl HW-40S, 150 mM NH₄HCO₃, 1.6 x 60 cm, 1 mL/min) or RP-HPLC (linear-gradient, 5 mL/min, Gemini-NX 5 μm C18, 110 Å, 250 x 10.0 mm) followed by lyophilization.

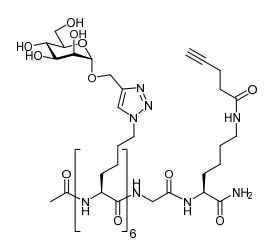
Ac-Lys(Man₁)-Gly-Lys(pent-4-ynoic amide)-NH₂ (141).



Compound **32** (5.72 mg, 9.28 µmol) was coupled with **140** using the general procedure. Compound **141** was obtained after RP-HPLC (linear-gradient 5 - 45% B, 10 min) as a white powder (4.01 mg, 5.75 µmol, 62%). <u>LC-MS</u>: $R_t = 4.48 \text{ min}$ (0 - 50% ACN; 13 min); <u>1H NMR</u> (400 MHz, D₂O) δ 8.03 (s, 1H, trzl), 4.93 (d, J = 1.7 Hz, 1H, H-1), 4.82 - 4.80 (m, 1H, O-CHH-trzl), 4.68 (d, J = 12.4 Hz, 1H, O-CHH-

trzl), 4.42 (t, J = 6.9 Hz, 2H, CH₂-trzl), 4.26 - 4.14 (m, 2H, CH), 3.92 - 3.57 (m, 8H, CH₂ (G), H-2, H-3, H-4, H-5, H-6), 3.16 (t, J = 6.9 Hz, 2H, CH₂-NH₂), 2.49 - 2.42 (m, 2H, CH₂), 2.42 - 2.36 (m, 2H, CH₂), 2.32 (t, J = 2.5 Hz, 1H, C \equiv CH), 1.97 (s, 3H, Ac), 1.89 (q, J = 7.3 Hz, 2H, CH₂), 1.85 - 1.62 (m, 4H, CH₂), 1.48 (q, J = 8.2, 7.5 Hz, 2H, CH₂), 1.34 (ddd, J = 23.0, 15.9, 7.4 Hz, 4H, CH₂); $\frac{13}{2}$ C NMR (101 MHz, D₂O) δ 174.9 (C=O), 99.4 (C-1), 72.9, 70.4, 70.1, 69.9, 66.6, 60.8, 59.7, 53.8, 50.1, 42.4, 39.0, 34.5, 30.5, 22.3, 21.8, 21.6 (Ac), 14.6; $\frac{1}{2}$ HRMS [C₃₀H₄₈N₈O₁₁ + H]+: 697.35147 found, 697.35153 calculated.

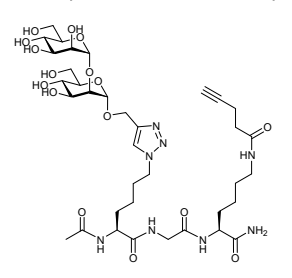
Ac-Lys(Man₁)-Lys(Man₁)-Lys(Man₁)-Lys(Man₁)-Lys(Man₁)-Lys(Man₁)-Gly-Lys(pent-4-ynoic amide)-NH₂ (145).



Compound **50** (8.0 mg, 2.1 μ mol) was coupled with **140** using the general procedure. Compound **145** was obtained after purification by gel filtration (eluted at 41 - 52 mL) or RP-HPLC (linear-gradient 5 - 45% B, 10 min) as a white powder (3.52 mg, 1.38 μ mol, 66%). <u>LC-MS</u>: R_t = 5.09 min (0 - 50% ACN; 13 min); <u>1H NMR</u> (500 MHz, D₂O) δ 7.95 (d, J = 5.6 Hz, 6H, trzl), 4.87 (d, J = 1.7 Hz, 6H, H-1), 4.71 (d, J

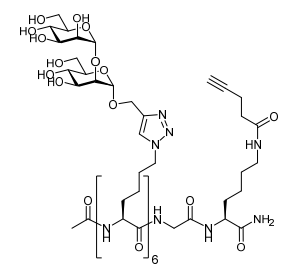
= 12.5, 3.9 Hz, 6H, O-C*H*H-trzl), 4.58 (d, J = 12.5 Hz, 6H, O-CH*H*-trzl), 4.31 (t, J = 6.5 Hz, 12H, CH₂-trzl), 4.20 - 3.99 (m, 7H, CH (K)), 3.91 - 3.49 (m, 38H, H-2, H-3, H-4, H-5, H-6, CH₂ (G)), 3.08 (t, J = 6.8 Hz, 2H, CH₂-NH(CO)), 2.39 - 2.22 (m, 5H, CH₂, CH₂, CH), 1.92 (s, 3H, Ac), 1.86 - 1.08 (m, 42H, CH₂); $\frac{13C \text{ NMR}}{126 \text{ MHz}}$ (126 MHz, D₂O) δ 160.5, 99.4 (C-1), 72.9, 70.5, 69.9, 66.6 (C-2, C-3, C-4, C5), 60.8 (C-6), 59.8 (O-CH₂-trzl); $\frac{13C \text{ NMR}}{126 \text{ NMS}}$ [C₁₀₅H₁₆₈N₂₈O₄₆ + 2H]²⁺: 1280.09306 found, 1280.09210 calculated.

Ac-Lys(1,2-Man₂)-Gly-Lys(pent-4-ynoic amide)-NH₂ (142).



Compound **33** (2.37 mg, 3.04 µmol) was coupled with **140** using the general procedure. Compound **142** was obtained after purification by gel filtration (eluted at 53.5 - 61 mL) as a white powder (1.86 mg, 2.16 µmol, 71%). <u>LC-MS</u>: $R_t = 4.72$ min (0 - 50% ACN; 13 min); <u>HRMS</u> [$C_{36}H_{58}N_8O_{16} + H$] +: 859.40447 found, 859.40435 calculated.

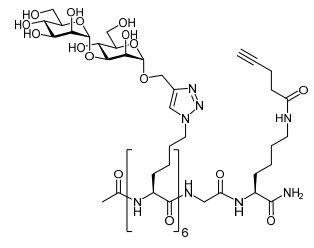
Ac-Lys(1,2-Man₂)-Lys(1,2-Ma



Compound **51** (7.06 mg, 2.04 µmol) was coupled with **140** using the general procedure. Compound **146** was obtained after purification by gel filtration (buffer contained 20% ACN, eluted at 25 - 40 mL) as a white powder (6.95 mg, 1.96 µmol, 96%). <u>LC-MS</u>: $R_t = 4.76 \text{ min}$ (0 - 50% ACN; 13 min); <u>1H NMR</u> (500 MHz, D₂O) δ 7.93 - 7.88 (m, 6H, trzl), 5.04 (s, 6H, H-1), 4.86 (s, 6H, H-1'), 4.66 (d, J = 12.4 Hz, 6H, O-CHH-trzl), 4.54 (d, J = 12.7 Hz, 6H, O-CHH-trzl), 4.27 (t, J = 6.4 Hz,

12H, CH₂-trzl), 4.18 - 3.97 (m, 7H, CH), 3.96 - 3.43 (m, 74H, CH₂ (G), H-2, H-2', H-3, H-3', H-4, H-4', H-5, H-5', H-6, H-6'), 3.03 (t, J = 6.4 Hz, 2H, CH₂NH₂), 2.35 - 2.17 (m, 5H, CH₂, CH₂, C≡CH), 1.87 (s, 3H, Ac), 1.82 - 1.03 (m, 42H, CH₂); <u>HRMS</u> [C₁₄₁H₂₂₈N₂₈O₇₆ + 3H]³⁺: 1177.83838 found, 1177.83618 calculated.

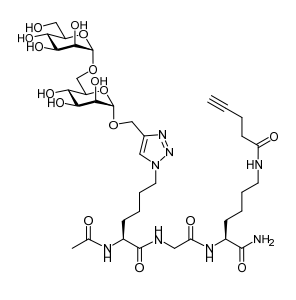
Ac-Lys(1,3-Man₂)-Lys(1,3-Ma



A solution of compound **52** (150 μ L, 5mM, 750 nmol, aq.) was coupled with **140** using the general procedure. Compound **147** was obtained after purification by gel filtration (buffer contained 20% ACN, eluted at 23.5 - 40 mL) as a white powder (2.23 mg, 645 nmol, 95%). <u>LC-MS</u>: R_t = 4.60 min (0 - 50% ACN; 13 min); <u>1H NMR</u> (500 MHz, D₂O) δ 7.93 - 7.88 (m, 6H, trzl), 4.96 (s, 6H, H-1),

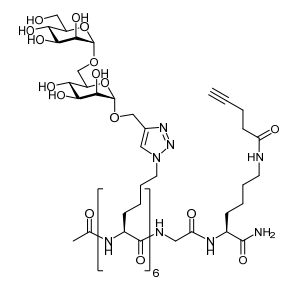
4.80 (s, 6H, H-1'), 4.66 (d, J = 5.8 Hz, 6H, O-CHH-trzl), 4.55 (d, J = 12.6 Hz, 6H, O-CHH-trzl), 4.26 (d, J = 6.3 Hz, 12H, CH₂-trzl), 4.14 - 3.96 (m, 7H, CH), 3.96 - 3.43 (m, 74H, CH₂ (G), H-2, H-2', H-3, H-3', H-4, H-4', H-5, H-5', H-6, H-6'), 3.03 (t, J = 6.7 Hz, 2H, CH₂NH₂), 2.39 - 2.16 (m, 5H, CH₂, CH₂, CH₂CH), 1.86 (s, 3H, Ac), 1.82 - 1.04 (m, 42H, CH₂); HRMS [C₁₄₁H₂₂₈N₂₈O₇₆ + 3H]³⁺: 1177.83747 found, 1177.83618 calculated.

Ac-Lys(1,6-Man₂)-Gly-Lys(pent-4-ynoic amide)-NH₂ (143).



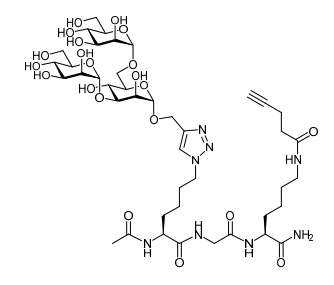
Compound **35** (2.32 mg, 2.99 μ mol) was coupled with **140** using the general procedure. Compound **143** was obtained after purification by gel filtration (eluted at 53.5 - 61 mL) as a white powder (1.81 mg, 2.11 μ mol, 71%). <u>LC-MS</u>: R_t = 4.73 min (0 - 50% ACN; 13 min); <u>HRMS</u> [C₃₆H₅₈N₈O₁₆ + H]⁺: 859.40439 found, 859.40435 calculated.

Ac-Lys(1,6-Man₂)-Lys(1,6-Ma



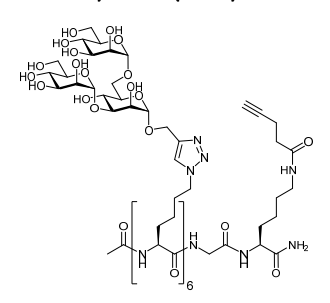
Compound **53** (2.35 mg, 679 nmol) was coupled with **140** using the general procedure. Compound **148** was obtained after purification by gel filtration (eluted at 31.5 - 42 mL) as a white powder (2.23 mg, 645 nmol, 95%). <u>LC-MS</u>: $R_t = 4.76$ min (0 - 50% ACN; 13 min); <u>HRMS</u> [$C_{141}H_{228}N_{28}O_{76} + 3H$]³⁺: 1177.83621 found, 1177.83618 calculated.

Ac-Lys(Man₃)-Gly-Lys(pent-4-ynoic amide)-NH₂ (144).



Compound **36** (4.53 mg, 4.81 µmol) was coupled with **140** using the general procedure. Compound **144** was obtained after purification by gel filtration (eluted at 44.5 - 50.5 mL) as a white powder (0.98 mg, 872 nmol, 18%). <u>LC-MS</u>: $R_t = 4.64$ min (0 - 50% ACN; 13 min); <u>HRMS</u> [$C_{42}H_{68}N_8O_{21} + H$]⁺: 1021.45725 found, 1021.45718 calculated.

Ac-Lys(Man₃)-Lys(Man₃)-Lys(Man₃)-Lys(Man₃)-Lys(Man₃)-Lys(Man₃)-Gly-Lys(pent-4-ynoic amide)-NH₂ (149).



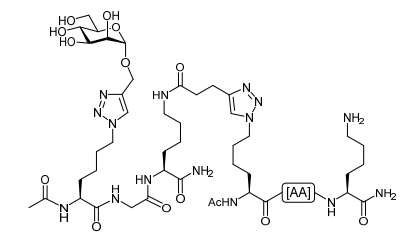
Compound **54** (18.77 mg, 4.24 µmol) was coupled with **140** using the general procedure. Compound **149** was obtained after purification by gel filtration (buffer contained 20% ACN, eluted at 26 - 38.5 mL) as a white powder (17.96 mg, 3.98 µmol, 94%). <u>LC-MS</u>: $R_t = 4.64 \text{ min } (0 - 50\% \text{ ACN}; 13 \text{ min}); \frac{1 \text{H NMR}}{1 \text{ H NMR}}$ (500 MHz, D₂O) δ 7.92 (s, 6H, trzl), 4.95 (s, 6H, H-1), 4.80 (s, 6H, H-1'), 4.76 (s, 6H, H-1"), 4.68 - 4.63 (m, 6H, O-CHH-trzl), 4.57 (d, J = 12.7 Hz, 6H, O-

CH*H*-trzl), 4.28 (t, J = 6.3 Hz, 12H, CH₂-trzl), 4.18 - 4.05 (m, 6H, CH), 4.05 - 3.39 (m, 111H, CH, CH₂ (G), H-2, H-2', H-3, H-3', H-3', H-4, H-4', H-4", H-5, H-5', H-5", H-6, H-6', H-6"), 3.04 (t, J = 6.7 Hz, 2H, CH₂NH₂), 2.41 - 2.18 (m, 5H, CH₂, CH₂, C≡CH), 1.87 (s, 3H, Ac), 1.84 - 1.01 (m, 42H, CH₂); 13 C NMR (126 MHz, D₂O) δ 143.5, 124.2 (CH trzl), 102.4, 99.7, 99.4 (C-1, C-1', C-1"), 78.6, 73.3, 72.7, 71.2, 70.6, 70.3, 70.0, 69.9, 69.5, 69.5, 66.7, 65.4, 64.9, 60.9 (C-2, C-2', C-2", C-3, C-3', C-3", C-4, C-4', C-4", C-5, C-5', C-5", C-6, C-6', C-6"), 59.8 (O-*C*H₂trzl), 53.9, 53.5 (CH), 50.0 (*C*H₂-trzl), 42.4 (CH₂ (G)), 39.1 (CH₂NH₂), 34.5 (CH₂), 30.0, 28.9, 22.0 (CH₂), 21.7 (Ac), 14.6 (CH₂); HRMS [C₁₇₇H₂₈₈N₂₈O₁₀₆ + 3H]³⁺: 1502.27589 found, 1502.27616 calculated.

General procedure for the CuAAC of alkyne mannoside clusters and azido-gp100 peptides:

The "general click protocol" used for the conjugation of alkynes and azido-gp100 peptides: All solvents used in these reactions were degassed by sonicating while bubbling argon through the solutions. A solution of azido-peptides 137 or 139 in DMSO was mixed with a solution of alkyne functionalized glycoclusters in water 141-149 followed by addition of an aliquot of a stock solution of CuI (0.1 eq), THPTA (0.3 eq) and DIPEA (0.2 eq) in water ([Cu⁺] = 0.5 M). The reaction was stirred at 45°C and the process was followed via LC-MS. When reactions did not progress and turned blue, a stock solution of sodium ascorbate (0.25 M) and arginine³⁴ (0.5 M, 0.2 - 1 eq ascorbate) in water was added. After completion a small amount of Quadrasil® AP (washed with water) was added, stirred for 1 h, filtered and purified by either gel filtration (Toyopearl HW-40S, 150 mM NH₄HCO₃, buffer contained 20% ACN, 1.6x60 cm, 1 mL/min) and/or RP-HPLC (linear-gradient, 5 mL/min, Gemini-NX 5 μm C18, 110 Å, 250 x 10.0 mm) followed by lyophilization.

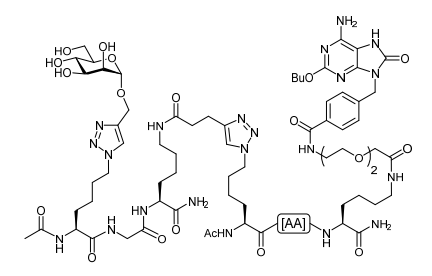
Ac-Lys(*[Ac-Lys(Man₁)-Gly-Lys(*triazolylpentyl-5-amide)-NH₂])-Val-Thr-His-Thr-Tyr-Leu-Glu-Pro-Gly-Pro-Val-Thr-Ala-Asn-Arg-Gln-Leu-Tyr-Pro-Glu-Trp-Thr-Glu-Ala-Gln-Arg-Leu-Asp- $_{\alpha}$ Abu-Trp-Arg-Gly-Lys-NH₂ (150).



A solution of mannosides cluster **141** (100 μ L, 0.02 M, 2.0 μ mol, 1.15 eq, aq.) and undecorated gp100 **137** in DMSO (88 μ L, 0.2 M, 1.75 μ mol, 1 eq) were conjugated using the general click protocol. After purification by RP-HPLC (linear-gradient 7 - 38% B, 10 min) compound **150** was obtained as a white powder (4.365 mg, 911 nmol, 52%). <u>LC-MS:</u> R_t =

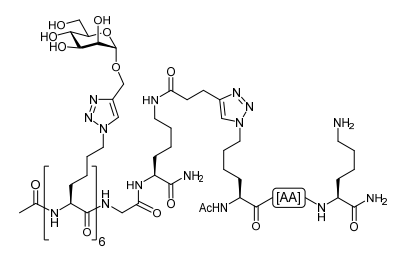
4.09 min (10 - 90% ACN; 13 min); $\frac{1}{1}$ H NMR (500 MHz, D₂O) δ 8.55 (d, J = 1.1 Hz, 1H, H_{arom} (H)), 7.99 (s, 1H, trzl), 7.71 (s, 1H, trzl), 7.48 (dd, J = 31.8, 7.9 Hz, 1Hz, 2H, H_{arom} (W)), 7.38 (dd, J = 16.5, 8.2 Hz, 4H, H_{arom} (W)), 7.26 - 7.10 (m, 5H, H_{arom}), 7.10 - 6.95 (m, 6H, H_{arom}), 6.83 - 6.65 (m, 4H, H_{arom} (Y)), 4.92 (d, J = 1.4 Hz, 1H, H-1), 4.77 - 4.51 (m, 7H), 4.47 - 4.00 (m, 34H), 3.99 - 3.47 (m, 20H), 3.35 - 2.65 (m, 31H), 2.53 (t, J = 7.3 Hz, 2H, CH_2NH_2 (K)), 2.50 - 2.29 (m, 7H), 2.29 - 2.15 (m, 8H), 2.14 - 1.02 (m, 92H), 1.01 - 0.69 (m, 30H); $\frac{1}{1}$ HRMS [$C_{214}H_{327}N_{63}O_{63}$ + 5H]⁵⁺: 958.89471 found, 958.89482 calculated.

Ac-Lys(*[Ac-Lys(Man₁)-Gly-Lys(*triazolylpentyl-5-amide)-NH₂])-Val-Thr-His-Thr-Tyr-Leu-Glu-Pro-Gly-Pro-Val-Thr-Ala-Asn-Arg-Gln-Leu-Tyr-Pro-Glu-Trp-Thr-Glu-Ala-Gln-Arg-Leu-Asp- α Abu-Trp-Arg-Gly-Lys(Peg-TLR7L)-NH₂ (151).



A solution of mannosides cluster **141** (75 μ L, 0.02 M, 1.50 μ mol, 1.5 eq, aq.) and TLR-decorated gp100 **139** in DMSO (100 μ L, 0.01 M, 1.0 μ mol, 1 eq) were conjugated using the general click protocol. After purification by RP-HPLC (linear-gradient 7 - 42% B, 11 min) compound **151** was obtained as a white powder (1.800 mg, 341 nmol, 34%). <u>LC-MS:</u> $R_t = 4.51 \text{ min}$ (10 - 90% ACN; 13 min); ¹H NMR (500

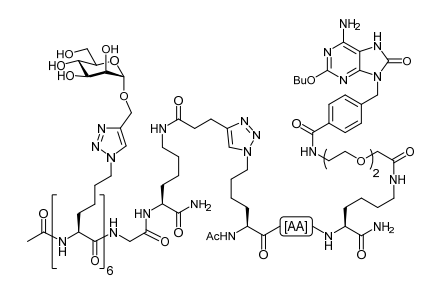
MHz, D₂O) δ 8.55 (s, 1H, H_{arom} (H)), 8.00 (s, 2H, trzl), 7.77 - 7.66 (m, 2H, H_{arom}), 7.48 - 6.62 (m, 21H, H_{arom}), 4.92 (s, 1H, H-1), 4.68 - 2.59 (m, ~106H), 2.54 (t, J = 7.0 Hz, 2H, CH₂NH₂ (K)), 2.49 - 0.64 (m, ~144H); <u>HRMS</u> [C₂₃₇H₃₅₅N₆₉O₆₉ + 5H]⁵⁺: 1055.93685 found, 1055.93678 calculated.



A solution of mannosides cluster (96 μ L, 0.005 M, 480 nmol, 1 eq, aq.) and undecorated gp100 **137** in DMSO (100 μ L, 0.005 M, 500 nmol, 1.05 eq) were conjugated using the general click protocol. After purification by RP-HPLC (linear-gradient 8 - 42% B, 10 min) compound **152** was obtained as a white powder (1.090 mg, 163 nmol, 34%). <u>LC-MS:</u> R_t =

6.46 min (0 - 50% ACN; 13 min); 1 H NMR (500 MHz, D₂O) δ 8.51 (s, 1H, H_{arom} (H)), 7.92 (s, 6H, trzl), 7.63 (s, 1H, trzl), 7.52 - 7.28 (m, 4H, H_{arom}), 7.25 - 6.93 (m, 11H, H_{arom}), 6.79 - 6.62 (m, 4H, H_{arom}), 4.87 (s, 6H, H-1), 4.64 - 2.56 (m, nd), 2.47 (t, J = 7.8 Hz, 2H, CH_2NH_2 (K)), 2.41 - 0.58 (m, nd). \underline{HRMS} [C₂₈₉H₄₄₇N₈₃O₉₈ + 5H]⁵⁺: 1331.25941 found, 1331.25988 calculated.

 $\label{eq:continuous} Ac-Lys(*[Ac-Lys(Man_1)-Lys(Man_$

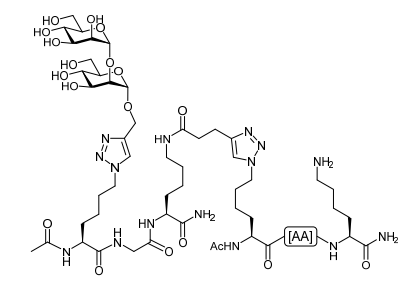


A solution of mannosides cluster **145** (120 μ L, 0.01 M, 1.20 μ mol, 1.2 eq, aq.) and TLR-decorated gp100 **139** in DMSO (100 μ L, 0.01 M, 1.0 μ mol, 1 eq) were conjugated using the general click protocol. After purification by RP-HPLC (linear-gradient 8 - 42% B, 10 min) compound **153** was obtained as a white powder (2.085 mg, 292 nmol, 29%). LC-MS: $R_t = 7.19$ min (0 - 50% ACN; 13 min); $R_t = 4.38$ min

(10 - 90% ACN; 13 min); 1H NMR (500 MHz, D₂O) δ 8.56 (s, 1H, H_{arom} (H)), 7.96 (s, 7H, trzl), 7.91 - 6.62

(m, 23H, H_{arom}), 4.89 (s, 6H, H-1), 4.76 - 0.64 (m, nd); <u>HRMS</u> [$C_{312}H_{475}N_{89}O_{104} + 6H$]⁶⁺: 1190.41891 found, 1190.41941 calculated.

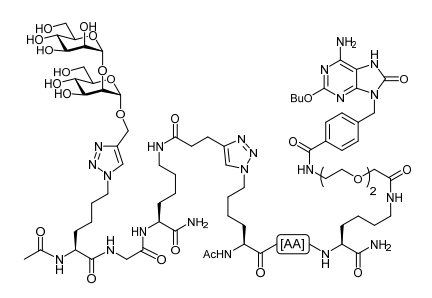
Ac-Lys(*[Ac-Lys(1,2-Man₂)-Gly-Lys(*triazolylpentyl-5-amide)-NH₂])-Val-Thr-His-Thr-Tyr-Leu-Glu-Pro-Gly-Pro-Val-Thr-Ala-Asn-Arg-Gln-Leu-Tyr-Pro-Glu-Trp-Thr-Glu-Ala-Gln-Arg-Leu-Asp- α Abu-Trp-Arg-Gly-Lys-NH₂ (154).



A solution of mannosides cluster **142** (80 μ L, 0.01 M, 0.80 μ mol, 1 eq, aq.) and undecorated gp100 **137** in DMSO (100 μ L, 0.01 M, 1.0 μ mol, 1.25 eq) were conjugated using the general click protocol. After purification by gel-filtration (eluted at 42 - 57 mL) compound **154** was obtained as a white powder (3.633 mg, 734 nmol, 91%). <u>LC-MS:</u> $R_t = 4.48 \text{ min}$ (10 - 90% ACN; 13 min); <u>HRMS</u> [C₂₂₀H₃₃₇N₆₃O₆₈ + 5H]⁵⁺:

991.30528 found, 991.30539 calculated.

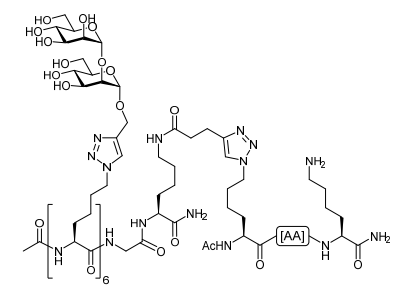
Ac-Lys(*[Ac-Lys(1,2-Man₂)-Gly-Lys(*triazolylpentyl-5-amide)-NH₂])-Val-Thr-His-Thr-Tyr-Leu-Glu-Pro-Gly-Pro-Val-Thr-Ala-Asn-Arg-Gln-Leu-Tyr-Pro-Glu-Trp-Thr-Glu-Ala-Gln-Arg-Leu-Asp- α Abu-Trp-Arg-Gly-Lys(Peg-TLR7L)-NH₂ (157).



A solution of mannosides cluster **142** (80 μ L, 0.01 M, 0.80 μ mol, 1 eq, aq.) and TLR-decorated gp100 **139** in DMSO (100 μ L, 0.01 M, 1.0 μ mol, 1.25 eq) were conjugated using the general click protocol. After purification by gel-filtration (eluted at 32 - 54.5 mL) compound **157** was obtained as a white powder (0.915 mg, 168 nmol, 21%). <u>LC-MS:</u> $R_t = 4.83$ min (10 - 90% ACN; 13 min); <u>HRMS</u> [C₂₄₃H₃₆₅N₆₉O₇₄ +

5Na]⁵⁺: 1110.78537 found, 1110.73038 calculated.

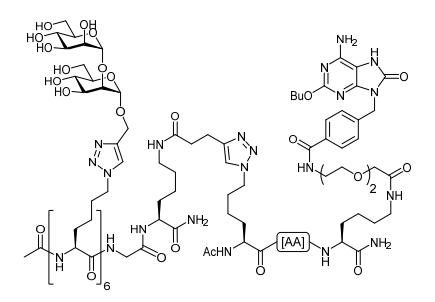
Ac-Lys(*[Ac-Lys(1,2-Man₂)-L



A solution of mannosides cluster **146** (125 μ L, 0.01 M, 1.25 μ mol, 1 eq, aq.) and undecorated gp100 **137** in DMSO (125 μ L, 0.016 M, 1.95 μ mol, 1.5 eq) were conjugated using the general click protocol. After purification by gel-filtration (eluted at 28 - 35.5 mL) compound **160** was obtained as a white powder (3.73 mg, 491 nmol, 39%). <u>LC-MS:</u> $R_t = 6.99$ min (0 - 50% ACN; 13 min); <u>1H NMR</u> (500 MHz, D₂O) δ 8.03 - 7.89 (m,

7H, trzl), 7.71 - 6.62 (m, 19H, H_{arom}), 5.12 (s, 6H, H-1), 4.94 (s, 6H, H-1'), 4.89 - 0.61 (m, nd); <u>HRMS</u> [$C_{325}H_{507}N_{83}O_{128} + 5H_{15}^{5+}$: 1525.72868 found, 1525.72330 calculated.

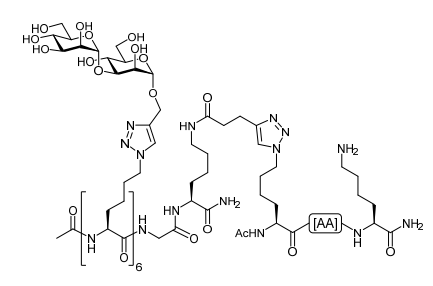
Ac-Lys(*[Ac-Lys(1,2-Man₂)-L



A solution of mannosides cluster **146** (71.5 μ L, 0.01 M, 715 nmol, 1 eq, aq.) and TLR-decorated gp100 **139** in DMSO (75 μ L, 0.01 M, 750 μ mol, 1.05 eq) were conjugated using the general click protocol. After purification by RP-HPLC (linear-gradient 8 - 42% B, 10 min) compound **164** was obtained as a white powder (1.395 mg, 172 nmol, 24%). LC-MS: $R_t = 7.10$ min (0 - 50% ACN; 13 min); HRMS

 $[C_{348}H_{535}N_{89}O_{134} + 6H]^{6+}$: 1352.47638 found, 1352.47226 calculated.

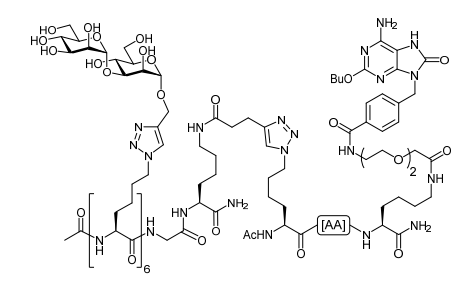
Ac-Lys(*[Ac-Lys(1,3-Man₂)-L



A solution of mannosides cluster 147 (112 μ L, 0.005 M, 560 nmol, 1 eq, aq.) and undecorated gp100 137 in DMSO (168 μ L, 0.01 M, 1.68 μ mol, 3 eq) were conjugated using the general click protocol. After purification by gel-filtration (eluted at 28 - 35.5 mL) compound 161 was obtained as a white powder (2.650 mg, 349 nmol, 62%). LC-MS: $R_t = 6.40$ min (10 - 50 % ACN; 13 min); $\frac{1}{1}$ NMR (500 MHz, D₂O)

 $\delta~8.32~(s,1H,H_{arom}~(H)),~7.88~(s,7H,trzl),~7.64~-6.51~(m,19H,H_{arom}),~4.96~(s,6H,H-1),~4.79~(s,6H,H-1),\\4.76~-0.46~(m,nd);~\frac{HRMS}{(C_{325}H_{507}N_{83}O_{128}+6H]^{6+}};~1271.77597~found,~1271.77109~calculated.$

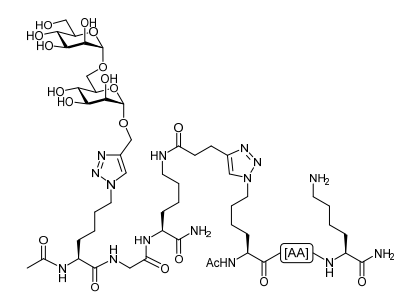
Ac-Lys(*[Ac-Lys(1,3-Man₂)-L



A solution of mannosides cluster **147** (38 μ L, 0.005 M, 190 nmol, 1 eq, aq.) and TLR-decorated gp100 **139** in DMSO (28.5 μ L, 0.01 M, 285 μ mol, 1.5 eq) were conjugated using the general click protocol. After purification by RP-HPLC (linear-gradient 8 - 42% B, 10 min) compound **165** was obtained as a white powder (0.630 mg, 78 nmol, 41%). LC-MS: $R_t = 7.12$ min (10 - 50% ACN; 13 min); HRMS

 $[C_{348}H_{535}N_{89}O_{134} + 6H]^{6+}$: 1352.47991 found, 1352.47226 calculated.

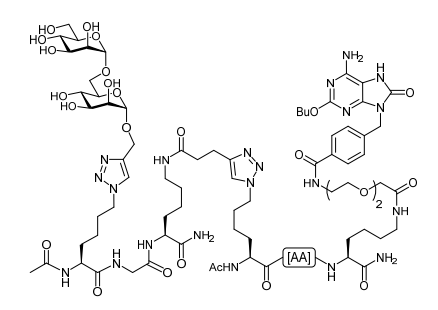
Ac-Lys(*[Ac-Lys(1,6-Man₂)-Gly-Lys(*triazolylpentyl-5-amide)-NH₂])-Val-Thr-His-Thr-Tyr-Leu-Glu-Pro-Gly-Pro-Val-Thr-Ala-Asn-Arg-Gln-Leu-Tyr-Pro-Glu-Trp-Thr-Glu-Ala-Gln-Arg-Leu-Asp- α Abu-Trp-Arg-Gly-Lys-NH₂ (155).



A solution of mannosides cluster **143** (80 μ L, 0.01 M, 0.80 μ mol, 1 eq, aq.) and undecorated gp100 **137** in DMSO (100 μ L, 0.01 M, 1.0 μ mol, 1.25 eq) were conjugated using the general click protocol. After purification by gel-filtration (eluted at 32 - 54.5 mL) compound **155** was obtained as a white powder (3.570 mg, 721 nmol, 90%). <u>LC-MS:</u> $R_t = 4.48 \text{ min} (10 - 90\% \text{ ACN}; 13 \text{ min}); <u>HRMS</u> [C₂₂₀H₃₃₇N₆₃O₆₈ + 5H]⁵⁺:$

991.30570 found, 991.30539 calculated.

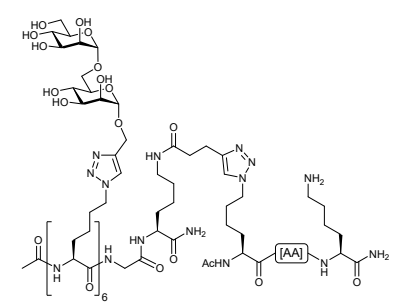
Ac-Lys(*[Ac-Lys(1,6-Man₂)-Gly-Lys(*triazolylpentyl-5-amide)-NH₂])-Val-Thr-His-Thr-Tyr-Leu-Glu-Pro-Gly-Pro-Val-Thr-Ala-Asn-Arg-Gln-Leu-Tyr-Pro-Glu-Trp-Thr-Glu-Ala-Gln-Arg-Leu-Asp- α Abu-Trp-Arg-Gly-Lys(Peg-TLR7L)-NH₂ (158).



A solution of mannosides cluster **143** (80 μ L, 0.01 M, 0.80 μ mol, 1 eq, aq.) and TLR-decorated gp100 **139** in DMSO (100 μ L, 0.01 M, 1.0 μ mol, 1.25 eq) were conjugated using the general click protocol. After purification by gel-filtration (eluted at 32 - 54.5 mL) compound **158** was obtained as a white powder (0.840 mg, 154 nmol, 19%). <u>LC-MS:</u> $R_t = 4.77$ min (10 - 90% ACN; 13 min); <u>HRMS</u> [C₂₄₃H₃₆₅N₆₉O₇₄ +

6H]6+: 906.82311 found, 906.78974 calculated.

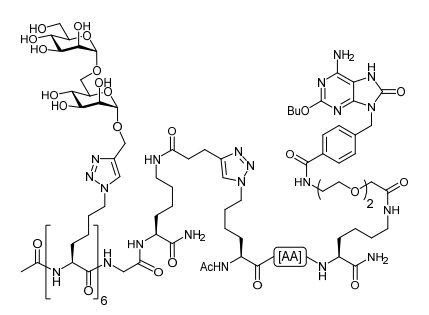
Ac-Lys(*[Ac-Lys(1,6-Man₂)-L



A solution of mannosides cluster **148** (35 μ L, 0.01 M, 350 nmol, 1 eq, aq.) and undecorated gp100 **137** in DMSO (40 μ L, 0.01 M, 400 nmol, 1.15 eq) were conjugated using the general click protocol. After purification by gel-filtration (eluted at 36 - 45 mL) compound **162** was obtained as a white powder (1.805 mg, 238 nmol, 68%). <u>LC-MS:</u> R_t = 4.32 min (10 - 90% ACN; 13 min); <u>HRMS</u> [C₃₂₅H₅₀₇N₈₃O₁₂₈ + H + Na

+ 3NH₃|5+: 1540.12657 found, 1540.13201 calculated.

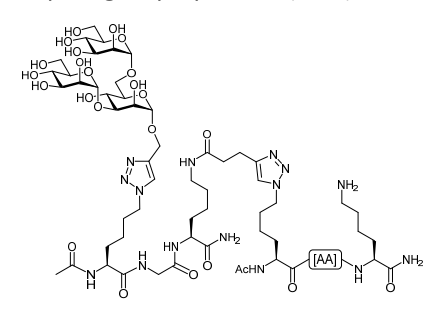
Ac-Lys(*[Ac-Lys(1,6-Man₂)-L



A solution of mannosides cluster **148** (35 μ L, 0.01 M, 350 nmol, 1 eq, aq.) and TLR-decorated gp100 **139** in DMSO (40 μ L, 0.01 M, 400 nmol, 1.15 eq) were conjugated using the general click protocol. After purification by gel-filtration (eluted at 37.5 - 49.5 mL) compound **166** was obtained as a white powder (0.520 mg, 64 nmol, 18%). <u>LC-MS:</u> R_t = 4.68 min (10 - 90% ACN; 13 min); <u>HRMS</u> [C₃₄₈H₅₃₅N₈₉O₁₃₄ + 5H]⁵⁺:

1622.56900 found, 1622.56470 calculated.

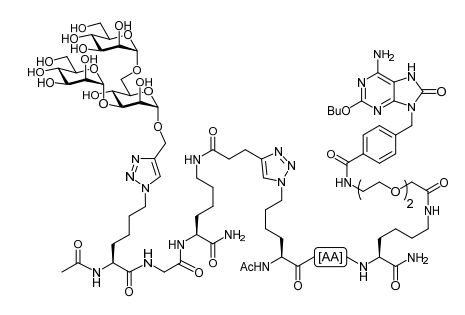
Ac-Lys(*[Ac-Lys(Man₃)-Gly-Lys(*triazolylpentyl-5-amide)-NH₂])-Val-Thr-His-Thr-Tyr-Leu-Glu-Pro-Gly-Pro-Val-Thr-Ala-Asn-Arg-Gln-Leu-Tyr-Pro-Glu-Trp-Thr-Glu-Ala-Gln-Arg-Leu-Asp- α Abu-Trp-Arg-Gly-Lys-NH₂ (156).



A solution of mannosides cluster **144** (40 μ L, 0.01 M, 400 nmol, 1 eq, aq.) and undecorated gp100 **137** in DMSO (45 μ L, 0.01 M, 450 μ mol, 1.13 eq) were conjugated using the general click protocol. After purification by gel-filtration (eluted at 30 - 54.5 mL) compound **156** was obtained as a white powder (1.802 mg, 352 nmol, 88%). <u>LC-MS:</u> $R_t = 4.48 \text{ min} (10 - 90\% \text{ ACN}; 13 \text{ min}); <u>HRMS</u> [C₂₂₆H₃₄₇N₆₃O₇₃ +$

4Na]4+: 1301.63838 found, 1301.62576 calculated.

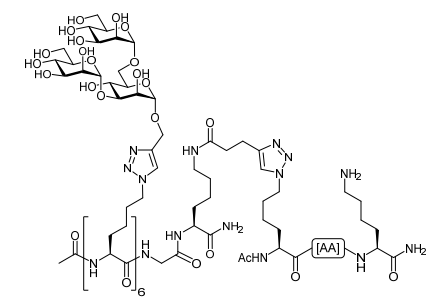
Ac-Lys(*[Ac-Lys(Man₃)-Gly-Lys(*triazolylpentyl-5-amide)-NH₂])-Val-Thr-His-Thr-Tyr-Leu-Glu-Pro-Gly-Pro-Val-Thr-Ala-Asn-Arg-Gln-Leu-Tyr-Pro-Glu-Trp-Thr-Glu-Ala-Gln-Arg-Leu-Asp- $_{\alpha}$ Abu-Trp-Arg-Gly-Lys(Peg-TLR7L)-NH₂ (159).



A solution of mannosides cluster **144** (40 μ L, 0.01 M, 400 nmol, 1 eq, aq.) and TLR-decorated gp100 **139** in DMSO (45 μ L, 0.01 M, 450 μ mol, 1.13 eq) were conjugated using the general click protocol. After purification by gel-filtration (eluted at 30 - 54.5 mL) compound **159** was obtained as a white powder (0.721 mg, 129 nmol, 32%). LC-MS: $R_t = 5.56 \text{ min} (10 - 90\% \text{ ACN}; 13 \text{ min}); HRMS$

 $[C_{249}H_{375}N_{69}O_{79} + 4Na]^{4+}$: 1421.97944 found, 1422.17613 calculated.

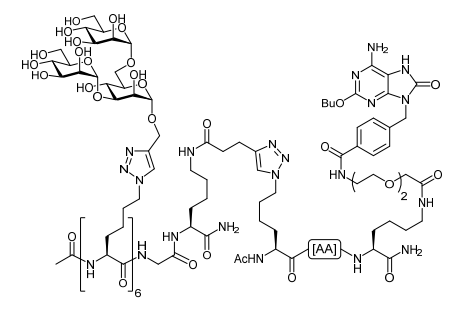
Ac-Lys(*[Ac-Lys(Man₃)-Lys(M



A solution of mannosides cluster **149** (175 μ L, 0.01 M, 1.75 μ mol, 1 eq, aq.) and undecorated gp100 **137** in DMSO (263 μ L, 0.01 M, 263 μ mol, 1.5 eq) were conjugated using the general click protocol. After purification by gel-filtration (eluted at 29 - 38 mL) followed by RP-HPLC (linear-gradient 8 - 42% B, 10 min) compound **163** was obtained as a white powder (6.760 mg, 786 nmol, 45%). <u>LC-MS:</u> $R_t =$

6.37 min (10 - 50% ACN; 13 min); 1 H NMR (500 MHz, D_{2} O) δ 8.40 (s, 1H, H_{arom} (H)), 7.90 (d, J = 11.1 Hz, 7H, trzl), 7.63 - 6.50 (m, 19H, H_{arom}), 4.94 (s, 6H, H-1), 4.79 (s, 6H, H-1), 4.76 (s, 6H, H-1"), 4.71 - 0.54 (m, nd); $\frac{HRMS}{HRMS}$ [$C_{361}H_{567}N_{83}O_{158} + 6H]^{6+}$: 1433.82676 found, 1433.82394 calculated.

 $\label{eq:continuous} Ac-Lys(*{\rm [Ac-Lys(Man_3)-Lys(M$



A solution of mannosides cluster **149** (200 μ L, 0.01 M, 2.0 μ mol, 2 eq, aq.) and TLR-decorated gp100 **139** in DMSO (100 μ L, 0.01 M, 1.0 μ mol, 1 eq) were conjugated using the general click protocol. After purification by RP-HPLC (linear-gradient 8 - 42% B, 10 min) compound **167** was obtained as a white powder (2.483 mg, 273 nmol, 27%). <u>LC-MS:</u> $R_t = 7.07 \text{ min}$ (10 - 50% ACN; 13 min); ${}^{1}H$

NMR (500 MHz, D₂O) δ 8.55 (s, 1H, H_{arom} (H)), 7.98 (s, 7H, trzl), 7.74 - 6.60 (m, 23H, H_{arom}), 5.03 (s, 6H, H-1), 4.88 (s, 6H, H-1), 4.85 (s, 6H, H-1"), 4.77 - 1.40 (m, nd), 1.38 (s, 3H, Ac), 1.36 (s, 3H, Ac), 1.35 - 0.66 (m, nd); HRMS [C₃₈₄H₅₉₅N₈₉O₁₆₄ + 6H]⁶⁺: 1514.69741 found, 1514.69225 calculated.

References

- (1) Li, R.-J. E.; Hogervorst, T. P.; Achilli, S.; Bruijns, S. C.; Arnoldus, T.; Vivès, C.; Wong, C. C.; Thépaut, M.; Meeuwenoord, N. J.; van den Elst, H.; Overkleeft, H. S.; van der Marel, G. A.; Filippov, D. V.; van Vliet, S. J.; Fieschi, F.; Codée, J. D. C. C.; van Kooyk, Y. Systematic Dual Targeting of Dendritic Cell C-Type Lectin Receptor DC-SIGN and TLR7 Using a Trifunctional Mannosylated Antigen. *Front. Chem.* **2019**, 7. https://doi.org/10.3389/fchem.2019.00650.
- (2) Hogervorst, T. P.; Li, E. R. J.; Achilli, S.; Bruijns, S. C. M.; Vivès, C.; van Vliet, S. J.; Fieschi, F.; Codée, J. D. C.; Van Kooyk, Y. Targeting of the Langerhans Cell C-Type Lectin Receptor Langerin Using Bifunctional Mannosylated Antigens. [Submitted] 2020.
- (3) Ribas, A.; Wolchok, J. D. Cancer Immunotherapy Using Checkpoint Blockade. *Science (80-.).* **2018**, *359*, 1350–1355. https://doi.org/10.1126/science.aar4060.
- (4) Sharma, P.; Wagner, K.; Wolchok, J. D.; Allison, J. P. Novel Cancer Immunotherapy Agents with Survival Benefit: Recent Successes and next Steps. *Nat. Rev. Cancer* **2011**, *11*, 805–812. https://doi.org/10.1038/nrc3153.
- (5) Disis, M. L.; Watt, W. C.; Cecil, D. L. Th1 Epitope Selection for Clinically Effective Cancer Vaccines. Oncoimmunology 2014, 3, e954971. https://doi.org/10.4161/21624011.2014.954971.
- (6) Chandran, S. S.; Klebanoff, C. A. T Cell Receptor-based Cancer Immunotherapy: Emerging Efficacy and Pathways of Resistance. *Immunol. Rev.* **2019**, *290*, 127–147. https://doi.org/10.1111/imr.12772.
- (7) Ackerman, A. L.; Cresswell, P. Regulation of MHC Class I Transport in Human Dendritic Cells and the Dendritic-Like Cell Line KG-1. *J. Immunol.* **2003**, *170*, 4178–4188. https://doi.org/10.4049/jimmunol.170.8.4178.
- (8) Koster, J.; Plasterk, R. H. A. A Library of Neo Open Reading Frame Peptides (NOPs) as a Sustainable Resource of Common Neoantigens in up to 50% of Cancer Patients. *Sci. Rep.* **2019**, *9*, 1–8. https://doi.org/10.1038/s41598-019-42729-2.
- (9) Hos, B. J.; Tondini, E.; van Kasteren, S. I.; Ossendorp, F. Approaches to Improve Chemically Defined Synthetic Peptide Vaccines. *Front. Immunol.* **2018**, *9*. https://doi.org/10.3389/fimmu.2018.00884.
- (10) Fujita, Y.; Taguchi, H. Overview and Outlook of Toll-like Receptor Ligand-Antigen Conjugate Vaccines. *Ther. Deliv.* **2012**, *3*, 749–760. https://doi.org/10.4155/tde.12.52.
- (11) Magarian Blander, J.; Medzhitov, R.; Blander, J. M.; Medzhitov, R. Toll-Dependent Selection of Microbial Antigens for Presentation by Dendritic Cells. *Nature* **2006**, 440, 808–812. https://doi.org/10.1038/nature04596.
- (12) Cho, H. J.; Takabayashi, K.; Cheng, P.-M.; Nguyen, M.-D.; Corr, M.; Tuck, S.; Raz, E. Immunostimulatory DNA-Based Vaccines Induce Cytotoxic Lymphocyte Activity by a T-Helper Cell-Independent Mechanism. *Nat. Biotechnol.* **2000**, *18*, 509–514. https://doi.org/10.1038/75365.
- (13) Deres, K.; Schild, H.; Wiesmüller, K.-H.; Jung, G.; Rammensee, H.-G. In Vivo Priming of Virus-Specific Cytotoxic T Lymphocytes with Synthetic Lipopeptide Vaccine. *Nature* **1989**, *342*, 561–564. https://doi.org/10.1038/342561a0.
- Willems, M. M. J. H. P.; Zom, G. G.; Khan, S.; Meeuwenoord, N.; Melief, C. J. M.; Stelt, M. van der; Overkleeft, H. S.; Codée, J. D. C.; Marel, G. A. van der; Ossendorp, F.; Filippov, D. V. N -Tetradecylcarbamyl Lipopeptides as Novel Agonists for Toll-like Receptor 2. J. Med. Chem. 2014, 57, 6873–6878. https://doi.org/10.1021/jm500722p.
- (15) Willems, M. M. J. H. P.; Zom, G. G.; Meeuwenoord, N.; Khan, S.; Ossendorp, F.; Overkleeft, H. S.; van der Marel, G. A.; Filippov, D. V.; Codée, J. D. C. Lipophilic Muramyl Dipeptide-Antigen Conjugates as Immunostimulating Agents. *ChemMedChem* **2016**, *11*, 190–198. https://doi.org/10.1002/cmdc.201500196.
- (16) Buskas, T.; Ingale, S.; Boons, G.-J. J. Towards a Fully Synthetic Carbohydrate-Based Anticancer Vaccine: Synthesis and Immunological Evaluation of a Lipidated Glycopeptide Containing the Tumor-Associated Tn Antigen. *Angew. Chemie Int. Ed.* **2005**, *44*, 5985–5988. https://doi.org/10.1002/anie.200501818.
- (17) Moyle, P. M.; Olive, C.; Ho, M.-F.; Pandey, M.; Dyer, J.; Suhrbier, A.; Fujita, Y.; Toth, I. Toward the Development of Prophylactic and Therapeutic Human Papillomavirus Type-16 Lipopeptide Vaccines. *J. Med.*

- Chem. 2007, 50, 4721–4727. https://doi.org/10.1021/jm070287b.
- (18) Sedaghat, B.; Stephenson, R. J.; Giddam, A. K.; Eskandari, S.; Apte, S. H.; Pattinson, D. J.; Doolan, D. L.; Toth, I. Synthesis of Mannosylated Lipopeptides with Receptor Targeting Properties. *Bioconjug. Chem.* **2016**, 27, 533–548. https://doi.org/10.1021/acs.bioconjchem.5b00547.
- (19) Zom, G. G.; Willems, M. M. J. H. J. H. P.; Meeuwenoord, N. J.; Reintjens, N. R. M.; Tondini, E.; Khan, S.; Overkleeft, H. S.; van der Marel, G. A.; Codee, J. D. C.; Ossendorp, F.; Filippov, D. V. Dual Synthetic Peptide Conjugate Vaccine Simultaneously Triggers TLR2 and NOD2 and Activates Human Dendritic Cells. *Bioconjug. Chem.* 2019, *30*, 1150–1161. https://doi.org/10.1021/acs.bioconjchem.9b00087.
- (20) Khan, S.; Bijker, M. S.; Weterings, J. J.; Tanke, H. J.; Adema, G. J.; Van Hall, T.; Drijfhout, J. W.; Melief, C. J. M.; Overkleeft, H. S.; Van Der Marel, G. A.; Filippov, D. V.; van der Burg, S. H.; Ossendorp, F. Distinct Uptake Mechanisms but Similar Intracellular Processing of Two Different Toll-like Receptor Ligand-Peptide Conjugates in Dendritic Cells. *J. Biol. Chem.* **2007**, *282*, 21145–21159. https://doi.org/10.1074/jbc.M701705200.
- (21) Ignacio, B. J.; Albin, T. J.; Esser-Kahn, A. P.; Verdoes, M. Toll-like Receptor Agonist Conjugation: A Chemical Perspective. *Bioconjug. Chem.* **2018**, *29*, 587–603. https://doi.org/10.1021/acs.bioconjchem.7b00808.
- Glaffig, M.; Stergiou, N.; Hartmann, S.; Schmitt, E.; Kunz, H. A Synthetic MUC1 Anticancer Vaccine Containing Mannose Ligands for Targeting Macrophages and Dendritic Cells. *ChemMedChem* **2018**, *13*, 25–29. https://doi.org/10.1002/cmdc.201700646.
- (23) McIntosh, J. D.; Brimble, M. A.; Brooks, A. E. S.; Dunbar, P. R.; Kowalczyk, R.; Tomabechi, Y.; Fairbanks, A. J. Convergent Chemo-Enzymatic Synthesis of Mannosylated Glycopeptides; Targeting of Putative Vaccine Candidates to Antigen Presenting Cells. *Chem. Sci.* **2015**, *6*, 4636–4642. https://doi.org/10.1039/c5sc00952a.
- (24) Srinivas, O.; Larrieu, P.; Duverger, E.; Boccaccio, C.; Bousser, M. T.; Monsigny, M.; Fonteneau, J. F.; Jotereau, F.; Roche, A. C. Synthesis of Glycocluster Tumor Antigenic Peptide Conjugates for Dendritic Cell Targeting. *Bioconjug. Chem.* **2007**, *18*, 1547–1554. https://doi.org/10.1021/bc070026g.
- (25) Fritz, J. H.; Girardin, S. E.; Fitting, C.; Werts, C.; Mengin-Lecreulx, D.; Caroff, M.; Cavaillon, J.-M.; Philpott, D. J.; Adib-Conquy, M. Synergistic Stimulation of Human Monocytes and Dendritic Cells by Toll-like Receptor 4 and NOD1- and NOD2-Activating Agonists. *Eur. J. Immunol.* **2005**, *35*, 2459–2470. https://doi.org/10.1002/eji.200526286.
- (26) Gringhuis, S. I.; den Dunnen, J.; Litjens, M.; van het Hof, B.; van Kooyk, Y.; Geijtenbeek, T. B. H. C-Type Lectin DC-SIGN Modulates Toll-like Receptor Signaling via Raf-1 Kinase-Dependent Acetylation of Transcription Factor NF-KB. *Immunity* 2007, 26, 605–616. https://doi.org/10.1016/j.immuni.2007.03.012.
- (27) Melssen, M.; Slingluff, C. L. Vaccines Targeting Helper T Cells for Cancer Immunotherapy. *Curr. Opin. Immunol.* **2017**, *47*, 85–92. https://doi.org/10.1016/j.coi.2017.07.004.
- Jin, G.; Wu, C. C. N.; Tawatao, R. I.; Chan, M.; Carson, D. A.; Cottam, H. B. Synthesis and Immunostimulatory Activity of 8-Substituted Amino 9-Benzyladenines as Potent Toll-like Receptor 7 Agonists. *Bioorg. Med. Chem. Lett.* **2006**, *16*, 4559–4563. https://doi.org/10.1016/j.bmcl.2006.06.017.
- (29) Chan, M.; Hayashi, T.; Kuy, C. S.; Gray, C. S.; Wu, C. C. N.; Corr, M.; Wrasidlo, W.; Cottam, H. B.; Carson, D. A. Synthesis and Immunological Characterization of Toll-Like Receptor 7 Agonistic Conjugates. *Bioconjug. Chem.* **2009**, *20*, 1194–1200. https://doi.org/10.1021/bc900054q.
- (30) Gential, G. P. P.; Hogervorst, T. P.; Tondini, E.; van de Graaff, M. J.; Overkleeft, H. S.; Codée, J. D. C.; van der Marel, G. A.; Ossendorp, F.; Filippov, D. V. Peptides Conjugated to 2-Alkoxy-8-Oxo-Adenine as Potential Synthetic Vaccines Triggering TLR7. *Bioorg. Med. Chem. Lett.* **2019**, *29*, 1340–1344. https://doi.org/10.1016/j.bmcl.2019.03.048.
- (31) Wlodawer, A.; Miller, M.; Jaskolski, M.; Sathyanarayana, B.; Baldwin, E.; Weber, I.; Selk, L.; Clawson, L.; Schneider, J.; Kent, S. Conserved Folding in Retroviral Proteases: Crystal Structure of a Synthetic HIV-1 Protease. *Science* (80-.). 1989, 245, 616–621. https://doi.org/10.1126/science.2548279.
- (32) Chan, W. C.; White, P. D. Fmoc Solid Phase Peptide Synthesis: A Practical Approach; Oxford University Press, 2000.
- (33) Horatscheck, A.; Wagner, S.; Ortwein, J.; Kim, B. G.; Lisurek, M.; Beligny, S.; Schütz, A.; Rademann, J. Benzoylphosphonate-Based Photoactive Phosphopeptide Mimetics for Modulation of Protein Tyrosine Phosphatases and Highly Specific Labeling of SH2 Domains. *Angew. Chemie Int. Ed.* **2012**, *51*, 9441–9447.

- https://doi.org/10.1002/anie.201201475.
- (34) Conibear, A. C.; Farbiarz, K.; Mayer, R. L.; Matveenko, M.; Kählig, H.; Becker, C. F. W. Arginine Side-Chain Modification That Occurs during Copper-Catalysed Azide–Alkyne Click Reactions Resembles an Advanced Glycation End Product. *Org. Biomol. Chem.* **2016**, *14*, 6205–6211. https://doi.org/10.1039/C6OB00932H.
- (35) Behrendt, R.; Offer, J. Advances in Fmoc Solid-Phase Peptide Synthesis. *J. Pept.* **2016**, No. October 2015, 4–27. https://doi.org/10.1002/psc.2836.

Development of a *C*-mannoside functionalized lysine for the synthesis of acid-stable mannosylated peptides

Introduction

The uptake, processing, and (cross)-presentation of antigens is a complex process, which has not yet been fully elucidated.^{2,3} Studying the process, starting from cellular uptake and ending with the presentation at the surface of antigen-presenting cells remains challenging, since the introduction of accessory molecular motives to follow the fate of the antigens, such as fluorescent labels, can influence the antigen processing pathway significantly.⁴ To circumvent this issue, small bioorthogonal handles with minimal impact on the structure of peptide conjugates can be applied, allowing the introduction of reporter groups during the process. Especially the azide-alkyne cycloaddition is ideal for this purpose since the conjugation of these reaction partners is selective and fast, with the small azide and alkyne handles being well tolerated in biological systems and usually only having minimal effects on biological processes.^{5,6} The tri-functional conjugates, described in Chapter 4, demonstrate the potential of combining ligands for C-type lectin receptors

Part of this work is published by Hogervorst & Li et al. 2020¹

(CLRs) and Toll-like receptors (TLRs) with an antigenic peptide in a single conjugate. The development of these conjugates comprised the incorporation of an azide handle in the peptide, allowing the introduction of an additional adjuvant after the solid-phase peptide synthesis (SPPS). This approach however, requires an extra azide-alkyne cycloaddition and an extra purification step to obtain the final conjugates. Furthermore, the use of an azide/alkyne combination limits the options for the inclusion of orthogonal handles for further conjugation and excludes the use of alkyne reporter groups that could help study antigen-conjugate processing in more detail.

This Chapter describes the design and synthesis of a *C*-mannose functionalized lysine building block that can be used in SPPS (168, Scheme 1). Utilizing a *C*-mannoside derivative that lacks the exo-cyclic anomeric oxygen, the glycosidic linkage can withstand the acidic conditions required for the release from resin and general deprotection that is part of a standard automated SPPS. The stabilized sugar amino acid block can be incorporated in an 'in-line' fashion, obviating the post-synthesis conjugation step and thus preventing the use of an azide-alkyne click reaction. Building block 168 is designed with a spacer of similar length as the previously described triazole *O*-mannoside conjugates in Chapter 2 and 4, allowing a side by side comparison. Potential side reactions on the mannose hydroxyls during peptide assembly are prevented by the protection of these functionalities with the acid-labile *para*-methoxybenzyl (PMB) groups which can be removed simultaneously with the amino acid side-chain protecting groups during the general deprotection and cleavage protocol of the projected peptide conjugates. Protection of the N-terminus with a temporary Fmoc protecting group allows for the controlled use of 168 in standard Fmoc-SPPS.

HOO OH HOO OH HOO OH HOO OPMB PMBO O

Scheme 1: Retrosynthesis of *C*-mannoside peptide conjugates.

Results and Discussion

The key step in the synthesis of **168** is the introduction of the α -*C*-glycosidic bond (Scheme 2). Based on previously reported work by Girard et al.⁷, the anomeric allyl was introduced *via* a Hosomi-Sakurai reaction using allyltrimethylsilane (allyl-TMS). In this reaction, the glycosyl donor is activated using a strong Lewis acid forming an electrophilic oxocarbenium ion that can react with the poor nucleophilic allyl-TMS. When peracetylated mannose **169** was used, it gave allyl **173** with poor stereoselectivity.⁸⁻¹⁰ On the other hand, a similar reaction with non-participating perbenzylated donor **171** gave allyl **172** almost exclusively as the α -anomer (α : β ; \geq 15:1).^{10,11} Since separation of the anomeric mixtures in initial experiments proved to be tedious, the additional steps accompanying the perbenzylated route were considered an unavoidable obstacle that had to be taken.

The synthetic route to 168 shown in Scheme 2 starts with the benzylation of methyl α-Dmannopyranoside 170 to obtain methyl 2,3,4,6-tetra-O-benzyl-α-D-mannopyranoside 171. The allyl group was introduced by treatment of the methyl mannoside with allyltrimethyl silane and trimethylsilyl triflate in acetonitrile to provide C-mannoside 172. This reaction proceeded with high stereoselectivity and was complete within an hour when assisted by ultrasound irradiation.¹² Selective removal of the benzyl ethers in the presence of the allyl functionality was achieved using BCl₃. Unfortunately, this reaction proved to be difficult to scale up. The recently described method using a Birch-type reduction in liquid ammonia¹³ was discarded because condensation of large volumes of toxic ammonia was considered too time-consuming and hazardous. Therefore, an alternative method was sought, and a Birch-type reduction using lithium naphthalenide in THF allowed for the removal of the four benzyls from 172. This reaction could be run on a 80 mmol scale, to provide the desired tetra-ol, which was acetylated to allow for easy purification, yielding 173. After the installment of four PMB ethers, allyl 174 was elongated by cross-metathesis with methyl acrylate or benzyl acrylate to afford α,β-unsaturated ketones 175 & 176, respectively. The reduction of the double bond in these products with RuCl₃ in the presence of NaBH₄ and MeOH, ¹⁴ was followed by saponification of the resulting esters 177 & 178 to obtain carboxylic acid 179. On a small scale, these three reactions gave the highest yield with the methyl ester, so the synthesis on large scale was performed with methyl acrylate. Fully protected amino acid 180 was obtained by coupling of carboxylic acid 179 with the methyl ester of N_{α} -Fmoc protected lysine 181, using HCTU as condensation agent. Selective hydrolysis of the ester in the presence of the Fmoc group was achieved with LiOOH, 15,16 which is more nucleophilic but less basic than LiOH, a resulting in

-

^a p K_a of H₂O₂ = 11.6; p K_a of H₂O = 15.8²⁷

the isolation of **168** in 79% yield.¹⁷ Altogether, SPPS compatible *C*-mannose functionalized lysine building block **168** was synthesized in 20% over 11 steps.

Scheme 2: Synthesis of *C*-mannoside lysine **168**.

Reagents and conditions: a) NaH, BnBr, TBAI, DMF, 78%; b) allyITMS, TMSOTf, ACN, 73%; c) either i. BCl3, DCM; ii. Ac_2O , pyridine 95% or i. Li, naphthalene, THF, -20°C; ii. Ac_2O , pyridine, 54%; d) i. NaOMe, MeOH; ii. NaH, PMBCl, TBAI, DMF, 69%; e) methyl acrylate or benzyl acrylate, Grubbs 2^{nd} gen. catalyst, DCM (175: 74%; 176: 73%); f) RuCl3, NaBH4, DCE/MeOH: (177: 91%; 178: 93%); g) KOH, THF/H2O (177 \rightarrow 179: 90%; 178 \rightarrow 179: qnt.); h) 181, HCTU, DIPEA, DMF, 99%; i) LiOH, H2O2, THF/H2O/t-BuOH, 79%.

With sufficient amounts of building block **168** available, the assembly of clusters containing 1, 2, 3, or 6 copies of the *C*-mannose lysine was undertaken *via* SPPS (Scheme 3). Using Tentagel[®] S-RAM amide resin, Fmoc-Lys(Boc)-OH and Fmoc-Gly-OH were introduced successively followed by elongation with *C*-mannose functionalized lysine building block **168** using a standard Fmoc protocol and HCTU as coupling agent. To prevent the use of a large excess of **168**, it was introduced manually, using fewer equivalents of the building block than commonly used in SPPS with prolonged coupling times (2eq, overnight). After completion of the sequence, the N-termini were capped with acetyls resulting in immobilized peptides **182-185** (Scheme 3). When resins **182**-

185 were subjected to a cleavage cocktail of TFA/TIS/H₂O (190/5/5, v/v/v), the Boc and PMB ethers were successfully removed and the peptide clusters were isolated after RP-HPLC purification to obtain monovalent- (186), bivalent- (187), trivalent- (188) and hexavalent- (189) clusters in 7%, 14%, 6%, and 2% yield, respectively. It was initially hypothesized that the relatively low yield originated from incomplete precipitation of the peptides after cleavage from the solid support, but when a different workup method was applied for 186 & 189, in which the cleavage cocktail was concentrated instead of precipitated, the yields were not increased. LC-MS analysis of the crude products showed multiple side products, possibly due to side reactions during the cleavage reaction which will be addressed later in this chapter.

To validate whether *C*-mannosides were able to bind the target CLRs, the clusters **186-189** were functionalized with a biotin moiety to enable the visualization of the clusters using fluorescently labeled streptavidin. The clusters were treated with biotin-*N*-hydroxysuccinimide (NHS) ester to give the biotinylated mannoside clusters **190-193** (R = R₂, Scheme 3). This allowed for the side by side comparison with their *O*-mannoside analogs **59**, **64**, **69**, and **74** *via* flow cytometry as described in Chapter 2. Thus, DC-SIGN expressing MoDCs were exposed to the *C*- and *O*-mannoside clusters at 4 °C, after which the cells were washed and treated with fluorescent streptavidin which was quantified by FACS analysis. Figure 1A shows that the *C*-mannoside clusters are binding equally as well as their *O*-counterparts, with better binding with an increasing number of mannosides on the scaffold. Similar to the experiments described in Chapter 2, the clusters were tested for their rate of uptake. Active internalization can take place when the cells are allowed to warm to room temperature, and the rate of reduction of the signal as a function of time, is an indication for the rate of uptake over time. Also, in these experiments, the *C*-mannose clusters behaved very similar to their *O*-mannose analogs (Figure 1B).

Scheme 3: Synthesis of *C*-mannoside clusters.

Reagents and conditions: a) Fmoc-SPPS (168, HCTU, DIPEA, DMF); b) TFA, TIS, H₂O, (octanethiol, phenol) (186: 7.0%; 187: 14%; 188: 6.0%; 189: 2.1%); c) Biotin-NHS, DIPEA, DMSO (190: 94%; 191: 72%; 192: 99%; 193: 80%); d) ATTO655-NHS, DIPEA, DMSO, 194: 55%.

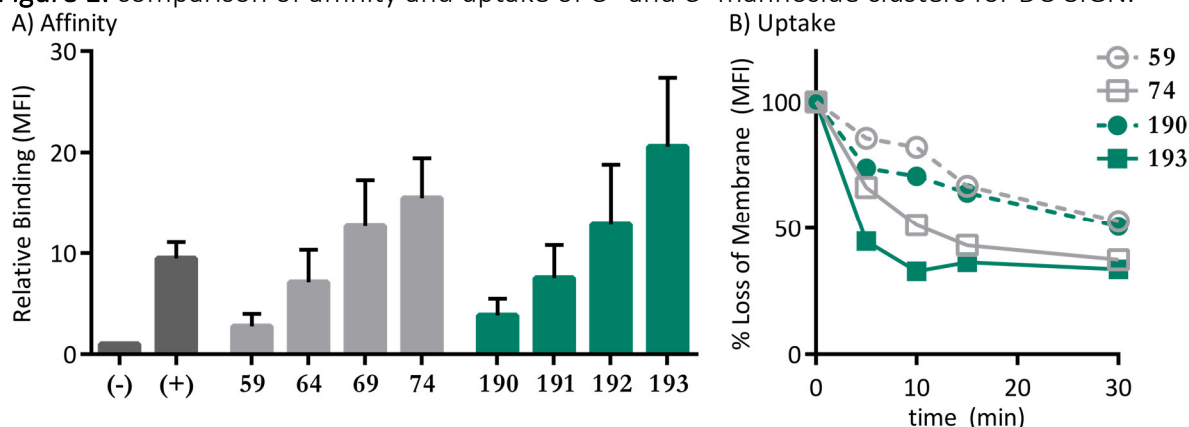
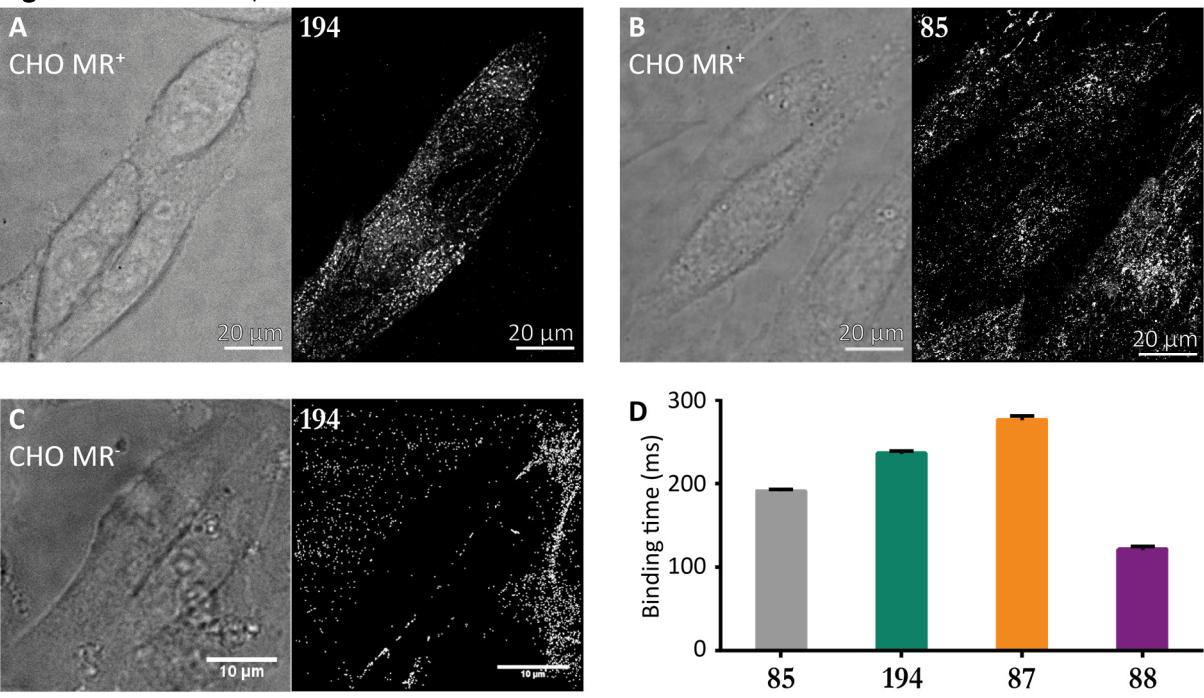


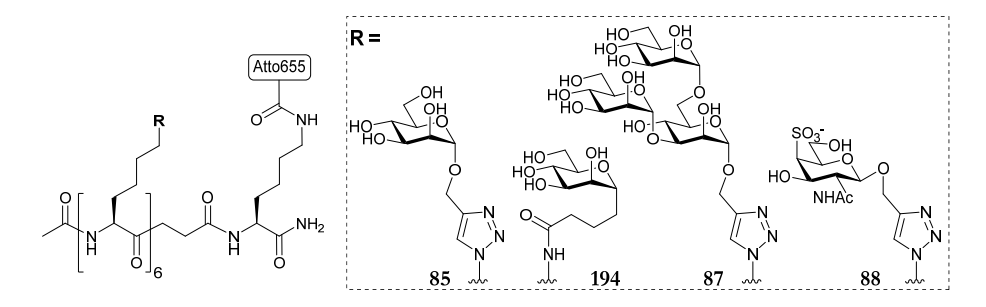
Figure 1: comparison of affinity and uptake of O- and C- mannoside clusters for DC-SIGN.

A) Binding of the biotinylated mannoside library to DC-SIGN on moDC was measured by flow cytometry. Normalized to the negative control. MoDCs were incubated with biotinylated constructs (30 min, 4 °C, 10 μ M). (-) = negative control (PBS); (+) = positive control (1 μ g/mL of Lewis Y conjugated polyacrylamide); Serie A in gray; C-mannoside in green; **B)** The internalization of the mannoside clusters by moDCs was measured by flow cytometry. One donor is depicted here as representation of four. Cells were incubated with clusters (20 μ M on ice for one hour and after incubated at 37 °C for different time spans). Quantification with an external fluorophore allowed quantification of the remaining clusters on the cell surface as an indirect measure of uptake.

Figure 2: STORM experiments.



A) CHO-MR cells were incubated with 194 (5 nM) and imaged with a 640 nm laser (40 mW); **B)** CHO-MR cells were incubated with 85 (5 nM) and imaged with a 640 nm laser (40 mW); **C)** CHO-K1 cells were incubated with 194 (5 nM) and imaged with a 640 nm laser (40 mW); **D)** Incubation of CHO-MR cells with probes 85, 194, 87 and 88 at 37°C allowed for single particle tracking. Trajectory lengths from at least 5 images per probes were combined, plotted in a histogram and fitted with a single exponential decay function wherefrom τ was determined. The used structures are depicted on the next page.



Finally, **189** was decorated with an ATTO655 laser dye (R = R₃, Scheme 2) to obtain **194**, which was compared with its *O*-analogue **85** in a mannose receptor (MR) binding experiment. In this setup for stochastic optical reconstruction microscopy (STORM) (As used in Chapter 2), only clusters that remain at the same location for a certain time will be observed. Since unbound clusters move to fast due to diffusion, only clusters that are fixed will be observed. This can be either in cellular compartments or bound to receptors. When Chinese hamster ovary (CHO) cells transfected with the MR were subjected to cluster **194**, the clusters were localized on the cell surface (see Figure 2A). When the same experiments were performed with CHO cells that lack the MR, the clusters did not localize indicating that this localization is MR dependent (Figure 2C). When these MR⁺ CHO cells were subjected to **85**, the *O*-analogue of **194** (see Figure 2B), both clusters showed similar localization. Additionally, by following individual fluorescent events, an average binding time can be determined, which correlates with the affinity of the cluster for the receptor. Both *C*- and *O*- mannoside clusters showed similar affinities (Figure 2D). Together these results indicated that DC-SIGN and the MR well tolerate the *O* to *CH*₂ modification, encouraging the use of such clusters in an antigen-adjuvant conjugate.

Encouraged by these results, the synthesis of *C*-mannose peptide conjugates in which the melanoma tumor antigen gp100 is incorporated were undertaken (see also Chapter 4). The SPPS of the gp100 antigen 134 containing the N-terminal monomethoxy trityl (Mmt) protected lysine, as described in Chapter 4, was followed by either one or six couplings with 168 to obtain *C*-mannosylated 195 & 196, respectively (Scheme 4). Next, 195 & 196 were functionalized at their N-termini with the TLR7 ligand 2-butoxy-8-oxo-adenine, using the building block described in Chapter 3, to give immobilized conjugates 197 & 198. Alternatively, the N-termini were acetylated to obtain resins 199 & 200, which could be further functionalized at the C-termini by subsequent selective removal of the monomethoxy trityl (Mmt) on the C-terminal lysines followed by the introduction of the TLR7 ligand to provide 201 & 202 bearing the TLR7 agonist on the C-terminus. Having fully protected and immobilized conjugates 197-202 available, the ensuing deprotection and cleavage from the solid support was evaluated. When resin 199 was treated with a cleavage cocktail of TFA/TIS/H₂O (190/5/5, v/v/v, Chapter 4), LC-MS analysis revealed the

formation of a complex mixture. It was hypothesized that the poor quality of the crude material was due to side reactions of the cleavage and deprotection step and not due to incomplete couplings. Reactive cationic species are liberated during the acidic removal of the PMB ethers, which could potentially react with functional groups in the unprotected peptide.²⁰ Howard et al.²¹ effectively scavenged PMB-cations using phenol as an electron-rich aromatic additive and when resin 199 was subjected to a modified cleavage cocktail, that included octanethiol and phenol, LC-MS analysis showed a crude mixture with improved quality and 203 as the main product. Further optimization of the cleavage cocktail was achieved by increasing concentration of the scavengers (up to 10% of the total volume) and increasing the volume of cleavage medium (effectively diluting the concentration of reactive cationic species and reactive functional groups on the peptide). Using this optimized cleavage protocol, bi-functional conjugates 203 & 204 were effectively released and deprotected to give the purified conjugates in 2.5% yield over 34 couplings and 0.7% yield over 39 couplings respectively (90% and 88% per step). The treatment of resin 197 with these optimized conditions resulted in tri-functional monovalent C-mannose conjugate 205 in 2.6% yield over 36 couplings (average of 90% per step). Exposure of 198 delivered the tri-functional hexavalent Cmannose conjugate 206 in 1.3% yield over 41 couplings (average of 90% per step). When resins 201 & 202 were treated with this optimized cocktail however, a complex mixture was obtained. LC-MS analysis of the crude of 207 indicated not only the formation of the desired product but also more lipophilic products, having a higher molecular mass increasing with 484.2 Da per step. This increment corresponded with the addition of an extra ethylene glycol - TLR7 ligand (PEG-TLR7L, see Figure 4A). Since this was not observed for the C-mannose conjugates without Cterminal elongation, it was hypothesized that PMB ethers were partly removed during the removal of the Mmt, liberating C-mannose hydroxyls, which could then react with the activated HCTU esters in the next coupling reaction. This was confirmed by treatment of the cleaved crude peptide mixture with aqueous ammonia, which removed the heavier ester byproducts (Figure 4B). Therefore milder conditions were explored for the removal of the C-terminal Mmt-group. Eventually it was found that the use of acetic acid in a mixture of trifluoroethanol (TFE) and DCM (1/2/7, v/v/v), a cocktail first described to selectively cleave the Mmt over methyltrityl and tritylgroups,²² was effective. After the introduction of the ethylene glycol moiety and TLR7 ligand 116, no byproducts were observed that contained additional PEG-TLR7L esters, supporting the notion that the previously observed side products were formed due to partial cleavage of PMB ethers during the Mmt removal. Using the milder AcOH/TFE/DCM Mmt removal conditions, trifunctional conjugates 207 & 208 were successfully synthesized and isolated in 2.1% over 36 couplings and 0.6% over 41 couplings respectively (90% and 88% per step).

Scheme 4: Synthesis of gp100 conjugates.

Reagents and conditions: a) Fmoc-SPPS (168, HCTU, DIPEA, DMF); b) Fmoc-SPPS (127 or 116, HCTU, DIPEA, DMF); c) Ac_2O , DIPEA, DMF; d) AcOH, TFE, DCM; e) TFA, TIS, H_2O , octanethiol, phenol (205: 2.60% over 36 couplings (90% per step); 206: 1.30% over 41 couplings (90% per step); 203: 2.51% over 34 couplings (90% per step); 204: 0.73% over 39 couplings (88% per step); 207: 2.10% over 36 couplings (90% per step); 208: 0.60% over 41 couplings (88% per step)).

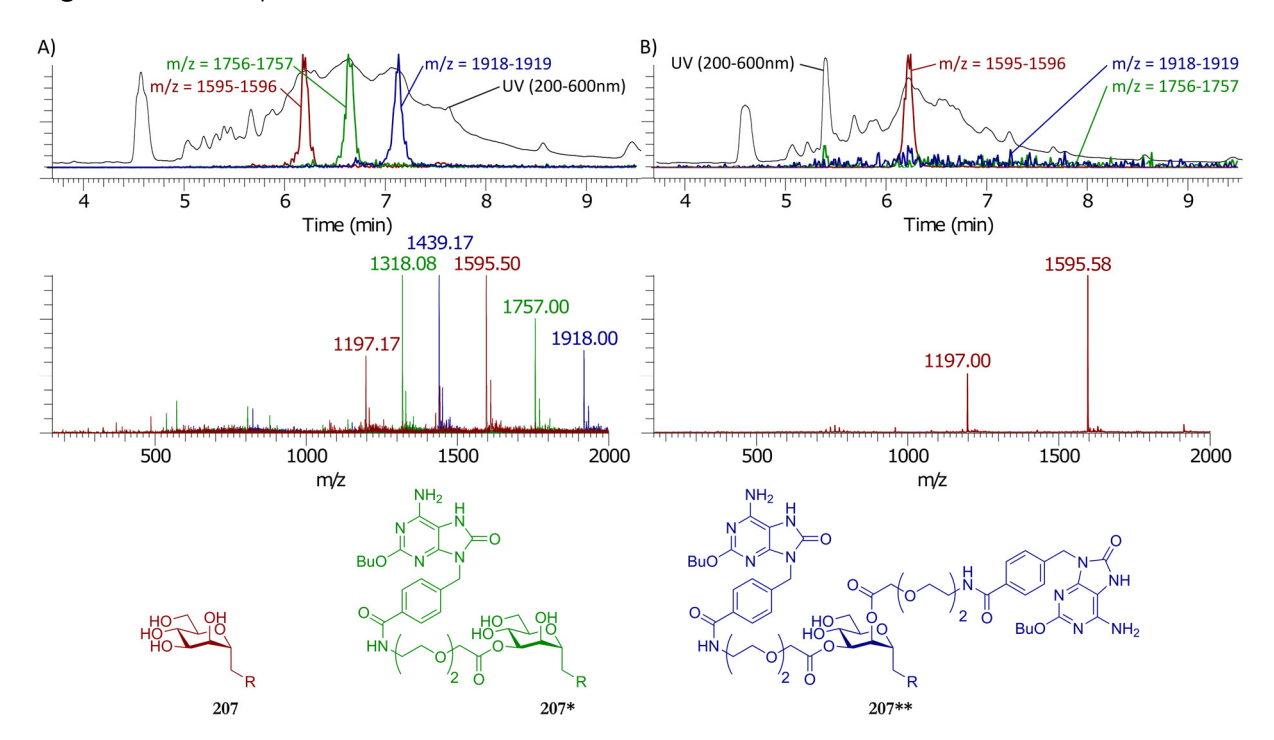


Figure 4: LC-MS spectra of 207 after release from resin.

A) LC-MS spectra of 207 (Mmt removal with 1% TFA); **B)** LC-MS Spectra of the same batch of 207 after treatment with aqueous ammonia.

These conjugates were tested for their ability to induce maturation, activation, and their antigen (cross-)presentation capacity. DC maturation is a necessity for the induction of an efficient immune response. By quantification of co-stimulatory molecules, maturation was measured (Figure 5B). All conjugates induced higher levels of CD86 when compared with the unfunctionalized gp100 **129**, and the *O* to *C* modification did not result in different expression levels. To determine whether these constructs were still able to activate DCs, the concentration of secreted cytokines from four donors were determined as a measure of activation by the quantification of four key cytokines. IL-6 and IL-12 are primarily inflammatory cytokines that help with DC maturation and Th1 skewing. IL-10 is an anti-inflammatory cytokine that interferes with DC maturation and can skew naïve T cells to regulatory T cells (Tregs). TNFα is an inflammatory cytokine required for DC activation and proliferation. When comparing the cytokine profiles of the here described *C*-mannoside conjugates with their *O*-mannoside analogs (Figure 5C), similar cytokine profiles are induced. However, for the conjugates with both *C*-mannoside and TLR ligand

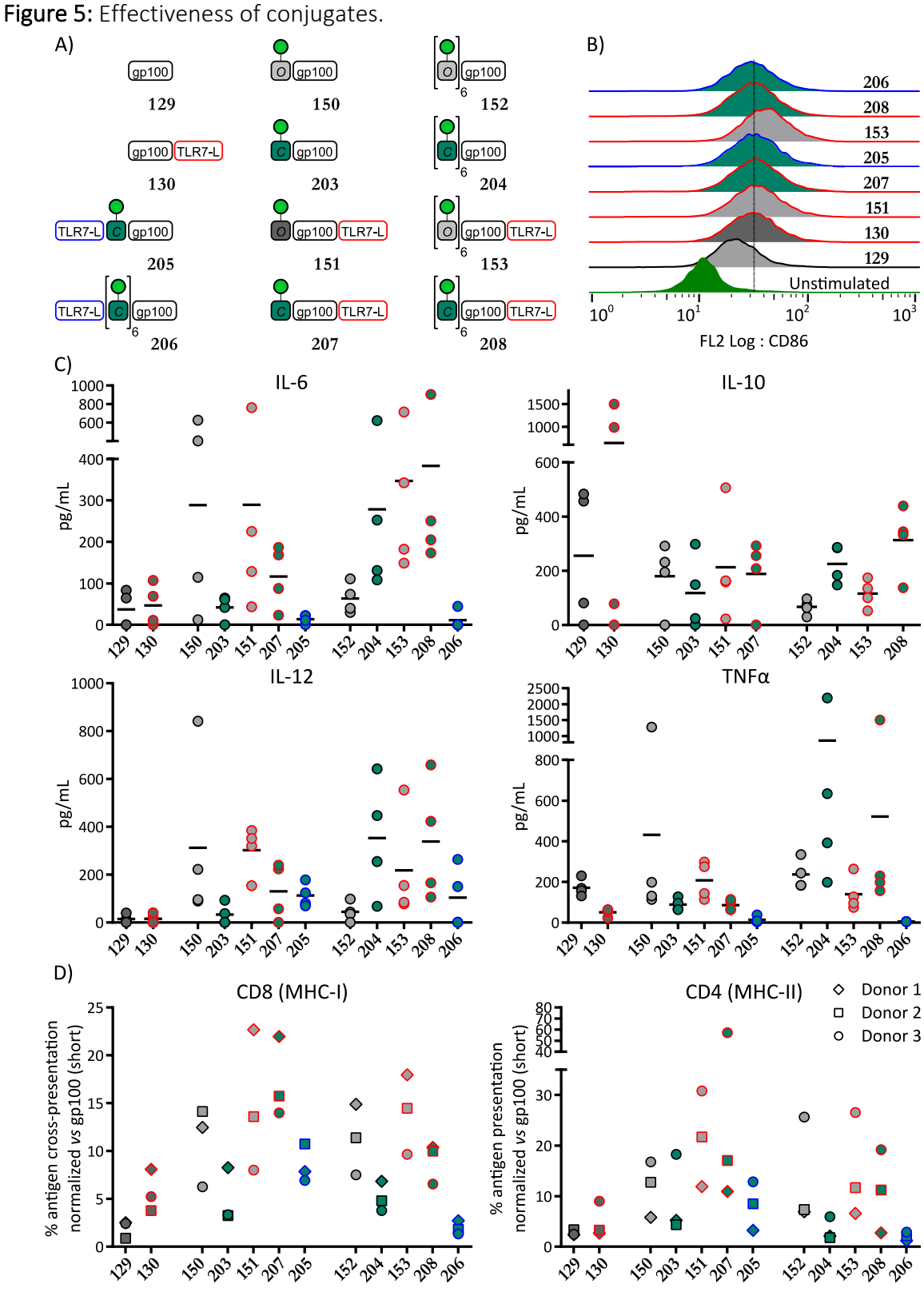
on the N-terminus (205 and 206), the production of inflammatory cytokines (IL-6, IL-12, $TNF\alpha$) was almost completely diminished.^a

Finally, the prepared clusters were tested for their antigen presentation ability using gp100 specific T cell clones (see Figure 5D). In short, five-day-old moDCs were incubated with the peptide conjugates, after which the moDcs were washed and co-cultured with either a CD8 cell clone that is specific for the gp100₂₈₀₋₂₈₈ MHC-I epitope or with a CD4 cell clone, specific for the gp100₄₀₋₅₉ MHC-II epitope. Interferon γ cytokine secretion was measured by sandwich ELISA as a measure for T-cell activation. Quantification of antigen presentation was achieved by normalization of the interferon γ cytokine production with secretion levels induced by short gp100 peptide (gp100₂₈₀₋₂₈₈, and long gp100 peptide (gp100₂₈₀₋₂₈₈, 40-59) set to 100%. The *C*-mannoside-conjugates (203-208) were tested side-by-side with the *O*-mannoside-conjugate conjugates (150-153) described in Chapter 4 to reveal any differences between the two types of conjugates.

When the antigen presentation induced by the monovalent O-mannose-clusters 150 & 151 and Cmannose-clusters 203 & 207 are compared it becomes clear that both conjugates induce antigen and cross-presentation equally well. Furthermore, when compared with the stand-alone gp100 peptide (129) or the TLR7-gp100 conjugate (130), antigen (cross)-presentation capacity was enhanced. However, conjugation of both the C-mannoside and the TLR7 ligand to the N-terminus of the peptide (205) led to a decrease in antigen presentation. Comparable effects were observed for the hexavalent clusters, although here, the C-mannoside conjugates (204 & 208) showed somewhat lower antigen presentation than their O-counterparts (152 & 153). The difference appears to be larger for MHC-II presentation than for the MHC-I mediated presentation, which could be the result of the effect that the metabolically stable C-mannosides have on the processing of the conjugates. Antigen (cross)-presentation was again significantly diminished when the TLR7 ligand and the hexavalent C-mannose clusters where both conjugated to the N-terminus of the peptide (206). This effect could be caused by steric hindrance preventing the TLR7 ligand to bind properly to its receptor, the TLR7 appendage hindering CLR mediated uptake, or because the processing of a longer sequence of unnatural amino acids hampers the processing and presentation of these conjugates.

122

^a Expression levels of CD86 however showed similar levels compared with the other conjugates bearing the TLR7 ligand.



A) Cartoon representation of used C- and O-conjugates; B) Expression of the DC maturation marker CD86 upon overnight stimulation with the trifunctional conjugates is measured by flow cytometry. LPS stimulation (10 ng/mL) is used as positive control; C) IL-6, IL-10, IL-12p70, and TNFa secretion of four donors was measured using ELISA upon overnight stimulation with conjugates; D) Antigen cross-presentation (left) and presentation (right) by the moDCs was determined by IFNy release of the activated T cells, after stimulation with conjugates (20 µM, 30 min).

Conclusion

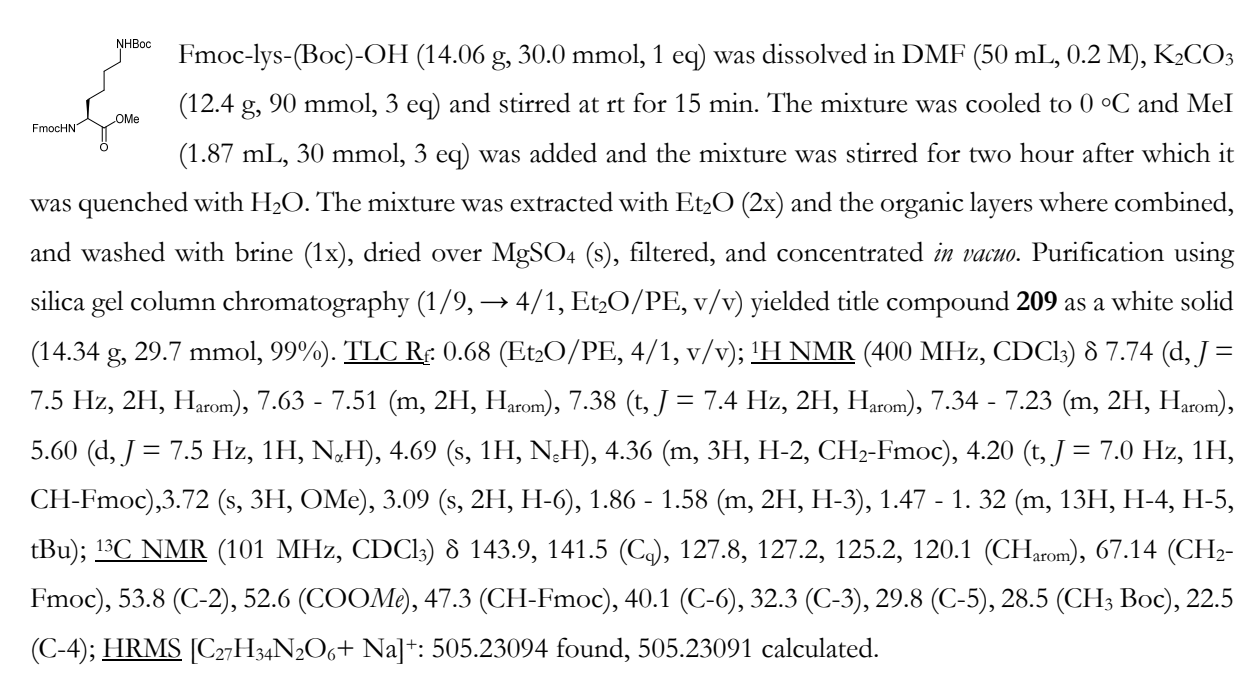
The synthesis of a new C-mannoside lysine building block has been reported. This building block is synthetically readily accessible and the C-glycosidic linkage renders it stable towards acidic reaction conditions. This, in combination with the temporary Fmoc-group installed on the lysine- N_{ω} and the permanent PMB protection, masking the mannose hydroxyl groups, enabled the use of this building block in online SPPS. The building block was successfully applied for the generation of various glycopeptide-conjugates. All these conjugates were synthesized on resin, which obviates post-SPPS conjugation steps after release from resin. At first, the cleavage and global deprotection of these conjugates were met with poor results, due to side reactions caused by the release of reactive PMB cations during the cleavage/deprotection step, that reacted with functional groups on the peptide. The addition of extra scavengers and dilution of the reaction mixture prevented these undesired side reactions. The assembly of the conjugates, functionalized at the C-terminal end, required the chemoselective removal of the C-terminal lysine Mmt group, for which the use of AcOH in a mixture of TFE and DCM proved effective. Different peptidic antigen conjugates were generated. First, it was established that clusters, comprising 1, 2, 3, or 6 copies of the C-mannose lysine show similar binding to, and similar uptake in moDCs compared with their O-mannose analogs. The retention time for the clusters bound to the MR on transfected CHO cells were also identical. These results show that the O to CH2 modification is well-tolerated by these CLRs. Next gp100-peptide antigens were equipped with multiple copies of the Cmannoside and an additional TLR7 ligand. Conjugates having both the mannose cluster and the TLR7 ligand on the same (N-terminal) side of the antigen, or attached to different sides of the antigen (the mannose cluster on the N-terminal side, the TLR7 ligand on the C-terminus), were successfully assembled. Evaluation of the conjugates in antigen (cross)-presentation assays revealed that the antigen (cross)-presentation of the conjugates was not significantly hampered by the O to CH₂ modification. The monovalent C-mannose conjugates with the TLR7 ligand on the C-terminus significantly enhanced the antigen presentation. The combination of both the TLR7 ligand and the C-mannoside cluster on the N-terminus hampered (cross)-presentation and maturation, likely due to the steric hindrance of the TLR7 ligand. With the 'SPPS-compatible' mannoside amino acid building block 168 available and chemistry developed for its introduction and deprotection, further conjugates can now be designed that employ mannose-binding lectins for enhanced uptake. In these conjugates, chemically or enzymatically labile spacers may be introduced to enhance the processing of the antigen-conjugates.²⁵ Azide-alkyne handles can be introduced to follow the processing of these glycopeptide conjugates in more detail.

Experimental

General procedures:

All reactions, purifications, and analyses were performed as described in the general procedures of Chapter 2.

N_{α} -Fmoc- N_{ϵ} -(Boc)-L-lysine-methyl ester (209).



N_{α} -Fmoc- N_{ϵ} -(HCl)-L-lysine-methyl ester (181).

Boc protected lysine **209** (4.74 g, 9.8 mmol, 1 eq) was dissolved in HCl (20 mL, 4.0 M in dioxane) at 0 °C. After four hours the solvent was partly removed *in vacuo* after which the product was precipitated, filtered, washed with little EtOAc and dried *in vacuo* to yield title compound **181** as a white solid (4.744 g, 9.1 mmol, 94%). TLC R_E: 0 (EtOAc/PE, 1/1, v/v); ¹H NMR (400 MHz, MeOD) δ 7.83 (d, *J* = 7.5 Hz, 2H, H_{arom}), 7.69 (t, *J* = 7.5 Hz, 2H, H_{arom}), 7.42 (t, *J* = 7.4 Hz, 2H, H_{arom}), 7.34 (td, *J* = 7.4, 0.9 Hz, 2H, H_{arom}), 4.55 – 4.33 (m, 2H, CH₂-Fmoc), 4.28 – 4.17 (m, 2H, CH-Fmoc, H-2), 3.74 (s, 3H, OMe), 2.94 (t, *J* = 7.0 Hz, 2H, H-6), 1.98 – 1.82 (m, 1H, H-3a), 1.82 – 1.60 (m, 3H, H-3b, H-5), 1.58 – 1.39 (m, 2H, H-4); ¹³C NMR (101 MHz, MeOD) δ 142.6, 141.5 (C_q), 128.8, 128.2, 126.2, 126.1, 121.0 (CH_{arom}), 67.9 (CH₂-Fmoc), 55.0 (C-2), 52.8 (COO*Me*), 48.4 (CH-Fmoc), 40.5 (C-6), 32.0 (C-3), 28.0 (C-5), 23.8 (C-4); HRMS [C₂₂H₂₆N₂O₄+ H]⁺: 383.1973 found, 383.19653 calculated.

Methyl 2,3,4,6-tetra-O-benzyl- α -D-mannopyranoside (171).

Methyl α-p-mannopyranoside (29.13 g, 150 mmol) was co-evaporated with toluene (2x), dissolved in DMF (900 mL, 0.17 M) and cooled to 0 °C. NaH (60% dispersion in mineral oil) (36.0 g, 900 mmol, 6 eq) was added in small portions under a continuous flow of argon. BnBr (80.28 mL, 675 mmol, 4.5 eq) and TBAI (5.54 g, 15 mmol, 0.1 eq) were added and the reaction mixture was stirred at room temperature. After three days the mixture was quenched with MeOH at 0°C, diluted in Et₂O and washed with brine. The aqueous layer was back-extracted with Et2O, the organic fractions combined, washed with brine (2x), dried over MgSO₄ (s), filtered and concentrated in vacuo. Purification using silica gel column chromatography (1/8, \rightarrow 1/4, PE/Et₂O/PE, v/v) yielded compound 171 as a colorless oil (64.5 g, 116.3 mmol, 77.5%). TLC R_f: 0.67 (1/4, EtOAc/PE, v/v); IR (neat, cm⁻¹): 3020, 2905, 1495, 1453, 1362, 1261, 1098, 1058, 1026, 967, 910, 846, 801, 733, 695; 1H NMR (400 MHz, CDCl₃) δ 7.40 - 7.22 (m, 18H, H_{arom}), 7.18 - 7.14 (m, 2H, H_{arom}), 4.88 (d, J = 10.8 Hz, 1H, CHH Bn), 4.79 - 4.64 (m, 4H, CHH-Bn, CH_2 -Bn, H-1), 4.61 (s, 2H, CH_2 -Bn), 4.53 (dd, J = 20.7, 11.5 Hz, 2H, CHH-Bn (2x)), 3.97 (t, J = 9.1 Hz, 1H, H-4), 3.88 (dd, J = 9.3, 3.1 Hz, 1H, H-3), 3.81 - 3.70 (m, 4H, H-2, H-5, H-6), 3.32 (s, 3H, OMe); $\frac{13C}{2}$ NMR (101 MHz, CDCl₃) δ 138.6, 138.6, 138.5, 138.5 (C_q), 128.4, 128.4, 128.4, 128.0, 127.9, 127.8, 127.7, 127.6, 127.6, 127.5 (CH_{arom}), 99.0 (C-1), 80.3 (C-3), 75.1 (CH₂-Bn), 75.0(C-4), 74.6 (C-2), 73.4, 72.6, 72.2 (CH₂-Bn), 71.8 (C-5), 69.4 (C-6), 54.8 (OMe); <u>HRMS</u> [C₃₅H₃₈O₆ + H]⁺: 555.27512 found, 555.27412 calculated.

3-(2,3,4,6-Tetra-O-benzyl- α -D-mannopyranoside)-1-propene (172).

Compound **171** (53.61 g, 96.64 mmol) was co-evaporated with toluene (3x) under argon, dissolved in ACN (133 mL, 0.73 M) and cooled to 0 °C. Allyltrimethylsilane (41.5 mL, 260.93 mmol, 2.7 eq) and TMSOTf (21.0 mL, 116.0 mmol, 1.2 eq) were added and the reaction mixture was irradiated with ultrasound for 50 min after which the reaction mixture was quenched by addition of Et₃N. The reaction mixture was diluted in Et₂O washed with brine (3x), dried over MgSO₄ (s), filtered and concentrated *in vacuo*. Purification using silica gel column chromatography (1/4, \rightarrow 1/1, Et₂O/PE, v/v) yielded compound **172** as a colorless oil (56.1 g, 70.48 mmol, 73%). TLC R_f: 0.61 (EtOAc/PE, 1/4, v/v); IR (neat, cm⁻¹): 3021, 2905, 2855, 1495, 1453, 1363, 1262, 1090, 1072, 1027, 1001, 912, 733, 695; IH NMR (400 MHz, CDCl₃) δ 7.39 - 7.24 (m, 18H, H_{arom}), 7.22 - 7.18 (m, 2H, H_{arom}), 5.83 - 5.68 (m, 1H, H-2), 5.08 - 4.93 (m, 2H, H-1), 4.70 (d, J = 11.3 Hz, 1H, CHH-Bn), 4.62 - 4.49 (m, 7H, CH₂-Bn (3x), CHH-Bn), 4.04 (q, J = 6.3 Hz, 1H, H-4), 3.92 - 3.66 (m, 5H, H-6, H-7, H-8, H-9), 3.62 (dd, J = 4.6, 3.1 Hz, 1H, H-5), 2.32 (hept, J = 6.8 Hz, 2H, H-3); J C NMR (101 MHz, CDCl₃) δ 138.5, 138.4, 138.3, 138.2 (C_q), 134.4 (C-2), 128.5, 128.4, 128.4, 128.1, 128.1, 128.0, 127.8, 127.8, 127.7, 127.5 (CH_{arom}), 117.3 (C-1), 76.9 (C-6/7/8), 75.2 (C-5), 75.0 (C-6/7/8), 73.9 (CH₂-Bn), 73.8 (C-6/7/8), 73.4 (CH₂-Bn), 72.4 (C-4), 72.1, 71.6 (CH₂-Bn), 69.2 (C-9), 34.7 (C-3); H RMS [C₃7H₄₀O₅ + H]⁺: 565.29569 found, 565.29485 calculated.

3-(2,3,4,6-Tetra-O-Acetyl- α -D-mannopyranoside)-1-propene (173). Method a) BCl₃

Compound 172 (6.44 g, 11.4 mmol) was co-evaporated with toluene (3x) under argon, dissolved in DCM (10 mL) and cooled to -78°C. To this solution BCl₃ (100 mL, 1.0 M in DCM, 100 mmol, >8 eq) was added dropwise. After overnight stirring at -78°C the reaction mixture was quenched by the addition of MeOH (100 mL) at -78°C after which the mixture was concentrated *in vacuo* and co-evaporated with toluene (5x). The crude pink oil was dissolved in pyridine (20 mL, 0.6 M) and Ac₂O (6.5 mL, 69.0 mmol, 6 eq) was added dropwise at 0°C. After overnight stirring at rt the reaction was quenched with MeOH, diluted in Et₂O and washed with HCl (1 M, aq., 4x). The organic layer was collected, dried over MgSO₄ (s), filtered, and concentrated *in vacuo*. Purification using silica gel column chromatography (1/9, \rightarrow 1/1, Et₂O/PE, v/v) yielded title compound 173 as a colourless oil (4.003 g, 10.7 mmol, 95%).

Method b) Li-naphthalenide

Compound 172 (45.8 g, 81 mmol) was co-evaporated with toluene (3x) under argon and dissolved in distilled anhydrous THF (180 mL). This solution was added dropwise to a lithium napthalenide solution at -78°C and stirred for five days at -20°C with a glass stirring rod. Li-napthalenide solution was prepared from Li (9.2 g, 1.3 mol, 14 eq) and naphthalene (15.5 g, 121 mmol, 1.5 eq) in distilled anhydrous THF (400 mL). The reaction was quenched with MeOH, neutralized with Amberlite H+ resin, filtered and concentrated *in vacuo*. After co-evaporation with toluene (3x) the mixture was dissolved in pyridine (135 mL, 0.6 M), cooled to 0°C and Ac₂O (46 mL, 486 mmol, 6 eq) was added dropwise. After overnight stirring at rt, the reaction was quenched with MeOH, diluted with Et₂O and washed with HCl (1 M, aq.). The aqueous layer was back-extracted with Et₂O (2x) and the organic layers were combined, washed with HCl (1.0 M, aq., 2x), dried over MgSO₄(s), filtered and concentrated *in vacuo*. Purification using silica gel column chromatography (1/9, \rightarrow 1/1, Et₂O/PE, v/v) yielded title compound 173 as a colorless oil (16.38 g, 44 mmol, 54%).

TLC R_E: 0.34 (Et₂O/PE, 6/4, v/v); <u>IR</u> (neat, cm⁻¹): 2905, 1739, 1369, 1213, 1144, 1114, 1045, 986, 918, 802; <u>¹H NMR</u> (400 MHz, CDCl₃) δ 5.78 (ddt, J = 17.1, 10.2, 6.9 Hz, 1H, H-2), 5.27 (dd, J = 8.9, 3.3 Hz, 1H, H-6), 5.23 - 5.13 (m, 4H, H-7, H-5, H-1), 4.33 (dd, J = 12.1, 6.3 Hz, 1H, H-9a), 4.11 (dd, J = 12.1, 2.9 Hz, 1H, H-9b), 4.08 - 4.02 (m, 1H, H-4), 3.90 (ddd, J = 8.9, 6.5, 2.9 Hz, 1H, H-8), 2.59 - 2.48 (m, 1H, H-3a), 2.48 - 2.36 (m, 1H, H-3b), 2.13 (s, 3H, Ac), 2.09 (s, 3H, Ac), 2.07 (s, 3H, Ac), 2.03 (s, 3H, Ac); <u>¹³C NMR</u> (101 MHz, CDCl₃) δ 170.8, 170.3, 170.0, 169.8 (C=O), 132.6 (C-2), 118.4 (C-1), 74.2 (C-4), 70.7 (C-8), 70.1 (C-5), 68.9 (C-6), 67.1 (C-7), 62.5 (C-9), 33.7 (C-3), 21.0, 20.8, 20.8 (Ac (4x)); <u>HRMS</u> [C₁₇H₂₄O₉ + H]+: 373.14931 found, 373.14931 calculated.

3-(2,3,4,6-Tetra-O-paramethoxybenzyl-α-p-mannopyranoside)-1-propene (174).

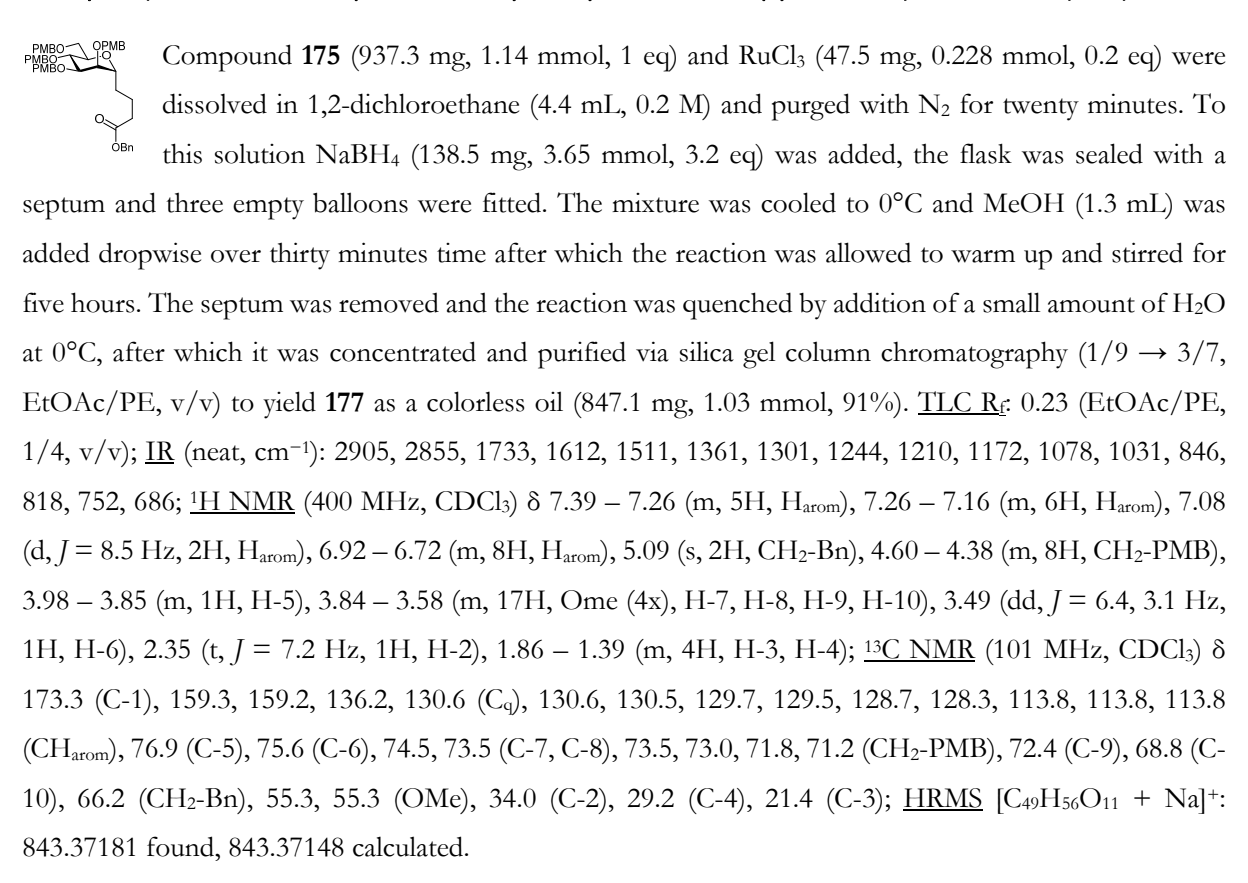
Compound 173 (18.84 g, 50.6 mmol) was dissolved in MeOH (83 mL, 0.6 M) and NaOMe (4.5 mL, ~5.4 M, 20.25 mmol, 0.4 eq) was added dropwise. After overnight stirring, the mixture was neutralized with Amberlite H+ resin, filtrated and concentrated in vacuo. After co-evaporation with toluene (3x) the crude was dissolved in DMF (253 mL, 0.2 M) cooled to 0°C and NaH (12.14 g, 60% wt dispersion in mineral oil, 303.6 mmol, 6 eq), PMBCl (41.2 mL, 303.6 mmol, 6 eq) and TBAI (3.7 g, 10.1 mmol, 0.2 eq) were added in portions. After overnight stirring at rt, the mixture was quenched with H₂O at 0°C and extracted with Et₂O (2x). The organic layers were combined, washed with brine (3x), dried over MgSO₄ (s), filtrated and concentrated in vacuo. Purification using silica gel column chromatography $(1/9, \rightarrow$ 1/4, EtOAc/PE, v/v) yielded title compound 174 as a colorless oil (23.8 g, 34.7 mmol, 69%). TLC R: 0.38 (EtOAc/PE, 1/4, v/v); <u>IR</u> (neat, cm⁻¹): 3054, 2988, 1612, 1514, 1422, 1264, 1174, 1083, 896, 824, 732, 704; 1 H NMR (400 MHz, CDCl₃) δ 7.24 (t, J = 8.3 Hz, 4H, H_{arom}), 7.18 (d, J = 8.6 Hz, 2H, H_{arom}), 7.09 (d, J = 8.6 Hz, 2H, H_{arom}), 6.87 - 6.79 (m, 8H, H_{arom}), 5.74 (ddt, J = 18.2, 9.1, 6.9 Hz, 1H, H-2), 5.06 - 4.96 (m, 2H, H-1), 4.61 (d, J = 10.9 Hz, 1H, CHH-PMB), 4.56 - 4.37 (m, 7H, CH₂-PMB (3x), CHH-PMB), 4.04 -3.94 (m, 1H, H-4), 3.84 - 3.75 (m, 14H, OMe (4x), H-6, H-8), 3.71 (dt, I = 7.4, 4.0 Hz, 2H, H-9a, H-7), 3.65(dd, J = 10.1, 2.9 Hz, 1H, H-9b), 3.57 (dd, J = 4.6, 3.1 Hz, 1H, H-5), 2.32 (tt, J = 12.2, 6.6 Hz, 2H, H-3); $\underline{^{13}C}$ NMR (101 MHz, CDCl₃) δ 159.3, 159.3, 159.2 (C_q), 134.6 (C-2), 130.7, 130.6, 130.5, 130.4 (C_q), 129.7, 129.7, 129.6, 129.5 (CH_{arom}), 117.2 (C-2), 113.8, 113.8, 113.8 (CH_{arom}), 76.5 (C-7), 74.7 (C-5), 74.6, 73.8 (C-6, C-8), 73.5, 73.0 (CH₂-PMB), 72.4 (C-4)), 71.7, 71.1 (CH₂-PMB), 68.9 (C-9), 55.4, 55.3 (OMe (4x)), 34.8 (C-3); <u>HRMS</u> $[C_{41}H_{48}O_9 + N_a]^+$: 707.31913 found, 707.31905 calculated.

Benzyl-but-4-(2,3,4,6-tetra-O-paramethoxybenzyl- α -D-mannopyranoside)-cis/trans-2-enoate (175).

Allyl **174** (803.1 mg, 1.17 mmol, 1 eq) and benzylacrylate (531.3 mg, 3.276 mmol, 2.8 eq) where combined and co-evaporated with toluene (3x) under argon after which they were dissolved in DCM (40 mL, 1 M) and purged by bubbling with N₂ gas for twenty minutes. Grubbs second generation catalyst (19,9 mg, 23.4 μ mol, 0.02 eq) was added and the reaction mixture was refluxed protected from light. After three days the mixture was concentrated on Celite and purified via silica gel column chromatography (1/9 \rightarrow 1/3, EtOAc/PE, v/v) to yield **175** as a brown oil (707.8 mg, 0.86 mmol, 74%). TLC R_i: 0.23 (EtOAc/PE, 1/4, v/v); IR (neat, cm⁻¹): 2920, 2880, 1716, 1610, 1511, 1318, 1302, 1244, 1210, 1171, 1082, 1030, 990, 845, 755; IH NMR (400 MHz, CDCl₃) δ 7.39 - 7.27 (m, 5H, H_{arom}), 7.20 (d, J = 8.4 Hz, 4H, H_{arom}), 7.12 (t, J = 8.7 Hz, 4H, H_{arom}), 6.97 (dt, J = 15.5, 7.1 Hz, 1H, H-3), 6.82 (t, J = 8.7 Hz, 8H, H_{arom}), 5.89 (d, J = 15.7 Hz, 1H, H-2), 5.16 (s, 2H, CH₂-Bn), 4.53 - 4.36 (m, 8H, CH₂-PMB), 4.05 - 3.93 (m, 1H, H-5), 3.88 - 3.66 (m, 16H, Ome (4x), H-7, H-8, H-9, H-10a), 3.61 (dd, J = 10.3, 4.6 Hz, 1H, H-10b), 3.51 (dd, J = 6.4, 2.6 Hz, 1H, H-6), 2.55 - 2.34 (m, 2H, H-4); $\frac{13}{2}$ C NMR (101 MHz, CDCl₃) δ 166.2 (C-1), 159.4, 159.2 (C_q), 145.8 (C-3), 130.5, 130.3, 130.2, 130.1 (C_q), 129.8, 129.6, 129.6, 129.5, 128.6, 128.3, 128.2 (CH_{arom}), 123.2 (C-2), 113.9, 113.9, 113.8 (CH_{arom}), 75.1, 74.8, 74.3, 74.1 (C-6, C-7, C-8, C-9), 73.0,

72.7, 71.9, 71.1 (CH₂-PMB), 70.4 (C-5), 68.3 (C-10), 66.1 (CH₂-Bn), 55.4, 55.4, 55.4 (OMe), 33.8 (C-4); $\underline{\text{HRMS}}$ [C₄₉H₅₄O₁₁ + H]⁺: 819.37936 found, 819.37389 calculated.

Benzyl-4-(2,3,4,6-tetra-O-paramethoxybenzyl- α -D-mannopyranoside)-butanoate (177).



Methyl-but-4-(2,3,4,6-tetra-O-paramethoxybenzyl- α -D-mannopyranoside)-cis/trans-2-enoate (176).

Compound 174 (24.77 g, 36.2 mmol) was co-evaporated with CHCl₃ (1x), dissolved in DCM (40 mL, 1 M) and purged by bubbling with N₂ gas for twenty minutes. To this mixture methyl acrylate (16.3 mL, 181 mmol, 5 eq) and Grubbs second generation catalyst (0.68 g, 0.80 mmol, 0.02 eq) were added, the mixture was purged with N₂ for twenty minutes more, after which it was refluxed protected from light. After two days the mixture was concentrated on Celite and purified via silica gel column chromatography (1/9 \rightarrow 1/3, EtOAc/PE, v/v) to yield unreacted starting material 174 (6.27 g, 9.16 mmol, 25%) and product 176 as a brown oil (19.60 g, 26.4 mmol, 73%). TLC R_f: 0.22 (EtOAc/PE, 1/4, v/v); IR (neat, cm⁻¹): 2936, 2837, 1720, 1659, 1611, 1586, 1512, 1463, 1440, 1362, 1302, 1245, 1172, 1082, 1033, 819, 733, 702; IH NMR (400 MHz, CDCl₃) δ 7.24 - 7.09 (m, 8H, H_{arom}), 6.96 - 6.87 (m, 1H, H-3), 6.87 - 6.80 (m, 8H, H_{arom}), 5.83 (d, J = 15.7 Hz, 1H, H-2), 4.51 (d, J = 11.4 Hz, 1H, CHH-PMB), 4.47 - 4.37 (m, 7H, CH₂-PMB (3x), CHH-PMB), 4.04 - 3.96 (m, 1H, H-5), 3.89 - 3.83 (m, 1H, H-9), 3.83 - 3.75 (m, 12H, OMe (3x)), 3.75 - 3.65 (m, 6H, H-7, H-8, CO₂Me, H-10a), 3.65 - 3.59 (m, 1H, H-10b), 3.50 (dd, J = 6.4, 2.5 Hz, 1H, H-6), 2.55 - 2.37 (m, 2H, H-4); $\frac{13}{2}$ NMR (101 MHz, CDCl₃) δ 166.7 (C-1), 159.3, 159.1 (C₉), 145.3 (C-3), 130.4, 130.2, 130.1, 130.0 (C₉), 129.7, 129.6, 129.4 (CH_{arom}), 123.0 (C-2), 113.8, 113.7

(CH_{arom}), 74.9 (C-6), 74.7, 74.2 (C-7, C-8), 73.9 (C-9), 72.9, 72.6, 71.8, 71.0 (CH₂-PMB), 70.3 (C-5), 68.2 (C-10), 55.3 (OMe (4x)), 51.4 (COOMe), 33.7 (C-4); <u>HRMS</u> [C₄₃H₅₀O₁₁ + Na]⁺: 765.32463 found, 765.32453 calculated.

Methyl-4-(2,3,4,6-tetra-O-paramethoxybenzyl- α -D-mannopyranoside)-butanoate (178).



Compound 176 (19.60 g, 26.4 mmol) and RuCl₃ (1.1 g, 5.3 mmol, 0.2 eq) were dissolved in 1,2dichloroethane (100 mL, 0.26 M) and purged with N2 for twenty minutes. To this solution NaBH₄ (3.2 g, 84.5 mmol, 3.2 eq) was added, the flask was sealed with a septum and three empty balloons were fitted. The mixture was cooled to 0°C and MeOH (34 mL) was added dropwise over thirty minutes time after which the reaction was allowed to warm up and stirred for four hours. The septum was removed and the reaction was quenched by addition of a small amount of H₂O at 0°C, after which it was concentrated and purified via silica gel column chromatography ($1/9 \rightarrow 3/7$, EtOAc/PE, v/v) to yield 178 as a yellow oil (18.35 g, 24.6 mmol, 93%). TLC R_f: 0.34 (EtOAc/PE, 3/7, v/v); 1H NMR (400 MHz, CDCl₃) δ 7.29 - 7.22 (m, 4H, H_{arom}), 7.19 (d, J = 8.6 Hz, 2H, H_{arom}), 7.08 (d, J = 8.6 Hz, 2H, H_{arom}), 6.88 -6.80 (m, 8H, H_{arom}), 4.63 - 4.38 (m, 8H, CH_2 -PMB), 3.90 (dd, I = 8.6, 4.2 Hz, 1H, H-5), 3.84 - 3.60 (m, 20H, OMe (5x), H-7, H-8, H-9, H-10), 3.50 (dd, J = 4.7, 3.1 Hz, 1H, H-6), 2.30 (t, J = 7.1 Hz, 2H, H-2), 1.83 - 1.41 (m, 4H, H-3, H-4); 13C NMR (101 MHz, CDCl₃) δ 173.6 (C-1), 159.1, 159.1, 159.0, 130.4, 130.3, 130.2 (C₉), 129.9, 129.4, 129.3, 129.2, 129.0, 113.6, 113.5, 113.5 (CH_{arom}), 76.5 (C-7, C-8, C-9), 75.4 (C-6), 74.3, 73.4 (C-7, C-8, C-9), 73.1, 72.7 (CH₂-PMB), 72.1 (C-5), 71.5, 71.0 (CH₂-PMB), 68.5 (C-10), 55.0, 55.0 (OMe), 51.2 (COOMe), 33.5 (C-2), 29.0, 21.1 (C-3, C-4); HRMS [C₄₃H₅₂O₁₁ + H]⁺: 745.35731 found, 745.35824 calculated.

4-(2,3,4,6-tetra-O-paramethoxybenzyl-α-p-mannopyranoside)-butanoic acid (179).



Methyl ester 178 (18.34 g, 24.6 mmol)^a was dissolved in THF (123 mL, 0.2 M) and cooled to 0°C, followed by the dropwise addition of KOH (31 mL, 4.0 M, aq., 124 mmol, 5 eq). The mixture was heated to 50°C and stirred overnight. After acidification of the reaction mixture with HCl (1 M aq., pH ± 2), the product was extracted with Et₂O (3x), the organic layers were combined, dried over MgSO₄ (s), filtered and concentrated in vacuo. Purification using silica gel column chromatography (3/7 \rightarrow 1/0, EtOAc/PE, v/v) yielded title compound 179 as a clear oil (18.01 g, 24.6 mmol, qnt.). TLC R_f: 0.27 (EtOAc/PE, 7/3, v/v); IR (neat, cm⁻¹): 3055, 2920, 1513, 1422, 1264, 1034, 896, 733, 704; 1 H NMR (400 MHz, CDCl₃) δ 7.27 - 7.21 (m, 4H, H_{arom}), 7.18 (d, J = 8.6 Hz, 2H, H_{arom}), 7.08 (d, J = 8.6 Hz, 2H, H_{arom}), 6.83 (ddd, J = 8.5, 5.4, 2.5 Hz, 8H, H_{arom}), 4.60 - 4.36 (m, 8H, CH₂-PMB), 3.90 (dt, $J = 8.5, 4.6 \text{ Hz}, 1\text{H}, \text{H}-5), 3.83 - 3.66 \text{ (m, 18H, OMe (4x) H}-7, H}-8, H}-9, H}-10a), 3.66 - 3.60 \text{ (m, 1H, H}-$ 10b), 3.50 (dd, J = 5.0, 2.9 Hz, 1H, H-6), 2.34 (t, J = 7.0 Hz, 2H, H-2), 1.81 - 1.49 (m, 4H, H-3, H-4); $\frac{13C}{1}$ NMR (101 MHz, CDCl₃) δ 178.5 (C-1), 159.3, 159.2, 130.5, 130.5, 130.4 (C₀), 129.7, 129.7, 129.6, 129.6, 113.9 (CH_{arom}), 76.6 (C-7, C-8, C-9), 75.6 (C-6), 74.5, 73.6 (C-7, C-8, C-9), 73.3, 73.0 (CH₂-PMB), 72.2 (C-

^a Using the same procedure, hydrolysis of 177 (847.1 mg, 1.03 mmol) resulted in 179 (764.4 mg, 0.92 mmol, 90 %).

5), 71.9, 71.3 (CH₂-PMB), 68.8 (C-10), 55.4, 55.4 (OMe), 33.6 (C-2), 29.1 (C-4), 21.2 (C-3); <u>HRMS</u> $[C_{42}H_{50}O_{11} + Na]^+$: 753.32470 found, 753.32453 calculated.

N_{α} -Fmoc- N_{ϵ} -[butan-4-(2,3,4,6-tetra-O-paramethoxybenzyl- α -D-mannopyranoside)-amide]-L-lysine-methyl ester (180).

Carboxylic acid 178 (6.25 g, 8.55 mmol) was combined with amine 181 (3.58 g, 8.55 mmol, 1 eq) and HCTU (3.54 g, 8.55 mmol, 1 eq), dissolved in DMF (42.8 mL, 0.2 M) and DIPEA (4.47 mL, 25.65 mmol, 3 eq) was added dropwise. After two hours the mixture diluted with EtOAc, washed with a mixture of HCl (1 M, aq.) and brine (1/1, v/v) after which] the aqueous layer was backextracted with EtOAc (1x). The organic layers were combined, washed with brine (1x), dried over MgSO₄ (s), filtered and concentrated in vacuo. Purification using silica gel column chromatography (1/1 \rightarrow 9/1, EtOAc/PE, v/v) yielded title compound **180** as a white solid (9.30 g, 8.49 mmol, 99%). <u>TLC Re</u>: 0.34 (EtOAc/PE, 4/1, v/v); IR (neat, cm⁻¹): 3331, 2934, 1720, 1648, 1611, 1585, 1512, 1451, 1301, 1246, 1173, 1082, 1033, 820, 760, 740; $\frac{1}{1}$ H NMR (400 MHz, CDCl₃) δ 7.75 (d, J = 7.5 Hz, 2H, H_{arom}), 7.60 (d, J7.1 Hz, 2H, H_{arom}), 7.39 (t, J = 7.4 Hz, 2H, H_{arom}), 7.30 (t, J = 7.4 Hz, 2H, H_{arom}), 7.27 - 7.14 (m, 6H, H_{arom}), 7.09 (d, J = 8.4 Hz, 2H, H_{arom}), 6.83 (dd, J = 7.5, 5.0 Hz, 8H, H_{arom}), 5.94 (s, 1H, N_{ϵ} H), 5.48 (d, J = 8.1 Hz, 1H, N_{α} H), 4.59 (d, J = 11.1 Hz, 1H, CHH-PMB), 4.53 - 4.36 (m, 9H, CHH-PMB, CH₂-PMB (3x), CH₂-Fmoc), 4.36 - 4.27 (m, 1H, H-2), 4.22 (t, J = 6.9 Hz, 1H, CH-Fmoc), 3.94 - 3.86 (m, 1H, H-5), 3.84 - 3.55(m, 21H, OMe (5x), H-7', H-8', H-9', H-10'), 3.51 - 3.45 (m, 1H, H-6'), 3.18 - 3.03 (m, 2H, H-6), 2.29 - 2.09 (m, 2H, H-2'), 1.86 - 1.58 (m, 4H, H-3, H-3'), 1.58 - 1.44 (m, 2H, H-4'), 1.44 - 1.25 (m, 4H, H-4, H-5); 13C NMR (101 MHz, CDCl₃) δ 173.4, 173.1 (C-1, C-1'), 159.4, 159.4, 159.4, 159.3, 143.9, 141.4, 130.5, 130.5, 130.3 (C_q), 129.7, 129.6, 129.6, 127.8, 127.2, 125.2, 120.1, 113.9, 113.9, 113.9 (CH_{arom}), 76.8 (C-7', C-8', C-9'), 75.9 (C-6'), 74.8, 73.6 (C-7',C-8', C-9'), 73.4 (CH₂-PMB), 73.2 (C-5'), 73.2, 71.9, 71.4(CH₂-PMB), 69.4 (C-10'), 67.1 (CH₂-Fmoc), 53.8 (C-2), 52.5 (COOMe), 47.3 (CH-Fmoc), 39.0 (C-6), 35.7 (C-2'), 32.1 (C-3), 29.2 (C-5), 28.3 (C-4), 22.9 (C-3), 22.6 (C-4); <u>HRMS</u> $[C_{64}H_{74}N_2O_{14} + N_a]^+$: 1117.50383 found, 1117.50323

N_{α} -Fmoc- N_{ϵ} -[butan-4-(2,3,4,6-tetra-O-paramethoxybenzyl- α -D-mannopyranoside)-amide]-L-lysine (168).

calculated.

Methyl ester **180** (2.19 g, 2.0 mmol) was dissolved in THF (20 mL, 0.1 M) and *t*-BuOH (2 mL) and cooled to 0°C. A solution of LiOH (240 mg, 10.0 mmol, 5 eq) in H₂O₂ (50% wt. aq., 4 mL, 2 M) was added dropwise (pH >10) and stirred at 0°C for four hours. The mixture was diluted with EtOAc, washed with HCl (1 M, aq., 1x), the organic layer was dried over MgSO₄ (s), filtered, concentrated *in vacuo* and purified using silica gel column chromatography (2/8 \rightarrow 8/2, Acetone/DCM, v/v) to yield title compound **168** as a fluffy white powder after lyophilization from 1,4-dioxane (1.70 g, 1.57 mmol, 79%). TLC R_E: 0.23 (AcOH/EtOAc/PE, 1/80/20, v/v/v); IR (neat, cm⁻¹): 3333, 2933, 1718, 1612, 1586, 1512, 1451, 1301, 1246, 1174, 1080, 1032, 819, 760, 740; H NMR (400 MHz, CDCl₃) δ 7.76 (d, J = 7.5 Hz, 2H, H_{arom}), 7.61 (d, J = 5.9 Hz, 2H, H_{arom}), 7.39 (t, J = 7.4 Hz, 2H, H_{arom}),

7.30 (t, J = 7.1 Hz, 2H, H_{arom}), 7.27 - 7.08 (m, 8H, H_{arom}), 6.89 - 6.78 (m, 8H, H_{arom}), 5.93 (t, J = 5.9 Hz, 1H, N_eH), 5.61 (d, J = 7.1 Hz, 1H, N_aH), 4.58 (d, J = 11.2 Hz, 1H, CHH-PMB), 4.52 - 4.30 (m, 10H, CHH-PMB, CH₂-PMB (3x), CH₂-Fmoc, H-2), 4.22 (t, J = 7.1 Hz, 1H, CH-Fmoc), 3.93 - 3.87 (m, 1H, H-5'), 3.83 - 3.76 (m, 13H, OMe (4x), H-7'/ H-8'/ H-9'), 3.72 - 3.55 (m, 4H, H-10', H-7'/ H-8'/ H-9'), 3.49 (dd, J = 5.4, 2.5 Hz, 1H, H-6'), 3.20 (dt, J = 11.6, 5.3 Hz, 1H, H-6a), 3.09 - 2.96 (m, 1H, H-6b), 2.26 (dt, J = 14.3, 6.5 Hz, 1H, H-2a'), 2.11 (dt, J = 13.8, 6.3 Hz, 1H, H-2b'), 1.90 - 1.58 (m, 4H, H-3, H-3'), 1.53 - 1.27 (m, 6H, H-4', H-4, H-5); $\frac{13}{12}$ C NMR (101 MHz, CDCl₃) δ 174.1, 173.8 (C-1, C-1'), 159.5, 159.5, 159.4, 156.1, 143.9, 141.4, 130.2 (C_q), 129.9, 129.8, 129.8, 129.6, 127.8, 127.2, 125.3, 120.1, 113.9, 113.9, 113.9 (CH_{arom}), 76.2 (C-7',C-8', C-9'), 75.9 (C-6'), 74.7, 73.5 (C-7',C-8', C-9'), 73.3 (CH₂-PMB), 73.2 (C-5'), 73.2, 72.0, 71.5 (CH₂-PMB), 69.1 (C-10'), 67.1 (CH₂-Fmoc), 55.4 (OMe), 53.6 (C-2), 47.3 (CH-Fmoc), 39.0 (C-6), 35.5 (C-2'), 31.8 (C-3), 29.8 (C-5), 28.8 (C-4'), 23.2 (C-3'), 21.9 (C-4); HRMS [C₆₃H₇₂N₂O₁₄ + H]+: 1081.50810 found, 1081.50588 calculated.

General procedure for manual solid phase synthesis:

The solid-phase peptide synthesis was performed starting with Tentagel[®] S-RAM resin (~0.22 mmol/g) on a 45-50 µmol scale using established Fmoc protocols.²⁶ The consecutive steps performed in each cycle were:

1) DMF wash (1x) followed by nitrogen purge; 2) Deprotection of the Fmoc-group with 20% piperidine in DMF (4 mL, 3 x 5 min); 3) DMF wash (3x) followed by nitrogen purge; 4) Coupling of the appropriate amino acid^a in five-fold excess (unless stated otherwise)^{b,c}; 5) DMF wash (3x) followed by nitrogen purge; 6) capping with a Ac₂O/DMF/DIPEA solution (4mL, 20/88/2, v/v/v) for 2 min; 7) DMF wash (2x).

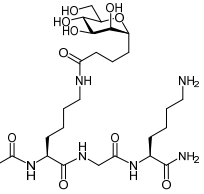
After the complete sequence capping was achieved by utilization of steps 1,2 & 3 followed by 6 and washing with DMF (3x), DCM (3x) and Et₂O (2x) followed by nitrogen purge.

^a The Fmoc amino acids applied in this synthesis were: Fmoc-Lys(Boc)-OH, Fmoc-Gly-OH, 168^c.

 $^{^{\}rm b}$ For couplings on 50 μ mol scale: generally the Fmoc amino acid was dissolved in a HCTU solution in DMF (1.25 mL ,0.20 M, 0.25 mmol, 5 eq) This solution was transferred to the reaction vessel followed by a DIPEA solution in DMF (1.00 mL, 0.50 M, 0.50 mmol, 10 eq) to initiate the coupling. Next, the reaction vessel was shaken for 60 min at room temperature.

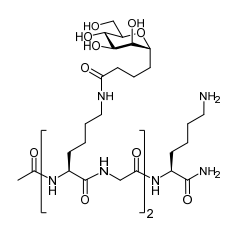
 $[^]c$ For C-mannoside couplings less equivalents with prolonged reaction times were used. Generally **168** (2eq) was dissolved in a solution of HCTU in DMF (0,5 mL ,0.20 M, 100 µmol, 2 eq), followed by a DIPEA solution in DMF (0.40 mL, 0.5 M, 200 µmol, 4 eq) and shaken overnight.

Ac-CMAN-Gly-Lys-NH2 (186).



Ac-CMAN-Glv-Lvs(Boc)-Tentagel® S-RAM (loading: 50 µmol) was transferred to a flask and treated for 120 minutes with a cleavage cocktail (20 mL, TFA/DCM/TIS/H₂O/phenol²¹/octanethiol, 3600/60/100/72/72/100, v/v/v/v/ w/v). The resin was filtered off and washed with neat TFA (3 x 1 mL). The filtrate was concentrated and purified via gel filtration (Toyopearl HW40S, 150 mM NH4HCO3, 1.6 x 60 cm, 1 mL/min, eluted at 51.5 - 60 mL) followed by purification via RP-HPLC (linear gradient 0 - 30% B in A, 10 min, Gemini-NX 5µm C18, 110 Å, 250 x 10.0 mm, 5 mL/min) yielded title compound 186 as a white powder after lyophilization (2.11 mg, 3.49 μ mol, 7.0% over 3 couplings, 41% per step). LC-MS: $R_t = 3.42$ min (0 - 50% ACN; 13 min); 1 H NMR (500 MHz, D₂O) δ 4.27 (dd, J = 9.5, 4.9 Hz, 1H, CH (Cman)), 4.19 (dd, J = 8.6, 5.8 Hz, 1H, CH (K)), 3.96 - 3.86 (m, 3H, CH₂ (G), H-5'), 3.86 - 3.79 (m, 2H, H-6', H-10a'),3.76 (dd, I = 9.4, 3.3 Hz, 1H, H-7'), 3.69 (dd, I = 12.2, 6.2 Hz, 1H, H-10b'), 3.59 (t, I = 9.5 Hz, 1H, H-8'),3.50 - 3.44 (m, 1H, H-9'), 3.15 (t, I = 7.0 Hz, 2H, CH_2 -NHC=O), 2.90 (t, I = 7.7 Hz, 2H, CH_2 -NH₂), 2.26 (hept, J = 7.2 Hz, 2H, H-2'), 2.01 (s, 3H, Ac), 1.91 - 1.27 (m, 16H, H-3', H-4', CH₂ (6x)); $\frac{13}{12}$ C NMR (126) MHz, D_2O) δ 176.7, 176.3, 175.2, 174.5, 171.4 (C=O), 77.9 (C-5'), 73.5 (C-9'), 71.4 (C-6'), 70.8 (C-7'), 67.3 (C-8), 61.2 (C-10), 54.1 (CH (K)), 53.2 (CH (CMan)), 42.5 (CH₂ (G)), 39.3 (CH₂-NH₂), 38.9 (CH₂-NH₂-NH₂), 38.9 (CH₂-NH₂-NH₂), 38.9 (CH₂-NH₂ NHC=O), 35.2 (C-2'), 30.3, 27.8, 26.9, 26.7, 22.3, 22.0, 21.8 (C-3', C-4', CH₂ (6x)), 21.6 (Ac); <u>HRMS</u> $[C_{26}H_{48}N_6O_{10} + H]^+$: 605.35031 found, 605.35047 calculated.

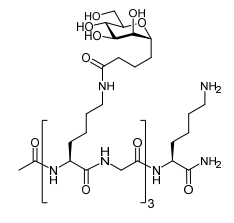
Ac-CMAN-Gly-CMAN-Gly-Lys-NH2 (187).



Ac-CMAN-Gly-CMAN-Gly-Lys(Boc)-Tentagel® S-RAM (loading: 45 µmol) was transferred to a flask and treated for 120 minutes with a cleavage cocktail (10 mL, TFA/TIS/H₂O, 190/5/5, v/v/v). The mixture was concentrated to approximately one mL after which the resin was filtered off into cold Et₂O (45 mL) and the resin was washed off with neat TFA (3 x 1 mL) into the ether solution. This solution was

centrifuged (10 min, 5000 rpm) after which the supernatant was removed and the precipitate was dried under nitrogen flow. Purification via RP-HPLC (linear gradient 0 - 30% B in A, 10 min, Gemini-NX 5µm C18, 110 Å, 250 x 10.0 mm, 5 mL/min) yielded title compound 187 as a white powder after lyophilization $(6.43 \text{ mg}, 6.29 \mu\text{mol}, 14\% \text{ over 5 couplings}, 67\% \text{ per step})$. <u>LC-MS</u>: $R_t = 0.91 \text{ min} (10 - 90\% \text{ ACN}; 13 \text{ min});$ <u>1H NMR</u> (400 MHz, CDCl₃) δ 4.28 (td, J = 8.6, 7.9, 5.3 Hz, 2H, CH (Cman)), 4.21 (dd, J = 8.7, 5.7 Hz, 1H, CH (K)), 3.96 - 3.91 (m, 4H, CH₂ (G)), 3.91 - 3.86 (m, 2H, H-5'), 3.86 - 3.80 (m, 4H, H-6', H-10a'), 3.77 (dd, J = 9.3, 3.3 Hz, 2H, H-7'), 3.70 (dd, J = 12.1, 6.2 Hz, 2H, H-10b'), 3.61 (t, J = 9.5 Hz, 2H, H-8'), 3.48(ddd, J = 9.1, 6.2, 2.2 Hz, 2H, H-9'), 3.16 (t, J = 6.9 Hz, 4H, CH₂-NHC=O), 2.98 (t, J = 7.5 Hz, 2H, CH₂-NH₂), 2.34 - 2.19 (m, 4H, H-2'), 2.02 (s, 3H, Ac), 1.93 - 1.23 (m, 26H, H-3', H-4', CH₂); ¹³C NMR (101 MHz, CDCl₃) 8 176.6, 176.3, 176.3, 175.2, 174.8, 174.5, 171.6, 171.4 (C=O), 77.9 (C-5'), 73.5 (C-9'), 71.4 (C-6'), 70.8 (C-7'), 67.3 (C-8'), 61.3 (C-10'), 54.2 (CH (K)), 53.9, 53.1 (CH (Cman)), 42.5, 42.4 (CH₂ (G)) 39.2 (CH₂-NH₂), 38.9 (*C*H₂-NHC=O), 35.2 (C-2'), 30.3, 27.8, 26.7, 26.1, 22.4, 22.0, 21.98 (C-3', C-4', CH₂), 21.7 (Ac); <u>ESI-MS</u> [C₄₄H₇₉N₉O₁₈ + H]⁺: 1022.400 found, 1022.562 calculated.

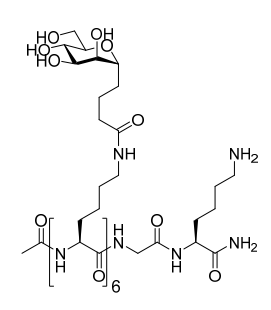
Ac-CMAN-Gly-CMAN-Gly-CMAN-Gly-Lys-NH₂ (188).



Ac-CMAN-Gly-CMAN-Gly-Lys(Boc)-Tentagel® S-RAM (loading: 45 μmol) was transferred to a flask and treated for 120 minutes with a cleavage cocktail (10 mL, TFA/TIS/H₂O, 190/5/5, v/v/v). The resin was filtered off into cold Et₂O (45 mL) and the resin was washed off with neat TFA (3 x 1 mL) into the ether solution. This solution was centrifuged (10 min, 5000 rpm) after which the supernatant was

removed and the precipitate was dried under nitrogen flow. Purification via RP-HPLC (linear gradient 0 - 30% B in A, 10 min, Gemini-NX 5μm C18, 110 Å, 250 x 10.0 mm, 5 mL/min) yielded title compound **188** as a white powder after lyophilization (3.91 mg, 2.71 μmol, 6.0% over 7 couplings, 67% per step). <u>LC-MS</u>: $R_t = 4.54$ min (20 - 50% ACN; 13 min); <u>1H NMR</u> (400 MHz, CDCl₃) δ 4.32 - 4.24 (m, 3H, CH (Cman)), 4.21 (dd, J = 8.6, 5.6 Hz, 1H, CH (K)), 3.96 - 3.86 (m, 9H, CH₂ (G), H-5'), 3.86 - 3.80 (m, 6H, H-6', H-10a'), 3.77 (dd, J = 9.3, 3.3 Hz, 3H, H-7'), 3.70 (dd, J = 12.1, 6.2 Hz, 3H, H-10b'), 3.61 (t, J = 9.5 Hz, 3H, H-8'), 3.48 (ddd, J = 9.3, 6.2, 2.2 Hz, 3H, H-9'), 3.15 (d, J = 6.5 Hz, 6H, CH₂-NHC=O), 2.98 (t, J = 7.4 Hz, 2H, CH_2 -NH₂), 2.34 - 2.18 (m, 6H, H-2'), 2.02 (s, 3H, Ac), 1.92 - 1.22 (m, 36H, H-3', H-4', CH₂); <u>ESI-MS</u> [C₆₂H₁₁₀N₁₂O₂₆ + H]⁺: 1439.533 found, 1439.773 calculated.

Ac-CMAN-CMAN-CMAN-CMAN-CMAN-Gly-Lys-NH2 (189).



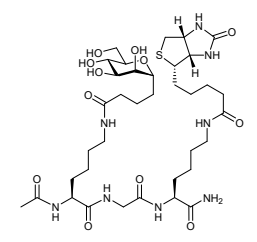
Ac-CMAN-CMAN-CMAN-CMAN-CMAN-Gly-Lys(Boc)-Tentagel[®] S-RAM (loading: 50 μmol) was transferred to a flask and treated for 120 minutes with a cleavage cocktail (20 mL, TFA/DCM/TIS/H₂O/phenol²¹/octanethiol, 3600/60/100/72/72/100, v/v/v/w/v). The resin was filtered off and washed with neat TFA (3 x 1 mL). The filtrate was concentrated and purified via gel filtration (Toyopearl HW40S, 150 mM NH₄HCO₃, 1.6 x 60 cm, 1 mL/min, eluted

at 34 - 49 mL) followed by purification via RP-HPLC (linear gradient 0 - 30% B in A, 10 min, Gemini-NX 5µm C18, 110 Å, 250 x 10.0 mm, 5 mL/min) to yield title compound **189** as a white powder after lyophilization (2.56 mg, 1.06 µmol, 2.1% over 8 couplings, 62% per step). <u>LC-MS</u>: $R_t = 4.22 \text{ min } (0 - 50\% \text{ ACN}; 13 \text{ min}); 1H NMR (500 MHz, D2O) δ 4.30 - 4.18 (m, 6H, CH (Cman)), 4.18 - 4.14 (m, 1H, CH (K)), 3.93 (s, 2H, CH₂ (G)), 3.88 (dd, J = 10.0, 3.4 Hz, 6H, H-5'), 3.86 - 3.79 (m, 12H, H-6', H-10a'), 3.76 (dd, J = 9.4, 3.3 Hz, 6H, H-7'), 3.69 (dd, J = 12.1, 6.2 Hz, 6H, H-10b'), 3.60 (t, J = 9.5 Hz, 6H, H-8'), 3.47 (ddd, J = 9.0, 6.2, 2.1 Hz, 6H, H-9'), 3.17 - 3.09 (m, 12H, CH₂-NHC=O), 2.97 (t, J = 7.2 Hz, 2H, CH₂-NH₂), 2.24 (hept, J = 7.6 Hz, 12H, H-2'), 2.01 (s, 3H, Ac), 1.89 - 1.25 (m, 66H, H-3', H-4', CH₂); HRMS <math>[C_{106}H_{188}N_{16}O_{45} + 3H]^{3+}$: 803.10536 found, 803.10546 calculated.

General procedure for biotinylation:

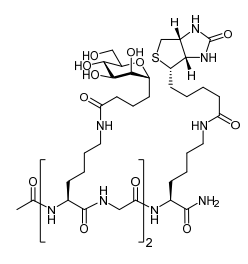
The general procedure to introduce the biotin handle: Glycoclusters described above with a free amine were dissolved in DMSO (0.02 M). To this, a stock solution of Biotin-NHS (0.15 M, 3-4 eq) and DIPEA (0.015M, 0.3-0.4 eq) in DMSO was added and shaken overnight after which compounds were purified via RP-HPLC (linear-gradient 10 - 16% B in A, 12 min, 5 mL/min, Develosil RPAQUEOUS 10.0 x 250 mm) followed by lyophilization.

Ac-CMAN-Gly-Lys(biotin)-NH₂ (190).



Compound **186** (1.54 mg, 1.23 μ mol) was coupled with biotin-NHS using the general procedure. Compound **190** was obtained after purification by RP-HPLC as a white powder (1.98 mg, 2.38 μ mol, 94%). <u>LC-MS:</u> R_t = 5.23 min (0 - 50% ACN; 13 min); <u>HRMS</u> [C₃₆H₆₂N₈O₁₂S +H]⁺: 831.42807 found, 831.42807 calculated.

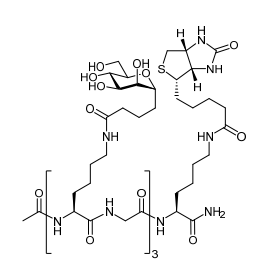
Ac-CMAN-Gly-CMAN-Gly-Lys(biotin)-NH2 (191).



Compound **187** (6.43 mg, 6.30 µmol) was coupled with biotin-NHS using the general procedure. Compound **191** was obtained after purification by RP-HPLC as a white powder (5.64 mg, 4.51 µmol, 72%). <u>LC-MS:</u> $R_t = 5.21 \text{ min } (0 - 50\% \text{ ACN; } 13 \text{ min)};$ $\frac{1}{1} \frac{1}{1} \frac$

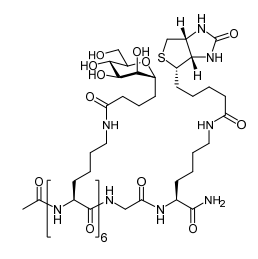
3.91 (m, 2H), 3.90 - 3.84 (m, 4H), 3.81 (dd, J = 9.4, 3.4 Hz, 2H), 3.74 (dd, J = 12.1, 6.2 Hz, 2H), 3.65 (t, J = 9.5 Hz, 2H), 3.52 (ddd, J = 9.2, 6.2, 2.3 Hz, 2H), 3.35 (dt, J = 9.7, 5.3 Hz, 1H), 3.20 (dt, J = 6.9, 3.6 Hz, 6H), 3.01 (dd, J = 13.1, 5.0 Hz, 1H), 2.79 (d, J = 13.0 Hz, 1H), 2.36 - 2.23 (m, 6H), 2.06 (s, 3H), 1.92 - 1.30 (m, 32H); HRMS [$C_{54}H_{93}N_{11}O_{20}S$ +2H] $^{2+}$: 624.82361 found, 624.82323 calculated.

Ac-CMAN-Gly-CMAN-Gly-CMAN-Gly-Lys(biotin)-NH₂ (192).



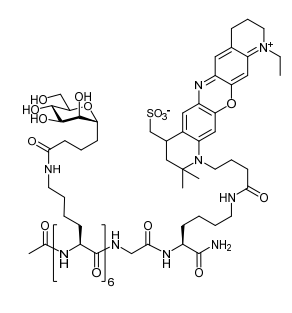
Compound **188** (3.91 mg, 2.72 μ mol) was coupled with biotin-NHS using the general procedure. Compound **192** was obtained after purification by RP-HPLC as a white powder (9.29 mg, 5.58 μ mol, 99%). <u>LC-MS:</u> R_t = 5.16 min (0 - 50% ACN; 13 min); <u>HRMS</u> [C₇₂H₁₂₄N₁₄O₂₈S +2H]²⁺: 833.42889 found, 833.42879 calculated.

Ac-CMAN-CMAN-CMAN-CMAN-CMAN-Gly-Lys(biotin)-NH₂ (193).



Compound **189** (2.09 mg, 0.87 μ mol) was coupled with biotin-NHS using the general procedure. Compound **193** was obtained after purification by RP-HPLC as a white powder (1.84 mg, 0.70 μ mol, 80%). <u>LC-MS</u>: $R_t = 5.06$ min (0 - 50% ACN; 13 min); <u>HRMS</u> [$C_{116}H_{202}N_{18}O_{47}S + 3H$]³⁺: 1317.19385 found, 1317.19348 calculated.

Ac-CMAN-CMAN-CMAN-CMAN-CMAN-Gly-Lys(ATTO655)-NH₂ (194).



Compound **189** (155 nmol) was dissolved in DMSO (2.0 mM). To this a solution of ATTO655-NHS (5.0 mM, 2 eq) and DIPEA (0.01 M, 2 eq) in DMSO was added, shaken protected from light for one hour. After which compound **194** was obtained after purification by gel filtration (eluted at 46 - 58 mL) as a blue powder after lyophilization (0.247 mg, 85 nmol, 55%). <u>LC-MS:</u> $R_t = 6.08 \text{ min } (0 - 50\% \text{ ACN; } 13 \text{ min}); <u>HRMS</u> [<math>C_{133}H_{219}N_{19}O_{50}S + 3H]^{3+}$: 972.83825 found, 972.83828

calculated.

General procedure for automated solid-phase synthesis of gp100 peptides:

The solid-phase peptide synthesis was performed on a TRIBUTE® Peptide Synthesizer (Gyros Protein Technologies AB, Arizona, USA) applying Fmoc based protocol starting with Tentagel® S-RAM resin (~0.22 mmol/g) on a 100-250 µmol scale using established synthetic protocols.²⁶ The consecutive steps for synthesis on 250 µmol scaleª performed in each cycle were:

1) DMF wash (1x) followed by nitrogen purge; 2) Deprotection of the Fmoc-group with 20% piperidine in DMF (8 mL)(3 x 3 min at 50 °C); 3) DMF wash (3x) followed by nitrogen purge; 4.1)

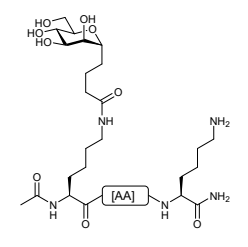
136

^a All amounts were scaled-down in equimolar proportions for smaller scale.

Coupling of the appropriate amino acid^a in four-fold excess (unless stated otherwise);^{b,c,d} 4.2) Step 4.1 was repeated 5) DMF wash (3x) followed by nitrogen purge; 6) capping with a solution of Ac₂O/DMF/DIPEA (8mL, 10/88/2, v/v/v) for 2 min; 7) DMF wash (2x).

After the complete sequence, the resin was washed with DMF (3x), DCM (3x), Et₂O (3x), followed by nitrogen purge before treatment with the cleavage cocktail.

Ac-CMAN-Val-Thr-His-Thr-Tyr-Leu-Glu-Pro-Gly-Pro-Val-Thr-Ala-Asn-Arg-Gln-Leu-Tyr-Pro-Glu-Trp-Thr-Glu-Ala-Gln-Arg-Leu-Asp- α Abu-Trp-Arg-Gly-Lys-NH₂ (203).



Resin 134 (theoretical loading: 25 μ mol) was elongated with 168 (54 mg, 50 μ mol, 2 eq) by shaking overnight at room temperature with HCTU (20.7 mg, 50 μ mol, 2 eq) and DIPEA (17.4 μ L, 100 μ mol, 4 eq) in DMF (450 μ L, 0.11 M of 168). After washing (steps 7,1) and Fmoc removal (steps 2, 3) the N-terminus was capped with Ac₂O/DMF/DIPEA (4mL, 10/88/2, v/v/v, 3 x 5 min) and the resin was washed

with DMF (3x), DCM (3x), Et₂O (3x) and dried by nitrogen purge to yield Ac-CMAN-Val-Thr(t/Bu)-His(Trt)-Thr(t/Bu)-Tyr(t/Bu)-Leu-Glu(Ot/Bu)-Pro-Gly-Pro-Val-Thr(t/Bu)-Ala-Asn(Trt)-Arg(Pbf)-Gln(Trt)-Leu-Tyr(t/Bu)-Pro-Glu(Ot/Bu)-Trp(Boc)-Thr(t/Bu)-Glu(Ot/Bu)-Ala-Gln(Trt)-Arg(Pbf)-Leu-Asp(Ot/Bu)-αAbu-Trp(Boc)-Arg(Pbf)-Gly-Lys(Mmt)-Tentagel® S-RAM (199). The resin was transferred to a flask and treated for 120 minutes with a cleavage cocktail (20 mL, TFA/DCM/TIS/H₂O/phenol²¹/octanethiol, 3600/60/100/72/72/100, v/v/v/w/v). The resin was filtered off and washed with neat TFA (3 x 1 mL). The filtrate was concentrated and transferred dropwise into a cold mixture of Et₂O/pentane (45 mL, 5/4, v/v) This solution was centrifuged (10 minutes, 5000 rpm) after which the supernatant was removed and the precipitate was dried under nitrogen flow, re-dissolved in magic (5 mL, t-BuOH/ACN/H₂O, 1/1/1, v/v/v) and lyophilized. Purification via RP-HPLC (linear-gradient 20 - 30% B in A, 10 min, Gemini-NX 5μm C18, 110 Å, 250 x 10.0 mm, 5 mL/min) yielded title compound 203 as a white powder after

^a The amino acids applied in this synthesis were: Fmoc-Lys(Mmt)-OH, Fmoc-Gly-OH, Fmoc-Arg(Pbf)-OH, Fmoc-Trp(Boc)-OH, Fmoc-Leu-OH^d, Fmoc-Gln(Trt)-OH, Fmoc-Ala-OH, Fmoc-Glu(O/Bu)-OH, Fmoc-Thr(/Bu)-OH, Fmoc-Pro-OH, Fmoc-Tyr(/Bu)-OH, Fmoc-Asn(Trt)-OH, Fmoc-Val-OH, Fmoc-His(Trt)-OH, Fmoc-AEEA-OH (Fmoc-8-amino-3,6-dioxaoctanoic acid), 116 and 168.°

^b Generally, the Fmoc amino acid is dissolved in a HCTU solution in DMF (5.00 mL ,0.20 M, 1.0 mmol, 4 eq) The resulting solution was transferred to the reaction vessel followed by a DIPEA solution in DMF (4.00 mL, 0.50 M, 2.0 mmol, 8 eq) to initiate the coupling. The reaction vessel was shaken for 30 min at 50 °C (unless stated otherwise).

 $^{^{\}rm c}$ Aspartic acid and the adjacent Leucine and Arginine were introduced at with one hour reaction time at room temperature. Fmoc removal was achieved with piperide/DMF in 3 x 5 min at room temperature. 28

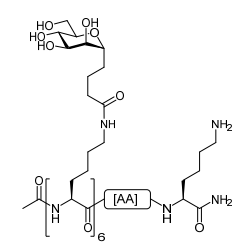
 $[^]d$ For C-mannoside couplings less equivalents with prolonged reaction times were used. Generally for elongation on 100 µmol scale, **168** (2eq) was dissolved in a solution of HCTU in DMF (1,0 mL ,0.20 M, 200 µmol, 2 eq), followed by a DIPEA solution in DMF (0.80 mL, 0.5 M, 400 µmol, 4 eq) and shaken overnight.

lyophilization (2.69 mg, 626 nmol, 2.51% over 34 couplings, 90% per step). <u>LC-MS</u>: $R_t = 4.16$ min (10 - 90% ACN; 13 min); <u>HRMS</u> [$C_{194}H_{297}N_{53}O_{58} + 4H$]⁴⁺: 1075.80691 found, 1075.80670 calculated.

Ac-CMAN-CMAN-CMAN-CMAN-CMAN-Val-Thr-His-Thr-Tyr-Leu-Glu-Pro-Gly-Pro-Val-Thr-Ala-Asn-Arg-Gln-Leu-Tyr-Pro-Glu-Trp-Thr-Glu-Ala-Gln-Arg-Leu-Asp- $_{\alpha}$ Abu-Trp-Arg-Gly-Lys-Tentagel S-RAM (200).

Resin 134 (theoretical loading: 100 μmol) was elongated with 168 (216 mg, 200 μmol, 2 eq) by shaking overnight at room temperature with HCTU (82.6 mg, 200 μmol, 2 eq) and DIPEA (69.5 μL, 400 μmol, 4 eq) in DMF (1.8 mL, 0.11 M of 168). followed by Fmoc removal and washing steps as described in general protocol (steps 7,1,2 and 3), these steps were repeated (6x total). After these cycles, the resin was washed (steps 7,1), the Fmoc removed (steps 2, 3), the N-terminus was capped with Ac₂O/DMF/DIPEA (8mL, 10/88/2, v/v/v, 3 x 5 min) and the resin was washed with DMF (3x), DCM (3x), Et₂O (3x) and dried by nitrogen purge to yield Ac-CMAN-CMAN-CMAN-CMAN-CMAN-CMAN-Val-Thr(*t*Bu)-His(Trt)-Thr(*t*Bu)-Tyr(*t*Bu)-Leu-Glu(O*t*Bu)-Pro-Gly-Pro-Val-Thr(*t*Bu)-Ala-Asn(Trt)-Arg(Pbf)-Gln(Trt)-Leu-Tyr(*t*Bu)-Pro-Glu(O*t*Bu)-Trp(Boc)-Thr(*t*Bu)-Glu(O*t*Bu)-Ala-Gln(Trt)-Arg(Pbf)-Leu-Asp(O*t*Bu)-αAbu-Trp(Boc)-Arg(Pbf)-Gly-Lys(Mmt)-Tentagel® S-RAM (200).

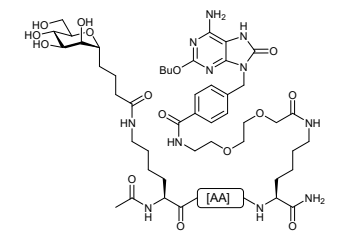
Ac-CMAN-CMAN-CMAN-CMAN-CMAN-Val-Thr-His-Thr-Tyr-Leu-Glu-Pro-Gly-Pro-Val-Thr-Ala-Asn-Arg-Gln-Leu-Tyr-Pro-Glu-Trp-Thr-Glu-Ala-Gln-Arg-Leu-Asp- $_{\alpha}$ Abu-Trp-Arg-Gly-Lys-NH $_{2}$ (204).



Resin **200** (theoretical loading: 25 μ mol) was transferred to a flask and treated for 120 minutes with a cleavage cocktail (40 mL, TFA/DCM/TIS/H₂O/phenol²¹/ octanethiol, 3600/60/100/72/72/100, v/v/v/v/v/v). The resin was filtered off and washed with neat TFA (3 x 1 mL). The filtrate was concentrated and transferred dropwise into a cold mixture of Et₂O/pentane (45 mL, 5/4, v/v) This solution was

centrifuged (10 minutes, 5000 rpm) after which the supernatant was removed and the precipitate was dried under nitrogen flow, re-dissolved in magic (5 mL, *t*-BuOH/ACN/H₂O, 1/1/1, v/v/v) and lyophilized. Purification via RP-HPLC (linear-gradient 20 - 30% B in A, 10 min, Gemini-NX 5µm C18, 110 Å, 250 x 10.0 mm, 5 mL/min) yielded title compound **204** as a white powder after lyophilization. (1.115 mg, 182 nmol, 0.73% over 39 couplings, 88% per step). <u>LC-MS</u>: $R_t = 3.91$ min (10 - 90% ACN; 13 min); <u>HRMS</u> $[C_{274}H_{437}N_{63}O_{93} + 5H]^{5+}$: 1221.23680 found, 1221.23707 calculated.

Ac-CMAN-Val-Thr-His-Thr-Tyr-Leu-Glu-Pro-Gly-Pro-Val-Thr-Ala-Asn-Arg-Gln-Leu-Tyr-Pro-Glu-Trp-Thr-Glu-Ala-Gln-Arg-Leu-Asp- α Abu-Trp-Arg-Gly-Lys(Peg-TLR7L)-NH₂ (207).



Resin 134 (theoretical loading: 25 μ mol) was elongated with 168 (54 mg, 50 μ mol, 2 eq) by shaking overnight at room temperature with HCTU (20.7 mg, 50 μ mol, 2 eq) and DIPEA (17.4 μ L, 100 μ mol, 4 eq) in DMF (450 μ L, 0.11 M of 168). After washing (steps 7,1) and Fmoc removal (steps 2, 3) the N-terminus was capped with Ac₂O/DMF/DIPEA (4mL, 10/88/2, v/v/v, 3 x

5 min) and the resin was washed with DMF (3x), DCM (3x), Et₂O (3x) and dried by nitrogen purge to yield 199. This resin was loaded in a syringe with frit and treated with a mixture of AcOH in TFE and DCM (1/2/7, v/v/v) shaken for 15 minutes followed by filtration²². This was repeated until the filtrate lost the vellow color (~ 8x). After which the resin was washed with DCM (5x), DMF (5x) Piperidine (20% in DMF, 2x) and DMF (5x). The lysine was elongated with Fmoc-AEEA-OH (127) using the general protocol followed by introduction of 116 (45.7 mg, 100 µmol, 4 eq) by shaking for one hour with HCTU (41.3 mg, 100 μmol, 4 eq) and DIPEA (35 μL, 200 μmol, 8 eq) in DMF (0.9 mL, 0.11 M of **116**) yielding Ac-CMAN-Val-Thr(tBu)-His(Trt)-Thr(tBu)-Tyr(tBu)-Leu-Glu(OtBu)-Pro-Gly-Pro-Val-Thr(tBu)-Ala-Asn(Trt)-Arg(Pbf)-Gln(Trt)-Leu-Tyr(tBu)-Pro-Glu(OtBu)-Trp(Boc)-Thr(tBu)-Glu(OtBu)-Ala-Gln(Trt)-Arg(Pbf)-Leu-Asp(OtBu)-αAbu-Trp(Boc)-Arg(Pbf)-Gly-Lys(PEG-TLR7L)-Tentagel® S-RAM (201). The resin was washed with DMF (3x), DCM (3x) and Et₂O (3x) and dried by nitrogen purge, transferred to a flask and treated for 120 minutes with a cleavage cocktail (20 mL, TFA/DCM/TIS/H₂O/phenol²¹/octanethiol, 3600/60/100/72/72/100, v/v/v/v/w/v). The resin was filtered off and washed with neat TFA (3 x 1 mL). The filtrate was concentrated and transferred dropwise into a cold mixture of Et₂O/pentane (45 mL, 5/4, v/v) This solution was centrifuged (10 min, 5000 rpm) after which the supernatant was removed and the precipitate was dried under nitrogen flow, re-dissolved in magic (5 mL, t-BuOH/ACN/H₂O, 1/1/1, v/v/v) and lyophilized. Purification via RP-HPLC (linear-gradient 21 - 36% B in A, 15 min, Gemini-NX 5µm C18, 110 Å, 250 x 10.0 mm, 5 mL/min) yielded title compound 207 as a white powder after lyophilization (2.51 mg, 525 nmol, 2.10% over 36 couplings, 90% per step) LC-MS: $R_t = 4.53 \text{ min} (10 - 90\% \text{ ACN}; 13 \text{ min});$ \underline{HRMS} [C₂₁₇H₃₂₅N₅₉O₆₄ + 5H]⁵⁺: 957.68821 found, 957.68822 calculated.

Ac-CMAN-CMAN-CMAN-CMAN-CMAN-Val -Thr-His-Thr-Tyr-Leu-Glu-Pro-Gly-Pro-Val-Thr-Ala-Asn-Arg-Gln-Leu-Tyr-Pro-Glu-Trp-Thr-Glu-Ala-Gln-Arg-Leu-Asp- $_{\alpha}$ Abu-Trp-Arg-Gly-Lys(Peg-TLR7L)-NH $_{2}$ (208).

Mmt removal with 1% TFA:

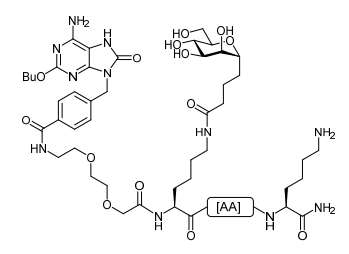
Resin 200 (theoretical loading: 12.5 µmol) was loaded in a syringe with frit and treated with TFA (1% in DCM) shaken for five minutes followed by filtration. This was repeated until the filtrate lost the orange/yellow color (~ 12x). After which the resin was washed with DCM (5x), DMF (5x) Piperidine (20%) in DMF, 2x) and DMF (5x). The lysine was elongated with Fmoc-AEEA-OH (127) using the general protocol followed by introduction of 116 (22.9 mg, 50 µmol, 4 eq) by shaking for one hour with HCTU (20.7 mg, 500 μmol, 4 eq) and DIPEA (17 μL, 100 μmol, 8 eq) in DMF (0.45 mL, 0.11 M of **116**) yielding Ac-CMAN-CMAN-CMAN-CMAN-CMAN-CMAN-Val-Thr(tBu)-His(Trt)-Thr(tBu)-Tyr(tBu)-Leu-Glu(OtBu)-Pro-Gly-Pro-Val-Thr(tBu)-Ala-Asn(Trt)-Arg(Pbf)-Gln(Trt)-Leu-Tyr(tBu)-Pro-Glu(OtBu)-Lys(PEG-TLR7L)-Tentagel® S-RAM (202). The resin was washed with DMF (3x), DCM (3x) and Et₂O (3x) and dried by nitrogen purge, transferred to a flask and treated for 120 minutes with a cleavage cocktail (10 mL, $TFA/DCM/TIS/H_2O/phenol^{21}/octanethiol$, 3600/60/100/72/72/100, v/v/v/v/w/v). The resin was filtered off and washed with neat TFA (3 x 1 mL). The filtrate was concentrated and transferred dropwise into a cold mixture of Et₂O/pentane (45 mL, 5/4, v/v) This solution was centrifuged (10 min, 5000 rpm) after which the supernatant was removed and the precipitate was dried under nitrogen flow, redissolved in magic (5 mL, t-BuOH/ACN/H₂O, 1/1/1, v/v/v) and lyophilized. LC-MS analysis showed multiple AEEA-TLR conjugations. Treatment of the crude mixture with ammonia (1mL, 35%wt NH₃ aq.) resulted in the disappearance of peaks corresponding with multiple conjugations. After lyophilization the mixture was purified by RP-HPLC (linear-gradient 22.5 - 30% B in A, 15 min, Gemini-NX 5µm C18, 110 Å, 250 x 10.0 mm, 5 mL/min) to yield title compound 208 as a white powder after lyophilization (0.247 mg, 37.4 nmol, 0.30% over 41 couplings, 86.8% per step).

Mmt removal with AcOH in TFE/DCM:

Resin 200 (theoretical loading: 62.5 μmol) was loaded in a syringe with frit and treated with a mixture of AcOH in TFE and DCM (1/2/7, v/v/v) shaken for 15 minutes followed by filtration²². This was repeated until the filtrate lost the yellow color (~ 8x). After which the resin was washed with DCM (5x), DMF (5x) Piperidine (20% in DMF, 2x) and DMF (5x). The lysine was elongated with Fmoc-AEEA-OH (127) using the general protocol followed by introduction of 116 (115 mg, 250 μmol, 4 eq) by shaking for one hour with HCTU (103 mg, 250 μmol, 4 eq) and DIPEA (87 μL, 500 μmol, 8 eq) in DMF (2.25 mL, 0.11 M of 116) yielding resin 202. The resin was washed with DMF (3x), DCM (3x) and Et₂O (3x) and dried by nitrogen purge, transferred to a flask and treated for 120 minutes with a cleavage cocktail (40 mL, TFA/DCM/TIS/H₂O/phenol²¹/octanethiol, 3600/60/100/72/72/100, v/v/v/w/v). The resin was filtered off and washed with neat TFA (3 x 1 mL). The filtrate was concentrated and transferred dropwise into a cold mixture of Et₂O/pentane (45 mL, 5/4, v/v) This solution was centrifuged (10 min, 5000 rpm) after which the supernatant was removed and the precipitate was dried under nitrogen flow, re-dissolved in magic (5 mL, t-BuOH/ACN/H₂O, 1/1/1, v/v/v) and lyophilized. LC-MS analysis of this crude mixture

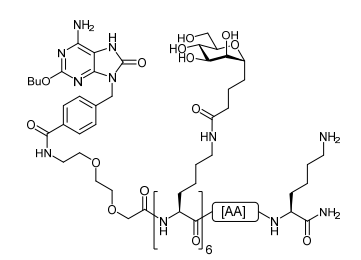
showed no ions for multiple AEEA-TLR conjugations. Purification via RP-HPLC (linear-gradient 22.5 - 30% B in A, 15 min, Gemini-NX 5µm C18, 110 Å, 250 x 10.0 mm, 5 mL/min) yielded title compound **208** as a white powder after lyophilization (2.48 mg, 376 nmol, 0.60% over 41 couplings, 88.3 % per step). <u>LC-MS</u>: $R_t = 7.11 \text{ min}$ (0 - 50% ACN; 13 min); <u>HRMS</u> [$C_{297}H_{465}N_{69}O_{99} + 4H$]⁴⁺: 1647.34697 found, 1647.34628 calculated.

TLR7L-PEG-CMAN-Val-Thr-His-Thr-Tyr-Leu-Glu-Pro-Gly-Pro-Val-Thr-Ala-Asn-Arg-Gln-Leu-Tyr-Pro-Glu-Trp-Thr-Glu-Ala-Gln-Arg-Leu-Asp- α Abu-Trp-Arg-Gly-Lys-NH $_2$ (205).



Resin 134 (theoretical loading: 25 μ mol) was elongated with 168 (54 mg, 50 μ mol, 2 eq) by shaking overnight at room temperature with HCTU (20.7 mg, 50 μ mol, 2 eq) and DIPEA (17.4 μ L, 100 μ mol, 4 eq) in DMF (450 μ L, 0.11 M of 168). Fmoc-AEEA-OH (127)(4eq) was introduced using the general protocol followed by introduction of 116 (46 mg, 100 μ mol, 4 eq) by shaking

TLR7L-PEG-CMAN-CMAN-CMAN-CMAN-CMAN-Val-Thr-His-Thr-Tyr-Leu-Glu-Pro-Gly-Pro-Val-Thr-Ala-Asn-Arg-Gln-Leu-Tyr-Pro-Glu-Trp-Thr-Glu-Ala-Gln-Arg-Leu-Asp- α Abu-Trp-Arg-Gly-Lys-NH₂ (206).



Resin Val-Thr(tBu)-His(Trt)-Thr(tBu)-Tyr(tBu)-Leu-Glu(OtBu)-Pro-Gly-Pro-Val-Thr(tBu)-Ala-Asn(Trt)-Arg(Pbf)-Gln(Trt)-Leu-Tyr(tBu)-Pro-Glu(OtBu)-Trp(Boc)-Thr(tBu)-Glu(OtBu)-Ala-Gln(Trt)-Arg(Pbf)-Leu-Asp(OtBu)-αAbu-Trp(Boc)-Arg(Pbf)-Gly-Lys(Boc)-Tentagel® S-RAM (theoretical loading: 50 μmol) was elongated with **168** (216 mg, 200 μmol, 2

eq) by shaking overnight at room temperature with HCTU (82.6 mg, 200 μmol, 2 eq) and DIPEA (69.5 μL,

400 µmol, 4 eq) in DMF (1.8 mL, 0.11 M of 168). followed by Fmoc removal and washing steps as described in general protocol (steps 7,1,2 and 3), these steps were repeated (6x total). Fmoc-AEEA-OH (127, 4 eq) was introduced using the general protocol followed by introduction of 116 (92 mg, 200 µmol, 4eq) by shaking for two hour with HCTU (82 mg, 200 µmol, 4eq) and DIPEA (70 µL, 400 µmol, 8 eq) in DMF (1.80 mL, 0.11 M of **116**) after which the resin was washed with DMF (3x), DCM (3x), Et₂O (3x) and dried by nitrogen purge to yield resin TLR7L-PEG-CMAN-CMAN-CMAN-CMAN-CMAN-CMAN-Val-Thr(tBu)-His(Trt)-Thr(tBu)-Tyr(tBu)-Leu-Glu(OtBu)-Pro-Gly-Pro-Val-Thr(tBu)-Ala-Asn(Trt)-Arg(Pbf)-Gln(Trt)-Leu-Tyr(tBu)-Pro-Glu(OtBu)-Trp(Boc)-Thr(tBu)-Glu(OtBu)-Ala-Gln(Trt)-Arg(Pbf)-Leu-Asp(O/Bu)-αAbu-Trp(Boc)-Arg(Pbf)-Gly-Lys(Boc)-Tentagel® S-RAM. This resin was transferred to a flask and treated for 120 minutes with a cleavage cocktail (20 mL, TFA/DCM/TIS/H₂O/phenol²¹/octanethiol, 3600/60/100/72/72/100, v/v/v/w/v). The resin was filtered off and washed with neat TFA (3 x 1 mL). The filtrate was concentrated and transferred dropwise into a cold mixture of Et₂O/pentane (45 mL, 5/4, v/v) This solution was centrifuged (10 min, 5000 rpm) after which the supernatant was removed and the precipitate was dried under nitrogen flow, re-dissolved in magic (5 mL, t-BuOH/ACN/H₂O, 1/1/1, v/v/v) and lyophilized. Purification via RP-HPLC (linear-gradient 16 - 28% B in A, 10 min, Gemini-NX 5µm C18, 110 Å, 250 x 12.0 mm, 5 mL/min) yielded title compound 206 as a white powder after lyophilization. (4.125 mg, 650 nmol, 1.30% over 41 couplings, 90% per step). <u>LC-MS</u>: $R_t = 7.73 \text{ min } (15 - 40\% \text{ ACN}; 15 \text{ min});$ $R_t = 5.82 \text{ min } (10 - 50\% \text{ ACN}; 13 \text{ min}); \frac{HRMS}{LRMS} [C_{295}H_{463}N_{69}O_{98} + 6H]^{6+}: 1091.56505 \text{ found, } 1091.56485]$ calculated.

References

- (1) Hogervorst, T. P.; Li, R.-J. E.; Marino, L.; Bruijns, S. C. M.; Meeuwenoord, N. J.; Filippov, D. V.; Overkleeft, H. S.; van der Marel, G. A.; van Vliet, S. J.; van Kooyk, Y.; Codée, J. D. C. C-Mannosyl Lysine for Solid Phase Assembly of Mannosylated Peptide Conjugate Cancer Vaccines. *ACS Chem. Biol. [Accepted]* **2020**.
- (2) York, I. A.; Goldberg, A. L.; Mo, X. Y.; Rock, K. L. Proteolysis and Class I Major Histocompatibility Complex Antigen Presentation. *Immunol. Rev.* **1999**, *172*, 49–66. https://doi.org/10.1111/j.1600-065X.1999.tb01355.x.
- Joffre, O. P.; Segura, E.; Savina, A.; Amigorena, S. Cross-Presentation by Dendritic Cells. *Nat. Rev. Immunol.* **2012**, *12*, 557–569. https://doi.org/10.1038/nri3254.
- (4) Khan, S.; Bijker, M. S.; Weterings, J. J.; Tanke, H. J.; Adema, G. J.; Van Hall, T.; Drijfhout, J. W.; Melief, C. J. M.; Overkleeft, H. S.; Van Der Marel, G. A.; Filippov, D. V.; van der Burg, S. H.; Ossendorp, F. Distinct Uptake Mechanisms but Similar Intracellular Processing of Two Different Toll-like Receptor Ligand-Peptide Conjugates in Dendritic Cells. J. Biol. Chem. 2007, 282, 21145–21159. https://doi.org/10.1074/jbc.M701705200.
- (5) Devaraj, N. K. The Future of Bioorthogonal Chemistry. *ACS Cent. Sci.* **2018**, *4*, 952–959. https://doi.org/10.1021/acscentsci.8b00251.
- (6) Pawlak, J. B.; Gential, G. P. P.; Ruckwardt, T. J.; Bremmers, J. S.; Meeuwenoord, N. J.; Ossendorp, F. A.; Overkleeft, H. S.; Filippov, D. V; van Kasteren, S. I. Bioorthogonal Deprotection on the Dendritic Cell Surface for Chemical Control of Antigen Cross-Presentation. *Angew. Chemie Int. Ed.* 2015, 54, 5628–5631. https://doi.org/10.1002/anie.201500301.
- (7) Girard, C.; Miramon, M.; de Solminihac, T.; Herscovici, J. Synthesis of 3-C-(6-O-Acetyl-2,3,4-Tri-O-Benzyl-α-d-Mannopyranosyl)-1-Propene: A Caveat. *Carbohydr*. Res. **2002**, *337*, 1769–1774. https://doi.org/10.1016/S0008-6215(02)00206-9.
- (8) Horton, D.; Miyake, T. Stereoselective Syntheses of C-(d-Glucopyranosyl)Alkenes. *Carbohydr. Res.* **1988**, *184*, 221–229. https://doi.org/10.1016/0008-6215(88)80020-X.
- (9) Nicolaou, K. C.; Hwang, C. K.; Duggan, M. E. Synthesis of the Brevetoxin B IJK Ring System. *J. Am. Chem. Soc.* **1989**, *111*, 6682–6690. https://doi.org/10.1021/ja00199a031.
- (10) Mousavifar, L.; Vergoten, G.; Roy, R. Deciphering the Conformation of C-Linked α-D-Mannopyranosides and Their Application toward the Synthesis of Low Nanomolar E. Coli FimH Ligands. *Arkivoc* **2018**, *2018*, 384–397. https://doi.org/10.24820/ark.5550190.p010.783.
- (11) Hosomi, A.; Sakata, Y.; Sakurai, H. Highly Stereoselective C-Allylation of Glycopyranosides with Allylsilanes Catalyzed by Silyl Triflate or Iodosilane. *Tetrahedron Lett.* **1984**, *25*, 2383–2386. https://doi.org/10.1016/S0040-4039(01)80261-6.
- Jarikote, D. V.; O'Reilly, C.; Murphy, P. V. Ultrasound-Assisted Synthesis of C-Glycosides. *Tetrahedron Lett.* **2010**, *51*, 6776–6778. https://doi.org/10.1016/j.tetlet.2010.10.113.
- (13) Touaibia, M.; Krammer, E.-M.; Shiao, T.; Yamakawa, N.; Wang, Q.; Glinschert, A.; Papadopoulos, A.; Mousavifar, L.; Maes, E.; Oscarson, S.; Vergoten, G.; Lensink, M.; Roy, R.; Bouckaert, J. Sites for Dynamic Protein-Carbohydrate Interactions of O- and C-Linked Mannosides on the E. Coli FimH Adhesin. *Molecules* 2017, 22, 1101. https://doi.org/10.3390/molecules22071101.
- (14) Sharma, P. K.; Kumar, S.; Kumar, P.; Nielsen, P. Selective Reduction of Mono- and Disubstituted Olefins by NaBH4 and Catalytic RuCl3. *Tetrahedron Lett.* **2007**, *48*, 8704–8708. https://doi.org/10.1016/j.tetlet.2007.10.017.
- (15) Newlander, K. A.; Callahan, J. F.; Moore, M. L.; Tomaszek, T. A.; Huffman, W. F. A Novel Constrained Reduced-Amide Inhibitor of HIV-1 Protease Derived from the Sequential Incorporation of .Gamma.-Turn Mimetics into a Model Substrate. *J. Med. Chem.* 1993, *36*, 2321–2331. https://doi.org/10.1021/jm00068a008.

- (16) Boger, D. L.; Yohannes, D.; Zhou, J.; Patane, M. A. Total Synthesis of Cycloisodityrosine, RA-VII, Deoxybouvardin, and N29-Desmethyl-RA-VII: Identification of the Pharmacophore and Reversal of the Subunit Functional Roles. *J. Am. Chem. Soc.* **1993**, *115*, 3420–3430. https://doi.org/10.1021/ja00062a004.
- (17) Evans, D. A.; Britton, T. C.; Ellman, J. A. Contrasteric Carboximide Hydrolysis with Lithium Hydroperoxide. Tetrahedron Lett. 1987, 28, 6141–6144. https://doi.org/10.1016/S0040-4039(00)61830-0.
- (18) Li, R.-J. E.; Hogervorst, T. P.; Achilli, S.; Bruijns, S. C.; Arnoldus, T.; Vivès, C.; Wong, C. C.; Thépaut, M.; Meeuwenoord, N. J.; van den Elst, H.; Overkleeft, H. S.; van der Marel, G. A.; Filippov, D. V.; van Vliet, S. J.; Fieschi, F.; Codée, J. D. C. C.; van Kooyk, Y. Systematic Dual Targeting of Dendritic Cell C-Type Lectin Receptor DC-SIGN and TLR7 Using a Trifunctional Mannosylated Antigen. *Front. Chem.* **2019**, 7. https://doi.org/10.3389/fchem.2019.00650.
- (19) Chan, M.; Hayashi, T.; Kuy, C. S.; Gray, C. S.; Wu, C. C. N.; Corr, M.; Wrasidlo, W.; Cottam, H. B.; Carson, D. A. Synthesis and Immunological Characterization of Toll-Like Receptor 7 Agonistic Conjugates. *Bioconjug. Chem.* **2009**, *20*, 1194–1200. https://doi.org/10.1021/bc900054q.
- (20) Volbeda, A. G.; Kistemaker, H. A. V.; Overkleeft, H. S.; van der Marel, G. A.; Filippov, D. V.; Codée, J. D. C. Chemoselective Cleavage of p -Methoxybenzyl and 2-Naphthylmethyl Ethers Using a Catalytic Amount of HCl in Hexafluoro-2-Propanol. *J. Org. Chem.* **2015**, *80*, 8796–8806. https://doi.org/10.1021/acs.joc.5b01030.
- (21) Howard, K. T.; Chisholm, J. D. Preparation and Applications of 4-Methoxybenzyl Esters in Organic Synthesis. Org. Prep. Proced. Int. 2016, 48, 1–36. https://doi.org/10.1080/00304948.2016.1127096.
- (22) Matysiak, S.; Böldicke, T.; Tegge, W.; Frank, R. Evaluation of Monomethoxytrityl and Dimethoxytrityl as Orthogonal Amino Protecting Groups in Fmoc Solid Phase Peptide Synthesis. *Tetrahedron Lett.* **1998**, *39*, 1733–1734. https://doi.org/10.1016/S0040-4039(98)00055-0.
- de Smedt, T.; van Mechelen, M.; De Becker, G.; Urbain, J.; Leo, O.; Moser, M. Effect of Interleukin-10 on Dendritic Cell Maturation and Function. *Eur. J. Immunol.* **1997**, *27*, 1229–1235. https://doi.org/10.1002/eji.1830270526.
- (24) Brossart, P.; Zobywalski, A.; Grünebach, F.; Behnke, L.; Stuhler, G.; Reichardt, V. L.; Kanz, L.; Brugger, W. Tumor Necrosis Factor Alpha and CD40 Ligand Antagonize the Inhibitory Effects of Interleukin 10 on T-Cell Stimulatory Capacity of Dendritic Cells. *Cancer Res.* **2000**, *60*, 4485–4492.
- (25) Wilson, D. S.; Hirosue, S.; Raczy, M. M.; Bonilla-Ramirez, L.; Jeanbart, L.; Wang, R.; Kwissa, M.; Franetich, J.-F.; Broggi, M. A. S.; Diaceri, G.; Quaglia-Thermes, X.; Mazier, D.; Swartz, M. A.; Hubbell, J. A. Antigens Reversibly Conjugated to a Polymeric Glyco-Adjuvant Induce Protective Humoral and Cellular Immunity. *Nat. Mater.* **2019**, *18*, 175–185. https://doi.org/10.1038/s41563-018-0256-5.
- (26) Chan, W. C.; White, P. D. Fmoc Solid Phase Peptide Synthesis: A Practical Approach; Oxford University Press, 2000
- Jencks, W. P.; Gilchrist, M. Nonlinear Structure-Reactivity Correlations. The Reactivity of Nucleophilic Reagents toward Esters. J. Am. Chem. Soc. 1968, 90, 2622–2637. https://doi.org/10.1021/ja01012a030.
- (28) Behrendt, R.; Offer, J. Advances in Fmoc Solid-Phase Peptide Synthesis. *J. Pept.* **2016**, No. October 2015, 4–27. https://doi.org/10.1002/psc.2836.

Synthesis of glycosylated BTA-coremonomers for the formation of dynamic self-assembling supramolecular fibers

Introduction

Carbohydrate recognition often requires multiple carbohydrates in close proximity to each other, so that the combined weak interaction of each separate carbohydrate and the effective local high concentration results in strong enough binding to induce an effect of the recognizing receptor. This multivalency-effect allows receptors to distinguish between single carbohydrates or larger glycosylated pathogens such as viruses and bacteria. Multivalent presentation of mannosides, for example, can result in inflammatory responses induced by the binding of C-type lectin receptors (CLRs), as described in previous chapters. Alternatively, multivalent macromolecules can also mimic natural systems with structural functions. An example would be mimicking the extracellular matrix (ECM), which serves functions such as signaling, water immobilization, cell attachment and aids in structural properties such as increasing stiffness of the framework around cells. The ECM

Part of this work is published in Hendrikse and Su et al.¹

consist of a network of proteins and carbohydrates such as heparin and hyaluronic acid (HA). A multitude of multivalent biomaterials have been described such as dendrimers, nanoparticles, and polymers, that are designed to mimic the ECM^{3–5} or viral particles.^{6–9} However, the synthesis of these materials usually requires many reaction steps, and variations in the composition of these materials often involve new synthetic approaches. Especially when variations in the ratio between components of such polymers are desired, the generation of these static polymers can be labor-intensive. Dynamic systems such as self-assembling polymers are considered to be an attractive alternative. Such systems would allow to more easily adapt the ratio of components by simply varying the ratio of the used monomers.

Self-assembling supramolecular polymer systems have been studied extensively as biomaterial mimics. 10,11 One of these systems is based on an N,N',N"-trialkylbenzene-1,3,5-tricarboxamide (BTA) scaffold, that bears three amphipathic arms (210, Figure 1), having a hydrophobic inner C12 spacer extended by an outer hydrophilic tetra-ethylene glycol (teEG) arm. These BTA based monomers can self-assemble into micrometer long fibers in aqueous solutions due to hydrogen bond formation between the amides and hydrophobic effects of the amphipathic arms. 12,13 In addition, polymerization of functionalized monomers allows for the introduction of additional functionality on the surface of the fibers (e.g., fluorophores).¹⁴ Combining different monomers would in principle allow for an infinite number of different polymers and materials. Such a feature could be useful for screening different combinations of adjuvants and antigens in the search for the most optimal vaccine formulation. However, a major drawback of this approach is that most of these monomer building blocks rely on poly(ethylene glycol) (PEG) moieties for their water solubility. This large number of PEG moieties on the surface of the fibers could induce immune responses against PEG, which would limit their in vivo application, 15-17 especially in combination with immuno-stimulating adjuvants. Previous work by Leenders et al.¹⁸ successfully incorporated glycosides on BTA based scaffolds using click chemistry of propargyl glycosides with azido functionalized teEG BTA monomers (211) to obtain glycosylated BTAs (212, Figure 1). This chapter describes different synthetic routes toward new BTA based monomeric building blocks (213-218), in which glycosides are used instead of tetra-ethylene glycol to form more "natural" BTA based fibers. By the incorporation of different glycosides, their effect on the behavior of the fibers can be assessed. The results of the self-assembly ability of the mannose, glucose, and cellobiose BTA monomers (213, 214, and 215) in comparison with the previously reported tetraethylene-glycol functionalized BTA monomer (210) are also presented. Finally, this chapter describes the synthesis of a glucoside based BTA in which one glucose residue is provided with an azide handle for the introduction of future functionalities (218).

Figure 1: BTA based monomers.

Results and discussion

The synthesis of the target glycosylated BTA cores comprises glycosylations and amide bond formations, the sequence of which can be reversed leading to two strategies (Scheme 1). Route A starts with glycosylation of a masked amino-dodecan-1-ol spacer, that after deprotection would result in an amine-functionalized glycoside which could be coupled with acyl chloride **219** or other BTA activated esters. The second route, route B, entails coupling of an amino-dodecan-1-ol spacer and BTA acyl chloride, subsequent glycosylation of the produced triol **220**, and finally, global deprotection. Route A would allow for the intermediate purification of the individual glycosides, which should be more straightforward compared with the purification of three coupled glycosides. The benefit of route B would be that incomplete amide formation for **220** would not waste more (synthetically) costly glycosides as could happen in route A. Both routes were evaluated to reveal the most suitable option (Scheme 1).

Scheme 1: Retrosynthesis of BTA-core-monomers.

$$\begin{array}{c} \begin{array}{c} \begin{array}{c} \\ \\ \\ \\ \end{array} \end{array} \begin{array}{c} \\ \\ \\ \end{array} \begin{array}{c} \\ \\ \\ \end{array} \begin{array}{c} \\ \\ \end{array} \begin{array}{c} \\ \\ \\ \end{array} \begin{array}{c} \\ \\ \\ \end{array} \begin{array}{c} \\ \\ \end{array} \begin{array}{c} \\ \\ \\ \end{array} \begin{array}{c} \\ \\ \\ \end{array} \begin{array}{c} \\ \\ \end{array} \begin{array}{c} \\ \\ \end{array} \begin{array}{c} \\ \\ \\ \end{array} \begin{array}{c} \\ \\ \\ \end{array} \begin{array}{c} \\ \\ \end{array} \begin{array}{c} \\ \\ \end{array} \begin{array}{c} \\ \\ \\ \end{array} \begin{array}{c} \\ \\ \end{array} \begin{array}{c} \\ \\ \end{array} \begin{array}{c} \\ \\ \end{array} \begin{array}{c} \\ \\$$

Monosaccharides D-mannose and D-glucose and disaccharides cellobiose, lactose, and maltose were selected to functionalize the BTA cores. All donors should be equipped with a participating protecting group on their 2-O position to achieve 1,2-trans-selective glycosylations. The benzoyl (Bz) protecting group is preferred over the acetyl (Ac) to minimize unwanted ortho-ester formation and potential acyl migration. The trichloroacetimidate method was chosen as the glycosylation procedure, and all trichloroacetimidoyl donors were synthesized from the starting carbohydrates by successive per-benzoylation, anomeric debenzoylation with hydrazine acetate and finally trichloroacetimidate introduction. This approach resulted in mannose donor 221, glucose donor 222, cellobiose donor 223, lactose donor 224, and maltose donor 225. Thiophenyl maltoside 226 was also synthesized, as an alternative for the imidate donor 225. Finally, the 6-azido glucoside donor 228 was synthesized using standard protecting and functional group manipulations, as previously reported, ¹⁹ for further functionalization of the BTA core.

Scheme 2: Synthesis of the glycosyl donors.

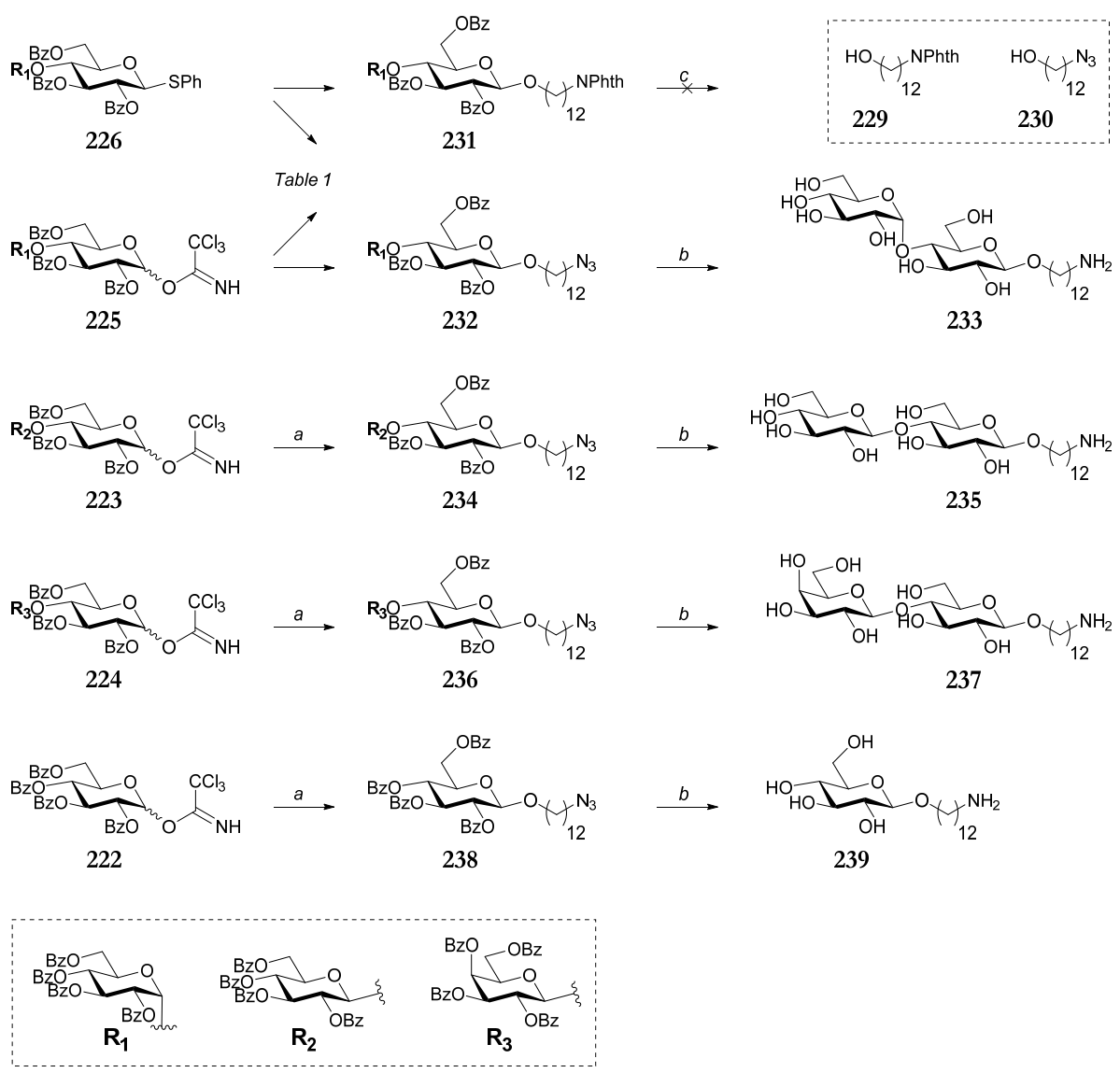
Reagents and conditions: a) i. BzCl, pyridine; ii. $H_2NNH_2 \cdot OAc$, DMF; iii. K_2CO_3 , CCl₃CN, DCM, (references: **221** 20 ; **222** 21 ; **223** 22 ; **224** 23 ; **225** 22); b) reference¹⁹; c) i. NIS, TFA, DCM; ii. K_2CO_3 , CCl₃CN, DCM, 70%; d) i. BzCl, pyridine; ii. PhSH, BF₃·OEt₂, DCM, 28%.

With these seven donors at hand, both glyco-BTA assembly routes were explored. The acceptors, 12-N-phthalimide-dodeca-1-ol (229), and the azido analog 12-azido-dodeca-1-ol (230) were synthesized according to published procedures. As part of route A, the glycosylation efficiency was tested using both thio and imidate maltose donors 226 and 225 and both linkers 229 and 230 (Table 1 and Scheme 3). Glycosylation of thio donor 226 and the phthalimide (Phth) linker 229 was met with poor conversion (Table 1, entry 1). Increasing the temperature, reaction time, equivalents of the acceptor, and concentration of the donor 226 improved the yield (entry 2). Coupling of imidate donor 225 with 229 at 0 °C resulted in the formation of the spacer equipped maltose in 51% yield (entry 3). Additional experiments demonstrated poor solubility of the phthalimide linker (229) at lower temperatures, but decreasing the concentration of the donor and using fewer equivalents of acceptor improved the yield to 99% (entry 4). Applying these conditions for the condensation of 225 with the azido acceptor 230 gave the same yield (entry 5).

Table 1: Glycosylations with dodecanol spacers.

Entry	Donor	Acceptor	Ratio	[Donor]	Activation (eq.)	Τ	time	yield
1	226	229	1/1.2	0.1 M	NIS (1.3), TfOH (0.3)	0°C	3h	25%
2	226	229	1/2	0.2 M	NIS (1.3), TfOH (0.3)	4°C	48h	55%
3	225	229	1/2	0.1 M	TMSOTf (0.2)	0° C a	4h	51%
4	225	229	1/1.2	$0.05~\mathrm{M}$	TMSOTf (0.2)	4°C	14h	99%
5	225	230	1/1.2	$0.05~\mathrm{M}$	TMSOTf (0.2)	4°C	14h	99%

Scheme 3: Glycosylations with dodecanol spacers.



Reagents and conditions: a) 230, TMSOTf, DCM (232: 99%; 234: 85%; 236: 61%; 238: 67%); b) i. NaOMe, MeOH/DCM; ii. PtO, H₂, dioxane, t-BuOH, H₂O (233: 48%; 235: 93%; 237: 88%; 239: 46%); c) ethylene-1,2-diamine, EtOH, inseparable mixture of products.

^a With lower temperatures than -10°C the reaction mixture crashes out and form a white solid.

Unfortunately, the simultaneous deprotection of all benzoyls and the phthalimide from 231 was not successful. A complex mixture resulted after refluxing the substrate in ethanol for ten days in the presence of ethyl diamine, and the product could not be isolated (Scheme 3). On the other hand, removal of the benzoyl groups of azido maltoside 232 was successful. Subsequent reduction of the azide was hindered since 232 formed micelles that shielded the azide from the aqueous phase. This micelle formation was due to the amphiphilic properties of the starting material, originating from the highly hydrophilic maltose residue and the hydrophobic C12-azide spacer. Therefore the hydrogenation of the azide was performed in a solvent mixture of \(\tau\)-BuOH/H2O with ultrasound irradiation and this protocol delivered the target amine 233 in 48% yield (Scheme 3). Following this approach, azide linker 230 was also condensed with cellobiose imidate donor 223, lactose imidate 224, and glucose imidate 222 to result in cellobioside 234, lactoside 236, and glucoside 238 in 85%, 61%, and 67% respectively. Benzoyl removal, followed by hydrogenation with the optimized conditions, proceeded uneventfully, resulting in cellobioside 235, lactoside 237, and glucoside 239 in 93%, 88%, and 46%, respectively (Scheme 3).

In the next phase of route A, the coupling of the amine-functionalized glycosides with benzene triacylchloride 219 was undertaken. (Scheme 4A). Unfortunately, the poor solubility of the reaction partners resulted in incomplete couplings, and purification of the target trifunctional BTAs could not be achieved at this stage. Therefore, route A was abandoned, and attention was directed to route B by condensing benzene triol 220 with glucose donor 222 or cellobiose donor 223 (Scheme 4B). Condensation of acceptor 220 and donors 222 or 223 resulted in a poor coupling efficiency because of poor solubility of the BTA-triol. The use of a large volume of dichloromethane did not improve the solubility of 220, which proved to be insoluble in other solvents that are commonly used in glycosylations. It appeared that 220 was too polar, necessitating the use of a highly polar solvent. Eventually it was found that a homogenous reaction mixture could be obtained using a solvent mixture of DCM and 1,1,1,3,3,3-hexafluoroisopropanol (HFIP), a combination previously described to dissolve poorly soluble peptides.²⁶ HFIP is a weak nucleophile which could potentially compete with triol 220 for activated donor, but a test glycosylation in which donor 222 was activated in HFIP/DCM (1/4, v/v) did not result in a significant amount the HFIP condensation product. De et al.27 have previously described the use of HFIP as a solvent for the synthesis of 2,3-unsaturated glucosides from an acetyl glucal, and in this synthesis, the condensation of HFIP was observed. The difference in reactivity between both systems can be explained by the more reactive glucal used by De et al. and the reluctance of dioxolenium ions to react with poor nucleophiles.

Scheme 4: Attempts toward glycosylated BTA monomers.

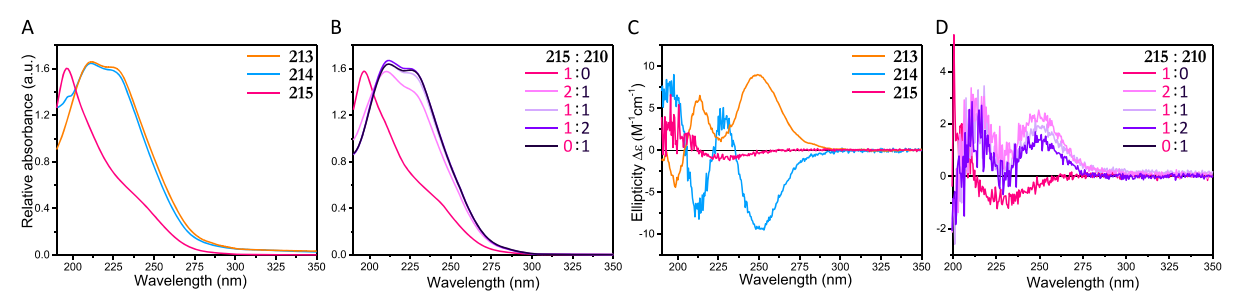
Donors 222, 221, 223, 224, and 225 were coupled with triol 220 in DCM/HFIP resulting in the protected mannoside 240, glucoside 241, cellobioside 242, lactoside 243, and maltoside 244 in 78%, 92%, 50%, 98%, and 70% yield, respectively (Scheme 5). Unfortunately, in the glycosylations of glucose 241 and cellobiose 242, (partial) benzoyl migration to one of the hydroxyls of the BTA acceptor was observed. The polarity of these side products was quite similar to the polarity of the target compounds, and the products could therefore not be purified at this stage. Therefore, the benzoyl groups in glucoside 241 were removed with sodium methanolate, and LC-MS analysis of the obtained crude mixture showed a difference in retention between product 214 and the side product having two glucosides. Purification via RP-HPLC gave pure 214 in 41% yield. The unwanted transesterification of the benzovls was averted using fewer equivalents of TfOH in the glycosylation reaction, but as a consequence, ortho-esters were formed. Eventually, the use of 0.5 equivalents of TfOH per triol 220 gave the most favorable ratio of product versus side-products for all donors. Coupling of the more reactive mannose donor 221 with 220 was completed in the shortest reaction time of all used donors. After removal of the benzoyl in 240, LC-MS analysis indicated that the mannosylation was not accompanied by benzoyl migration, and mannoside 213 was isolated in 48% yield. All other BTA-glycosides were subjected to similar benzoyl removal conditions as described for glucose-BTA 214 and purification via RP-HPLC delivered cellobioside **215**, lactoside **216**, and maltoside **217** in 19%, 13%, and 27% yield, respectively.

Scheme 5: Glycosylation with BTA core.

Reagents and conditions: a) 220, TfOH, DCM, HFIP (240: 92%; 241: 78%; 242: 50%; 243: 98%; 244: 70%); b) NaOMe, MeOH, t-BuOH, dioxane (213: 48%; 214: 41%; 215: 19%; 216: 13%; 217: 27%).

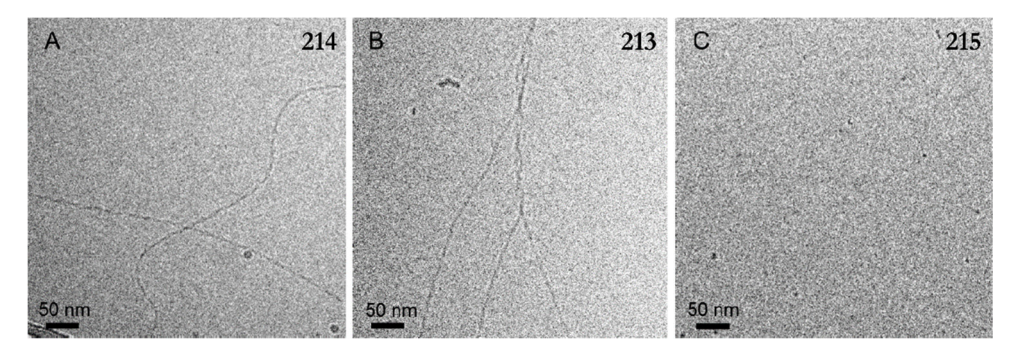
The self-assembly of the glucose, mannose, and cellobiose BTA monomers (213, 214, and 215) were assessed and compared with the previously reported tetra-ethylene-glycol functionalized BTA monomer (210, see Figure 1). In short, aqueous solutions of the constructs were investigated using UV spectroscopy, circular dichroism (CD) spectroscopy, static light scattering (SLS), cryogenic transmission electron microscopy (cryo-TEM) and hydrogen/deuterium exchange mass spectrometry (HDX-MS). These results are summarized in Figure 2 and Figure 3 and show that both the mannose (213) and glucose (214) can assemble in supramolecular fibers (two absorption maxima at 211 and 225 nm, characteristic of fibrous structures, Figure 2A). Cellobiose 215 was only able to form fibers when co-assembled with the ethylene glycol 210), since assembly of solely 215 generated small micellar aggregates (one maximum at 196 nm, Figure 2A, 2B). Unlike the fibers formed from the teEG BTA 210, the fibers formed with 213 and 214 assembled with a preference in helicity. CD spectroscopy indicated a biphasic Cotton effect for glucose 214 and a mirror image biphasic Cotton effect for mannose 213 (Figure 2C). Surprisingly, co-assembly of 210 with cellobiose 215 (glucose-\beta1,4-glucose) displayed a mirror image biphasic Cotton effect opposite of 214 (β-glucose, Figure 2D). Micrometers long fibers for 214 and 213 with a diameter between 5 and 10 nm were observed using cryogenic transmission electron microscopy (cryo-TEM, see Figure 3). Cellobiose 215 assembled into small micelles of approximately 5 nm.

Figure 2: UV and CD spectra of assembled BTA monomers.



A) UV spectra of 213, 214 and 215. 213 and 214 show the typical BTA maxima at 211 and 225 nm, whereas 215 show maxima at 196 nm; **B)** UV spectra of 215 co assembled with 210 in different ratios; **C)** CD spectra of 214, 213 and 215. 213 and 214 show a biphasic positive and negative mirror Cotton effect, whereas 215 is CD silent; **D)** CD spectra of 215 co-assembled with 210 in different ratios.

Figure 3: Cryo-TEM of fibers.



Cryo-TEM of **A)** 214; **B)** 213 and; **C)** 215; Micrometers long fibrous structures were observed for 213 and 214 while micellar structures for 215. Scale bars indicate 50 nm. Used concentrations of BTA = 250 or 500 μ M.

The result of the self-assembly study was an incentive to investigate the synthesis of an azido functionalized glucose-BTA monomer. The target structure contains two glucoses and a single 6azido-6-deoxy glucose moiety (218, Scheme 6). First attempts towards the target molecule were directed at the functionalization of the BTA-triol with a single 6-azido glucoside or a double glycosylation with glucose donor 222 with triol 220 (Route A and B, Scheme 6). However, both condensations resulted in a complex mixture of various products, differing in glycosylation degree. The mixture of the glycosylation with azido donor 228 contained acceptor 220, the expected product 245, and the double coupled side product. For the glycosylation with glucose donor 222 not only the product 246 was obtained, but also single and triple coupled side products. In addition, ortho-esters were formed, or benzoyl migration to acceptor 220 occurred. Besides, the purification was hindered by the poor solubility of 220 in common eluents and the similar polarity of the product, ortho-ester, and benzoylated BTA side products. The ortho-ester formation and the benzoyl migration could be partially suppressed by adjusting the amount of activator, but these side reactions could never be completely prevented. Together these side reactions hindered the isolation of the relevant intermediates in sufficient yields. However, a test glycosylation using starting material 245 that was partly purified delivered 247, in a mixture of compounds. Debenzovlation of this mixture of compounds provided a mixture that was analyzed by LC-MS to show a distinct peak for the desired product. Therefore, a one-pot procedure was performed, comprising of an initial glycosylation of acceptor 220 with one equivalent of azido glucose donor 228, after which two equivalents of donor 222 were added (Route C, Scheme 6). Purification by size exclusion gave a mixture of compounds, of which the BTA arms were functionalized with either benzoyl, glucose or 6-azido-6-deoxy glucose. NMR analysis of this mixture indicated the presence of 0.3 eq. of migrated benzoyl groups, 1.6 eq. of the glucose appendage, and 1.1 eq of azido glucose per BTA core. After benzoyl removal with NaOMe, LC-MS analysis showed not

only the presence of triple glycosylated BTA compounds such as product 218, tri-glucose 214, double azido glucose and another glucose (248) but also BTA compounds originating from benzoyl migration, bearing two glycosides (249 and 250). The five BTA products, 218/214/248/249/250, were formed in an approximate 3/2/2/1/1 ratio as indicated by LC-MS analysis. RP-HPLC purification resulted in the isolation of both target 218 and 214 in 9% and 13% yield, respectively. With the recovery of the side products, this methodology can produce the target molecule and other relevant functionalized BTA monomers in a short amount of time. Further assessment of the effect of the azide on the self-assembly is under evaluation.

Scheme 6: Synthesis of azido functionalized BTA monomer 218.

A RO
$$\frac{1}{12}$$
 O RO $\frac{1}{12}$ O RO $\frac{1}{12$

Reagents and conditions: a) 220, TfOH, DCM, HFIP; b) 222, TfOH, DCM; c) 220, TfOH, DCM, HFIP; d) 228, TfOH, DCM; e) 220, TfOH, DCM, HFIP, then 222 (qnt."); f) NaOMe, MeOH (218: 9%; 214: 13%).

^a As a mixture of products

Conclusion

The synthesis of benzene-1,3,5-tricarboxyamide (BTA) monomers functionalized with various glycosides has been reported. Two different synthetic approaches have been assessed, both of which were hampered by solubility issues. The first approach in which glycosides containing amino-dodecyl spacer were condensed with activated BTA cores proved to be unsuccessful. The second approach in which imidate donors were coupled with a BTA-triol, provided with an aminododecyl spacer was successful when an unusual solvent mixture, composed of 1,1,1,3,3,3hexafluoroisopropanol and DCM, was used to dissolve the acceptor. Most glycosylations also suffered from the competition of side reactions such as ortho-ester formation and benzoyl migration. The formation of the side products could not be completely avoided, but the pure target BTA monomers were isolated after removal of the benzoyl protecting groups and RP-HPLC purification. Using this methodology, BTA monomers bearing glucose, mannose, cellobiose, lactose, and maltose were synthesized. The first three have been tested for their ability to selfassemble. The cellobiose BTA showed micelle aggregates and could only assemble in fibers when co-assembled with other monomers. Both the mannose and glucose constructs were able to selfassemble in 2D fibers. Notably, the sugar residues induced the formation of fibers of opposite helicity. Furthermore, the synthesis of a BTA monomer, bearing two glucose and one 6-azido-6deoxy-glucose residue, is described. Different approaches were evaluated, and eventually, a onepot glycosylation procedure led to the isolation of the target BTA monomer. Further co-assembly studies of the obtained BTA monomers could shed light on the dynamics of glycosylated fibers and could be the start to obtain bio-compatible self-assembling fibers.

Experimental

General procedures:

All reactions, purifications, and analyses were performed as described in the general procedures of Chapter 2.

General procedure for generation of perbenzylated trichloro imidate donors:

Per-benzoylated donors were dissolved in DMF (0.2 M) and hydrazine acetate (2 eq) was added at 0°C in portions after which the reaction mixture was stirred at 0°C until the starting material was consumed (2-6 h). After this, the reaction mixture was diluted in Et₂O and washed with HCl (1 M, aq., 3x), NaHCO₃ (sat. aq., 2x) and brine after which the organic layer was dried over MgSO₄ (s), filtered, concentrated and when necessary purified by silica gel column chromatography (Et₂O/PE). The hemi-acetals were re-dissolved in DCM (0.2 M) and K₂CO₃ (4 eq) and trichloro acetonitrile (3 eq) were added at 0°C and the mixture was stirred at rt until starting material was consumed (4-16 h). After filtration over Celite, imidate donors were purified by silica gel column chromatography (Et₂O/PE) and stored under N₂ at -20°C.

2,3,4,6-Tetra-O-benzoyl-1-O-(N-trichloroacetimidoyl)- α/β -D-mannopyranoside (221).

BZO COLO Spectral data as described in previous literature. 20

2,3,4,6-Tetra-O-benzoyl-1-O-(N-trichloroacetimidoyl)- α/β -p-glucopyranoside (222).

Spectral data as described in previous literature.²¹

4-O-(2,3,4,6-tetra-O-benzoyl-β-D-glucopyranosyl)-2,3,6-tri-O-benzoyl-1-O-(Ntrichloroacetimidoyl)- α/β -D-glucopyranoside (223).



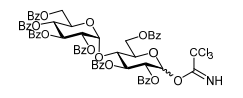
Spectral data as described in previous literature.²²

4-O-(2,3,4,6-tetra-O-benzoyl-β-p-galactopyranosyl)-2,3,6-tri-O-benzoyl-1-O-(Ntrichloroacetimidoyl)- α/β -D-glucopyranoside (224).



Spectral data as described in previous literature.²³

4-O-(2,3,4,6-tetra-O-benzoyl-α-p-glucopyranosyl)-2,3,6-tri-O-benzoyl-1-O-(Ntrichloroacetimidoyl)- α/β -D-glucopyranoside (225).



Spectral data as described in previous literature.²²

Phenyl 4-O-(2,3,4,6-tetra-O-benzoyl- α -D-glucopyranosyl)-2,3,6-tri-O-benzoyl-1-thio- β -D-glucopyranoside (226).

Per-benzoylated lactose (5.27 g, 4.49 mmol) was co-evaporated with toluene (2x) and dissolved in anhydrous DCM (5 mL, 0.9 M) under N2. The solution was cooled to 0°C and thiophenol (0.46 mL, 4.45 mmol, 0.99 eq) and BF₃·OEt₂ (1.11 mL, 9 mmol, 2eq) were added dropwise. After overnight stirring, the reaction mixture was quenched with Et₃N, diluted in DCM, washed with NaOH (1 M, aq. 3x) after which the organic layer was dried over MgSO₄ (s) filtered and concentrated in *vacuo*. Purification using silica gel column chromatography $(1/8, \rightarrow 1/1, Et_2O/PE, v/v)$ yielded compound 226 as a white foam (1.44 g, 1.24 mmol, 28%). TLC R_f: 0.35 (3/2, Et₂O/PE, v/v); IR (neat, cm⁻¹): 1734, 1717, 1506, 1264, 1090, 1067, 1026, 705; $\underline{^{1}H}$ NMR (400 MHz, CDCl₃) δ 8.14 (dd, J = 8.3, 1.2 Hz, 2H, H_{arom}), 8.08 - 8.03 (m, 2H, H_{arom}), 7.96 - 7.87 (m, 4H, H_{arom}), 7.78 (ddd, J = 8.4, 3.5, 1.2 Hz, 4H, H_{arom}), 7.69 - 7.63 (m, 3H, H_{arom}), 7.58 - 7.13 (m, 25H, H_{arom}), 6.13 (t, J = 10.1 Hz, 1H, H-3'), 5.86 (t, J = 9.2 Hz, 1H, H-3), 5.78 (d, J = 3.9 Hz, 1H, H-2), 5.71 (t, J = 9.8 Hz, 1H, H-4'), 5.37 - 5.28 (m, 2H, H-2, H-2'), 5.12 -5.03 (m, 2H, H-6a', H-1), 4.79 (dd, J = 12.1, 4.7 Hz, 1H, H-6b'), 4.55 - 4.45 (m, 3H, H-4, H-5', H-6a), 4.38- 4.31 (m, 1H, H-6b), 4.20 (ddd, J = 9.5, 4.6, 2.2 Hz, 1H, H-5); $\frac{13}{13}$ C NMR (101 MHz, CDCl₃) δ 166.2, 165.9, 165.7, 165.5, 165.2, 165.1, 165.1 (C=O), 133.6, 133.5, 133.5, 133.3, 133.2, 133.2, 133.2, 132.1 (CH_{arom}), 131.4 (C_q), 130.0, 130.0, 129.9, 129.9, 129.8, 129.7 (CH_{arom}), 129.6, 129.5, 129.5, 129.2, 129.1, 128.9 (C_q), 128.9, 128.8, 128.7, 128.6, 128.5, 128.5, 128.4, 128.4, 128.3, 128.2 (CH_{arom}), 96.5 (C-1'), 85.7 (C-1), 76.9 (C-5), 76.3 (C-3), 73.0 (C-4/C-5'), 70.9 (C-2, C-2'), 69.9 (C-3'), 69.3, 69.2 (C-4', C-4/C-5'), 63.6 (C-6'), 62.6 (C-6); HRMS $[C_{67}H_{54}O_{17}S + NH_4]^+$: 1180.34275 found, 1180.34200 calculated.

Phenyl 6-azido-2,3,4,-tri-O-benzoyl-6-deoxy-1-thio-β-p-mannopyranoside (227).

 $_{\text{BB20}}$ Synthesis and spectral data as described in previous literature. 19

6-Azido-2,3,4,-tri-O-benzoyl-6-deoxy- α/β -D-mannopyranoside (251).

Thioglycoside **227** (3.34 g, 5.50 mmol) was dissolved in DCM (55 mL, 0.1 M) and cooled to 0°C, *N*-Iodosuccinimide (1.37 g, 6.05 mmol, 1.1 eq) and TFA (0.50 mL, 6.05 mmol, 1.1 eq) were added and the mixture was stirred for 1.5 h. The reaction mixture was quenched with Na₂S₂O₃ (sat. aq.) and NaHCO₃ (sat. aq.) and stirred for an extra hour after which the mixture was extracted with EtOAc. The organic layer was washed with brine (2x), dried over MgSO₄ (s) filtered and concentrated *in vacuo*. Purification using silica gel column chromatography (3/7, \rightarrow 1/1, Et₂O/PE, v/v) yielded compound **251** as a colorless oil (2.31 g, 4.46 mmol, 81%, α/β ratio = 4/1). TLC R_f: 0.29 (1/4, EtOAc/PE, v/v); IR (neat, cm⁻¹): 3019, 2106, 1728, 1602, 1452, 1263, 1214; HNMR (400 MHz, CDCl₃) δ 8.01 - 7.81 (m, 6H, H_{arom}), 7.56 - 7.23 (m, 9H, H_{arom}), 6.23 (t, *J* = 9.9 Hz, 1H, H-3), 5.79 (d, *J* = 3.6 Hz, 1H, H-1), 5.55 (t, *J* = 9.8, 1.6 Hz, 1H, H-4), 5.31 (dd, *J* = 10.2, 3.6 Hz, 1H, H-2), 4.54 - 4.47 (m, 1H, H-5), 3.53 - 3.40 (m, 2H, H-6); ¹³C NMR (101 MHz, CDCl₃) δ 166.0, 165.0, 165.6 (C=O), 133.7, 133.6, 133.3, 130.1, 130.0, 130.0, 130.0, 129.8,

129.8 (CH_{arom}), 129.1, 129.0, 128.7, 128.6 (C_q), 128.6, 128.6, 128.5, 128.4 (CH_{arom}), 90.4 (C-1), 72.3 (C-2), 70.1, 70.0 (C-3, C-4), 69.0 (C-5), 51.3 (C-6); <u>HRMS</u> [$C_{27}H_{23}N_3O_8 + Na$]⁺: 540.1387 found, 540.13774 calculated.

6-Azido-2,3,4,-tri-O-benzoyl-6-deoxy-1-O-(N-trichloroacetimidoyl)- α/β -D-mannopyranoside (228).

Hemiacetal **251** (1.55 g, 3.00 mmol) was dissolved in DCM (15 mL, 0.2 M), cooled to 0°C and trichloroacetonitrile (0.90 mL, 9.0 mmol; 3 eq) and K₂CO₃ (1.66 g, 12.0 mmol; 4 eq) were added successfully. After stirring overnight, the reaction mixture was filtered over Celite and concentrated *in vacuo*. Purification using silica gel column chromatography (2/8, \rightarrow 1/1, Et₂O/PE, v/v) yielded compound **228** as a yellow oil (1.71 g, 2.58 mmol, 86%). TLC R_F: 0.73 (1/4, EtOAc/PE, v/v); IR (neat, cm⁻¹): 3345, 3019, 2106, 1731, 1677, 1602, 1452, 1262, 1091, 1068; IH NMR (400 MHz, CDCl₃) δ 8.72 (s, 1H, NH), 8.00 - 7.94 (m, 4H, H_{arom}), 7.89 - 7.85 (m, 2H, H_{arom}), 7.54 - 7.42 (m, 2H, H_{arom}), 7.42 - 7.29 (m, 6H, H_{arom}), 7.25 (t, J = 7.8 Hz, 2H, H_{arom}), 6.89 (d, J = 3.6 Hz, 1H, H-1), 6.28 (t, J = 9.9 Hz, 1H, H-3), 5.72 (t, J = 9.9 Hz, 1H, H-4), 5.64 (dd, J = 10.2, 3.7 Hz, 1H, H-2), 4.54 - 4.45 (m, 1H, H-5), 3.56 - 3.46 (m, 2H, H-6); I³C NMR (101 MHz, CDCl₃) δ 165.6, 165.3, 165.2 (C=O), 160.3 (C=N), 133.7, 133.6, 133.3, 129.9, 129.9, 129.7 (CH_{arom}), 128.8 (C_q), 128.5, 128.4, 128.3 (CH_{arom}), 92.9 (C-1), 71.9 (C-2), 70.6 (C-5), 69.9 (C-3), 69.2 (C-4), 50.7 (C-6); HRMS [C₂₉H₂₃Cl₃N₄O₈ + Na]⁺: 685.0465 found, 685.04442 calculated.

N^1 , N^3 , N^5 -Tris(dodecan-12-ol)-benzene-1,3,5-tricarboxamide (220).



To a co-evaporated solution of benzene-1,3,5-tricarbonyl trichloride (0.535 g, 2.04 mmol, 1 eq) in anhydrous DCM (20 mL, 0.1 M) at 0°C under N₂, was added dropwise (>4 h) a co-evaporated solution of 12-amino-dodecan-1-ol (1.32 g, 6.56 mmol, 3.3 eq) and Et₃N (0.94

mL, 6.73 mmol, 3.3 eq) in anhydrous DCM (33 mL, 0.2 M). The mixture was stirred overnight after which the mixture was absorbed on silica and purified using silica gel column chromatography (1/19, MeOH/CHCl₃, v/v) yielded compound **220** as a white solid (1.09 g, 1.44 mmol, 71%). <u>TLC R</u>_f: 0.73 (1/9, MeOH/CHCl₃, v/v); <u>IR</u> (neat, cm⁻¹): 3266, 2916, 1629, 1541, 1466, 1293, 1056; <u>1H NMR</u> (400 MHz, MeOD) δ 8.34 (s, 3H, BTA-H_{arom}), 3.51 (t, J = 6.6 Hz, 6H, CH₂-O), 3.37 (t, J = 7.1 Hz, 6H, CH₂-N), 1.66 - 1.55 (m, 6H, CH₂), 1.55 - 1.44 (m, 6H, CH₂), 1.44 - 1.23 (m, 48H, CH₂); <u>13C NMR</u> (101 MHz, MeOD) δ 168.7 (C=O), 136.9 (C_q), 129.7 (CH_{arom}), 63.0 (CH₂-O), 41.2 (CH₂-N), 33.7, 30.8, 30.7, 30.7, 30.6, 30.5, 30.5, 28.1, 27.0 (CH₂); <u>HRMS</u> [C₄₅H₈₁N₃O₆ + H]⁺: 760.6223 found, 760.61981 calculated.

12-N-Phthalimido-dodecan-1-ol (229).

HO WIPHIN Synthesis and spectral data as described in previous literature.²⁴

12-azido-dodecan-1-ol (230).

HOW Synthesis and spectral data as described in previous literature.²⁵

12-*N*-Phthalimido-dodecyl 4-O-(2,3,4,6-tetra-O-benzoyl- α -D-glucopyranosyl)-2,3,6-tri-O-benzoyl- β -D-glucopyranoside (231).

Acceptor 230 (38 mg, 0.11 mmol, 1.2eq) and donor 225 (116 mg, 95 μmol, 1eq) were combined and co-evaporated with toluene (3x) under N2 atmosphere, dissolved in anhydrous DCM (1.9 mL, 0.05 M) and stirred with activated molecular sieves (3Å) for 30 min. The reaction mixture was cooled to 0 °C, TMSOTf (3.4 µL, 19 µmol, 0.2eq) was added dropwise and the mixture was stirred at 4 °C overnight. The reaction was quenched with Et₃N (0.1 mL), diluted in DCM, washed with NaHCO3 (sat aq. 1x), dried over MgSO4 (s), filtered and concentrated in vacuo. Purification using size exclusion (Sephadex LH20, 1/1, MeOH/DCM, v/v) yielded compound 231 as a white solid (130 mg, 94 μmol, 99%). TLC R_f: 0.31 (3/2, Et₂O/PE, v/v); IR (neat, cm⁻¹): 1709, 1264, 1090, 1067, 1024, 705; ¹H NMR (400 MHz, CDCl₃) δ 8.14 - 8.07 (m, 2H, H_{arom}), 8.02 - 7.96 (m, 2H, H_{arom}), 7.91 - 7.80 (m, 6H, H_{arom}), 7.78 - 7.62 (m, 8H, H_{arom}), 7.60 - 7.27 (m, 18H, H_{arom}), 7.25 - 7.16 (m, 4H, H_{arom}), 6.09 (t, J = 10.0 Hz, 1H, H-3'), 5.80 - 5.72 (m, 2H, H-3, H-1'), 5.65 (t, J = 9.8 Hz, 1H, H-4'), 5.31 (dd, J = 9.5, 7.6 Hz, 1H, H-2), 5.25 (dd, J = 10.5, 3.9 Hz, 1H, H-2'), 4.91 (dd, J = 12.0, 2.4 Hz, 1H, H-6a'), 4.81 - 4.72 (m, 2H, H-1, H-6b'), 4.55-4.42 (m, 2H, H-4, H-5'), 4.39 (dd, J = 12.3, 3.0 Hz, 1H, H-6a), 4.26 (dd, J = 12.3, 3.8 Hz, 1H, H-6b), 4.13 -4.06 (m, 1H, H-5), 3.87 (dt, J = 9.7, 6.2 Hz, 1H, CHH-O), 3.71 - 3.63 (m, 2H, CH₂-N), 3.48 (dt, J = 9.6, 6.7 Hz, 1H, CHH-O), 1.65 (dd, J = 14.3, 7.1 Hz, 2H, CH₂), 1.47 (dq, J = 14.9, 6.6 Hz, 2H, CH₂), 1.38 -1.25 (m, 4H, CH₂), 1.21 - 0.93 (m, 12H, CH₂); 13C NMR (101 MHz, CDCl₃) δ 168.6, 166.3, 166.0, 165.8, 165.5, 165.3, 165.2 (C=O), 134.0, 133.6, 133.5, 133.4, 133.3, 133.2, 133.1 (CH_{arom}), 132.3 (C_q), 130.1, 130.0, 129.9, 129.8, 129.7 (CH_{arom}), 129.6, 129.5, 129.4, 129.0, 128.9, 128.8 (C_q), 128.7 (CH_{arom}), 128.6 (C_q), 128.5, 128.5, 128.3, 128.2, 123.3 (CH_{arom}), 100.9 (C-1), 96.5 (C-1'), 75.1 (C-3), 73.3 (C-4), 72.9 (C5), 72.4 (C-2), 71.0 (C-2'), 70.3 (CH₂-O), 70.0 (C-3), 69.2 (C-5', C-4'), 63.7 (C-6'), 62.6 (C-6), 38.2 (CH₂-N), 29.6, 29.6, 29.5, 29.5, 29.3, 29.3, 28.7, 27.0, 25.9 (CH₂); <u>HRMS</u> [C₈₁H₇₇NO₂₀ + H]⁺: 1384.51389 found, 1384.51117 calculated.

12-Azido-dodecyl 4-O-(2,3,4,6-tetra-O-benzoyl- α -D-glucopyranosyl)-2,3,6-tri-O-benzoyl- β -D-glucopyranoside (232).

Acceptor **230** (31.3 mg, 0.138 mmol, 1.2eq) and donor **225** (139.3 mg, 0.115 mmol, 0.115 mmol, 1.2eq) and donor **225** (139.3 mg, 0.115 mmol, 1.2eq) and donor **225** (139.3 mg, 0.115 mmol, 1.2eq) and donor **225** (139.3 mg, 0.115 mmol, 0.2eq) were combined and co-evaporated with toluene (3x) under N₂ atmosphere, dissolved in anhydrous DCM (2.29 mL, 0.05 M) and stirred with activated molecular sieves (3Å) for 30 min. The reaction mixture was cooled to 0 °C, a stock solution of TMSOTf in DCM (100 μL, 0.23 M, 23 μmol, 0.2eq) was added dropwise and the mixture was stirred at 4 °C overnight. The reaction was quenched with Et₃N (0.1 mL), diluted in DCM, washed with NaHCO₃ (sat aq. 1x), dried over MgSO₄ (s), filtered and concentrated *in vacuo*. Purification using size exclusion (Sephadex LH20, 1/1, MeOH/DCM, v/v) yielded compound **232** as a white solid (146 mg, 0.115 mmol, 99%). TLC R_f: 0.67 (3/2, Et₂O/PE, v/v); IR (neat, cm⁻¹): 2924, 2853, 2094, 1720, 1264, 1092, 1068, 1026, 703; HNMR (400 MHz, CDCl₃) δ 8.10 (d, *J* = 7.5 Hz, 2H, H_{arom}), 7.99 (d, *J* = 7.4 Hz, 2H, H_{arom}), 7.85 (t, *J* = 6.7 Hz, 4H, H_{arom}), 7.78 - 7.62 (m, 6H, H_{arom}),

7.62 - 7.27 (m, 18H, H_{arom}), 7.24 - 7.15 (m, 4H, H_{arom}), 6.08 (t, J = 10.0 Hz, 1H, H-3'), 5.83 - 5.71 (m, 2H, H-3, H-1'), 5.65 (t, J = 9.8 Hz, 1H, H-4'), 5.30 (dd, J = 11.1, 6.0 Hz, 1H, H-2), 5.25 (dd, J = 10.5, 3.8 Hz, 1H, H-2'), 4.91 (d, J = 10.1 Hz, 1H, H-6a'), 4.79 - 4.68 (m, 2H, H-6b', H-1), 4.54 - 4.35 (m, 3H, H-4, H-5', H-6a), 4.26 (dd, J = 12.3, 3.6 Hz, 1H, H-6b), 4.13 - 4.03 (m, 1H, H-5), 3.86 (dt, J = 9.7, 6.3 Hz, 1H, CHH-O), 3.54 - 3.42 (m, 1H, CHH-O), 3.24 (t, J = 7.0 Hz, 2H, CH₂-N₃), 1.57 (q, J = 7.3 Hz, 2H, CH₂), 1.53 - 1.40 (m, 2H, CH₂), 1.40 - 0.95 (m, 16H, CH₂); $\frac{13}{12}$ C NMR (101 MHz, CDCl₃) δ 166.3, 166.0, 165.8, 165.5, 165.3, 165.2 (C=O), 133.6, 133.5, 133.4, 133.3, 133.2, 133.1, 132.1, 131.7, 130.1, 130.0, 129.9, 129.8, 129.7 (CH_{arom}), 129.6, 129.5, 129.4, 129.1, 129.0, 128.9(C_q), 128.7 (CH_{arom}), 128.6 (C_q), 128.5, 128.3, 128.2, 128.1, 127.9, 114.4, 113.9 (CH_{arom}), 100.9 (C-1), 96.5 (C-1'), 75.1 (C-3), 73.3 (C-4), 72.9 (C-5), 72.4 (C-2), 71.0 (C-2'), 70.3 (CH₂-O), 70.0 (C-3'), 69.2 (C-5', C-4'), 63.7 (C-6'), 62.6 (C-6), 51.6 (CH₂-N₃), 29.6, 29.5, 29.3, 29.3, 29.0, 26.8, 25.9 (CH₂); HRMS [C₇₃H₇₃N₃O₁₈ + NH₄]+: 1297.52278 found, 1297.52274 calculated.

12-Amino-dodecyl 4-*O*-(α-D-glucopyranosyl)-β-D-glucopyranoside (233).

232 (144 mg, 0.10 mmol) was dissolved in a mixture of MeOH/DCM (0.5 mL, 0.2 M, 1/1, v/v) and NaOMe (0.010 mL, 5.4 M, 0.05 mmol, 0.5eq) was added dropwise. and the mixture was stirred for 2 h after which it was neutralized using Amberlite H⁺ resin, filtrated and concentrated *in vacuo*. This crude was dissolved in a mixture of H₂O/*t*-BuOH/dioxane (2 mL, 0.05 M, 1/1/1, v/v/v) and HCl (1 M, 1 drop) was added. The mixture was flushed with N₂ gas, and PtO (scoop) was added. The mixture was flushed with H₂ and was sonicated for 1 h. After which the mixture was filtered over a Whatman filter. Purification using size exclusion (Sephadex LH20, 1/9, H₂O/MeOH, v/v) yielded compound 233 as a white powder after lyophilization (25 mg, 0.048 mmol, 48%). TLC R₅: 0.52 (3/7, NH₃ (aq.)/*i*-PrOH, v/v); IR (neat, cm⁻¹): 3330, 2921, 2852, 1060, 1027, 992; HNMR (400 MHz, DMSO) δ 5.00 (d, J = 3.8 Hz, 1H, H-1'), 4.14 (d, J = 7.8 Hz, 1H, H-1), 3.79 - 3.16 (m, 12H), 3.06 (t, J = 9.2 Hz, 1H), 3.02 - 2.95 (m, 1H, H-2, H-3, H-4, H-5, H-6, H-2', H-3'. H-4', H-5', H-6', CH₂-O), 2.57 (t, J = 7.0 Hz, 2H, CH₂-NH₂), 1.56 - 1.45 (m, 2H, CH₂), 1.36 (dd, J = 13.5, 6.9 Hz, 2H, CH₂), 1.24 (s, 6H, CH₂); $\frac{13C}{12}$ NMR (101 MHz, DMSO) δ 102.7 (C-1), 100.8 (C-1'), 79.7, 76.5, 75.1, 73.5, 73.3, 73.0, 72.5, 69.9, 68.7 (C-2, C-3, C-4, C-5, C-2', C-3', C-4', C-5'), 60.8 (CH₂-O), 60.6 (C-6, C-6'), 40.9 (CH₂-N), 31.6, 29.3, 29.0, 28.9, 26.3, 25.5 (CH₂); HRMS [C₂4H₄7NO₁₁ + H]⁺: 526.32237 found, 526.32219 calculated.

12-Azido-dodecyl 4-*O*-(2,3,4,6-tetra-*O*-benzoyl-β-D-glucopyranosyl)-2,3,6-tri-*O*-benzoyl-β-D-glucopyranoside (234).

Acceptor **230** (1.12 g, 4.90 mmol, 1.1eq) and donor **223** (5.47 g, 4.50 mmol, 1eq) were combined and co-evaporated with toluene (3x) under N₂ atmosphere, dissolved in anhydrous DCM (45 mL, 0.1 M) and stirred with activated molecular sieves (3Å) for 30 min. The reaction mixture was cooled to 0 °C, TMSOTf (160 μ L, 0.9 mmol, 0.2eq) was added dropwise and the mixture was stirred at 0 °C for 4 h. The reaction was quenched with Et₃N (0.1 mL), diluted in DCM, washed with NaHCO₃ (sat aq. 1x), dried over MgSO₄ (s), filtered and concentrated *in vacuo*. Purification using silica gel column chromatography (1/9 \rightarrow 7/13, Et₂O/PE, v/v) yielded compound **234** as a white solid (4.89 g, 3.81

mmol, 85%). TLC R₅: 0.38 (3/2, Et₂O/PE, v/v); IR (neat, cm⁻¹): 2926, 2096, 1720, 1266, 1093, 1067, 1027, 704; 1 H NMR (400 MHz, CDCl₃) δ 8.02 - 7.88 (m, 10H, H_{arom}), 7.79 - 7.71 (m, 4H, H_{arom}), 7.60 - 7.18 (m, 21H, H_{arom}), 5.78 (t, J = 9.4 Hz, 1H, H-3), 5.72 (t, J = 9.6 Hz, 1H, H-3'), 5.51 (dd, J = 9.8, 8.0 Hz, 1H, H-2'), 5.44 - 5.33 (m, 2H, H-2, H-4'), 4.92 (d, J = 7.9 Hz, 1H, H-1'), 4.68 - 4.56 (m, 2H, H-1, H-6a), 4.45 (dd, J = 12.1, 4.4 Hz, 1H, H-6b), 4.23 (t, J = 9.5 Hz, 1H, H-4), 4.05 (dd, J = 11.8, 2.8 Hz, 1H, H-6a'), 3.84 - 3.75 (m, 3H, H-5, H-5', CHH-O), 3.72 (dd, J = 11.8, 5.7 Hz, 1H, H-6b'), 3.44 - 3.35 (m, 1H, CH*H*-O), 3.25 (t, J = 7.0 Hz, 2H, CH₂-N₃), 1.63 - 1.52 (m, 4H, CH₂), 1.50 - 0.92 (m, 16H, CH₂); 13 C NMR (101 MHz, CDCl₃) δ 165.9, 165.8, 165.7, 165.6, 165.3, 165.1, 164.9 (C=O), 133.5, 133.4, 133.2, 129.9, 129.9, 129.9 (CH_{arom}), 129.6, 129.5, 128.8, 128.7 (C_q), 128.6, 128.4, 128.4, 128.4 (CH_{arom}), 101.1, 101.0 (C-1, C-1'), 76.7 (C-4), 73.1, 72.9 (C-3, C-3'), 72.5 (C-5, C-5'), 72.0 (C-2, C-2'), 70.4 (CH₂-O), 69.5 (C-4'), 62.7, 62.6 (C-6, C-6'), 51.6 (CH₂-N₃), 29.5, 29.3, 29.0, 26.8, 25.8 (CH₂); HRMS [C₇₃H₇₃N₃O₁₈ + NH₄]+: 1297.52353 found, 1297.52274 calculated.

12-Azido-dodecyl 4-*O*-(β-D-glucopyranosyl)-β-D-glucopyranoside (252).

Compound **234** (3.47 g, 2.70 mmol) was dissolved in a mixture of MeOH/DCM (13.5 mL, 0.2 M, 1/1, v/v) and NaOMe (0.1 mL, 5.4 M, 0.54 mmol, 0.2eq) was added dropwise. and the mixture was stirred for 2 h after which it was neutralized using Amberlite H⁺ resin, filtrated and concentrated *in vacuo* to yield **252** as a white solid (1.38 g, 2.50 mmol, 93%). TLC R_i: 0.08 (1/9, MeOH/DCM, v/v); IR (neat, cm⁻¹): 3421, 2920, 2850, 2094, 1087, 1025, 990; ¹H NMR (400 MHz, MeOD) δ 4.39 (d, J = 7.8 Hz, 1H, H-1'), 4.26 (d, J = 7.8 Hz, 1H, H-1), 3.90 - 3.81 (m, 4H, H-6', H-6a, CHH-O), 3.68 - 3.61 (m, 1H, H-6b), 3.58 - 3.45 (m, 3H, CHH-O, H-3, H-4), 3.41 - 3.15 (m, 8H, H-3', H-4', H-5, H-5', H-2, H-2', CH₂-N₃), 1.58 (dp, J = 14.4, 6.8 Hz, 4H, CH₂), 1.42 - 1.25 (m, 16H, CH₂); ¹³C NMR (101 MHz, MeOD) δ 104.6 (C-1'), 104.2 (C-1), 80.7 (C-4), 78.1, 77.8, 76.4 (C-5, C-5', C-3'), 76.4 (C-3), 74.9, 74.8(C-2, C-2'), 71.3 (C-4'), 70.9 (CH₂-O), 62.4, 61.8 (C-6, C-6'), 52.4 (CH₂-N₃), 30.8, 30.7, 30.7, 30.7, 30.6, 30.6, 30.3, 29.9, 27.8, 27.1 (CH₂); HRMS [C₂₄H₄₅N₃O₁₁ + NH₄]⁺: 569.33907 found, 569.33923 calculated.

12-Amino-dodecyl 4-*O*-(β-D-glucopyranosyl)-β-D-glucopyranoside (235).

Azide **252** (57 mg, 0.10 mmol) was dissolved in a mixture of H₂O/*t*-BuOH/dioxane (3 mL, 0.033 M, 1/1/1, v/v/v) and HCl (1 M, 2 drops) was added. The mixture was flushed with N₂ gas, and PtO (1 scoop) was added. The mixture was flushed with H₂ and was sonicated for 1 h. After which the mixture was filtered over a Whatman filter. Purification using size exclusion (Sephadex LH20, 1/9, H₂O/MeOH, v/v) yielded compound **235** as a white powder after lyophilization (54 mg, 0.10 mmol, qnt). TLC R_E: 0.05 (3/7, MeOH/DCM, v/v); IR (neat, cm⁻¹):3421, 3321, 2920, 2851, 2094, 1074, 1027, 991; IH NMR (400 MHz, DMSO) δ 7.86 (s, 2H, NH₂), 5.26 (d, J = 4.9 Hz, 1H, 2-OH/2'-OH), 5.14 - 5.02 (m, 3H, 3-OH, 3'-OH, 2-OH/2'-OH), 4.67 (s, 1H, 4'-OH), 4.61 (dt, J = 16.5, 5.7 Hz, 2H, 6-OH, 6'-OH), 4.25 (d, J = 7.9 Hz, 1H, H-1/H-1'), 4.15 (d, J = 7.9 Hz, 1H, H-1/H-1'), 3.79 - 3.52 (m, 4H, H-6', H-6a, C*H*H-O), 3.46 - 3.32 (m, 2H, CH*H*-O, H-6b), 3.32 - 3.22 (m, 3H, H-4, H-5, H-5'), 3.21 - 3.11 (m, 2H, H-3, H-3'), 3.09 - 3.02 (m, 1H, H-4'), 3.02 - 2.93 (m, 2H, H-2, H-2'), 2.77 - 2.69 (m, 2H, CH₂-N), 1.60 - 1.43

(m, 4H, CH₂), 1.25 (s, 16H, CH₂); 13 C NMR (101 MHz, DMSO) δ 103.2, 102.5 (C-1, C-1'), 80.6 (C-4), 76.8, 76.5 (C-3, C-3'), 75.1, 74.8 (C-5, C-5'), 73.3, 73.1 (C-2, C-2'), 70.0 (C-4'), 68.7 (CH₂-O), 61.0 (C-6), 60.4 (C-6'), 38.7 (CH₂-N), 29.3, 29.0, 28.9, 28.9, 28.5, 27.0, 25.8, 25.5 (CH₂); 13 HRMS [C₂₄H₄₇NO₁₁ + H]+: 526.32220 found, 526.32219 calculated.

12-Azido-dodecyl 4-*O*-(2,3,4,6-tetra-*O*-benzoyl-β-D-galactopyranosyl)-2,3,6-tri-*O*-benzoyl-β-D-glucopyranoside (236).

Acceptor **230** (106 mg, 466 μmol, 1.1eq) and donor **224** (515.0 mg, 424 μmol, 1eq) were combined and co-evaporated with toluene (3x) under N2 atmosphere, dissolved in anhydrous DCM (4.24 mL, 0.1 M) and stirred with activated molecular sieves (3Å) for 30 min. The reaction mixture was cooled to 0 °C, TMSOTf (15 µL, 85 µmol, 0.2eq) was added dropwise and the mixture was stirred at 0 °C for 2 h. The reaction was quenched with Et₃N (0.1 mL), diluted in DCM, washed with NaHCO3 (sat aq. 1x), dried over MgSO4 (s), filtered and concentrated in vacuo. Purification using silica gel column chromatography (1/9 \rightarrow 7/13, Et₂O/PE, v/v) yielded compound **236** as a white foam (328.6 mg, 257 μmol, 61%). TLC R_f: 0.39 (3/2, Et₂O/PE, v/v); IR (neat, cm⁻¹): 2927, 2855, 2095, 1724, 1259, 1090, 1067, 1026, 705; $\frac{1}{1}$ H NMR (400 MHz, CDCl₃) δ 8.06 - 7.93 (m, 10H, H_{arom}), 7.90 (d, J = 7.3 Hz, 2H, H_{arom}), 7.73 (d, J = 7.4 Hz, 2H, H_{arom}), 7.67 - 7.28 (m, 17H, H_{arom}), 7.21 (t, J = 7.8 Hz, 2H, H_{arom}), 7.14 (t, J = 7.7Hz, 2H, H_{arom}), 5.80 (t, J = 9.5 Hz, 1H, H-3), 5.76 - 5.67 (m, 2H, H-2', H-4'), 5.45 (dd, J = 9.7, 8.0 Hz, 1H, H-2), 5.36 (dd, J = 10.3, 3.3 Hz, 1H, H-3'), 4.86 (d, J = 7.9 Hz, 1H, H-1'), 4.67 (d, J = 7.9 Hz, 1H, H-1), 4.60 (dd, J = 11.0, 1.5 Hz, 1H, H-6a), 4.48 (dd, J = 12.1, 4.2 Hz, 1H, H-6b), 4.25 (t, J = 9.5 Hz, 1H, H-4),3.92 - 3.78 (m, 3H, H-5', H-5, CHH-O), 3.78 - 3.64 (m, 2H, H-6'), 3.49 - 3.38 (m, 1H, CHH-O), 3.25 (t, I = 7.0 Hz, 2H, $C\text{H}_2$ - N_3), 1.58 (p, J = 7.0 Hz, 2H, $C\text{H}_2$), 1.51 - 1.40 (m, 2H, $C\text{H}_2$), 1.40 - 0.94 (m, 16H, $C\text{H}_2$); 13C NMR (101 MHz, CDCl₃) δ 166.0, 165.7, 165.5, 165.3, 165.3, 164.9 (C=O), 133.7, 133.5, 133.4, 133.3, 130.1, 129.9, 129.8, 129.8, 129.7 (CH_{arom}), 129.7, 129.5, 129.0, 128.8 (C_q), 128.8, 128.7, 128.7, 128.4, 128.4 (CH_{arom}), 101.3 (C-1), 101.1 (C-1), 76.2 (C-4), 73.1, 73.0 (C-3, C-5), 71.9, 71.9 (C-2, C-3), 71.5 (C-5), 70.5 (CH_2-O) , 70.0, 67.6 (C-2', C-4'), 62.6 (C-6), 61.2 (C-6'), 51.6 (CH_2-N_3) , 29.6, 29.5, 29.5, 29.3, 29.3, 29.0, 26.8, 25.8 (CH₂); <u>HRMS</u> $[C_{73}H_{73}N_3O_{18} + NH_4]^+$: 1297.52439 found, 1297.52274 calculated.

12-Azido-dodecyl 4-*O*-(β-D-galactopyranosyl)-β-D-glucopyranoside (253).

Compound **236** (305.7 mg, 0.24 mmol) was dissolved in a mixture of MeOH/DCM (1.2 mL, 0.2 M, 1/1, v/v) and NaOMe (0.025 mL, 5.4 M, 0.048 mmol, 0.2eq) was added dropwise. and the mixture was stirred for 2 h after which it was neutralized using Amberlite H⁺ resin, filtrated and concentrated *in vacuo* to yield **253** as a white solid (118.3 mg, 0.21 mmol, 89%). <u>TLC R</u>_ε: 0.07 (1/9, MeOH/DCM, v/v); <u>IR</u> (neat, cm⁻¹): 3650, 3384, 2920, 2850, 2095, 1096, 1061, 770; <u>¹H NMR</u> (400 MHz, DMSO) δ 4.22 - 4.13 (m, 2H, H-1', H-1), 3.80 - 3.69 (m, 2H, CHH-O, H-6a), 3.63 - 3.22 (m, 13H, H-4, CHH-O, H-6b, H-6', H-3, H-3',CH₂-N₃, H-5, H-5', H-4',H-2'), 3.03 - 2.95 (m, 1H, H-2), 1.51 (q, *J* = 6.4, 5.8 Hz, 4H, CH₂), 1.25 (s, 16H, CH₂); <u>¹³C NMR</u> (101 MHz, DMSO) δ 103.9 (C-1'), 102.5 (C-1), 80.9, 75.5, 75.0, 74.8 (C-2'/C-3/C-3'/C-4'/C-5/C-5'), 73.2 (C-2), 73.2, 70.5 (C-2'/C-3/C-3'/C-4'/C-5/C-5'), 68.7

(CH₂-O), 68.1 (C-4), 60.5, 60.4 (C-6, C-6'), 50.6 (CH₂-N₃), 29.3, 29.1, 29.0, 29.0, 29.0, 28.6, 28.3, 26.2, 25.5 (CH₂); <u>HRMS</u> [$C_{24}H_{45}N_3O_{11} + H$]⁺: 552.31251 found, 552.31269 calculated.

12-Amino-dodecyl 4-*O*-(β-D-galactopyranosyl)-β-D-glucopyranoside (237).

Azide **253** (70.5 mg, 0.13 mmol) was dissolved in a mixture of H_2O/t -BuOH/dioxane (3 mL, 0.033 M, 1/1/1, v/v/v) and HCl (1 M, 2 drops) was added. The mixture was flushed with H_2 and was sonicated for 1 h. After which the mixture was filtered over a Whatman filter. Purification using size exclusion (Sephadex LH20, 1/9, $H_2O/MeOH$, v/v) yielded compound **237** as a white powder after lyophilization (67.9 mg, 0.13 mmol, 99%). IR (neat, cm⁻¹): 3381, 3245, 2919, 2850, 1097, 1062, 1020; $H_1 = 100$ MHz, DMSO) δ 7.94 (s, 2H, NH₂), 4.22 - 4.18 (m, 1H, H-1'), 4.16 (d, J = 7.8 Hz, 1H, H-1), 3.78 - 3.68 (m, 2H, CHH-O, H-6a), 3.64 - 3.22 (m, 11H, H-4, CHH-O, H-6b, H-6', H-3, H-3', H-5, H-5', H-4',H-2'), 2.98 (t, J = 8.1 Hz, 1H, H-2), 2.80 - 2.68 (m, 2H, CH₂-N), 1.58 - 1.44 (m, 4H, CH₂), 1.36 - 1.16 (m, 16H, CH₂); $H_2 = 100$ MHz, DMSO) δ 103.9 (C-1'), 102.5 (C-1), 80.8, 75.5, 75.0, 74.8, 73.3, 73.2, 70.6 (C-2, C-2', C-3, C-3', C-4', C-5, C-5'), 68.7 (CH₂-O), 68.1 (C-4), 60.5, 60.3 (C-6, C-6'), 38.7 (CH₂-N), 29.3, 29.1, 29.0, 29.0, 28.9, 28.6, 27.0, 25.8, 25.5 (CH₂); $H_1 = 100$ HRMS $H_2 = 10$

12-Azido-dodecyl-2,3,4,6-tetra-*O*-benzoyl-β-D-glucopyranoside (238).

BBCO OBZ O_{0BZ} Acceptor **230** (403 mg, 1.77 mmol, 1.5eq) and donor **222** (874 mg, 1.18 mmol, 1eq) were combined and co-evaporated with toluene (3x) under N2 atmosphere, dissolved in anhydrous DCM (12 mL, 0.1 M) and stirred with activated molecular sieves (3Å) for 30 min. The reaction mixture was cooled to 0 °C, TMSOTf (43 µL, 236 µmol, 0.2eq) was added dropwise and the mixture was stirred at 0 °C for 3 h. The reaction was quenched with Et₃N (0.1 mL), diluted in DCM, washed with NaHCO3 (sat aq. 1x), dried over MgSO4 (s), filtered and concentrated in vacuo. Purification using size exclusion (Sephadex LH20, 1/1, MeOH/DCM, v/v) followed by silica gel column chromatography (1/9 \rightarrow 1/4, Et₂O/PE, v/v) yielded compound 238 as a clear oil (634 mg, 0.786 mmol, 67%). TLC R_c: 0.39 (3/2, Et₂O/PE, v/v); <u>IR</u> (neat, cm⁻¹): 2926, 2855, 2095, 1724, 1259, 1090, 1067, 1026, 705; <u>1H NMR</u> (400 MHz, CDCl₃) δ 8.05 - 7.99 (m, 2H, H_{arom}), 7.99 - 7.93 (m, 2H, H_{arom}), 7.93 - 7.87 (m, 2H, H_{arom}), 7.87 - 7.81 $(m, 2H, H_{arom}), 7.57 - 7.27 (m, 12H, H_{arom}), 5.91 (t, J = 9.7 Hz, 1H, H-3), 5.68 (t, J = 9.7 Hz, 1H, H-4), 5.53$ (dd, J = 9.7, 7.9 Hz, 1H, H-2), 4.84 (d, J = 7.9 Hz, 1H, H-1), 4.64 (dd, J = 12.1, 3.3 Hz, 1H, H-6a), 4.51(dd, I = 12.1, 5.2 Hz, 1H, H-6b), 4.21 - 4.11 (m, 1H, H-5), 3.92 (dt, I = 9.7, 6.3 Hz, 1H, CHH-O), 3.54 (dt, I = 9.6, 6.7 Hz, 1H, CHH-O), 3.25 (t, $I = 7.0 \text{ Hz}, 2H, \text{CH}_2$ -N₃), 1.54 (dh, $I = 30.3, 7.9, 7.4 \text{ Hz}, 4H, \text{CH}_2$), 1.40 - 0.99 (m, 16H, CH₂); ¹³C NMR (101 MHz, CDCl₃) δ 166.3, 166.0, 165.3, 165.2 (C=O), 133.5, 133.3, 133.3, 133.2, 129.9, 129.9, 129.9 (CH_{arom}), 129.7, 129.5, 128.9, 128.9 (C_q), 128.5, 128.5, 128.4, 128.4 (CH_{arom}), $101.4 \text{ (C-1)}, 73.0 \text{ (C-3)}, 72.3 \text{ (C-5)}, 72.0 \text{ (C-2)}, 70.5 \text{ (CH}_2\text{-O)}, 70.0 \text{ (C-4)}, 63.4 \text{ (C-6)}, 51.6 \text{ (CH}_2\text{-N}_3), 29.6$ 29.6, 29.5, 29.5, 29.5, 29.3, 29.0, 26.8, 25.9 (CH₂); \underline{HRMS} [C₄₆H₅₁N₃O₁₀ + Na]⁺: 828.34680 found, 828.34667 calculated.

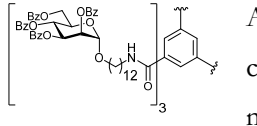
12-Azido-dodecyl-β-D-glucopyranoside (254).

Glucoside **238** (600 mg, 0.70 mmol) was dissolved in a mixture of MeOH/DCM (3.5 mL, 0.2 M, 1/1, v/v) and NaOMe (0.025 mL, 5.4 M, 0.14 mmol, 0.2eq) was added dropwise. and the mixture was stirred for 2 h after which it was neutralized using Amberlite H+ resin, filtrated and concentrated *in vacno*. Purification using size exclusion (Sephadex LH20, 1/1, MeOH/DCM, v/v) yielded compound **254** as a white solid (150 mg, 0.382 mmol, 55%). TLC R_C: 0.33 (1/9, MeOH/DCM, v/v); IR (neat, cm⁻¹): 3380, 3247, 2921, 2850, 2095, 1284, 1254, 1167, 1070, 1034, 994; HNMR (400 MHz, MeOD) δ 4.22 (d, J = 7.8 Hz, 1H, H-1), 3.92 - 3.80 (m, 2H, CHH-O, H-6a), 3.64 (dd, J = 11.8, 5.1 Hz, 1H, H-6b), 3.51 (dt, J = 9.3, 6.8 Hz, 1H, CHH-O), 3.36 - 3.18 (m, 5H, CH₂-N₃, H-3, H-4, H-5), 3.14 (t, J = 8.4 Hz, 1H, H-2), 1.66 - 1.49 (m, 4H, CH₂), 1.43 - 1.22 (m, 16H, CH₂); $\frac{13}{12}$ C NMR (101 MHz, MeOD) δ 104.3 (C-1), 78.1 (C-3), 77.9 (C-4/C-5), 75.1 (C-2), 71.6 (C-4/C-5), 70.9 (CH₂-O), 62.7 (C-6), 52.4 (CH₂-N₃), 30.8, 30.7, 30.7, 30.7, 30.6, 30.3, 29.9, 27.8, 27.1 (CH₂); HRMS [C₁₈H₃₅N₃O₆ + Na]+: 412.24191 found, 412.24181 calculated.

12-Amino-dodecyl-β-D-glucopyranoside (239).

Glucose **254** (131 mg, 0.34 mmol) was dissolved in a mixture of H₂O/*t*-BuOH/dioxane (6 mL, 0.05 M, 1/1/1, v/v/v) and HCl (1 M, 2 drops) was added. The mixture was flushed with N₂ gas, and PtO (1 scoop) was added. The mixture was flushed with H₂ and was sonicated for 1 h. After which the mixture was filtered over a Whatman filter. Purification using size exclusion (Sephadex LH20, 1/9, H₂O/MeOH, v/v) yielded compound **239** as a white powder after lyophilization (102 mg, 0.28 mmol, 83%). TLC R_E: 0.05 (1/9, MeOH/DCM, v/v); IR (neat, cm⁻¹): 3367, 2921, 2852, 1077, 989; IH NMR (400 MHz, DMSO) & 7.92 (s, 1H, NH), 7.51 - 7.14 (m, 2H, NH), 4.09 (d, *J* = 7.7 Hz, 1H, H-1), 3.78 - 3.69 (m, 1H, CHH-O), 3.65 (d, *J* = 11.4 Hz, 1H, H-6a), 3.47 - 3.35 (m, 2H, H-6b, CHH-O), 3.14 (t, *J* = 8.5 Hz, 1H, H-3), 3.10 - 2.99 (m, 2H, H-4, H-5), 2.93 (t, *J* = 8.3 Hz, 1H, H-2), 2.81 - 2.66 (m, 2H, CH₂-N), 1.59 - 1.43 (m, 4H, CH₂), 1.24 (s, 16H, CH₂); 13C NMR (101 MHz, DMSO) & 103.0 (C-1), 76.9 (C-3, C-4/C-5), 73.7 (C-2), 70.3 (C-4/C-5), 68.8 (CH₂-O), 61.3 (C-6), 39.0 (CH₂-N), 29.5, 29.2, 29.1, 29.0, 28.8, 28.3, 27.1, 26.0, 25.8, 24.9 (CH₂); HRMS [C₁₈H₃₇NO₆ + H]⁺: 364.26926 found, 364.26936 calculated.

N^1 , N^3 , N^5 -Tris-(dodecyl-12-O-[2,3,4,6-tetra-O-benzoyl- α -D-mannopyranosyl])-benzene-1,3,5-tricarboxamide (240).

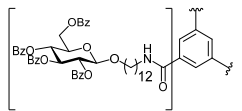


Acceptor 220 (76 mg, 0.10 mmol, 1 eq) and donor 221 (296 mg, 0.40 mmol, 4 eq) were combined and co-evaporated with toluene (3x) under N_2 atmosphere, dissolved in a mixture of anhydrous DCM/HFIP (4 mL, 0.025 M, 4/1, v/v) and stirred with

activated molecular sieves (3Å) for 30 min. The reaction mixture was cooled to 0 °C, TfOH (9 μL, 0.1 mmol, 1 eq) was added dropwise and the mixture was stirred at 0 °C for three hours. The reaction was quenched with Et₃N (0.1 mL), diluted in DCM, washed with NaHCO₃ (sat aq., 3x), dried over MgSO₄ (s), filtered and concentrated *in vacuo*. Purification using size exclusion (Sephadex LH20, 1/1, MeOH/DCM, v/v) yielded compound **240** as a transparent solid (229 mg, 0.092 mmol, 92%). <u>TLC R</u>_E: 0.72 (Et₂O); <u>IR</u>

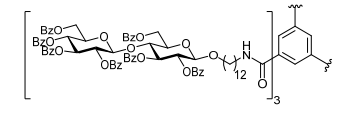
(neat, cm⁻¹): 2942, 2853, 1717, 1560, 1507, 1259, 1066, 1026, 705; 1H NMR (400 MHz, CDCl₃) δ 8.34 (s, 3H, BTA-H_{arom}), 8.12 - 8.01 (m, 12H, H_{arom}), 7.99 - 7.93 (m, 6H, H_{arom}), 7.86 - 7.81 (m, 6H, H_{arom}), 7.63 -7.33 (m, 30H, H_{arom}), 7.27 (t, J = 8.2 Hz, 6H, H_{arom}), 6.47 (t, J = 5.6 Hz, 3H, NH), 6.10 (t, J = 10.0 Hz, 3H, H-4), 5.93 (dd, J = 10.1, 3.3 Hz, 3H, H-3), 5.70 (dd, J = 3.2, 1.8 Hz, 3H, H-2), 5.09 (d, J = 1.5 Hz, 3H, H-1), 4.69 (dd, J = 12.0, 2.4 Hz, 3H, H-6a), 4.49 (dd, J = 12.1, 4.5 Hz, 3H, H-6b), 4.45 - 4.38 (m, 3H, H-5), 3.82 (dt, I = 9.5, 6.8 Hz, 3H, CHH-O), 3.57 (dt, I = 9.5, 6.7 Hz, 3H, CHH-O), 3.44 (q, I = 6.8 Hz, 6H, CH₂-N), 1.75 - 1.65 (m, 6H, CH₂), 1.65 - 1.55 (m, 6H, CH₂), 1.45 - 1.23 (m, 48H, CH₂); 13C NMR (101 MHz, CDCl₃) δ 166.3, 165.7, 165.6, 165.6, 165.6, 165.6 (C=O), 135.4 (C₉), 133.6, 133.3, 133.2, 130.0, 129.9, 129.9 (CH_{arom}), 129.5, 129.2, 129.1 (C_q), 128.7, 128.6, 128.4, 128.0 (CH_{arom}), 97.8 (C-1), 70.8 (C-2), 70.3 (C-1) 3), 68.9 (CH₂-O), 68.9 (C-5), 67.1 (C-4), 63.1 (C-6), 40.5 (CH₂-N), 29.7, 29.7, 29.7, 29.5, 29.4, 27.1, 26.3 (CH_2) ; HRMS $[C_{147}H_{159}N_3O_{33} + H + NH_4]^{2+}$: 1257.06660 found, 1257.06502 calculated.

N^1 , N^3 , N^5 -Tris-(dodecyl-12-O-[2,3,4,6-tetra-O-benzoyl- β -D-glucopyranosyl])-benzene-1,3,5tricarboxamide (241).



Acceptor 220 (0.99 g, 1.30 mmol, 1 eq) and donor 222 (4.82 g, 6.50 mmol, 5 eq) were combined and co-evaporated with toluene (3x) under N2 atmosphere, dissolved in a mixture of anhydrous DCM/HFIP (57 mL, 0.023 M, 4/1, v/v) and stirred with activated molecular sieves (3Å) for 30 min. The reaction mixture was cooled to 0 °C, TfOH (115 µL, 1.3 mmol, 1 eq) was added dropwise and the mixture was stirred at 4 °C overnight. The reaction was quenched with Et₃N (0.6 mL), diluted in DCM, washed with NaHCO₃ (sat aq., 3x), dried over MgSO₄ (s), filtered and concentrated in vacuo. Purification using size exclusion (Sephadex LH20, 1/1, MeOH/DCM, v/v) and silica gel column chromatography (3/7, Et₂O/PE, v/v \rightarrow 100% Et₂O) yielded title compound 241 as a white solid (2.52 g, 1.01 mmol, 78%). TLC R_E: 0.51 (Et₂O); IR (neat, cm⁻¹): 2925, 2853, 1720, 1560, 1260, 1090, 1067, 1026, 705; 1H NMR (400 MHz, CDCl₃) δ 8.37 (s, 3H, BTA-H_{arom}), 8.05 - 7.80 (m, 24H, H_{arom}), 7.57 -7.24 (m, 36H, H_{arom}), 6.61 (t, J = 5.3 Hz, 3H, NH), 5.92 (t, J = 9.7 Hz, 3H, H-3), 5.68 (t, J = 9.7 Hz, 3H, H-4), 5.53 (dd, J = 9.8, 7.9 Hz, 3H, H-2), 4.85 (d, J = 7.9 Hz, 3H, H-1), 4.64 (dd, J = 12.1, 3.2 Hz, 3H, H-6a), 4.51 (dd, I = 12.1, 5.2 Hz, 3H, H-6b), 4.21 - 4.13 (m, 3H, H-5), 3.91 (dt, I = 9.7, 6.3 Hz, 3H, CHH-O), 3.54 (dt, I = 9.7, 6.7 Hz, 3H, CHH-O), 3.43 (q, I = 6.7 Hz, 6H, CH₂-N), 1.65 - 1.46 (m, 12H, CH₂), 1.40 -0.95 (m, 48H, CH₂); 13 C NMR (101 MHz, CDCl₃) δ 166.3, 165.9, 165.8, 165.3, 165.2 (C=O), 135.4 (C_q), 133.5, 133.3, 133.3, 133.2, 129.9, 129.8 (CH_{arom}), 129.8 (C_q), 129.7 (CH_{arom}), 129.6, 129.4, 128.9, 128.9 (C_q), 128.5, 128.4, 128.4, 128.4, 128.1 (CH_{arom}), 101.4 (C-1), 73.0 (C-3), 72.2 (C-5), 72.0 (C-2), 70.5 (CH₂-O), 69.9 (C-4), 63.3 (C-6), 40.5 (CH₂-N), 29.6, 29.6, 29.6, 29.5, 29.5, 29.5, 29.4, 29.3, 27.1, 25.8 (CH₂); HRMS $[C_{147}H_{159}N_3O_{33} + 2H]^{2+}$: 1248.55472 found, 1248.55174 calculated.

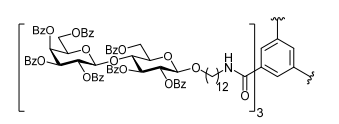
N^{1} , N^{3} , N^{5} -Tris-(dodecyl-12-O-[4-O-(2,3,4,6-tetra-O-benzoyl- β -D-glucopyranosyl])-benzene-1,3,5-tricarboxamide (242).



Acceptor **220** (1.33 g, 1.75 mmol, 1 eq) and donor **223** (10.66 g, 8.77 mmol, 5 eq) were combined and co-evaporated with toluene (3x) under N_2 atmosphere, dissolved in a mixture of anhydrous DCM/HFIP (76 mL, 0.023)

M, 4/1, v/v) and stirred with activated molecular sieves (3Å) for 30 min. The reaction mixture was cooled to 0 °C, TfOH (155 μL, 1.75 mmol, 1 eq) was added dropwise and the mixture was stirred at 4 °C overnight. The reaction was quenched with Et₃N (0.5 mL), diluted in DCM, washed with NaHCO₃ (sat aq., 3x), dried over MgSO₄ (s), filtered and concentrated in vacuo. Purification using silica gel column chromatography (1/1, EtOAc/PE, v/v) followed by purification using size exclusion (Sephadex LH20, 1/1, MeOH/DCM, v/v) yielded compound 242 as a white powder (3.46 g, 0.88 mmol, 50%). TLC R: 0.75 (9/1, Et₂O/PE, v/v); IR (neat, cm⁻¹): 2924, 2853, 1684, 1670, 1654, 1636, 1617, 1497,1260, 1090, 1070, 1025, 705; 1H NMR (400 MHz, CDCl₃) δ 8.35 (s, 3H, BTA-H_{arom}), 8.01 - 7.89 (m, 30H, H_{arom}), 7.79 - 7.71 (m, 12H, H_{arom}), 7.60 -7.17 (m, 63H, H_{arom}), 6.49 (t, J = 5.3 Hz, 3H, NH), 5.78 (t, J = 9.4 Hz, 3H, H-3), 5.72 (t, J = 9.6 Hz, 3H, H-3'), 5.51 (dd, J = 9.8, 7.9 Hz, 3H, H-2'), 5.43 - 5.33 (m, 6H, H-2, H-4'), 4.93 (d, J = 7.9 Hz, 3H, H-1'), 4.69 - 4.55 (m, 6H, H-1, H-6a), 4.45 (dd, J = 12.1, 4.5 Hz, 3H, H-6b), 4.23 (t, J = 9.4 Hz, 3H, H-4), 4.05(dd, J = 11.9, 2.9 Hz, 3H, H-6a'), 3.87 - 3.67 (m, 12H, H-5, H-5', CHH-O, H-6b'), 3.50 - 3.35 (m, 9H, CH₂-N, CHH-O), 1.66 - 1.52 (m, 6H, CH₂), 1.51 - 1.39 (m, 6H, CH₂), 1.39 - 0.93 (m, 48H, CH₂); 13C NMR (101 MHz, CDCl₃) δ 165.9, 165.8, 165.7, 165.6, 165.3, 165.1, 164.9 (C=O), 135.4 (C_q), 133.5, 133.4, 133.2, 129.9, 129.8, 129.8, 129.6 (CH_{arom}), 129.5, 128.8, 128.7, 128.7 (C_q), 128.6, 128.6, 128.4, 128.4, 128.4, 128.1 (CH_{arom}), 101.1, 101.0 (C-1, C-1'), 76.6 (C-4), 73.1, 72.9 (C-3, C-3'), 72.5 (C-5, C-5'), 72.1, 72.0 (C-2, C-2'), 70.4 (CH₂-O), 69.5 (C-4'), 62.8 (C-6'), 62.6 (C-6), 40.5 (CH₂-N), 29.6, 29.6, 29.5, 29.4, 29.3, 27.1, 25.8 (CH₂); HRMS $[C_{228}H_{221}D_3N_3O_{57} + 2H]^{2+}$: 1961.60894 found, 1961.76000 calculated.

N^1 , N^3 , N^5 -Tris-(dodecyl-12-*O*-[4-*O*-(2,3,4,6-tetra-*O*-benzoyl- β -D-galactopyranosyl)-2,3,6-tri-*O*-benzoyl- β -D-glucopyranoside])-benzene-1,3,5-tricarboxamide (243).

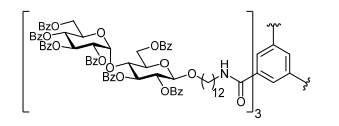


Acceptor **220** (84 mg, 0.11 mmol, 1 eq) and donor **224** (674 mg, 0.55 mmol, 5 eq) were combined and co-evaporated with toluene (3x) under N₂ atmosphere, dissolved in a mixture of anhydrous DCM/HFIP (4.8 mL, 0.023)

M, 4/1, v/v) and stirred with activated molecular sieves (3Å) for 30 min. The reaction mixture was cooled to 0 °C, TfOH (10 μ L, 0.11 mmol, 1 eq) was added dropwise and the mixture was stirred at 4 °C overnight. The reaction was quenched with Et₃N (0.1 mL), diluted in DCM, washed with NaHCO₃ (sat aq., 3x), dried over MgSO₄ (s), filtered and concentrated *in vacuo*. Purification using size exclusion (Sephadex LH20, 1/1, MeOH/DCM, v/v) yielded compound **243** as a white foam (425 mg, 0.108 mmol, 98%). <u>TLC Recolor</u>: 0.80 (9/1, Et₂O/PE, v/v); <u>IR</u> (neat, cm⁻¹): 2923, 2853, 1734, 1717, 1647, 1560, 1260, 1093, 1066, 1025, 704; <u>1H NMR</u> (400 MHz, CDCl₃) δ 8.35 (s, 3H, BTA-H_{arom}), 8.04 - 7.93 (m, 30H, H_{arom}), 7.92 - 7.88 (m, 6H, H_{arom}), 7.74 - 7.69 (m, 6H, H_{arom}), 7.66 - 7.27 (m, 51H, H_{arom}), 7.21 (t, J = 7.8 Hz, 6H, H_{arom}), 7.14 (t, J = 7.8 Hz,

6H, H_{arom}), 6.63 - 6.47 (m, 3H, NH), 5.80 (t, J = 9.5 Hz, 3H, H-3), 5.76 - 5.68 (m, 6H, H-2', H-4'), 5.45 (dd, J = 9.8, 8.0 Hz, 3H, H-2), 5.37 (dd, J = 10.3, 3.4 Hz, 3H, H-3'), 4.87 (d, J = 7.9 Hz, 3H, H-1'), 4.68 (d, J = 7.9 Hz, 3H, H-1), 4.63 - 4.56 (m, 3H, H-6a), 4.49 (dd, J = 12.2, 4.3 Hz, 3H, H-6b), 4.25 (t, J = 9.5 Hz, 3H, H-4), 3.89 (t, J = 6.5 Hz, 3H, H-5'), 3.86 - 3.77 (m, 6H, H-5, CHH-O), 3.77 - 3.63 (m, 6H, H-6'), 3.51 - 3.37 (m, 9H, CH₂-N, CHH-O), 1.66 - 1.53 (m, 6H, CH₂), 1.53 - 1.39 (m, 6H, CH₂), 1.39 - 0.92 (m, 48H, CH₂); $\frac{13}{3}$ C NMR (101 MHz, CDCl₃) 8 166.0, 165.7, 165.7, 165.6, 165.5, 165.3, 165.3, 164.9 (C=O), 135.4 (C_q), 133.7, 133.5, 133.5, 133.5, 133.4, 133.3, 133.2, 130.1, 129.9, 129.8, 129.8, 129.7 (CH_{arom}), 129.6, 129.6, 129.5, 129.5, 128.9, 128.8, 128.7 (Cq), 128.6, 128.4, 128.4, 128.3, 128.0 (CH_{arom}), 101.3 (C-1), 101.1 (C-1'), 76.2 (C-4), 73.1, 73.0 (C-3, C-5), 71.9, 71.9 (C-2, C-3'), 71.5 (C-5'), 70.5 (CH₂-O), 70.0, 67.6 (C-2', C-4'), 62.6 (C-6), 61.2 (C-6'), 40.5 (CH₂-N), 29.7, 29.6, 29.6, 29.5, 29.4, 29.4, 29.4, 29.3, 27.1, 25.8 (CH₂); HRMS [C₂₂₈H₂₂₂D₃N₃O₅₇ + H]²⁺: 1961.60487 found, 1961.76000 calculated.

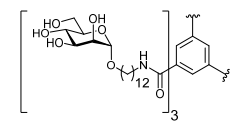
N^{1} , N^{3} , N^{5} -Tris-(dodecyl-12-O-[4-O-(2,3,4,6-tetra-O-benzoyl- α -D-glucopyranosyl)-2,3,6-tri-O-benzoyl- β -D-glucopyranosyl])-benzene-1,3,5-tricarboxamide (244).



Acceptor **220** (100 mg, 0.132 mmol, 1 eq) and donor **225** (814 mg, 0.66 mmol, 5 eq) were combined and co-evaporated with toluene (3x) under N_2 atmosphere, dissolved in a mixture of anhydrous DCM/HFIP (5.7 mL, 0.023)

M, 4/1, v/v) and stirred with activated molecular sieves (3Å) for 30 min. The reaction mixture was cooled to 0 °C, TfOH (12 µL, 0.132 mmol, 1 eq) was added dropwise and the mixture was stirred at 4 °C overnight. The reaction was quenched with Et₃N (0.1 mL), diluted in DCM, washed with NaHCO₃ (sat aq., 3x), dried over MgSO₄ (s), filtered and concentrated in vacuo. Purification using size exclusion (Sephadex LH20, 1/1, MeOH/DCM, v/v) yielded compound 244 as a transparent glasslike solid (360 mg, 0.092 mmol, 70%). TLC R_f: 0.60 (19/1, Et₂O/PE, v/v); IR (neat, cm⁻¹): 1721, 1654, 1601, 1451, 1262, 1090, 1025, 705; 1H <u>NMR</u> (500 MHz, CDCl₃) δ 8.29 (s, 3H, BTA-H_{arom}), 8.04 (dd, J = 8.3, 1.3 Hz, 7H, H_{arom}), 7.98 (dd, J = 8.4, 1.3 Hz, 7H, H_{arom}), 7.95 - 7.89 (m, 14H, H_{arom}), 7.88 - 7.79 (m, 14H, H_{arom}), 7.57 - 7.18 (m, 63H, H_{arom}), 6.61 (t, J = 5.6 Hz, 3H, NHCO), 6.17 (t, J = 9.9 Hz, 3H, H-3, H-3), 5.96 (d, J = 3.8 Hz, 3H, H-1), 5.72 (t, J = 3.8 Hz, 3H, NHCO)9.9 Hz, 3H, H-4), 5.40 (dd, J = 10.4, 3.8 Hz, 3H, H-2), 4.93 (dd, J = 9.0, 7.9 Hz, 3H, H-2), 4.83 (dd, J = 9.0, 7.9 Hz, 4.83 (dd, 11.9, 1.8 Hz, 3H, H-6a), 4.62 - 4.54 (m, 9H, H-5', H-1, H-6b), 4.51 (dd, *J* = 12.4, 2.9 Hz, 3H, H-6a'), 4.41 (dd, J = 12.4, 4.1 Hz, 3H, H-6b'), 3.99 (dd, J = 9.6, 8.5 Hz, 3H, H-4), 3.95 - 3.79 (m, 9H, H-3, H-5, CHH-O), 3.49 - 3.35 (m, 9H, CHH-O, CH₂-N), 1.62 - 1.52 (m, 6H, CH₂), 1.52 - 1.38 (m, 6H, CH₂), 1.38 - 0.99 (m, 48H, CH₂); ¹³C NMR (126 MHz, CDCl₃) δ 166.5, 166.3, 166.2, 166.0, 165.8, 165.8, 165.3 (C=O), 135.2 (C_q), 133.5, 133.4, 133.3, 133.3, 133.3, 133.1, 130.0, 129.9, 129.9, 129.8 (CH_{arom}), 129.8, 129.7 (C_q), 129.7 (CH_{arom}), 129.5, 129.3, 129.2, 129.0 (C_q), 128.6, 128.5, 128.5, 128.4, 128.4, 128.1 (CH_{arom}), 100.7 (C-1), 97.0 (C-1), 78.3 (C-4), 75.9 (C-3), 75.4 (C-2), 72.6 (C-5), 71.6 (C-2), 70.2 (CH₂-O), 70.2 (C-3), 69.3 (C-4), 69.0 (C-5'), 63.8 (C-6), 62.9 (C-6'), 40.5 (CH₂-N), 29.6, 29.5, 29.4, 29.3, 29.2, 27.1, 25.9 (CH₂); HRMS $[C_{228}H_{221}D_3N_3O_{57} + 2H]^{2+}$: 1961.60642 found, 1961.76000 calculated.

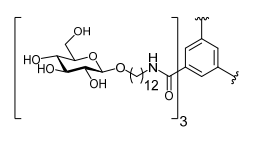
N^1 , N^3 , N^5 -Tris-(dodecyl-12-O- α -D-mannopyranoside)-benzene-1,3,5-tricarboxamide (213).



Mannoside **240** (38 mg, 15 μ mol) was dissolved in a mixture of dioxane, *t*-BuOH and MeOH (3 mL, 0.005 M, 1/1/1, v/v/v), a solution of NaOMe was added (3 drops) and the mixture was stirred overnight. Purification via RP-HPLC (linear gradient 15 -

85 % B in A, 10 min, Gemini-NX 5μm C18, 110 Å, 250 x 12.0 mm, 5 mL/min) yielded title compound **213** as a white powder after lyophilization (9.0 mg, 7.2 μmol, 48%). <u>LC-MS</u>: $R_t = 6.83$ min (0 - 90% ACN; 13 min); <u>IR</u> (neat, cm⁻¹): 3567, 3012, 1647, 1560, 1013, 952; <u>1H NMR</u> (500 MHz, DMSO) δ 8.62 (t, J = 5.6 Hz, 3H, NH), 8.35 (s, 3H, BTA-H_{arom}), 4.57 (d, J = 1.5 Hz, 3H, H-1), 3.63 (dd, J = 11.6, 2.1 Hz, 3H, H-6a), 3.61 - 3.55 (m, 6H, CHH-O, H-2), 3.46 - 3.40 (m, 6H, H-6b, H-3), 3.36 (t, J = 9.4 Hz, 3H, H-4), 3.32 - 3.24 (m, 12H, H-5, CHH-O, CH₂-N), 1.57 - 1.43 (m, 12H, CH₂), 1.35 - 1.20 (m, 48H, CH₂); <u>13C NMR</u> (126 MHz, DMSO) δ 165.4 (C=O), 135.1 (C_q), 128.3 (CH_{arom}), 99.7 (C-1), 73.9 (C-5), 71.0 (C-3), 70.4 (C-2), 67.0 (C-4), 66.2 (CH₂-O), 61.3 (C-6), 39.4 (CH₂-N), 29.1, 29.0, 29.0, 28.9, 28.8, 26.5, 25.8 (CH₂); <u>13C-GATED</u> (126 MHz, DMSO) δ 99.7 (d, J = 169 Hz, C-1); <u>HRMS</u> [C₆₃H₁₁₁N₃O₂₁ + NH₄]⁺: 1263.80652found, 1263.80483 calculated.

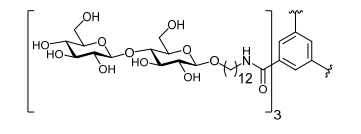
N^1 , N^3 , N^5 -Tris-(dodecyl-12-O- β -D-glucopyranoside)-benzene-1,3,5-tricarboxamide (214).



Glucoside **241** (1.47 g, 0.59 mmol) was dissolved in a mixture of dioxane, *t*-BuOH and MeOH (17 mL, 0.035 M, 3/5/10, v/v/v), a solution of NaOMe was added (10 mL, 25% wt, 44 mmol, 75 eq) and the mixture was refluxed for three days. The

mixture was quenched with Amberlite H⁺ and concentrated. After purification by RP-HPLC compound **214** was isolated as a white powder after lyophilizing (305 mg, 0.24 mmol, 41%). <u>LC-MS</u>: R_t = 6.03 min (0 - 90% ACN; 13 min); <u>IR</u> (neat, cm⁻¹): 3307, 2922, 2852, 1641, 1540, 1435, 1077, 1023; <u>1H NMR</u> (400 MHz, DMSO) δ 8.65 (t, J = 5.5 Hz, 3H, NH), 8.35 (s, 3H, BTA-H_{arom}), 4.08 (d, J = 7.8 Hz, 3H, H-1), 3.74 (dt, J = 9.4, 6.8 Hz, 3H, CHH-O), 3.69 - 3.61 (m, 3H, H-6a), 3.48 - 3.33 (m, 6H, H-6b, CHH-O), 3.26 (q, J = 6.5 Hz, 6H, CH₂-N), 3.15 - 2.97 (m, 9H, H-3, H-4, H-5), 2.92 (t, J = 8.3 Hz, 3H, H-2), 1.58 - 1.44 (m, 12H, CH₂), 1.37 - 1.19 (m, 48H, CH₂); <u>13C NMR</u> (101 MHz, DMSO) δ 165.4 (C=O), 135.1 (C_q), 128.3 (BTA-CH_{arom}), 102.9 (C-1), 76.8, 76.8 (C-3, C-4/C-5), 73.5 (C-2), 70.1 (C-4/C-5), 68.6 (CH₂-O), 61.1 (C-6), 39.4 (CH₂-N), 29.3, 29.1, 28.9, 26.6, 25.6 (CH₂); <u>HRMS</u> [C₆₃H₁₁₁N₃O₂₁ + H]+: 1246.78139 found, 1246.77828 calculated.

N^1 , N^3 , N^5 -Tris-(dodecyl-12-O-[4-O-(β -D-glucopyranosyl)- β -D-glucopyranoside])-benzene-1,3,5-tricarboxamide (215).

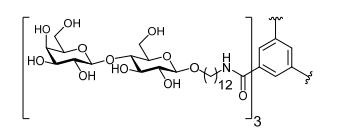


Compound **242** (3.46 g, 0.88 mmol) was dissolved in a mixture of water, MeOH, t-BuOH (65 mL, 1/6/6, v/v/v) to which KOH (15 mL, 1 M, aq., 15 mmol, 17eq) was added dropwise after which the mixture was refluxed for

three days after which it was neutralized with acetic acid. Purification usig C18 functionalized silica gel column chromatography (100% H2O \rightarrow 1/1, H₂O/ACN, v/v) yielded compound **215** as a white powder after lyophilizing (683 mg, 0.17 mmol, 19%). <u>LC-MS</u>: $R_t = 5.82 \text{ min}$ (5 - 100% ACN; 10 min); <u>1H NMR</u>

(400 MHz, MeOD) δ 8.35 (s, 3H, BTA-H_{arom}), 4.39 (d, J = 7.8 Hz, 3H, H-1'), 4.25 (d, J = 7.8 Hz, 3H, H-1), 3.93 - 3.80 (m, 12H, H-6', H-6a, C*H*H-O), 3.64 (dd, J = 11.8, 5.3 Hz, 3H, H-6b), 3.59 - 3.44 (m, 9H, CH*H*-O, H-3, H-4), 3.40 - 3.27 (m, 18H, CH₂-N, H-5, H-5', H-3', H-4'), 3.25 - 3.18 (m, 6H, H-2, H-2'), 1.58 (dd, J = 15.0, 6.7 Hz, 12H, CH₂), 1.31 (d, J = 26.4 Hz, 48H, CH₂); $\frac{13}{12}$ C NMR (101 MHz, MeOD) δ 136.8 (C_q), 129.8 (CH_{arom}), 104.6, 104.2 (C-1, C-1'), 80.7 (C-4), 78.1, 77.8 (C-3, C-3'), 76.4, 76.4 (C-5, C-5'), 74.9, 74.8 (C-2, C-2'), 71.3 (C-4'), 70.9 (CH₂-O), 62.4, 61.8 (C-6, C-6'), 41.2 (CH₂-N), 30.7, 30.6, 30.5, 28.1, 27.1 (CH₂); HRMS [C₈₁H₁₄₁N₃O₃₆ + H]+: 1732.93776 found, 1732.93675 calculated.

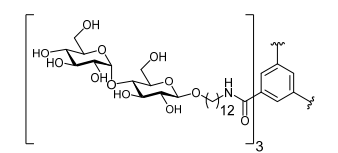
N^1 , N^3 , N^5 -Tris-(dodecyl-12-O-[4-O-(β -D-galactopyranosyl)- β -D-glucopyranoside])-benzene-1,3,5-tricarboxamide (216).



Lactoside **243** (153.1 mg, 39 μ mol) was dissolved in a mixture of dioxane, *t*-BuOH and MeOH (4 mL, 0.01 M, 1/1/1, v/v/v), a solution of NaOMe was added (3 drops) and the mixture was stirred overnight. Purification via RP-

HPLC (linear gradient 25 - 70 % B in A, 10 min, Gemini-NX 5μm C18, 110 Å, 250 x 12.0 mm, 5 mL/min) yielded title compound **216** as a white powder after lyophilization (8.9 mg, 5.1 μmol, 13%). <u>LC-MS</u>: $R_t = 6.02$ min (10 - 90% ACN; 13 min); <u>IR</u> (neat, cm⁻¹): 3565, 2921, 2852, 1647, 1064, 1024, 704; <u>¹H NMR</u> (500 MHz, DMSO) δ 8.62 (t, J = 5.6 Hz, 3H, NH), 8.34 (s, 3H, BTA-H_{arom}), 5.07 (t, J = 5.1 Hz, 6H, 2-OH, -OH), 4.82 - 4.73 (m, 3H, -OH), 4.69 - 4.60 (m, 6H, -OH), 4.56 - 4.47 (m, 6H, 6-OH, 6'-OH), 4.19 (d, J = 7.5 Hz, 3H, H-1'), 4.16 (d, J = 7.9 Hz, 3H, H-1), 3.78 - 3.69 (m, 6H, CHH-O, H-6a), 3.64 - 3.23 (m, 39H, CHH-O, H-6b, H-6', H-4, H-3', H-5, H-5', H-2', H-3, CH₂-N), 3.02 - 2.95 (m, 3H, H-2), 1.57 - 1.45 (m, 12H, CH₂), 1.35 - 1.19 (m, 48H, CH₂); $\frac{13}{C}$ NMR (126 MHz, DMSO) δ 165.4 (C=O), 135.1 (C_q), 128.3 (CH_{arom}), 103.9 (C-1'), 102.5 (C-1), 80.8, 75.5, 75.0, 74.8, 73.2, 73.1, 70.5 (C-2, C-2', C-3, C-3', C-4', C-5, C-5'), 68.7 (CH₂-O), 68.1 (C-4), 60.5 (C-6'), 60.4 (C-6), 39.7 (CH₂-N), 29.3, 29.1, 29.0, 29.0, 29.0, 28.8, 26.5, 25.5 (CH₂); $\frac{13}{C}$ -GATED (126 MHz, CDCl₃) δ 103.9 (d, J = 160 Hz, C-1'), 102.5 (d, J = 159 Hz, C-1); HRMS [C₈₁H₁₄₁N₃O₃₆ + 2H]²⁺: 866.97174 found, 866.97202 calculated.

N^1 , N^3 , N^5 -Tris-(dodecyl-12-O-[4-O-(α -D-glucopyranosyl)- β -D-glucopyranoside])-benzene-1,3,5-tricarboxamide (217).

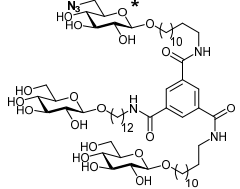


Maltoside **244** (166.4 mg, 42 μ mol) was dissolved in a mixture of dioxane, *t*-BuOH and MeOH (4 mL, 0.01 M, 1/1/1, v/v/v), a solution of NaOMe was added (3 drops) and the mixture was stirred overnight. Purification via RP-

HPLC (linear gradient 29 - 66 % B in A, 10 min, Gemini-NX 5μm C18, 110 Å, 250 x 12.0 mm, 5 mL/min) yielded title compound **217** as a white powder after lyophilization (19.8 mg, 11.4 μmol, 27%). <u>LC-MS</u>: R_t = 9.69 min (0 - 50% ACN; 13 min); <u>IR</u> (neat, cm⁻¹): 3328, 2923, 2853, 1647, 1289, 1021, 912; <u>¹H NMR</u> (500 MHz, DMSO) δ 8.63 (t, J = 5.6 Hz, 3H, NH), 8.36 (s, 3H, BTA-H_{arom}), 5.01 (d, J = 3.9 Hz, 3H, H-1'), 4.15 (d, J = 7.8 Hz, 3H, H-1), 3.75 (dt, J = 9.5, 6.8 Hz, 3H, C*H*H-O), 3.70 (d, J = 10.3 Hz, 3H, H-6a), 3.64 - 3.60 (m, 3H, H-6a'), 3.59 - 3.34 (m, 18H, H-3, H-3', CH*H*-O, H-6b', H-6b', H-5'), 3.34 - 3.25 (m, 9H, CH₂-N, H-4), 3.25 - 3.19 (m, 6H, H-2', H-5), 3.07 (t, J = 9.2 Hz, 3H, H-4'), 3.03 - 2.96 (m, 3H, H-2), 1.52 (dq, J

= 14.1, 6.8 Hz, 12H, CH₂), 1.28 (d, J = 22.2 Hz, 48H, CH₂); $\frac{13C \text{ NMR}}{2}$ (126 MHz, DMSO) δ 165.4 (C=O), 135.1 (C_q), 128.3 (CH_{arom}), 102.7 (C-1), 100.8 (C-1), 79.7 (C-4), 76.4 (C-3), 75.1 (C-5), 73.5 (C-5), 73.3 (C-3), 73.0 (C-2), 72.5 (C-2), 69.9 (C-4), 68.7 (CH₂-O), 60.8 (C-6), 60.6 (C-6), 39.4 (CH₂-N), 29.3, 29.1, 29.1, 29.0, 28.8, 26.5, 25.5 (CH₂); $\frac{13C-GATED}{2}$ (126 MHz, DMSO) δ 102.7 (d, J = 160 Hz, C-1), 100.8 (d, J = 170 Hz, C-1); HRMS [C₈₁H₁₄₁N₃O₃₆ + H]+: 1732.93655 found, 1732.93675 calculated.

N^{1} -(Dodecyl-12-O-[6-azido-6-deoxy- β -D-glucopyranoside])- N^{3} , N^{5} -bis-(dodecyl-12-O- β -D-glucopyranoside)-benzene-1,3,5-tricarboxamide (218).



Acceptor 220 (78 mg, 0.10 mmol, 1 eq) and donor 228 (112.4 mg, 0.17 mmol, 1.7 eq) were combined and co-evaporated with toluene (3x) under N_2 atmosphere, dissolved in a mixture of anhydrous DCM/HFIP (4 mL, 0.025 M, 4/1, v/v) and stirred with activated molecular sieves (3Å) for 30 min. The reaction mixture was

cooled to 0 °C, TfOH (8.8 µL, 0.1 mmol, 1 eq) was added dropwise and the mixture was stirred at 0 °C for 15 min after which a solution of donor 221 (222.2 mg, 0.30 mmol, 3 eq) in anhydrous DCM (0.6 mL, 0.5 M) was added dropwise over 10 minutes. The reaction mixture was stirred for an additional 3 hours after which it was quenched by addition of Et₃N (0.3 mL). The mixture was filtrated, concentrated in vacuo and purified using size exclusion (Sephadex LH20, 1/1, MeOH/DCM, v/v) yielding a mixture of compounds as a transparent solid (251 mg, 0.1 mmol, qnt). Based on ¹H NMR the mixture contains an average of 0.3 equivalent of migrated benzoyl, 1.6 equivalent of normal glucosides and 1.1 eq of azido glucose per BTA (based on bold integrals). 1H NMR (400 MHz, CDCl₃) δ 8.38 (s, **3.00H, BTA-H**_{arom}), 8.05 – 7.77 (m, 21H, H_{arom} , 7.57 – 7.23 (m, 34H, H_{arom}), 6.72 (s, 3H, NH), 5.91 (dt, I = 11.9, 9.7 Hz, 2.68H, H-3, H-3*), 5.68 (t, J = 9.7 Hz, 1.67 H, H-4), 5.57 - 5.48 (m, 2.76 H, H-2, H-2*), 5.45 (t, J = 9.7 Hz, 1 H, H-4*), 4.85 (d, J = 7.8 Hz)Hz, 2.64H, H-1, H-1*), 4.64 (dd, J = 12.1, 3.2 Hz, **1.60H, H-6a**), 4.51 (dd, J = 12.1, 5.2 Hz, 1.59H, H-6b), 4.31 (t, J = 6.7 Hz, **0.56H**, CH_2 -OBz), 4.21 – 4.13 (m, 1.63H, H-5), 4.03 – 3.87 (m, 3.96H, H-5*, CHH-O-Glu), 3.62 - 3.50 (m, 4.01H, C- $6a^*$, CHH-O-Glu), 3.42 (q, J = 6.7 Hz, 6.24H, CH₂-N), 3.30 (dd, J = 6.7 Hz, 6.24H, 13.4, 2.3 Hz, **1.09H, C-6b***), 1.65 – 1.45 (m, 12H, CH₂), 1.39 – 0.92 (m, 48H, CH₂); $\frac{13C \text{ NMR}}{12C \text{ NMR}}$ (101 MHz, CDCl₃) δ 166.2, 165.9, 165.9, 165.8, 165.4, 165.3, 165.2, 165.1 (C=O), 135.4 (C_q), 133.7, 133.5, 133.3, 133.3, 133.3, 133.2, 133.2, 129.9, 129.9, 129.8, 129.8 (CH_{arom}), 129.7, 129.6, 129.4, 129.4, 128.9, 128.9, 128.8, 128.6 (C_q) , 128.6, 128.5, 128.4, 128.4, 128.4, 128.1 (CH_{arom}), 101.4 (C-1), 101.1 (C-1*), 74.2 (C-5*), 73.0, 72.7 (C-1*) 3, C-3*), 72.2 (C-5), 72.0, 71.9 (C-2, C-2*), 70.5 (C-4*), 70.5, 70.3 (CH₂-O-Glu), 69.9 (C-4), 65.2 (CH₂-OBz), 63.3 (C-6), 51.4 (C-6*), 40.5 (CH₂-N), 29.6, 29.6, 29.6, 29.5, 29.5, 29.5, 29.4, 29.3, 27.1, 25.8, 25.8 (CH₂). This mixture of compounds (125 mg, ~51 µmol) was dissolved in a mixture of dioxane, t-BuOH and MeOH (2 mL, 0.01 M, 1/1/1, v/v/v), a solution of NaOMe was added (3 drops) and the mixture was stirred overnight. Purification via RP-HPLC (linear gradient 35 - 66 % B in A, 10 min, Gemini-NX 5µm C18, 110 Å, 250 x 12.0 mm, 5 mL/min) followed by a second RP-HPLC purification (linear gradient 36 -42~% B in A, 12 min, Vydac 219TP Diphenyl, $5~\mu m$, 250~x 10.0 mm, 5~mL/min) yielded title compound 218 as a white powder after lyophilization (6 mg, 4.7 µmol, 9%) (careful separation also allowed for the isolation of **214** as side product in 8.2 mg, 6.6 μ mol, 13%). LC-MS: $R_t = 6.62 \min (10 - 90\% ACN; 13 \min);$

<u>I.C.-MS</u>: R_t = 10.20 min (10 - 90% ACN; 21 min, Diphenyl) <u>IR</u> (neat, cm⁻¹): 3370, 2922, 2852, 2097, 1641, 1528, 1075, 1023; <u>1H NMR</u> (500 MHz, DMSO) δ 8.64 (t, J = 5.4 Hz, 3H, NH), 8.35 (s, 3H, BTA-H_{arom}), 5.41 (s, 1H, -OH), 5.20 – 5.02 (m, 3H, -OH), 4.96 – 4.84 (m, 5H, -OH), 4.46 (t, J = 5.8 Hz, 2H, -OH), 4.19 (d, J = 7.8 Hz, 1H, H-1*), 4.08 (d, J = 7.8 Hz, 2H, H-1), 3.73 (ddd, J = 15.6, 9.1, 6.9 Hz, 3H, C*H*H-O), 3.65 (dd, J = 10.9, 4.9 Hz, 2H, H-6a), 3.47 – 3.30 (m, 8H, H-6b, CH*H*-O, H-6*, H-5*), 3.26 (q, J = 6.6 Hz, 6H, CH_2 -NH), 3.17 – 2.98 (m, 8H, H-3, H-4, H-5, H-4*, H-3*), 2.97 (dd, J = 8.3, 3.6 Hz, 1H, H-2*), 2.92 (td, J = 8.5, 4.7 Hz, 2H, H-2), 1.50 (dt, J = 14.1, 6.9 Hz, 12H, CH₂), 1.36 – 1.16 (m, 48H, CH₂); $\frac{13}{2}$ C NMR (126 MHz, DMSO) δ 165.4 (C=O), 135.1 (C_q), 128.3 (BTA-CH_{arom}), 102.8 (C-1), 102.7 (C-1*), 76.8, 76.8 (C-3, C-5), 76.3 (C-3*), 75.4 (C-5*), 73.4 (C-2), 73.3 (C-2*), 71.0 (C-4*), 70.1 (C-4), 68.6 (CH₂-O), 61.1 (C-6), 51.4 (C-6*), 39.3 (CH₂-N), 29.3, 29.1, 29.0, 29.0, 28.8, 26.5, 25.6 (CH₂); $\frac{13}{2}$ C-GATED (126 MHz, CDCl₃) δ 102.8 (d, J = 159 Hz, C-1), 102.7 (d, J = 158 Hz, C-1*); HRMS [C₆3H₁₁₀N₆O₂₀ + H]+: 1271.78499 found, 1271.78477 calculated.

References

- (1) Hendrikse, S. I. S.; Su, L.; Hogervorst, T. P.; Lafleur, R. P. M.; Lou, X.; van der Marel, G. A.; Codée, J. D. C.; Meijer, E. W. Elucidating the Ordering in Self-Assembled Glycocalyx Mimicking Supramolecular Copolymers in Water. *J. Am. Chem. Soc.* **2019**, *141*, 13877–13886. https://doi.org/10.1021/jacs.9b06607.
- (2) Mammen, M.; Choi, S.-K.; Whitesides, G. M. Polyvalent Interactions in Biological Systems: Implications for Design and Use of Multivalent Ligands and Inhibitors. *Angew. Chemie Int. Ed.* **1998**, *37*, 2754–2794. https://doi.org/10.1002/(SICI)1521-3773(19981102)37:20<2754::AID-ANIE2754>3.0.CO;2-3.
- (3) Célia Monteiro de Paula, R.; Andrade Feitosa, J.; Beserra Paula, H. Polysaccharide Based Copolymers as Supramolecular Systems in Biomedical Applications. *Curr. Drug Targets* **2015**, *16*, 1591–1605. https://doi.org/10.2174/1389450116666151001113537.
- (4) Sasisekharan, R.; Raman, R.; Prabhakar, V. GLYCOMICS APPROACH TO STRUCTURE-FUNCTION RELATIONSHIPS OF GLYCOSAMINOGLYCANS. *Annu. Rev. Biomed. Eng.* **2006**, *8*, 181–231. https://doi.org/10.1146/annurev.bioeng.8.061505.095745.
- (5) Freudenberg, U.; Liang, Y.; Kiick, K. L.; Werner, C. Glycosaminoglycan-Based Biohybrid Hydrogels: A Sweet and Smart Choice for Multifunctional Biomaterials. *Adv. Mater.* **2016**, *28*, 8861–8891. https://doi.org/10.1002/adma.201601908.
- (6) García-Vallejo, J. J.; Ambrosini, M.; Overbeek, A.; van Riel, W. E.; Bloem, K.; Unger, W. W. J.; Chiodo, F.; Bolscher, J. G.; Nazmi, K.; Kalay, H.; van Kooyk, Y. Multivalent Glycopeptide Dendrimers for the Targeted Delivery of Antigens to Dendritic Cells. *Mol. Immunol.* **2013**, *53*, 387–397. https://doi.org/10.1016/j.molimm.2012.09.012.
- (7) Chiodo, F.; Enríquez-Navas, P. M.; Angulo, J.; Marradi, M.; Penadés, S. Assembling Different Antennas of the Gp120 High Mannose-Type Glycans on Gold Nanoparticles Provides Superior Binding to the Anti-HIV Antibody 2G12 than the Individual Antennas. *Carbohydr. Res.* **2015**, *405*, 102–109. https://doi.org/10.1016/j.carres.2014.07.012.
- (8) Wilson, D. S.; Hirosue, S.; Raczy, M. M.; Bonilla-Ramirez, L.; Jeanbart, L.; Wang, R.; Kwissa, M.; Franetich, J.-F. F.; Broggi, M. A. S. S.; Diaceri, G.; Quaglia-Thermes, X.; Mazier, D.; Swartz, M. A.; Hubbell, J. A. Antigens Reversibly Conjugated to a Polymeric Glyco-Adjuvant Induce Protective Humoral and Cellular Immunity. *Nat. Mater.* 2019, *18*, 175–185. https://doi.org/10.1038/s41563-018-0256-5.
- (9) Zhu, D.; Hu, C.; Fan, F.; Qin, Y.; Huang, C.; Zhang, Z.; Lu, L.; Wang, H.; Sun, H.; Leng, X.; Wang, C.; Kong, D.; Zhang, L. Co-Delivery of Antigen and Dual Agonists by Programmed Mannose-Targeted Cationic Lipid-Hybrid Polymersomes for Enhanced Vaccination. *Biomaterials* **2019**, *206*, 25–40. https://doi.org/10.1016/j.biomaterials.2019.03.012.
- (10) Meyers, M. A.; Chen, P.-Y.; Lin, A. Y.-M.; Seki, Y. Biological Materials: Structure and Mechanical Properties. *Prog. Mater. Sci.* **2008**, *53*, 1–206. https://doi.org/10.1016/j.pmatsci.2007.05.002.
- (11) Webber, M. J.; Appel, E. A.; Meijer, E. W.; Langer, R. Supramolecular Biomaterials. *Nat. Mater.* **2015**, *15*, 13–26. https://doi.org/10.1038/nmat4474.
- (12) Leenders, C. M. A.; Albertazzi, L.; Mes, T.; Koenigs, M. M. E.; Palmans, A. R. A.; Meijer, E. W. Supramolecular Polymerization in Water Harnessing Both Hydrophobic Effects and Hydrogen Bond Formation. *Chem. Commun.* **2013**, *49*, 1963. https://doi.org/10.1039/c3cc38949a.
- (13) Leenders, C. M. A.; Baker, M. B.; Pijpers, I. A. B.; Lafleur, R. P. M.; Albertazzi, L.; Palmans, A. R. A.; Meijer, E. W. Supramolecular Polymerisation in Water; Elucidating the Role of Hydrophobic and Hydrogen-Bond Interactions. *Soft Matter* **2016**, *12*, 2887–2893. https://doi.org/10.1039/C5SM02843D.
- (14) Albertazzi, L.; van der Zwaag, D.; Leenders, C. M. A.; Fitzner, R.; van der Hofstad, R. W.; Meijer, E. W. Probing Exchange Pathways in One-Dimensional Aggregates with Super-Resolution Microscopy. *Science (80-.)*. 2014, 344, 491–495. https://doi.org/10.1126/science.1250945.
- (15) Armstrong, J. K.; Hempel, G.; Koling, S.; Chan, L. S.; Fisher, T.; Meiselman, H. J.; Garratty, G. Antibody against Poly(Ethylene Glycol) Adversely Affects PEG-Asparaginase Therapy in Acute Lymphoblastic Leukemia Patients. *Cancer* **2007**, *110*, 103–111. https://doi.org/10.1002/cncr.22739.
- (16) Richter, A. W.; Åkerblom, E. Polyethylene Glycol Reactive Antibodies in Man: Titer Distribution in Allergic Patients Treated with Monomethoxy Polyethylene Glycol Modified Allergens or Placebo, and in Healthy

- Blood Donors. Int. Arch. Allergy Immunol. 1984, 74, 36–39. https://doi.org/10.1159/000233512.
- (17) Pelegri-O'Day, E. M.; Lin, E.-W.; Maynard, H. D. Therapeutic Protein–Polymer Conjugates: Advancing Beyond PEGylation. *J. Am. Chem. Soc.* **2014**, *136*, 14323–14332. https://doi.org/10.1021/ja504390x.
- (18) Leenders, C. M. A.; Jansen, G.; Frissen, M. M. M.; Lafleur, R. P. M.; Voets, I. K.; Palmans, A. R. A.; Meijer, E. W. Monosaccharides as Versatile Units for Water-Soluble Supramolecular Polymers. *Chem. A Eur. J.* **2016**, 22, 4608–4615. https://doi.org/10.1002/chem.201504762.
- (19) Takahashi, T.; Inoue, H.; Yamamura, Y.; Doi, T. Synthesis of a Trisaccharide Library by Using a Phenylsulfonate Traceless Linker on Synphase Crowns. *Angew. Chemie Int. Ed.* **2001**, *40*, 3230–3233. https://doi.org/10.1002/1521-3773(20010903)40:17<3230::AID-ANIE3230>3.0.CO;2-Z.
- (20) Becker, B.; Furneaux, R. H.; Reck, F.; Zubkov, O. a. A Simple Synthesis of 8-(Methoxycarbonyl)Octyl 3,6-Di-O-(α-d-Mannopyranosyl)-α-d-Mannopyranoside and Derivatives and Their Use in the Preparation of Neoglycoconjugates. *Carbohydr. Res.* **1999**, *315*, 148–158. https://doi.org/10.1016/S0008-6215(98)00330-9.
- Egusa, K.; Kusumoto, S.; Fukase, K. Solid-Phase Synthesis of a Phytoalexin Elicitor Pentasaccharide Using a 4-Azido-3-Chlorobenzyl Group as the Key for Temporary Protection and Catch-and-Release Purification. *European J. Org. Chem.* **2003**, 2003, 3435–3445. https://doi.org/10.1002/ejoc.200300248.
- Cammarata, A.; Upadhyay, S. K.; Jursic, B. S.; Neumann, D. M. Antifungal Activity of 2α,3β-Functionalized Steroids Stereoselectively Increases with the Addition of Oligosaccharides. *Bioorg. Med. Chem. Lett.* **2011**, *21*, 7379–7386. https://doi.org/10.1016/j.bmcl.2011.10.015.
- (23) Biswas, G.; Jeon, O.-Y.; Lee, W. S.; Kim, D.-C.; Kim, K.-T.; Lee, S.; Chang, S.; Chung, S.-K. Novel Guanidine-Containing Molecular Transporters Based on Lactose Scaffolds: Lipophilicity Effect on the Intracellular Organellar Selectivity. *Chem. A Eur. J.* **2008**, *14*, 9161–9168. https://doi.org/10.1002/chem.200801160.
- (24) Sprung, I.; Ziegler, A.; Flitsch, S. L. Enzymatic Synthesis of β-Mannosyl Phosphates on Solid Support. *Chem. Commun.* **2002**, *2*, 2676–2677. https://doi.org/10.1039/B206451K.
- (25) Hilário, F. F.; de Paula, R. C.; Silveira, M. L. T.; Viana, G. H. R.; Alves, R. B.; Pereira, J. R. C. S.; Silva, L. M.; de Freitas, R. P.; de Pilla Varotti, F. Synthesis and Evaluation of Antimalarial Activity of Oxygenated 3-Alkylpyridine Marine Alkaloid Analogues. *Chem. Biol. Drug Des.* **2011**, *78*, 477–482. https://doi.org/10.1111/j.1747-0285.2011.01154.x.
- (26) Kuroda, H.; Chen, Y. N.; Kimura, T.; Sakakibara, S. Powerful Solvent Systems Useful for Synthesis of Sparingly-Soluble Peptides in Solution. *Int. J. Pept. Protein Res.* **1992**, 40, 294–299. https://doi.org/10.1111/j.1399-3011.1992.tb00304.x.
- De, K.; Legros, J.; Crousse, B.; Bonnet-Delpon, D. Synthesis of 2,3-Unsaturated Glycosides via Metal-Free Ferrier Reaction. *Tetrahedron* **2008**, *64*, 10497–10500. https://doi.org/10.1016/j.tet.2008.09.005.

Summary and future prospects

The adaptive immune system is able to efficiently and selectively battle pathogens and aberrant cells. Tailored immune responses have been exploited in many therapeutic approaches, combatting both infections and tumors. One of these approaches trains naïve immune cells using a vaccine strategy, in which antigens and adjuvants are administered to antigen-presenting cells (APCs). The adjuvant is a necessary component of a vaccine, as it stimulates the APC to mature, thereby upregulating the levels of antigen presentation and co-stimulatory factors. Adjuvants can be recognized by pathogen recognizing receptors (PRRs) present on APCs. Two sub-families of PRRs have been targeted extensively with synthetic ligands and vaccines: the toll-like receptors (TLRs) and C-type lectin receptors (CLRs). TLRs are often exploited for their ability to mature APCs, while CLRs are targeted for their capacity to endocytose pathogens. A subset of these CLRs (MR, DC-SIGN, and langerin) can recognize mannose based glycans and these receptors have been extensively studied and targeted with mannosylated constructs, as summarized in Chapter 1. Signaling pathways initiated by these CLRs often work in concert with those triggered by TLR activation, and it has been demonstrated that simultaneous targeting of these receptors can improve and prolong the immune response synergistically. The work presented in this thesis studies and exploits the activation of the immune system with antigen-adjuvant conjugates, equipped with well-defined mannosylated conjugates.

The affinity of mannosylated constructs for DC-SIGN, langerin, and the mannose receptor have been extensively studied. Due to the multimeric nature of the three CLRs, a large number of multivalent constructs has been designed and tested in a variety of assays. Because of the variation in structure and nature of the interaction assays, clear structure-activity relationship can be difficult to assess. Chapter 2 describes the synthesis of a systematic library that investigates the effect of the number of mannoside copies and the structure of these mannosides on binding affinity for DC-SIGN, langerin and the MR, and cell uptake by these receptors. It has previously been difficult to study the MR in vitro due to the lability of this receptor when isolated. To allow affinity studies with this receptor, selected members from the mannoside library have been decorated with a laserdye to enable the tracking of single molecules in a super-resolution microscopy assay. This approach allowed, for the first time, the determination of relative affinities for the MR in a natural setting. The affinity studies for all three CLRs have revealed a similar structure-activity trend, with an increasing number of mannosides leading to increased affinity, in line with previous reports. Affinity for the MR significantly increases when comparing constructs bearing 1 or 2 mannosides with that carrying 6 copies. The difference in affinity for DC-SIGN was neglectable for clusters bearing 3 or 6 mannoside copies. However, the type of mannosides in the clusters had a large influence on the affinity for DC-SIGN, which shows a preference for α1,2-dimannosides. Since the affinity of the largest mannoside (an $\alpha 1,3-\alpha 1,6$ -tri-mannoside) seemed to decrease when six instead of three copies were installed on the clusters, it would be relevant to test whether this was the result of the scaffold used. By synthesizing a scaffold containing six azido lysines which are all spaced with glycines similar to the n = 3 scaffold (255, Scheme 1), followed by CuAAC ligation of the propargyl mannosides, hexavalent mannoside clusters 256 could be synthesized. These clusters could be compared with their shorter analogs described in Chapter 2. Longer spacers between the mannosides and the lysine scaffold may also be explored.

Langerin and the MR did not show a clear preference for the configuration of the mannosides in the clusters, as observed for DC-SIGN. Both di- and tri- mannosides showed comparable affinities for these receptors. Since the MR has multiple CRDs that can recognize mannosides, but only one domain that can bind sulfated galactosides, both ligands could be used to gain a deeper insight of the binding interactions with the MR. The results of this assay for example, indicated that the increase in binding affinity for mannosides with higher valency is most likely due to rebinding of the CRDs in close proximity rather than the binding of multiple CRDs simultaneously or even multiple receptors simultaneously.

Scheme 1: Synthesis of hexavalent clusters with similar spacing as the previously described n=3 & n=2 clusters.

The simultaneous targeting of both TLR and CLR has been a promising approach to generate more effective vaccines. To improve the synthetic accessibility of conjugates targeting TLR7, **Chapter 3** describes improvements in the synthesis of a TLR7 agonist which can be incorporated 'in-line' during a solid-phase peptide synthesis (SPPS) campaign. The alterations made to the synthetic steps improved the workability of the synthetic route and allowed for the large scale preparation of a Boc-protected building block. Chapter 3 also describes the synthesis of bifunctional ligands that can bind both mannose-binding CLRs and TLR7.

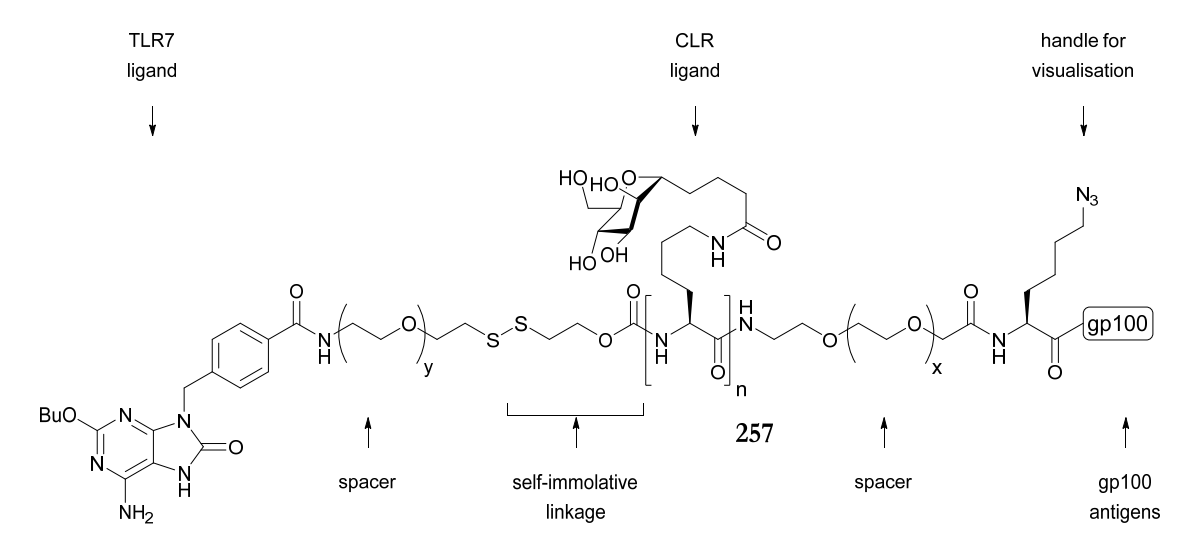
In Chapter 4, elements from the previous two chapters are combined in the synthesis of trifunctional conjugates that bear both a TLR7 ligand and mannoside clusters combined with a model gp100 antigen. The SPPS of the azido gp100 peptide required double couplings at elevated temperature and the addition of phenol to the cleavage cocktail to obtain sufficient quantities of product. For the introduction of the mannosides, both the simultaneous CuAAC of multiple propargyl mannosides and the conjugation of a pre-assembled mannoside clusters were planned. The pre-assembly of conjugatable mannoside clusters was easily achieved, whereas the synthesis of the gp100 peptide bearing six azides proved difficult. Therefore, the route requiring multiple simultaneous CuAAC events was abandoned. Evaluation of the conjugates showed that the addition of the TLR7 ligand improved the effectiveness of the conjugates. Conjugation to the hexavalent mannoside clusters further improved the activity of the gp100 conjugates. The synthetic route towards this gp100 platform allows for the conjugation of a carbohydrate cluster at a late stage of the synthesis, which allows for the generation of conjugates bearing different type of adjuvants. The presence of both an MHC-II and MHC-II epitope in the same peptide can be used to establish which combination of adjuvants would lead to optimal (cross-)presentation. The

platform allows for the variation of the ligands introduced via CuAAC (**R**₂, Figure 1) and ligands introduced during SPPS on either the N-terminus, C-terminal lysine or both (**R**₁, Figure 1). Instead of the TLR7 adjuvant, other TLR-ligands can be introduced, such as Pam3Cys targeting TLR2,¹ CPG like conjugates to target TLR9,² or a poly-I:C ligand to target TLR3.³ Combining lipophilic conjugates such as Pam3Cys with hydrophilic carbohydrates such as the mannosides clusters can enhance the poor water solubility of the lipophilic peptides.⁴ Instead of (oligo)mannosides, the antigen can also be combined with other glycans or adjuvants. For example, the introduction of fucosylated glycans such as the Lewis antigens can skew the type of T_h cell response.^{5,6} Another possibility would be to pivot the immune response from inflammatory towards anti-inflammatory. By the introduction of sialic acid-containing structures, sialic acid-binding immunoglobulin-type lectins (SIGLECs) can be targeted.⁷ Instead of targeting CLRs, an alternative would be the introduction of a muramyl dipeptide (MDP) which can lead to the engagement of the NOD2 receptor.⁸

Figure 1: Variations on the gp100 conjugates.

To improve the stability, and to allow the 'inline' introduction of mannoside clusters, Chapter 5 describes the synthesis of a stabilized C-mannosyl functionalized Fmoc protected lysine building block, in which acid-labile para-methoxybenzyl (PMB) groups are used to mask the hydroxyl groups to prevent unwanted side reactions on these functionalities. This C-mannosyl building block was successfully used in SPPS to generate both small clusters and gp100 conjugates. The deprotection and cleavage from the resin required additional scavengers to prevent side reactions originating from the released PMB cations. The use of PMB groups could be combined with the use of a monomethoxy trityl (Mmt) protecting group, when the latter was removed with a mixture of acetic acid, trifluoroethanol, and dichloromethane. The C-mannoside clusters and conjugates bind with similar affinity to CLRs as their O-mannoside analogs, and also the antigen presentation of conjugates bearing the C-mannosides was comparable to their O-mannoside counterparts. The ability to introduce these clusters 'in-line' allowed for the synthesis of clusters with both CLR and TLR clusters on the same terminus. However, this configuration hampered the effectiveness of these constructs. A potential solution for this would be to use a self-immolative linker between the C-mannosides and TLR7 agonist. The use of the C-mannoside also allows for the introduction of an azide handle in the conjugates, which can be used for tracking of the antigens (e.g., 257, Figure 2).

Figure 2: Second generation of *C*-mannosyl conjugates.



Chapter 6 describes the synthesis of glycosylated benzene-1,3,5-tricarboxyamide (BTA) monomers, which can self-assemble into supramolecular fibers in an aqueous environment. Two synthetic strategies have been assessed, both suffering from solubility issues. Eventually, the assembly of the BTA monomers was successful by the condensation of glycosyl imidate donors

and a BTA-triol in an unusual solvent system, compromising a mixture of 1,1,1,3,3,3hexafluoroisopropanol (HFIP) and DCM. The nucleophilicity of the HFIP proved to be sufficiently low to prevent any significant competition during the condensation reactions. The glycosylations was met with side reactions such as the formation of ortho-esters and benzoyl migration. These side-products proved to be difficult to remove from the product mixture, but after cleavage of the benzoyl groups, the products and side-products could be separated via RP-HPLC. Both the mannose and glucose BTAs were able to self-assemble in 2D fibers. Notably, the sugar residues induced the formation of fibers of opposite helicity. Since these two constructs differ at two positions in the carbohydrate appendage, it would be of interest to determine whether the helicity is caused by the configuration at C-2 or the stereochemistry of the anomeric bond. By synthesis of the 1,2-cis gluco and manno-isomers, this could be studied. A potential synthetic route towards these constructs can use donor 258 bearing acid-labile benzyl-like protecting groups (Nap or PMB, see Scheme 2). Activation of donor 258 by TMSI in the presence triphenyl oxide allows for as-selective couplings with a primary alcohol such as 220. The obtained α -glucoside 259 could then be deprotected using HCl in HFIP to obtain target construct 260.11 For the β-mannoside BTA, a benzylidene protected mannoside imidate donor such as 261 could be used at low temperature to generate cis-mannoside 262. This mannoside could generate β-mannoside 263 by acidic deprotection. It will be of interest to establish whether these glycosylations tolerate the use of HFIP as a co-solvent.

Scheme 2: Synthetic route towards the BTA mannose and glucose stereoisomers.

Reagents and conditions: a) TMSI, Ph₃P=O, DCM, HFIP; ¹⁰ b) HCl/HFIP, DCM/HFIP; ¹¹ c) TMSOTf, DCM, HFIP, -40°C. ^{12,13}

The synthesis of a BTA monomer that bears two glucose and one 6-azido-6-deoxy-glucose residue is also described in Chapter 6. The azide handle in this monomer can be used for further decoration with reporter groups, adjuvants (e.g., 265), or epitopes (e.g., 264). For example, the co-assembly of mannosylated-BTA monomers (213) in combination with BTA cores functionalized with the gp100 epitope (266) and TLR7 agonist (267) could form a multivalent system that can target both CLRs and TLR7. By mixing the components in different ratios, many self-assembled polymers (268) can be evaluated (see Scheme 3).

Scheme 3: Assembly of BTA fibers that bear antigen, a TLR7 agonist and mannosides.

References

- (1) Khan, S.; Weterings, J. J.; Britten, C. M.; de Jong, A. R.; Graafland, D.; Melief, C. J. M.; van der Burg, S. H.; van der Marel, G.; Overkleeft, H. S.; Filippov, D. V.; Ossendorp, F. Chirality of TLR-2 Ligand Pam3CysSK4 in Fully Synthetic Peptide Conjugates Critically Influences the Induction of Specific CD8+ T-Cells. *Mol. Immunol.* **2009**, *46*, 1084–1091. https://doi.org/10.1016/j.molimm.2008.10.006.
- (2) Khan, S.; Bijker, M. S.; Weterings, J. J.; Tanke, H. J.; Adema, G. J.; Van Hall, T.; Drijfhout, J. W.; Melief, C. J. M.; Overkleeft, H. S.; Van Der Marel, G. A.; Filippov, D. V.; van der Burg, S. H.; Ossendorp, F. Distinct Uptake Mechanisms but Similar Intracellular Processing of Two Different Toll-like Receptor Ligand-Peptide Conjugates in Dendritic Cells. *J. Biol. Chem.* **2007**, *282*, 21145–21159. https://doi.org/10.1074/jbc.M701705200.
- (3) Naumann, K.; Wehner, R.; Schwarze, A.; Petzold, C.; Schmitz, M.; Rohayem, J. Activation of Dendritic Cells by the Novel Toll-Like Receptor 3 Agonist RGC100. *Clin. Dev. Immunol.* **2013**, 2013, 1–11. https://doi.org/10.1155/2013/283649.
- (4) Gential, G. P. P.; Ho, N. I.; Chiodo, F.; Meeuwenoord, N.; Ossendorp, F.; Overkleeft, H. S.; van der Marel, G. A.; Filippov, D. V. Synthesis and Evaluation of Fluorescent Pam3Cys Peptide Conjugates. *Bioorg. Med. Chem. Lett.* **2016**, *26*, 3641–3645. https://doi.org/10.1016/j.bmcl.2016.05.094.
- (5) Gringhuis, S. I.; den Dunnen, J.; Litjens, M.; van der Vlist, M.; Geijtenbeek, T. B. H. Carbohydrate-Specific Signaling through the DC-SIGN Signalosome Tailors Immunity to Mycobacterium Tuberculosis, HIV-1 and Helicobacter Pylori. *Nat. Immunol.* **2009**, *10*, 1081–1088. https://doi.org/10.1038/ni.1778.
- (6) Geijtenbeek, T. B. H.; Gringhuis, S. I. C-Type Lectin Receptors in the Control of T Helper Cell Differentiation. *Nat. Rev. Immunol.* **2016**, *16*, 433–448. https://doi.org/10.1038/nri.2016.55.
- (7) Schwarz, F.; Landig, C. S.; Siddiqui, S.; Secundino, I.; Olson, J.; Varki, N.; Nizet, V.; Varki, A. Paired Siglec Receptors Generate Opposite Inflammatory Responses to a Human-specific Pathogen. *EMBO J.* **2017**, *36*, 751–760. https://doi.org/10.15252/embj.201695581.
- (8) Willems, M. M. J. H. P.; Zom, G. G.; Meeuwenoord, N.; Ossendorp, F. A.; Overkleeft, H. S.; Van Der Marel, G. A.; Codée, J. D. C.; Filippov, D. V. Design, Automated Synthesis and Immunological Evaluation of NOD2-Ligand-Antigen Conjugates. *Beilstein J. Org. Chem.* **2014**, *10*, 1445–1453. https://doi.org/10.3762/bjoc.10.148.
- (9) Wilson, D. S.; Hirosue, S.; Raczy, M. M.; Bonilla-Ramirez, L.; Jeanbart, L.; Wang, R.; Kwissa, M.; Franetich, J.-F. F.; Broggi, M. A. S. S.; Diaceri, G.; Quaglia-Thermes, X.; Mazier, D.; Swartz, M. A.; Hubbell, J. A. Antigens Reversibly Conjugated to a Polymeric Glyco-Adjuvant Induce Protective Humoral and Cellular Immunity. *Nat. Mater.* 2019, 18, 175–185. https://doi.org/10.1038/s41563-018-0256-5.
- (10) Wang, L.; Overkleeft, H. S.; van der Marel, G. A.; Codée, J. D. C. Reagent Controlled Stereoselective Synthesis of α-Glucans. *J. Am. Chem. Soc.* **2018**, *140*, 4632–4638. https://doi.org/10.1021/jacs.8b00669.
- Volbeda, A. G.; Kistemaker, H. A. V.; Overkleeft, H. S.; van der Marel, G. A.; Filippov, D. V.; Codée, J. D. C. Chemoselective Cleavage of p -Methoxybenzyl and 2-Naphthylmethyl Ethers Using a Catalytic Amount of HCl in Hexafluoro-2-Propanol. *J. Org. Chem.* **2015**, *80*, 8796–8806. https://doi.org/10.1021/acs.joc.5b01030.
- (12) Crich, D. Mechanism of a Chemical Glycosylation Reaction. Acc. Chem. Res. 2010, 43, 1144–1153. https://doi.org/10.1021/ar100035r.
- (13) Volbeda, A. G. Novel Protecting Group Strategies in the Synthesis of Oligosaccharides (Dissertation), 2018.

Samenvatting

Het adaptieve immuunsysteem is in staat om efficiënt en selectief pathogenen en afwijkende cellen te bestrijden. Veel therapeutische behandelingen tegen infecties en tumoren maken gebruik van specifieke immuunreacties om zieke of vreemde cellen op te ruimen. Een van deze behandelingen traint naïeve immuun cellen tegen specifieke structuren (antigenen) welke tot expressie komen op het pathogeen of de zieke cel. Deze vaccinatiestrategie combineert een antigeen met een moleculaire structuur die kan worden herkend door een antigeen presenterende cel (APC) en die instaat is om deze cel te activeren, een zogenaamd adjuvans. Het adjuvans is een noodzakelijke component van een vaccin, omdat het de APCs stimuleert tot maturiteit waardoor de mate van antigen presentatie en de productie van co-stimulatoire factoren toenemen. Adjuvans kunnen worden herkend met behulp van pathogeen herkennende receptoren (PRRs) die aanwezig zijn/tot expressie komen op APCs. Twee subfamilies van de pathogeen herkennende receptoren zijn het aangrijpingspunt voor vele synthetische liganden en vaccins: de Toll-like receptoren (TLRs) en de C-type lectine receptoren (CLRs). TLRs worden vaak gebruikt voor hun capaciteit om APCs te matureren terwijl de CLRs worden gebruikt voor hun capaciteit om pathogenen te endocyteren. Een sub-set van deze CLRs, namelijk de mannose receptor (MR, CD206), DC-SIGN (CD-209) en langerin (CD-207), kunnen op mannose gebaseerde koolhydraten herkennen. Deze receptoren zijn uitgebreid bestudeerd en veelal het aangrijpingspunt voor gemannosyleerde constructen zoals

beschreven in **Hoofdstuk 1**. Signaleringsroutes geïnitieerd door deze CLRs werken vaak samen met door TLR geactiveerde signaleringsroutes en het is voorheen aangetoond dat het simultaan activeren van zowel een TLR als CLR de immuunrespons synergistisch kan verbeteren en verlengen. Het werk beschreven in dit proefschrift bestudeert en gebruikt de activatie van het immuunsysteem met behulp van antigeen-adjuvans conjugaten die zijn uitgerust met goed gedefinieerde gemannosyleerde conjugaten.

De affiniteit van gemannosyleerde constructen voor DC-SIGN, langerin en de MR is uitgebreid getest. Omdat alle drie de receptoren een multimere structuur hebben, zijn er in het verleden een groot aantal multivalente constructen getest. Echter, door verschillen in de structuur en opzet van de test opstellingen, is het lastig om een duidelijke structuur-activiteit relatie te bepalen voor deze constructen. Daarom wordt in Hoofdstuk 2 de synthese van een systematische bibliotheek van verbindingen beschreven, die zowel het effect van het aantal mannoside kopieën als het effect van de mannoside structuur op de affiniteit voor DC-SIGN, MR en langerin bepaald, alsmede het effect op cel opname via de respectievelijke receptoren. Het is voorheen gebleken dat het bestuderen van de MR in vitro lastig is door de labiliteit van de geïsoleerde receptor. Om deze receptor toch te kunnen bestuderen, is een deel van de constructen in de hiervoor beschreven bibliotheek gefunctionaliseerd met een fluorescent label, dat gebruikt kan worden voor superresolutie microscopie om de constructen per molecuul te kunnen volgen. Hiermee kan voor het eerst de relatieve affiniteit voor de MR worden bepaald in een 'natuurlijke' omgeving. De resultaten van deze affiniteit studies zijn vergelijkbaar met eerder beschreven structuur-activiteit trends waarbij affiniteit toeneemt met het verhogen van het aantal mannoside kopieën. Affiniteit voor de MR wordt significant vergroot wanneer constructen met één of twee kopieën worden vergeleken met zes kopieën. Voor DC-SIGN zijn de verschillen tussen clusters met drie of zes mannoside kopieën verwaarloosbaar, maar de structuur van de gebruikte mannosides heeft een grote invloed op de affiniteit, met de hoogste affiniteit voor clusters uitgerust met α1,2-dimannosides. Voor zowel de MR als langerin is de voorkeur voor mannoside structuur niet zo duidelijk als voor DC-SIGN, en zowel de di- als tri-mannosides vertonen vergelijkbare affiniteiten voor deze receptoren. Gezien het feit dat de MR verscheidene mannose herkennende bindingsdomeinen (CRDs) kent, maar slechts één domein heeft dat gesulfateerde galactosides kan herkennen, zijn beide liganden gebruikt om een beter begrip van de bindingsinteracties van de receptor te krijgen. Uit deze experimenten is het af te leiden dat het meer waarschijnlijk is dat de verhoogde affiniteit voor multivalente mannoside clusters wordt veroorzaakt door het her-binden van de naastgelegen CRDs in plaats van het tegelijk binden van verschillende CRDs op dezelfde receptor, of zelfs het binden van verschillende CRDs op verschillende receptoren.

Het simultaan gebruiken van zowel een TLR als CLR is een veelbelovende aanpak voor het creëren van meer effectieve vaccins. Om de synthetische toegankelijkheid van conjugaten die op TLR7 gericht zijn te vergroten, wordt in **Hoofdstuk 3** een verbetering in de synthese van een TLR7 agonist beschreven. Dit ligand kan worden ingebouwd tijdens een vaste drager peptide chemie synthese (SPPS). De aanpassingen van de synthese stappen verbeteren de werkbaarheid van de route en maken het mogelijk om een *tert*-butyloxycarbonyl (Boc) beschermde TLR7-bouwsteen op grote schaal te produceren. Verder beschrijft hoofdstuk 3 de synthese van bi-functionele liganden die zowel kunnen binden aan mannose bindende CLRs als TLR7.

In Hoofdstuk 4 worden elementen uit de voorgaande hoofdstukken gebruikt voor de synthese van tri-functionele conjugaten, die een TLR7-ligand en een mannose cluster combineren met een gp100 antigen. De SPPS van het azide gefunctionaliseerde gp100 peptide vereiste dubbele koppelingen bij verhoogde temperaturen en toevoeging van phenol aan de afsplitscocktail om voldoende hoeveelheden product te kunnen isoleren. Voor de introductie van de mannose clusters waren twee strategieën bedacht. De eerste strategie behelst het simultaan koppelen van meerdere propargyl mannosides met behulp van een koper gekatalyseerde "klik-reactie" (CuAAC), terwijl de tweede aanpak gebruik maakt van vooraf geassembleerde oligomannoside clusters. Waar de synthese van vooraf geassembleerde conjugeerbare mannoside clusters gemakkelijk werd gerealiseerd, bleek de uitvoering van de eerste strategie moeilijker en daarom werd deze route niet verder uitgewerkt. Evaluatie van de conjugaten liet zien dat de toevoeging van het TLR-ligand de effectiviteit van de conjugaten vergroot. De conjugatie van hexavalente clusters verbeterde de activiteit van de conjugaten verder. Een bijkomend voordeel van de ontwikkelde synthese route is dat dit gp100 platform het mogelijk maakt om een koolhydraat cluster in een laat stadium van de synthese te introduceren. Dit maakt het makkelijk om verschillende conjugaten te genereren met variërende adjuvantia.

Om de stabiliteit van de mannoses te verbeteren en om de introductie van mannose clusters, middels een directe vaste drager synthese mogelijk te maken, beschrijft **Hoofdstuk 5** de synthese van een *C*-mannose gefunctionaliseerde lysine bouwsteen. In deze verbinding worden de mannose hydroxyl groepen gemaskeerd met zuur-labiele *para*-methoxybenzyl (PMB) groepen om ongewenste neven reacties op deze functionele groepen te voorkomen. Deze *C*-mannosyl lysine bouwsteen werd succesvol toegepast in SPPS om zowel kleine clusters als gp100 conjugaten te genereren. Het afsplitsen en ontschermen van de peptiden van de vaste drager vereiste additionele scavengers om neven reacties te voorkomen van de PMB-kationen, die gegenereerd werden tijdens de ontscherming. De PMB-groepen konden worden gebruikt in combinatie met een tijdelijke monomethoxy trityl (Mmt) bescherm-groep, wanneer deze laatste selectief werd verwijderd met

een mengsel van azijnzuur, trifluoroethanol en dichloromethane. De *C*-mannose clusters en conjugaten binden CLRs met vergelijkbare affiniteit als hun *O*-mannoside tegenhangers. Ook de antigen presentatie van de *C*-mannoside conjugaten was vergelijkbaar met de *O*-analogen. De mogelijkheid om deze clusters direct te introduceren in de peptide antigenen middels een SPPS aanpak, maakte het mogelijk om constructen te maken waarbij de CLR- en TLR-liganden aan dezelfde kant van het peptide werden verbonden. Deze configuratie belemmerde echter de effectiviteit van de constructen.

Hoofdstuk 6 omschrijft de synthese van geglycosyleerde benzene-1,3,5-tricarboxyamide (BTA) monomeren die in waterig milieu kunnen zelf-assembleren tot supramoleculaire vezels. Voor de synthese zijn twee strategieën beoordeeld en beide hadden te kampen met de geringe oplosbaarheid van de bouwstenen. Uiteindelijk zijn de BTA-monomeren succesvol geassembleerd met behulp van condensatie van glycosyl imidaat donoren en een BTA-triol in een ongebruikelijk oplosmiddel systeem, bestaande uit een mengsel van 1,1,1,3,3,3-hexafluoroisopropanol (HFIP) en dichloromethaan. De nucleofiliciteit van HFIP bleek voldoende laag te zijn om significante competitie tijdens de condensatiereactie te voorkomen. Tijdens deze reactie traden er echter andere nevenreacties op, die leidden tot de vorming van ortho-esters en migratie van benzoyl groepen. Deze bijproducten waren lastig te verwijderen uit het reactiemengsel, maar na het afsplitsen van de benzoyl groepen, konden de producten worden gezuiverd met behulp van HPLC. Zowel de mannose- en glucose-BTAs waren in staat om te zelf-assembleren tot 2D vezels, welke een tegengestelde heliciteit hadden. Ook omschrijft Hoofdstuk 6 de synthese van BTA-monomeren met twee glucose eenheden en één 6-azido-glucose functionaliteit. Het azide handvat in dit monomeer kan worden gebruikt voor verdere decoratie met functionele groepen zoals adjuvantia (bv. 265) of epitopen (bv. 264). Deze kunnen worden gebruikt voor bijvoorbeeld de co-assemblage van het gemannosyleerde BTA-monomer (213) in combinatie met gp100 gedecoreerde BTAmonomeren (226) en een TLR7-agonist (267) zodat ze een multivalent systeem kunnen vormen, dat interacties kan aangaan met zowel CLRs als TLRs. Door de componenten in verschillende verhoudingen te mengen kunnen gemakkelijk verschillende zelf-assemblerende polymeren worden verkregen en vergeleken (zie Schema 1).

Schema 1: Opbouw van BTA vezels, die een antigen, TLR7 agonist en mannosides.

List of publications

Manuscript in preparation [Glycopaint]

Roger Riera Brillas; <u>Tim P. Hogervorst</u>; Ward Doelman; Sander I. van Kasteren; Jeroen D.C. Codée; Lorenzo Albertazzi

Manuscript in preparation

C-mannosyl lysine for solid phase assembly of mannosylated peptide conjugate cancer vaccines

<u>Tim P. Hogervorst</u>*; & R.J. Eveline Li*; Laura Marino; Sven C.M. Bruijns; Nico J. Meeuwenoord; Dmitri V. Filippov; Herman S. Overkleeft; Gijsbert A. van der Marel; Sandra J. van Vliet; Yvette van Kooyk; and Jeroen D.C. Codée

ACS Chemical Biology, 2020, Manuscript accepted

Targeting of the Langerhans Cell C-Type Lectin Receptor Langerin Using Bifunctional Mannosylated Antigens

<u>Tim P. Hogervorst</u>*; & R.J. Eveline Li*; Silvia Achilli; Sven C.M. Bruijns; Corinne Vivès; Michel Thépaut; Dmitri V. Filippov; Gijsbert A. van der Marel; Sandra J. van Vliet; Franck Fieschi; Jeroen D.C. Codée; and Yvette van Kooyk

Manuscript submitted

Systematic Dual Targeting of Dendritic Cell C-Type Lectin Receptor DC-SIGN and TLR7 Using a Trifunctional Mannosylated Antigen

<u>Tim P. Hogervorst</u>*; & Eveline RJ Li*; Silvia Achilli; Sven C. Bruijns; Tim Arnoldus; Corinne Vivès; Chung C. Wong; Michel Thépaut; Nico J. Meeuwenoord; Hans van den Elst; Herman S. Overkleeft; Gijsbert A. van der Marel; Dmitri V. Filippov; Sandra J. van Vliet; Franck Fieschi; Jeroen D. C. C. Codée; and Yvette van Kooyk.

Frontiers in Chemistry, 2019, 7

https://doi.org/10.3389/fchem.2019.00650

Elucidating the Ordering in Self-Assembled Glycocalyx Mimicking Supramolecular Copolymers in Water

Simone I. S. Hendrikse*; & Lu Su*; <u>Tim P. Hogervorst</u>; René P. M. Lafleur; Xianwen Lou; Gijsbert A. van der Marel; Jeroen D. C. Codée; and Egbert Willem Meijer

Journal of the American Chemical Society, 2019, 141(35):13877–13886

https://doi.org/10.1021/jacs.9b06607

Peptides Conjugated to 2-Alkoxy-8-Oxo-Adenine as Potential Synthetic Vaccines Triggering TLR7

<u>Tim P. Hogervorst</u>*; & Geoffroy P. P. Gential*; Elena Tondini; Michel J. van de Graaff; Herman S. Overkleeft; Jeroen D. C. Codée; Gijsbert A. van der Marel; Ferry Ossendorp; and Dmitri V. Filippov.

Bioorganic & Medicinal Chemistry Letters, 2019, 29(11):1340-1344.

https://doi.org/10.1016/j.bmcl.2019.03.048



https://orcid.org/0000-0002-4686-6251

Curriculum Vitae

Tim Hogervorst was born on the 7th of April 1991 in Pijnacker, the Netherlands. After graduating from the high school Stanislascollege Westplantsoen (VWO) in 2009, he started the bachelor Molecular Science and Technology at Leiden University and the Technical University of Delft. He received his bachelor's degree in 2012 after completing a research internship on the synthesis of β-glycans, under the supervision of A.R. de Jong, prof. dr. G.A. van der Marel and dr. J.D.C. Codée. He continued his studies with the Master Chemistry (Research, Design and Synthesis) at Leiden University. After a short internship on the synthesis of an Artificial Electron-Relay for Cytochrome P450 at Occidental College (USA) under the supervision of prof. dr. Michael G. Hill, he started his masters internship under supervision of A.G. Volbeda, prof. dr. G.A. van der Marel and dr. J.D.C. Codée. The topic of this internship was on the synthesis of sulfated polymannuronates, wherefore different donors were generated and evaluated for their ability to generate oligo mannuronates both in solutions as on solid support.

After obtaining his Master's degree in 2015, the author commenced his PhD studies in May 2015 in the Bio-organic Synthesis department of the Leiden Institute of Chemistry, under the supervision of prof. dr. G.A. van der Marel and dr. J.D.C. Codée. Parts of this research were presented orally on the 20th European Carbohydrate Symposium in Leiden (2019), the 29th International Carbohydrate Symposium in Lisbon (2018) and the 4th annual symposium of the

Institute of Chemical Immunology in Amsterdam (2018). Posters were presented on CHAINS in Veldhoven (2016 & 2017), on the 19th European Carbohydrate Symposium in Barcelona (2017), the Molecular Machines Nobel Prize Conference in Groningen (2017), the 2nd and 3rd annual symposium of the Institute of Chemical Immunology in Amsterdam (2016 & 2017) where the 2017 poster was awarded with the poster price and on the 26th Dutch Peptide Symposium in Maastricht (2018) were the poster was awarded with the Bert L Schram Awards for best posters 2nd Price.

Since September 2019, the author is working as a Technology Scout with Findest B.V. in Amsterdam.